Human embryonic stem cell-derived mesenchymal stem cells as a therapy for spinal cord injury

Submitted in fulfilment of the requirements for the Degree of Doctor of Philosophy

Institute of Neuroscience and Psychology

College of Medical, Veterinary and Life Sciences

University of Glasgow

By

Che Anuar Che Mohamad

MBBS, International Islamic University Malaysia, 2006
MSc Human Anatomy, University of Dundee, 2009

August 2014

Abstract

Traumatic injury to the spinal cord interrupts ascending and descending pathways leading to severe functional deficits of sensory motor and autonomic function which depend on the level and severity of the injury. There are currently no effective therapies for treating such injuries and the adult central nervous system has very limited capacity for repair so that recovery is very limited and functional deficits are usually permanent. Cell transplantation is a potential therapy for spinal cord injury and a range of cell types are being investigated as candidates. Mesenchymal stem cells (MSCs) obtained from bone marrow are one cell type quite extensively studied. When transplanted into animal models of spinal cord injury these cells are reported to affect various aspects of repair and in some cases to improve functional outcome according to behavioural measures. However, the use of these cells has several limitations including the need for an invasive harvesting procedure, variability in cell quality and slow expansion in culture. This project therefore had two main aims: Firstly to investigate whether MSC-like cells closely equivalent to bone marrow derived MSCs could be reliably and consistently differentiated from human embryonic stem cells (hESCs) in order to provide an “off the shelf” cellular therapy product for spinal cord injury and secondly, to transplant such cells into animal models of spinal cord injury in order to, determine whether hESC-derived MSCs replicate or improve on the repair mechanisms reported for bone marrow MSCs.

To accomplish the first aim of the study, hESCs (H1) were repeatedly differentiated into MSC-like cells in several runs performed in duplicate, using an optimize protocol based on a non embryoid body (EB) based method previously described. Mesenchymal-like stem cells were reproducibly derived from hESCs after 28 days of differentiation and repeated passaging for 10-15 days. The cells were characterized according to morphology and adherence capacity to plastic, surface marker expression (eg. CD73 and CD105), gene expression and functional differentiation into adipocytes and osteoblasts. The MSC-like cells from this study grew very robustly and displayed a better proliferation capacity than is generally repeated for MSCs. Cells from each of the differentiation runs of were cryopreserved and five of them were recovered later for use in cell

transplantation in an animal model of SCI. Re-characterization of these cells indicates that they retain their MSC-like properties and ability to grow robustly even after being cryopreserved. The data from this part of study indicates that MSC-like cells can be generated reproducibly from hESCs, will proliferate more rapidly than adult cells and can be cryopreserved without detriment to their properties. This part of the work therefore provides proof of principle for the idea that hESC derived MSCs could be developed as an "off the shelf" cell therapy product.

In the second part of the project, the hESC-MSCs that were differentiated and characterised in the first part of the project were tested *in vivo* by transplanting cells into an animal model of traumatic spinal cord injury. Cells were transplanted three weeks after a contusion injury. In some animals an additional operation was performed to inject a tract tracer in order to assess axonal regeneration. All animals were perfusion fixed and the spinal cord removed and processed for immunocytochemistry using antibodies for different combinations of markers before being examined using fluorescence and confocal microscopy. The cells showed good survival within the injury provided that immunosuppressive treatment was used. They usually filled the injury area so that the cavities present in non-transplanted animals were never seen in transplanted spinal cords. There was no evidence that the cells differentiated into neurons or glia though their morphology could differ from that in culture especially for cells outwith the transplant area. There was some glial activation in response to the cells but the glial scar around the injury did not differ obviously in transplanted compared to non-transplanted animals. Laminin was frequently found at the injury site in both transplanted and non-transplanted animals but blood vessels were more numerous in transplanted animals as judged from both laminin and smooth muscle actin staining. The transplants supported axonal regeneration which included ascending dorsal column but not corticospinal fibres.

Cells were frequently seen outwith the injury site and could form tracks leading rostral and/or caudal to the injury. These tracks appeared to clear endogenous glial cells and in the white matter also axons yet also provided an environment which could encourage very modest regeneration of dorsal column axons beyond the rostral margins of the injury site.

Table of Contents

List of Tables

List of Figures

Acknowledgement

I am extremely thankful to Allah the almighty who gave health and patience to complete this noble effort.

I would like to thank my supervisor Dr. John S Riddell for giving me his full support, advice and knowledge to complete this challenging project. I am very grateful for the time you have dedicated to me and this project. I would also like to thank my co-supervisor Dr. Jo Mountford for her support in the work related to cell biology.

Many thanks to my friends and colleagues in the Spinal Cord Group for their support and help, in particular Mr. Andrew Toft and Dr. Syed Hamid Habib for their great support in my experimental work. Not forgotting Prof Andrew Todd, Dr Anne Bannatyne, Dr. Erika Polgar, Dr. David Hughes, Dr. Jacob Griffin, Dr. Ahmed Emraja, Mr. Robert Kerr, Mrs. Christine Watt, Dr. Zilli Huma, Dr. Najma Baseer, Robert Ganley, Victoria Morley and Emma Mitchell. Thanks to my friends and colleagues in the Stem Cell group, in particular Dr Emmanuel Oliver who introduce me to the technical details of cell culture. A special thanks to Dr. Scott Cowan, Dr. Angela, Dr. Lamin, Dr. Niove, Dr. Nik, Allision and John as each of you has helped me along the way during my time in the stem cell laboratory. Thanks to Dr. Susan Lindsay for her guidance in the preparation of cells for transplantation. Thank you to Dr. Rossi for some help with my histological work.

Very special thanks to my amazing family both in Kelantan and Perlis. In particular my mother in law, Zainab bt Majid who has been extraordinary since the first day I knew her. Many thanks to my siblings, Che Zulkifli Che Mohamad, Che Zuriati Che Mohamad and Che Zamrudi Che Mohamad for their tireless support. The biggest thanks and love go to my wife, Dr. Rosazra Roslan, you are a tower of strength and I value your patience to sustain me throughout these 4 years with love and sincerity despite your busy schedule.

I dedicate this piece of work to my beloved late father, Che Mohamad Che Abdullah who passed away in the final year of my project, and my late mother

Siti Fatimah bt Yaacob. May this work be considered as a good deed from your son that would further raise your rank in the hereafter.

Author's Declaration

I declare that this thesis comprises my own original work except where otherwise stated, and has not been accepted in any previous application for a degree. All sources of information have been referenced.

Definitions/Abbreviations

ºC	Degrees Celcius
µ	Micro
ANOVA	Analysis of variance
ASIA	American Spinal Cord Injury Association
BBB	Basso, Beattie, Breshnan locomotor scale
BDA	Biotin Dextran Amine
BDNF	Brain-derived neurotrophic factor
bFGF	basic fibroblast growth factor
CNS	Central nervous system
CSF	cerebro-spinal fluid
CST	Corticospinal tract
DMEM	Dulbecco's modified eagle medium
EB	Embryoid body
FBS	Fetal bovine serum
GDNF	Glial cell line derived neurotrophic factor
GFAP	Glial fibrillary acidic protein
GFP	Green fluorescent protein
hESC	Human embryonic stem cells

hESC-MSCs	Human embryonic stem cells drived mesenchymal stem cells
MSC	Mesenchymal stem cells
NF	Neurofilament
NGF	Nerve Growth Factor
NT-3	Neurotrophin 3
SCI	Spinal cord injury

Chapter 1

Introduction

Introduction

1.1 Overview of spinal cord injury

Spinal cord injury (SCI) is a devastating condition which can cause loss of sensory, motor and autonomic function rendering long-term personal difficulty to the sufferers. The majority of spinal cord injuries lead to paralysis and this loss of function is normally permanent due to the limited capacity of the spinal cord for repair and a lack of effective treatment to either prevent the secondary damage or to promote the repair (Di Giovanni, 2006; Luo *et al.*, 2009). In the long run, this condition is associated with a higher risk of developing cardiovascular complications, deep vein thrombosis, osteoporosis, pressure ulcers, autonomic dysreflexia and neuropathic pain (Vawda *et al.*, 2012). Additionally, patients are also very likely to suffer emotional and social problem which are primarily attributed to their immobility. Spinal cord injury tends to affect people in their 3rd decade of life, a time usually associated with prime earning potential which further contributes to the significant economic strain, on top of the necessity to provide lifelong healthcare (Baptiste *et al.*, 2007). The suffering as a result of permanent neurological deficits also extends to the patient's family who endure emotional, physical and financial burdens that are directly or indirectly related to the patient's immobility. The effort to reverse paralysis following SCI is among the most difficult challenges in neuroscience research and the damage to the spinal cord cannot currently be repaired by any available therapy.

The current best available treatment for SCI includes early surgical intervention, methylprednisolone and hypertensive therapy with vasoactive agents (Oliveri *et al.*, 2013). Methylprednisolone was previously introduced as a standard care for acute treatment of SCI but the American College of Surgeons subsequently declared there was insufficient evidence for it to be routinely used in SCI (Lammertse, 2012). A further systematic review conducted by a committee of experts from various fields following the request of the Canadian Spine Society and the Canadian Neurological Society have also concluded that there is insufficient evidence to support the use of high-dose methylprednisolone as a standard treatment due to weak clinical evidence but could still be regarded as an option for SCI treatment (Canadian Association of Emergency

Physicians,2009). Another treatment which is also regarded as one of the current standards of care is decompression surgery despite uncertainty regarding the appropriate timing (Furlan *et al.*, 2011). However, neither of these 2 treatments is able to prevent the progression of the pathological events following SCI. Other supporting treatments which have also been tested in clinical trials like GM1 ganglioside and 4-aminopyridine also so far produced marginal benefits with adverse side effects (Geffner *et al.*, 2008).

It is estimated that there are 130,000 new cases of spinal cord injury around the world each year (Illes *et al.*, 2011). According to the National Spinal Cord Injury Statistical Centre (NSCISC), there are around 40 cases of new spinal cord injury per million of population worldwide (Forostyak *et al.*, 2013). In the UK alone, there are approximately 1000 new cases each year which contribute a total of 40,000 people living with SCI. In the USA, the annual incidence is about 12,000 cases (40 cases per million), not including those who died immediately after the accident (National Spinal Cord Injury Stastitical Centre, 2012). While long term survival after injury keeps improving in developed countries, the figures of patients with chronic SCI will inevitably increase. Despite the tremendous efforts being made towards the development of new treatment strategies, this devastating injury remains one of the most challenging areas in neuroscience research and an extremely difficult clinical condition to manage.

1.2 Anatomy of the spinal cord

The spinal cord is a cylindrical elongated caudal extension of the brain and its function is to transmit and integrate the different signals of sensory, motor and autonomic function. It is located inside the bony vertebral column which supports and protects the spinal cord. It is covered by three layer of meninges and further surrounded by cerebral spinal fluid which gives added protection. In the human adult, it occupies the upper two-thirds of the vertebral canal and is divided into 31 segments: 8 cervical, 12 thoracic, 5 lumbar, 5 sacral 1 coccygeal. The spinal cord varies in diameter in different parts where there are two areas of enlargement, located in the mid cervical and lumbosacral segments. The cervical enlargement is from the third cervical to the first or second thoracic segments representing the sites of neurons that innervate the upper limb. The lumbosacral enlargement is from the first lumbar to the third sacral segments

and corresponds where the origin of the neurons that innervate the lower limbs (Afifi and Bergman, 2005). The cord then gradually tapers to form the *conus medullaris* which continues with the *filum terminale*.

The spinal cord is the major pathway containing millions of neuronal and glial cells for transmitting information toward and from the limb, trunk and organ of the body. The sensory nerve roots enter the dorsal aspect and the motor nerve roots exit from the ventral aspect and they combine peripherally to form spinal nerves (Figure 1-1). The spinal nerves exit from each segment of the spinal cord in pairs and are numbered following the corresponding spinal segment. Spinal nerves carry information from the spinal cord to the whole body. In general cervical nerves are responsible for movement and sensation in the arms, neck and upper trunk. Thoracic nerves transmit signals to and from the trunk and abdomen. The remaining lumbar and sacral nerves transmit information to and from the legs, the bladder, bowel and sexual organs (Afifi and Bergman, 2005).

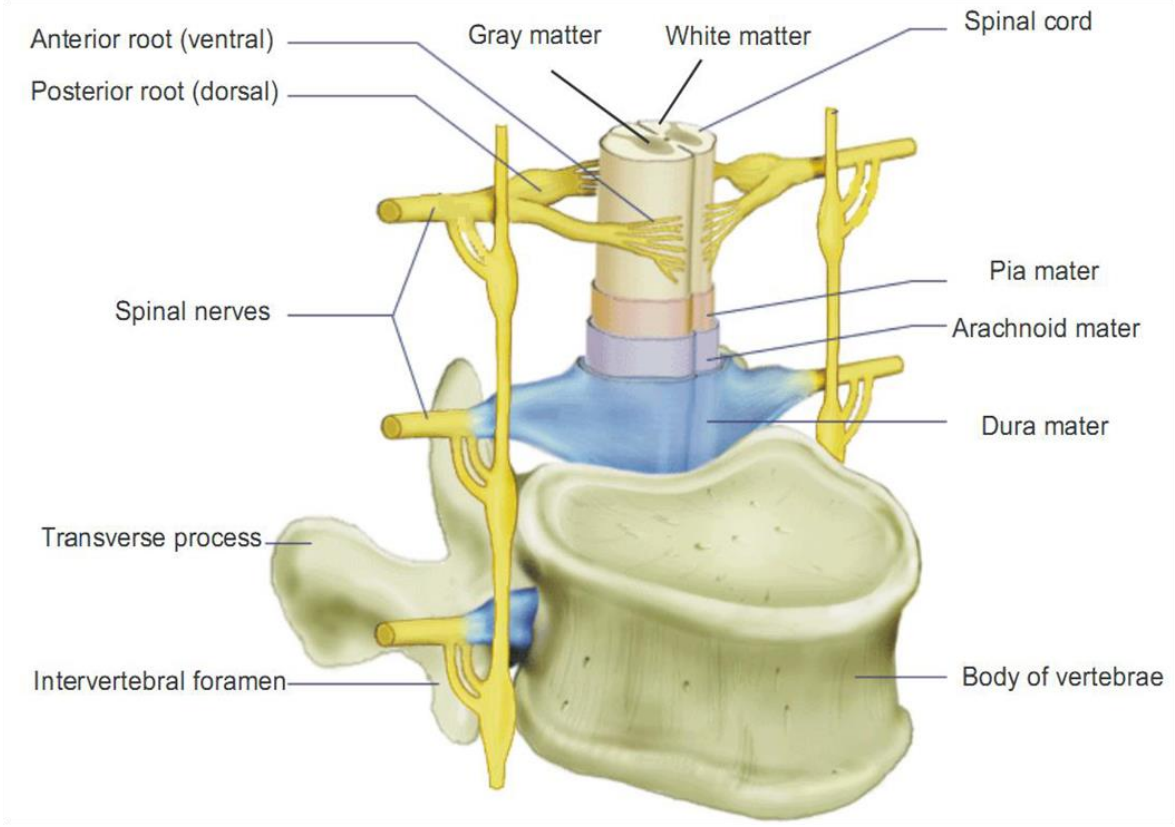

Figure 1-1. Structure of the spinal cord:

Diagram of the spinal cord which illustrates the surrounding vertebral column and the meninges (dura mater, arachnoid mater and pia mater) together with a centrally located butterfly shaped region of grey matter, surrounded by white matter. Also shown are the anterior (ventral) roots and posterior (dorsal) roots which carry motor and sensory signals respectively. (Adapated from www.mcgill.ca, 2008)

1.3 Anatomy of the rat spinal cord

Since this thesis involves work on the laboratory rodent, including tract tracing of specific pathways, an introduction to some of the anatomy of rat spinal cord is useful. The rat spinal cord is divided into 8 cervical segments, 13 thoracic segments, 6 lumbar segments, 4 sacral and 3 coccygeal. The grey matter which is located centrally contains the cell bodies of neurons which are further divided into the dorsal horn, the intermediate grey, the central grey and the ventral horn. The white matter embraces ascending and descending pathways and is divided into dorsal, dorsolateral, ventrolateral and ventral funiculi. From dorsal to ventral, the grey matter can be subdivided into 10 laminae (Molander *et al.*, 1984; Molander *et al.*,1989).

1.3.1 Corticospinal tract

The corticospinal tract (CST) is one of the main descending pathways which is found only in the mammalian CNS. It is an important descending pathway and particularly associated with fine control of the hand in human and non-human primates (Afifi and Bergman, 2005). Experimentally, the CST has been commonly chosen for the assessment of regeneration studies due to the relative ease with which it can be anatomically traced.

1.3.1.1 The origin and course of the CST in the rat

Corticospinal neurons are called pyramidal neurons and located in layer 5 of sensorimotor cortex. Corticospinal fibres have been shown to send collaterals to various brain stem nuclei which include the red nucleus, pontine nuclei, inferior olivary nuclei and dorsal column nuclei (O'Leary and Terashima, 1988)

The CST is divided into a crossed and uncrossed component where the crossed components form the majority (Terashima, 1995). The axons cross to the contralateral side in the medulla oblongata (pyramidal decussation) to descend through the dorsal column of the spinal cord. The majority of the main crossed component (90% of fibres) are located in the ventromedial aspect of the dorsal funiculus (Hicks and D'Amato, 1975; Miller, 1987; Rouiller *et al.*, 1991). The minor components are found in the ipsilateral dorsal, contralateral lateral and ipsilateral ventral funiculi (Casale *et al.*, 1988; Brosamle and Schwab, 1997; Rouiller *et al.*, 1991; Liang *et al.*, 1991).

1.3.2 Ascending pathways in the dorsal column

Ascending pathways in the spinal cord conduct information from sensory receptors in the trunk and limbs to the brain. There are essentially two main groups of ascending fibres in the dorsal columns of the spinal cord, a direct dorsal column pathway and a postsynaptic dorsal column pathway (Tracey and Waite, 1995).

The direct dorsal column pathway is comprised of the ascending branches from primary afferents of sensory neurons. The cell bodies of sensory neurons within the dorsal root ganglia give rise to axons that bifurcate to form 2 major branches

(Figure 1-2). There is one branch which innervates receptors in the skin, muscle and viscera while the other branch enters the spinal cord via the dorsal roots. This central branch bifurcates again into descending and ascending fibres (Willis and Coggeshall, 2004). The descending fibres usually maintain a less organised topographic distribution and only a small number of fibres descend two segments from their entry site (Smith and Bennett, 1987). Only a fraction of the ascending branches of primary afferents reach the dorsal column nuclei while other fibres end in the grey matter at some level of the spinal cord. A much larger number of dorsal root ganglion cells in the cervical enlargement project to the dorsal column nuclei compared with lumbar dorsal root ganglion cells (Smith and Bennett, 1987, Giuffrida and Rustioni, 1992). Axons which travel within the dorsal columns may give rise to collateral braches and terminate in various region of grey matter, including dorsal horn, intermediate region, and ventral horn (Willis and Coggeshall, 2004)(Figure 1-2).

The ascending branches of primary afferents are topgraphically organized in the dorsal columns such that fibres from the tail project close to the midline while fibres from the hindlimb, trunk and forelimb are added to the lateral border of the column at progressively more rostral levels (Willis and Coggeshall, 2004; Smith and Bennet, 1987).

About 25% of primary afferents in the dorsal columns are shown to be unmyelinated in the rat (Chung *et al.*, 1987). It is suggested that these unmyelinated afferents in the dorsal columns might carry information from nociceptors or visceral receptors to the dorsal column nuclei (McNeill *et al.*, 1988; Tamatani *et al.*, 1989; Patterson *et al.*, 1990).

The postsynaptic dorsal column pathway is formed by the axons of spinal neurons in the spinal cord projecting to the dorsal colum nuclei (Giesler *et al.*, 1984). The cells are in the nucleus proprius that is located ventral to the substantia gelatinosa. The axons of postsynaptic dorsal column neurons terminate at all rostrocaudal levels of the gracile and cuneate nuclei as well as in the external cuneate nucleus (de Pommery *et al.*, 1984).

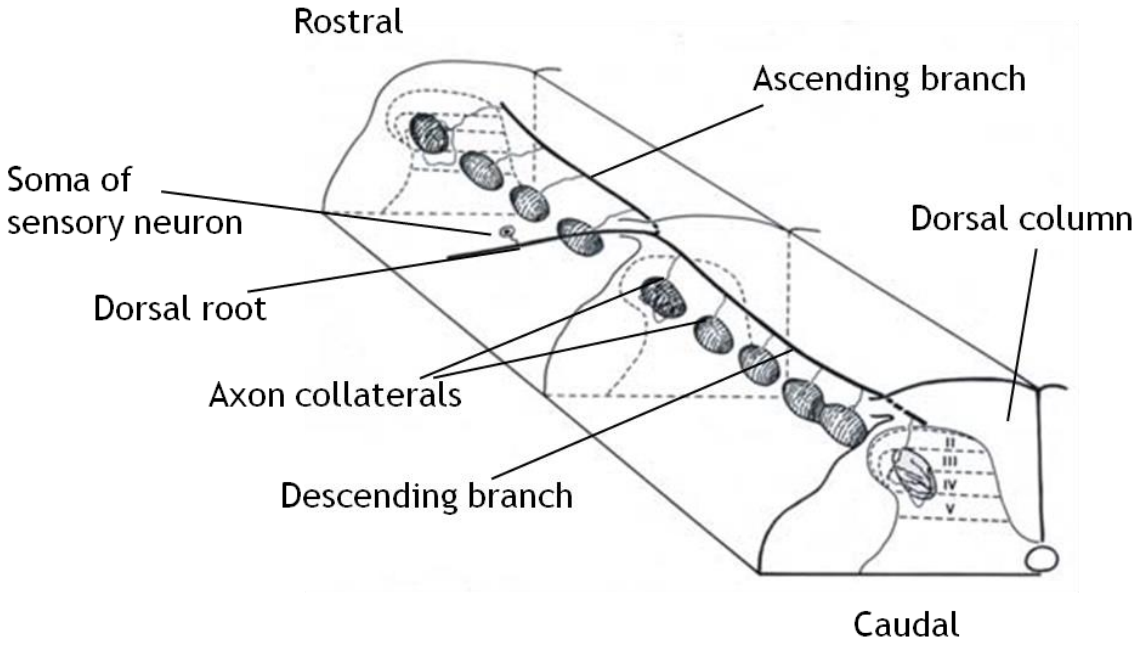

Figure 1-2. Schematic representation of the anatomy of a primary afferent fibres:

Diagram showing the organization of dorsal root ganglion neurons and their central processes. The cell bodies of sensory neurons are located in the dorsal root ganglia and give rise to both peripherally and centrally directed axons. The central axons of large myelinated sensory neurons enter the dorsal columns via the dorsal roots where they bifurcate into ascending and descending branches. These give off axon collaterals at regular intervals which arbourize in the grey matter. A proportion of the ascending axons travel to the brain to terminate in the dorsal column nuclei (Adapted from Brown *et al*, 1981).

1.4 Pathophysiology of spinal cord injury

1.4.1 Overview

The primary injury of traumatic SCI is usually caused by vertebral fracture or dislocation resulting in either contusion or compression injury to the spinal cord (Kigerl and Popovich, 2009). The cellular and molecular events following SCI have been studied in various different animal models and contusion and crush models in animals have been shown to demonstrate a histological picture that mimics the typical pathology in human SCI (Sahni and Kessler, 2010). Spinal cord contusion injury in both rodent and human directly induces damage ranging from membrane disruption, vascular damage and haemorrhage (Sahni and Kessler, 2010). While haemorrhage is immediately grossly visible, the microscopic signs of axon and myelin damage are delayed for about 24-48 hours after the injury (Rosenberg and Wrathall, 1997; Balentine, 1978) except in the event of axotomy where they appear immediately. In general, SCI presentation in human is highly variable depending on the location, extent and duration after the injury even though the major pathological signs are similar.

1.4.2 Phases of SCI responses after injury

Principally, SCI occurs in three phases of responses which range from acute, secondary and chronic responses following the injury event (Hulsebosch, 2002).

1.4.2.1 Acute phase

In the acute phase, there is immediate mechanical damage to neural and other soft tissues including endothelial cells of the vasculature, causing instantaneous necrosis and cell death (Hulsebosch, 2002). This leads to a variable degree of cell loss including neuronal and oligodendrocyte death due to necrosis in the immediate hours (Di Giovanni, 2006). Over the next few minutes, the affected nerve cells respond with an injury-induced barrage of action potentials accompanied with significant electrolyte shifts leading to functional neural failure and spinal shock (Hulsebosch, 2002). In addition, haemorrhage which is accompanied by oedema, loss of microcirculation by thrombosis, vasospasm and

mechanical damage and loss of auto regulation further aggravate the neural injury. The acute phase usually persists for hours up to days before being subsequently resolved into the subacute phase.

1.4.2.2 Secondary phase

The secondary and chronic injury phases are strategically feasible therapeutic targets. The secondary injury is the pathologic outcome of the cascades of cellular and molecular events intrigued by mechanical trauma (Lu *et al.*, 2000). In the secondary phase of SCI, ischaemic cellular death, electrolyte shifts and oedema occur. The ischaemic cell death or necrosis is an accidental cell death, characterized by swelling, energy loss, intense mitochondrial damage and homeostasis disturbance which collectively lead to cell rupture (Lu *et al.*, 2000). Cell lysis causes the release of intracellular constituent which evokes further inflammatory processes (Cohen, 1993). Subsequently, extracellular concentrations of glutamate and other excitatory amino acids reach toxic levels (Hulsebosch, 2002) due to cell lysis and synaptic and non synaptic transport. Later on, apoptosis will take place associated with increased expression of glial fibrillary acidic protein (GFAP) and astrocytic proliferation. Apoptosis, a programmed cell death, plays a major role in oligodendrocyte cell death (Crowe *et al.*, 1997; Liu *et al.*, 1997) that leads to axonal demyelination. Invading inflammatory cells such as neutrophils and lymphocytes increase the local concentration of cytokines and chemokines (Hulsebosch, 2002) which cause more cellular necrosis and apopotosis. Meanwhile, inhibitory factors and barriers to axonal regeneration begin to be expressed in the perilesion area. This is subsequently followed by enlargement of the lesion size/cavity leading to a larger amount of cell death.

1.4.2.3 Chronic phase

In the chronic phase, which occurs from weeks to years, apoptosis continues bidirectionally orthogradely and retrogradely and several different types of receptors and ion channels become altered in their expression levels and activation states (Hulsebosch, 2002). In penetrating injury, scarring and tethering of the cord occurs. These events will eventually lead to demyelination which results in conduction deficits and there will also be formation of a CSF-

filled cyst or cysts which continue to enlarge . Neural circuits are altered due to disruption in excitatory and inhibitory function which can cause permanent hyper excitability, resulting in chronic pain syndromes (Christensen and Hulsebosch, 1997; Christensen *et al*., 1996).

1.4.3 Main Pathology following SCI

1.4.3.1 Axonal degeneration following SCI

Axonal degeneration is an extremely important pathology in many diseases of the nervous system (Vargas and Barres, 2007) as the axon represents the largest functional element in many neuronal populations (Lingor *et al*., 2012) including the human spinal cord. In most cases, traumatic spinal cord injury would result in a partial transection of ascending and/or descending tracts causing an incomplete impairment of sensory or motor functions while only a small percentage may result in complete transections (Rowland *et al*., 2008). By definition, it is an active, tightly controlled and versatile process of self-destruction of an axon segment (Wang *et al*., 2012) leading to sequential degeneration. Axonal degeneration usually involves rapid blebbing and fragmentation of an entire axonal stretch which is subsequently removed by phagocytic cells (Wang *et al*., 2012). The axonal degeneration following a traumatic lesion is the most extensively studied (Lingor *et al*., 2012). In traumatic SCI, the injury force or lesion would cause membrane disruption which eventually results in calcium influx, calpain-mediated cleavage and axonal transport breakdown (Lingor *et al*., 2012). These events would finally lead to axonal degeneration in the vicinity of the lesion and distal to the lesion site, characterised by distinct morphological and chemical changes. The axonal degeneration distal to the lesion is also known as Wallerian degeneration (Wang *et al*., 2012). While the primary damage or the direct lesion induces Wallerian degeneration of the distal axons that project to the spinal cord, the neighbouring axons which have not been primarily injured may also degenerate after time due to secondary damage as a result of a local increase of Iba-1-positive microglia (Lingor *et al*., 2012). The above described events in axonal degeneration are responsible for the sensory-motor dysfunction following spinal cord injury. Being the largest functional entity in neuronal populations, the effort to repair and regenerate the injured axon has been regarded as the

ultimate way to restore the function of the injured spinal cord by reconnecting the severed long tracts for motor and sensory function (Tuszynski and Steward, 2012). Furthermore, an increasing amount of data nowadays supports the concept of axonal degeneration as the initial pathological mechanism so the consideration of axonal degeneration as a major event to be targeted and prevented by neuroprotective strategies is therefore crucial for the development of successful SCI treatments (Lingor *et al.*, 2012).

1.4.3.2 Axonal demyelination following SCI

Demyelination of the axon is a loss of the myelin sheath surrounding the axons and tends to happen early in the event of SCI. Chronic and progressive demyelination is a persistent feature in spinal cord injury (Totoiu and Keirstead, 2005). This pathology has been investigated in various studies of different animal species (Siegenthaler *et al.*, 2007) where oligodendrocyte death was identified as the main immediate and delayed event contributing to demyelination after SCI (Siegenthaler *et al.*, 2007). Functionally, demyelination of intact axons would result in impaired signal conduction and attenuated action potential propagation (Cao *et al.*, 2005). The malfunction is also due to the exposure of voltage-gated ion channels at the internodes of the demyelinated axons following spinal cord injury (Nashmi and Fehlings, 2001) which may finally lead to overt nerve conduction block.

Demyelination usually starts at the epicentre of the injured spinal cord and slowly progresses into adjacent white matter (Wu and Ren, 2008). One study has demonstrated that demyelination is a persistent feature of SCI. The overall numbers of demyelinated axons after SCI were highest at day one post injury, declining by 7 to 14 days following injury before again progressively increasing up to 450 days (Totoiu and Keirstead, 2005). Despite the endogenous remyelination that often follows demyelination in SCI (Smith and Jeffery, 2006; Lasiene *et al.*, 2008; Siegenthaler *et al.*, 2007), several studies have revealed that this process is incomplete and abortive (Salgado-Ceballos *et al.*, 1998; Siegenthaler *et al.*, 2007), and thus is unable to achieve the desired level of recovery. In addition, other studies have also demonstrated that oligodendrocytes which survive within a region of demyelination do not divide to expand their numbers to produce sufficient myelin, and are thus unable to

effectively contribute to remyelinating injured axons (Keirstead and Blakemore, 1997).

1.5 Endogenous regenerative repair after SCI

The classical dogma in neuroscience is that injured CNS neurons are incapable of regeneration. However, numerous studies have revealed that this is not necessarily the case. This classical view has been revised and challenged following several observations which revealed evidences of axonal regeneration after SCI. Early observations by Liu and Chambers in 1958 demonstrated that the central projections of primary afferent fibres are able to sprout after injury (Liu and Chambers, 1958). Subsequent research by Richardson *et al* in the 1980s using grafts of peripheral nerve tissue showed that central axons could regenerate if the nature of their environment was changed with peripheral type tissue (Richardson *et al.*, 1980). These studies showed that it was the CNS environment that is non-permissive to axon regeneration and not that axons cannot regenerate. At a molecular level, there is an increase in the expression of regeneration associated genes in the damaged neurons (Gardiner *et al.*, 2005; Filbin, 2003), as well as a surge in proliferation of local adult stem cells and progenitor cells which form the basis of the endogenous regeneration. However, these regenerative inputs are limited by growth inhibitors present on oligodendrocyte myelin debris and on cells forming the scar tissue (Nandoe Tewarie *et al.*, 2009) while certain populations of regenerating axons do not express certain key proteins like GAP-43 which is involved in neurite elongation (Hulsebosch, 2002). Furthermore, the newly regenerating endogenous stem cells and progenitors fail to functionally integrate into the damaged spinal cord to support a meaningful endogenous regeneration that is able to repair the injured spinal cord (Nandoe Tewarie *et al.*, 2009). These limiting or inhibiting factors result in inadequate endogenous regeneration to support a meaningful or efficient axonal regeneration thus necessitating an external supporting treatment.

Endogenous regeneration may contribute to the modest recovery seen in incomplete SCI patients although most of this probably involves plastic reorganisation in the brain (Baptiste *et al.*, 2007). There is some activation of

endogenous spinal cord ependymal progenitors (Foret *et al.*, 2010, Ruff *et al.*, 2012) which occurs over the rostro-caudal extent of the cord. Ependymal and sub-ependymal cells are known to be an endogenous source of neural stem cells in the adult spinal cord and proliferation of these cells increases dramatically after spinal cord injury forming oligodendrocytes and astrocytes (Meletis *et al.*, 2008).

1.6 Factors preventing efficient axonal regeneration

There are several limiting factors which are thought to affect the ability of injured neurons in the adult spinal cord to regenerate far enough to re-establish lost function. These factors include 1) inhibitory molecules in the environment of the injured spinal cord, 2) glial scarring and 3) cavity formation.

There are various inhibitory factors that have been identified that contribute to regeneration failure. Amongst them are the inhibitory factors from oligodendrocyte-derived CNS myelin. There are major myelin components that have been identified as inhibitors to the regeneration process in CNS (Schwab and He, 2007). One of the factors is Nogo, which has been shown to inhibit axonal growth. The administration of a function blocking antibody which targeted Nogo was shown to promote sprouting and was reported to result in long distance fibre growth in the adult CNS (Bregman *et al.*, 1995, Schnell and Schwab, 1990, Thallmair *et al.*, 1998). These studies verify the involvement of Nogo in limiting axonal regeneration. In addition to Nogo, myelin-associated glycoprotein (MAG) is another major inhibitory protein in the myelin which has been shown to limit axonal regeneration in vitro (Li *et al.*, 1996, Mukhopadhyay *et al.*, 1994; Tang *et al.*, 1997). The inhibitory effect was shown to be reduced after MAG denaturation in vitro (Li *et al.*, 1996) and the axonal regeneration significantly increased in MAG deficient knockout animals (Schafer *et al.*, 1996). Another major inhibitor in CNS myelin is oligodendrocyte myelin glycoprotein (OMgp) which has been shown to be a potent inhibitor for neurite outgrowth in in vitro and OMgp knockout animal studies (Wang *et al.*, 2002; Ji *et al.*, 2008). These three myelin-associated inhibitors are thought to account for the majority of the inhibitory effect associated with CNS myelin and block of axonal regeneration in the adult spinal cord (Wang *et al.*, 2002).

Regenerating fibres are typically blocked by the glial scar reaction that forms around the injury (Schwab and He, 2007). A glial scar is composed of glial cells and tissue elements (Fawcett and Asher, 1999; Silver and Miller, 2004; Stichel and Muller, 1998a) and forms after the injury to seal off the lesion as well as reduce the exit of cytotoxic molecules (Rolls and Schwartz, 2006). This scar is thought to act as a mechanical barrier which is impenetrable to the regenerating axon thus preventing regeneration. Further study however has revealed that the glial scar contains components which are able to disrupt axon regeneration such as the glycoprotein tenascin-C and chondroitin sulphate proteoglycans (CSPGs) (Davies *et al.*, 1997; Davies *et al.*, 1999; Grimpe and Silver, 2002; McKeon *et al.*, 1991). CSPG consists of a repeated disaccharide glycosaminoglycan chain which forms a barrier to axonal regeneration (Asher *et al.*, 2002; Dou and Levine, 1994). Following the injury, the expression of several different CSPGs is increased and the enzymatic degradation of these molecules by chondroitinase ABC (ChABC) has been shown to enhance axonal regeneration and functional recovery (Bradbury *et al.*, 2002; Moon *et al.*, 2001) verifying the inhibitory effect of the CSPGs.

A cerebrospinal fluid-filled cavity develops in the injured tissue following the necrotic and apoptotic events (Willerth and Sakiyama-Elbert, 2008). The formation of this cystic cavity creates another physical barrier to the regenerating axons (Radojicic *et al.*, 2005). Cell transplantation could potentially overcome this problem by either bridging the lesion or by secreting factors that help promote regeneration and cell migration as exhibited by recent studies using different type of cells (Ohta *et al.*, 2004; Wu *et al.*, 2003; Tuszynski *et al.*, 1994).

1.7 Treatment strategies in spinal cord injury

Delayed pathology which occurs during secondary and chronic phases due to secondary injury could be diminished by inhibiting one or more secondary injury cascades. The strategies for intervention in SCI need to address a whole list of various underlying pathologies or issues:

- Reduction of oedema and free radicals
- Rescue of neural tissues at risk of dying in secondary processes
- Control of inflammation
- Rescue of neuronal/glial populations at risk of continued apoptosis
- Repair of demyelination and conduction deficits
- Promotion of neurite growth through improved extracellular environment

The issues or pathologies mentioned are addressed via four main strategies. These strategies are by 1) promoting neuroprotection and repairing or supporting pre-existing/spared pathways, 2) promoting axonal regeneration, 3) promoting remyelination and 4) cell replacement therapies.

1.7.1 Neuroprotection and trophic support/ support spared pathway

Neuroprotection is a first line therapeutic strategy that could lead to an improved neurological outcome. It is a loose term referring to any process which prevents the spinal cord from continuously degenerating after the injury as a result of the secondary process. Several neuroprotective agents are currently being studied and one of the earliest discovered was methylprednisolone. It is thought to provide a neuroprotective effect through downregulation of pro-inflammatory genes and inhibition of peroxidation related processes (Almon *et al.*, 2002; Fu and Saporta, 2005; Hall, 1992). Stem cells have been shown to be able to provide neurotrophic support which would promote survival of injured

nerves as well as prevent cell atrophy and loss of neurons (Sahni and Kessler, 2010). Stem cells can secrete a variety of useful factors like nerve growth factors (NGF) or brain derived neurotrophic factors (BDNF) which apart from promoting axonal regeneration, have also been shown to promote neuroprotective effects in animal model of SCI (Mori *et al.*, 1997; Tobias *et al.*, 2003; Tang and Low, 2007).

NGF, BDNF and NT-3 are the best investigated neurotrophins in normal and injured spinal cord (Widenfalk *et al.*, 2001; Dougherty *et al.*, 2000; Dreyfus *et al.*, 1999; Nieto-Sampedro *et al.*, 1982; Finklestein *et al.*, 1988; Zvarova *et al.*, 2004; Tokumine *et al.*, 2003; Uchida *et al.*, 2003; Ikeda *et al.*, 2001; Li *et al.*, 2007). Neurotrophic factors have been demonstrated to enhance mechanisms involved in regeneration after SCI such as vascular proliferation, regeneration of transected axons, sprouting from intact axons and prevention of retrograde death of axotomized brainstem spinal projections neurons (Hardy *et al.*, 2008; Hawryluk, 2012). By providing these useful factors, transplanted cells may establish a permissive environment for axonal regeneration and further enhance functional recovery.

1.7.2 Promoting axonal regeneration

Axonal regeneration is regarded as the only way to restore the original lost function of the injured spinal cord and is probably one of the most desirable goals to be achieved (Tuszynski and Steward, 2012). Adequate and meaningful axonal regeneration would enable the severed axons to re-connect with their target neurons in order to restore function in ascending and descending spinal projections and provide functional recovery. Axonal regeneration refers to re-growth of transacted axons from the distal stump of a crushed or transacted nerve to re-innervate its normal target (Tuszynski and Steward, 2012). This is distinct from axon sprouting which can be defined as any growth arising from spared and intact axons (Tuszynski and Steward, 2012).

Following spinal cord injury, severed axons attempt to regenerate during the first 6-24 hours but they fail to achieve complete regeneration due to their failure to navigate into the right direction (Kerschensteiner *et al.*, 2005) and because of inhibitory factors which prevent their growth. Regeneration of an

injured CNS axonal projection depends on a series of events which can be regarded as a recapitulation of those occurring during normal development. This series of events includes 1) regrowth (spontaneous sprouting) of the damaged axon, 2) passage through the lesion site, 3) elongation in the correct direction, 4) topographic reinnervation of the normal target, and 5) restoration of former electrophysiological properties (Stichel and Muller, 1998b). It is clear from several recent studies that an external factor or treatment would be required to achieve such precise regeneration and several studies have showed that different types of cell transplants could promote different levels of axonal regeneration (Bonner *et al.*, 2010; Gu *et al.*, 2010; Sasaki *et al.*, 2009; Lu *et al.*, 2003a; Lu *et al.*, 2012). Without effective treatment to support regeneration, the restoration process will cease prior to any circuit reconnection leading to atrophy of the nerve sprouts (Ramon y Cajal, 1928).

1.7.3 Promoting axonal remyelination

Axonal demyelination is another important pathological event to be targeted which could have a major therapeutic effect in treating SCI. Apart from being essential for functional recovery, remyelination processes also have a role in protecting the axons and supporting regeneration of the injured axons. Therefore any treatment to either halt the continuing process of demyelination or promote the post injury remyelination would potentially lead to significant improvement in neural function. Amongst potential treatments which have been shown to promote remyelination is cell transplantation. Oligodendrocyte progenitor cells (OPC) show the potential to promote remyelination as they are able to form central myelin on demyelinated axons (Xu and Onifer 2009). They were shown to differentiate into mature oligodendrocytes after being transplanted into injured spinal cord (Cao *et al.*, 2005). Another study by Hawryluk *et al.* has revealed some degree of remyelination of the injured spinal cord following endogenous and exogenous NPC transplantation which contributed towards functional recovery of the injured animal (Hawryluk *et al.*, 2013).

1.7.4 Cell replacement

Treatment of SCI by replacing damaged and cut cells with functional cells, in order to either reconnect severed long tracts or remyelinate spared and

regenerating axons would require pre-differentiated high purity populations of desired cells or *in situ* differentiation of transplanted cells. Stem cells offer great promise as a source of new neurons or glial cells due to their ability to differentiate into multiple lineages, including neural cells. The best documented specific cell replacement study is using myelinogenic cells to form new myelin sheath (Rossi and Keirstead, 2009). This followed the successful derivation of high purity oligodendrocyte populations, which when transplanted were shown to remyelinate the demyelinated axons of the injured spinal cord (Nistor *et al.*, 2005; Izrael *et al.*, 2007; Keirstead *et al.*, 2005; Totoiu *et al.*, 2004). It has been suggested that the gliogenic nature of the lesion area further supports the remyelination ability of the transplanted cells in SCI (Cao *et al.*, 2002; Cao *et al.*, 2001; Horky *et al.*, 2006), while reducing the neuronal differentiation. Studies have shown that transplantation of NSCs into the injured spinal cord results in only 38% neuronal differentiation as compared 95% when transplanted into normal spinal cord (Tarasenko *et al.*, 2007; Wu *et al.*, 2002).

1.8 Stem cell-based transplants for treatment of spinal cord injury

There is evidence that cell transplants have the ability to promote neuroprotection, reduce the glial scar, reduce inflammation, induce or perform remyelination and promote axonal regeneration. With advances in stem cell biology, there are now a large number of different cell types that are candidates for transplant mediated repair after SCI (Rossi and Keirstead, 2009). The benefits of stem cell-based treatments have been well documented in the pre-clinical literature. Stem cells-based therapies offer several therapeutic promises through different mechanisms which could increase anatomical plasticity and sensorimotor recovery (Ruff *et al.*, 2012). These 2 elements are the key factors in promoting tissue repair and functional recovery following spinal cord injury. Plasticity could be loosely defined as an adaptive reorganisation of connectivity through axonal regeneration, collateral sprouting, unmasking of existing synapses, and activation of ascending and descending pathways (Ruff *et al.*, 2012). Stem cell transplants could increase and permit anatomic plasticity through lesion modification and glial scar degradation, improved growth and

survival through trophic signalling and removal of inhibitory signalling (Lu *et al.*, 2007; Lakatos *et al.*, 2003; Lopez-Vales *et al.*, 2006; Karimi-Abdolrezaee *et al.*, 2010). Apart from those elements of anatomical recovery, several investigations of cell therapies in SCI have also shown some degree of functional recovery (Abrams *et al.*, 2009; Boido *et al.*, 2012; Toft *et al.*, 2007; Tarasenko *et al.*, 2007). Functional recovery after spinal cord injury is defined as a return in the conductance and physiology of the spinal cord and improved motor and sensory function based on repair factors. In SCI transplant studies, functional recovery would usually be measured through electrophysiological and behavioural assessments.

Stem cell based therapies could be performed using either allogenic or autologous cells. Autologous cells have the advantage of avoiding host rejection and the need for immunosuppression. Stem cell based therapies have been in use since early 1968 following the first successful bone marrow transplant (Carpenter *et al.*, 2009; Bach *et al.*, 1968; Gatti *et al.*, 1968). Since then, it has been further developed clinically as one of the treatment options in leukaemia and other types of cancer (Tabbara *et al.*, 2002).

1.8.1 Embryonic stem cells/induced pluripotent stem cells(ESCs/iPSCs)

ESCs are a population of pluripotent cells derived from the inner cell mass of a pre-implantation blastocyst (Thomson *et al.*, 1998; Mountford, 2008; Rossi and Keirstead, 2009). Originally, ESCs were derived from the pre-implantation mouse embryo in the early 1980s (Evans and Kaufman, 1981) and then followed by the establishment of embryonic germ cell lines from primordial germ cells (Stewart *et al*, 1994). The successful isolation of hESCs by Thompson *et al*, has further heightened the interest in the field of ESCs (Thompson *et al.*, 1998) and has evoked tremendous discussion concerning the potential application of hESCs in regenerative medicine. At the laboratory level, ESCs can be prepared from pre-implantation or blastocyst stage embryos, by somatic cell nuclear transfer or by parthenogenetic egg activation (Bhattacharya *et al.*, 2004). In general, ESCs are characterized by two unique features which are the ability of unlimited self-renewal and the capacity to differentiate into all lineages. This type of cells also

can be grown in virtually unlimited numbers as they do not undergo senescence, are able to retain high telomerase activity (an enzyme which causes the cells to become immortal in culture without inducing any malignant transformation) and normal cell cycle signalling (Coutts and Keirstead, 2008). Amongst the currently available stem cells, hESCs show the greatest potential for the broadest range of cell replacement therapies as they were regarded as commercially viable. This is because they could be propagated in vitro almost indefinitely, stabley banked while maintaining a normal karyotype and differentiation potential even after very long duration in culture (Coutts and Keirstead, 2008).

One strategy is to derive differentiated cells from hESCs. Several studies have demonstrated that both rodent and human ESCs can be differentiated into neuronal or glial cells with some studies reporting that they support regeneration and remyelination after SCI (Finley *et al.*, 1996; Liu *et al.*, 2000; Reubinoff *et al.*, 2001; Carpenter *et al.*, 2001; Lang *et al.*, 2004; Li *et al.*, 2005; Keirstead *et al.*, 2005; Nistor *et al.*, 2005; Billon *et al.*, 2006). These studies demonstrate the possibility of directed differentiation of hESCs into high purity neural populations which enhance the therapeutic potential in treating SCI while reducing the risk of tumorigenesis as compared to direct application of hESCs into the lesion.

Induced pluripotent stem cells (iPSCs) are an interesting alternative to hESCs as they circumvent the ethical issues as well as reducing the risk of immunological rejection yet could act like hESCs. They can be produced from mouse and human fibroblasts by introducing Sox2, Klf4, Oct3/4 and c-Myc in culture (Takahashi and Yamanaka, 2006; Takahashi *et al.*, 2007). Human iPSCs have been shown to be similar to hESCs in morphology, proliferation, surface antigens, gene expression, epigenetic status of pluripotent cell-specific genes and telomerase activity (Takahashi *et al.*, 2007). These cells offer another possibility for providing an unlimited supply of cells for therapy. More interestingly, they have been shown to differentiate into functional neurons, astrocytes and oligodendrocytes (Miura *et al.*, 2009). However, the same study also indicated that iPSCs could form teratocarcinomas. The association with teratocarcinomas warrants a rigorous safety evaluation before treatment based on iPSCs is translated into the clinic. Recently, Fujimoto *et al.* have reported that iPSCs which were pre-differentiated into neuroepithelial like stem cells (hips-lt-NES) are able to

support the reconstruction of CST pathways, promote endogenous neuron survival and promote functional recovery of hind limbs in mice (Fujimoto *et al.*, 2012).

1.8.2 Neural stem/progenitor cells(NSPCs)

Neural stem cells or neural progenitor cells (NSPCs) are another interesting candidate for cell transplantation in SCI. NSPCs are endogenous stem cells which were found to exist within the central nervous system and can be isolated from different regions of the developing and adult brain and spinal cord (Synder *et al*, 1992; Reynolds and Weiss, 1992; Lois and Alvarez-Buylla, 1993; Mayer-Proschel *et al*, 1997; Uchida *et al*, 2000). These cells have been amplified as neurospheres with epidermal growth factor (EGF) and/or fibroblast growth factor (FGF) for several rounds of passages. EGF and FGF are two vital nutritional growth factors which can promote NSPC growth (Lee *et al.*, 2009; Tureyen *et al.*, 2005). The neurosphere culture system is the main method of NSPC study, developed by Reynold and Weiss (Reynolds and Weiss, 1992). They contain precursors for neurons, astroglia and oligodendrocytes. Being of exclusively neural origin, NSPCs are believed to be highly committed to a neural fate and thus easier to differentiate into mature neural phenotypes while very unlikely to become neoplastic. Human NSPCs are taken from cadavers which significantly and restricts the potential supply (Coutts and Keirstead, 2008). In rodents, the NSPCs can be obtained from the CNS of embryos (Tetzlaff *et al.*, 2011).

Following their isolation, these cells can be expanded by exposure to different growth factors. They maintain some capacity for self-renewal even after several freeze-thaw cycles and are capable of generating differentiated and mature neural cells which repair the injured CNS (Caldwell *et al.*, 2001; Nunes *et al.*, 2003; Cummings *et al.*, 2006; Ogawa *et al.*, 2002; Iwanami *et al.*, 2005). They have been shown to protect against excitotoxicity and secrete neurotrophic factors (Llado *et al.*, 2004; Lu *et al.*, 2003b). There have been several transplantation studies using NSPCs in therapeutic studies of SCI with evidence of axonal regeneration and functional improvement (Tarasenko *et al.*, 2007; Yan *et al.*, 2007; Yasuda *et al.*, 2011; Hwang *et al.*, 2009; Alexanian *et al.*, 2011b). In most cases, transplanted NSCs tend to differentiate into glial lineages *in vivo*,

especially into astrocyes (Cao *et al.*, 2001) which partly limit the efficiency of direct transplantation of NSCs without prior pre-differentiation into more committed lineages. Studies by Hwang *et al* and Alexanian *et al* have demonstrated a significant improvement in locomotor and sensory functional recovery following transplantation of pre-differentiated NSCs (Hwang *et al.*, 2009; Alexanian *et al.*, 2011b). Both studies indicated that oligodendrocyte differentiation from NSPCs is absolutely vital to the functional recovery likely promoted by remyelination. Another study demonstrated large-scale differentiation into neurons, axon regeneration with extensive synaptic contacts formed with host neurons in the lumbar cord of adult nude rats following transplantation of NSCs from human fetal spinal cord (Yan *et al.*, 2007). This study indicates the possibility of neural circuit restoration by implanting the NSCs in the injured spinal cord.

Nevertheless, despite some promising studies involving NSPCs, they have been associated with certain limitations which could restrain their application in a clinical setting. Firstly, their derivation from either human cadaver or foetuses (Coutts and Keirstead, 2008) would significantly restrict their supply. Secondly, the NSPCs from adult sources have been shown to divide less frequently so maybe difficult to expand into the large numbers required for clinical applications (Doetsch *et al.*, 1999; Morshead *et al.*, 1998). There is also evidence of a reduction in their differentiation potential after time in culture (Wright *et al.*, 2006) which further limits their therapeutic potential.

1.9 Other type of cells

1.9.1 Schwann Cells

Schwann cells (SCs) have become one of the most intensely studied cell types in the context of spinal cord injury repair. These cells are the myelinating cells of the peripheral nervous system (PNS), and play a crucial role in endogenous repair of peripheral nerves by contributing to axon regeneration and remyelination (Park *et al.*, 2010a). They have the ability to dedifferentiate, migrate, proliferate and express growth promoting factors which contribute toward their therapeutic properties (Xu *et al.*, 1997; Tuszynski *et al.*, 1998; Weidner *et al.*, 1999). SCs have been shown to produce different neurotrophic

factors such as NGF, BDNF and CNTF which can stimulate the survival and intrinsic regeneration ability of injured neurons (Park *et al.*, 2010a). They can also generate several cell adhesion molecules and extracellular matrix proteins to support axonal growth (Pierucci *et al.*, 2009; Ghosh *et al.*, 2012).

One of the great advantages of Schwann cells is that they can be readily isolated from peripheral nerves and easily purified and expanded in culture to generate a large number of cells, from both rat and human tissue. More recently, SCs were shown to be derived from other categories of stem cells including MSCs, adipose-derived stem cells, and skin-derived stem cells (Park *et al.*, 2010a; Xu *et al.*, 2008; Biernaskie *et al.*, 2007). Previous studies have demonstrated that Schwann cells can help to re-myelinate axons as well as promote regeneration (Li and Raisman, 1994; Tuszynski *et al.*, 1998; Kohama *et al.*, 2001). However these cells seems to provoke a robust astrocytic reaction that results in a less effective integration into the host spinal cord (Baron-Van Evercooren *et al.*, 1992; Shields *et al.*, 2000; Lakatos *et al.*, 2000). In addition, their *in vitro* expansion may take several weeks which imposes a delay in the intervention.

1.9.2 Olfactory ensheathing cells (OECs)

OECs are a unique glial population which are present only in the olfactory system and are derived from precursors originating from ectoderm in the olfactory placode (Ramón-Cueto and Avila, 1998; Chuah and Au, 1991). They are support cells that wrap olfactory axons and facilitate their regeneration throughout the life of mammalian species (Coutts and Keirstead, 2008). They are found to exist as two distinct cell sub-types *in vivo* namely a spindle-like cell that ensheaths the axons of ORNs and traverses from the mucosa to within the olfactory bulb and a cell that does not ensheath ORN axons. They have been reported to display an exceptional plasticity and could allow neurons to cross a glial scar including the PNS-CNS boundary (Richter and Roskams, 2008; Raisman and Li, 2007). OECs are relatively easy to isolate from nasal biopsies and could potentially provide an autologous source for cell transplantation. There have been various outcomes reported following experimental studies using OECs in SCI with some studies describing evidence of remyelination and regeneration of damaged axons while other groups have failed to reproduce these results (Ziegler *et al.*, 2011; Takeoka *et al.*, 2011).

1.10 MSCs for transplant in SCI

1.10.1 Introduction

MSCs could loosely be defined as heterogenous multipotent mesenchymal stromal cells that proliferate *in vitro* as plastic adherence cells, have fibroblast like morphology, form colonies in vitro and can be differentiated into bone, cartilage and fat cells (Uccelli *et al.*, 2008; Horwitz *et al.*, 2005). Developmentally, they originated from the embryonic mesodermal layer (Eftekharpour *et al.*, 2008). These cells are located in adult tissues such as bone marrow and other connectives tissues like adipose tissue, cartilage and dermis. MSCs are also found in the developing embryo, in umbilical cord blood, amniotic fluid and the foetal liver. In addition, MSCs are also found in synovial fluid and muscle tissue (Barberi *et al.*, 2006; Olivier *et al.*, 2006; Eftekharpour *et al.*, 2008). In the laboratory, cells with MSC-like characteristics have been isolated or derived from almost every tissue that have been analysed so far (da Silva Meirelles *et al.*, 2006). MSCs derived from human bone marrow are the best studied and characterized so far but there are still several biological aspects of MSCs which remain elusive and require further investigation.

1.10.2 The origin and location of MSCs

Although they were initially isolated from bone marrow, further research has demonstrated the existance of MSCs in other tissues. As a result, MSCs have been regarded as a cell that is lacking tissue specificity compared with other tissue-specific stem cells such as neural stem cells or intestinal stem cells where these cells progeny will usually develop to become the tissue of residence (Zipori, 2009). The embryonic origin of mesenchyme or MSCs in particular is also unclear. There are different views on the embryonic origin of MSCs with one suggesting that MSCs could be generated through epithelial-mesenchymal transformation (EMT) at different time points in embryogenesis (Hay, 2005; Prindull and Zipori, 2004). Another justified opinion is that an ancestral MSC may already exist in early development and later on give rise to the widely distributed MSCs in the adult body (Zipori, 2005). There were other studies which imply divergent

sources of MSCs including a study which found that MSCs start to appear in Sox1-positive neuroepithelium during embryogenesis instead of mesoderm (Takashima *et al.*, 2007). While this study adds to the puzzle in determining the exact origin of the MSCs, it could explain the potential of MSCs for regenerative therapies, particularly in relation to their axon growth promoting effect in SCI.

1.10.3 MSCs and therapeutic properties for SCI

The application of MSCs in SCI is favoured because they have several advantages as therapeutic agents compared to other type of cells. 1) they are relatively easy to isolate and to expand in culture, up to 50 population doublings in 10 weeks with only subtle potency loss (Jiao *et al.*, 2011); 2) they are able to produce various cell types including neuronal like cells (Kassem, 2004; Alexanian *et al.*, 2008a; Uccelli *et al.*, 2008); 3) they have immunomodulatory properties (Aggarwal and Pittenger, 2005b; Uccelli *et al.*, 2008; Tasso and Pennesi, 2009); 4) they are relatively free from the risk of developing into tumours (Lee *et al.*, 2010) following experimental transplant surgery and 5) they have not yet been found to cause adverse immune responses in both autologous (Pedram *et al.*, 2010) and allogenic transplantation recipients (Jiao *et al.*, 2011). Additionally, their safety in human subjects has been demonstrated following earlier clinical trials involving 15 patients receiving the infusion of the MSCs (Lazarus *et al.*, 1995).

Both autologous and allogenic MSCs have been shown to have positive therapeutic outcome in haematological, cardiovascular, neurological and inherited disease in pre-clinical studies (Le Blanc *et al.*, 2004; Ringden *et al.*, 2006). The first transplantation of MSCs for CNS repair was reported by Chen *et al* in 2000 where cells from bone marrow combined with BDNF were administered into an animal model of middle cerebral artery occlusion and demonstrated some degree of motor recovery (Chen *et al.*, 2000). In the field of SCI research, MSCs from bone marrow are the most widely studied cells and have been tested in rodents, large mammals and primates (Tetzlaff *et al.*, 2011). Furthermore, both human and rodent BM-MSCs have been equally well studied and both demonstrate some degree of functional improvement in many rodent model of SCI (Lee *et al.*, 2007; Abrams *et al.*, 2009; Boido *et al.*, 2012). However

there is a knowledge gap regarding the exact physiological and therapeutic role of transplanted MSCs in SCI and mechanisms through which the transplanted MSCs promote recovery remain elusive.

1.10.3.1 MSCs: survival, proliferation, differentiation and interaction with the host tissues

There are mixed reports on the survival and differentiation ability of MSCs following their transplantation into the injured spinal cord. Some studies have reported a low survival rate of grafted cells (Sheth *et al.*, 2008; Boido *et al.*, 2012; Hofstetter *et al.*, 2002; Zhou *et al.*, 2013) with only 1% of transplanted cells survived at 4 weeks after a 1 week delayed or later transplantation. In one study, delayed transplants were found to improve the cells survival compared with to an acute transplant which resulted in a fewer cells surviving (Hofstetter *et al.*, 2002). This was attributed to encountering a more hostile environment in the injured spinal cord comprising of ischaemia, necrosis and potentially toxic compounds such as oxygen radicals. However, even though less than 1% of MSCs survived after 4 weeks or later, it was suggested that this was adequate to promote functional recovery (Hofstetter *et al*, 2002; Zhou *et al*, 2013).

Despite being controversial, there have been several studies which have reported the ability of transplanted MSCs to differentiate into neuronal lineages (Akiyama *et al.*, 2002; Azizi *et al.*, 1998; Song *et al.*, 2004; Chiba *et al.*, 2009; Kang *et al.*, 2012). In one study, the transplanted MSCs were shown to express different markers for different neuronal lineage phenotypes such as NeuN, CC-1 and GFAP (Kang *et al.*, 2012). However there were other studies which indicate the absence of neural differentiation (Castro *et al.*, 2002; Ankeny *et al.*, 2004; Parr *et al.*, 2008; Sheth *et al.*, 2008; Gu *et al.*, 2010; Zhou *et al.*, 2013) following transplantation of MSCs into SCI. In these later studies recovery of function was seen which was suggested to be due to secretion of neurotrophic factors or neuroprotection.

1.10.3.2 MSCs and remyelination

As previously mentioned, apart from being essential for functional recovery, remyelination has also been found to play a role in protecting axons to further supporting regeneration. MSCs have been reported to promote axonal

remyelination following transplantation into spinal cord injury in rodents (Bizen *et al.*, 2003; Zhang *et al.*, 2012; Liu *et al.*, 2011; Chopp *et al.*, 2000). In one of the earliest experimental studies in the rat spinal cord using the ethidium bromide/X-irradiation demyelination model, transplantation of MSCs from bone marrow were reported to promote extensive remyelination (Bizen *et al.*, 2003). A further study by Liu *et al.* has also revealed an increase in remyelination as demonstrated by the increased expression of MBP, after transplantation of bFGF gene modified MSCs into spinal cord-injured rats (Liu *et al.*, 2011). More importantly the enhancement of the remyelination was consistent with significant axonal regeneration and associated with an improvement in neurological function.

1.10.3.3 MSCs and axonal regeneration

There have been many studies addressing the ability of MSCs to promote axonal regeneration (Hofstetter *et al.*, 2002; Chiba *et al.*, 2009; Sheth *et al.*, 2008; Lu *et al.*, 2005; Sasaki *et al.*, 2009; Zhou *et al.*, 2013; Ankeny *et al.*, 2004; Gu *et al.*, 2010). These have proposed different mechanisms that might underlay the axonal regeneration-promoting abilities of MSCs including production of growth factors and physical guidance of the regenerated axons through the formation of a biological scaffold acting as a regeneration permissive bridge (Hofstetter *et al.*, 2002). In this later study, it was reported that the transplanted MSCs formed bundles which bridged the epicentre of the lesion and the regenerating host neuropil was associated with these MSC aggregates in the bridge. Further work by Ankeny *et al.* supports the notion that transplanted MSCs can serve as a scaffold after partially filling in cysts thus supporting extensive axon growth (Ankeny *et al.*, 2004). In addition, immature astrocytes have been found to populate MSCs bundles which could be another mechanism by which a growth-permissive surface is promoted (Hofstetter *et al.*, 2002). 5-HT-positive nerve fibres have been identified in such MSCs bundles and these have been suggested to contribute to the observed behavioural improvement as the 5-HT-system of the spinal cord has been shown to be important in functional recovery after SCI (Hofstetter *et al.*, 2002; Nygren *et al.*, 1974; Bregman *et al.*, 1993). Chiba *et al.*, 2009 have made remarkable claims of axonal regeneration following BM-MSCs transplantation. This group used anterograde tract tracing and claimed

that the number of fibres of the dorsal corticospinal tract (dSCT) which positively stained for Fluoro-ruby (FR) caudal to the injury site were significantly higher in animals receiving MSCs compared with vehicle-treated animal. They also claimed that some of the GFP positive cells co-localized neuronal markers such as NeuN and MAP2.

A study by Sheth *et al* concluded that the transplanted MSCs are able to promote linear axonal growth, possibly due to the production and secretion of growth factors (Sheth *et al.*, 2008). A recent study comparing the efficacy of using MSCs from human bone marrow and human adipose tissue (Zhou *et al.*, 2013) reported that regeneration was better in animals that received hADSCs with large numbers of NF200 positive fibres and more 5-HT positive fibres. The anatomical findings were further supported by functional improvement and were attributed to increased BDNF levels in the injured spinal cord. It was also demonstrated that there was higher level of BDNF and better functional improvement in animal receiving hADSCs compared with animals receiving hBMSCs. There have been other studies which indicate the role of BDNF as an important mediator of the action of MSCs in promoting axonal regeneration, as well as synapse formation and plasticity (Sasaki *et al.*, 2009; Lu *et al.*, 2005).

1.10.3.4 MSC and anti-inflammatory/immunosuppressive/immune-modulatory properties

The inflammatory response that occurs following SCI has been extensively investigated and the 3 inflammatory mediators *IL-1, il-6* and *TNF-a* are inflammatory mediators commonly upregulated (Hawryluk, 2012). MSCs have been reported by several different groups to possess anti-inflammatory or immunosuppressive properties after being transplanted in injured spinal cord (Wright *et al.*, 2011). These properties are thought to reduce the acute inflammatory process after SCI and thus reduce the cavity formation and decrease astrocyte and microglia/macrophage reactivity (Neuhuber *et al.*, 2005; Himes *et al.*, 2006). Studies have also demonstrated the ability of transplanted MSCs to lessen the chronic inflammatory response in the injured spinal cord (Abrams *et al.*, 2009; Tyndall *et al.*, 2007). One of the possible mechanisms of

their immune modulatory properties is thought to be the upregulation of certain anti-inflammatory factors like *TGF-β1* which has been shown to be dominant over the other pro-inflammatory cytokines (Hawryluk, 2012). In addition, the transplantation of MSCs after SCI has also been shown to modify the inflammatory environment through shifting the macrophage phenotype from M1 (pro-inflammatory) to M2 (anti-inflammatory) as well as sparing the axons and myelin (Nakajima *et al.*, 2012). The immunomodulatory properties of MSCs could therefore create a more favourable environment for regeneration which limits tissue damage and promotes regeneration (Aggarwal and Pittenger, 2005a; Noel *et al.*, 2007).

MSCs have also been shown to possess the ability to target injured spinal cord tissue (Kang *et al.*, 2012a) even when adminstered by intravenous injection. The homing ability of the MSCs to injured tissues depends on the state of both local and systemic inflammation which is under the control of a large range of receptors, tyrosine kinase growth factors and chemokines (Ponte *et al.*, 2007). This particular homing ability is thought to offer the possibility of avoiding the more invasive direction injection approach.

1.10.3.5 MSCs reduce lesion cavity

Different studies using MSCs in SCI report the ability of grafted MSCs to reduce the size of the lesion cavity via reduction of the glial cyst and increased sparing of white matter (Ankeny *et al.*, 2004; Boido *et al.*, 2012; Gu *et al.*, 2010; Ohta *et al.*, 2004). This is suggested to be due to the neuroprotective properties of transplanted MSCs (Ankeny *et al.*, 2004). Boido *et al* suggested that the ability of transplanted MSCs to penetrate into the glial cyst and reduce its volume could enhance axonal regeneration and degrade the nerve-inhibitory molecules at the injury site (Boido *et al.*, 2012). MSCs have also been shown to secrete different matrix components which support nerve regeneration such as laminin, which can contribute to further reduction of the lesion cavity (Wu *et al.*, 2003; Ankeny *et al.*, 2004).

1.10.3.6 MSCs promote angiogenesis

MSCs have been shown to provide support for the reestablishment of blood vessels (da Silva Meirelles *et al.*, 2009; Quertainmont *et al.*, 2012), which is likely to be important to the recovery process following injury. Several pro-angiogenic factors such as bFGF and VEGF have been detected in both conditioned medium from MSCs and around transplanted cells (Kinnaird *et al.*, 2004). Another study demonstrated the ability of MSCs to support the formation of blood vessel-like structures by endothelial cells *in vitro* (Sorell *et al.*, 2009). In the field of SCI, MSC transplantation has been shown to promote angiogenesis evidenced by a significantly enhanced density of vWF positive blood vessels (Zhou *et al.*, 2013). The angiogenic effect of transplanted MSCs in this study was thought to be one of the contributing factors toward recover of motor function.

1.10.3.7 MSCs promote functional recovery

There have been several studies demonstrating the ability of transplanted MSCs to promote different levels of functional recovery in animal models of SCI (Abrams *et al.*, 2009; Osaka *et al.*, 2010; Boido *et al.*, 2012; Alexanian *et al.*, 2011a; Lee *et al.*, 2007; Pal *et al.*, 2010; Kang *et al.*, 2012b). In one study using allogenic hMSCs, Kang *et al.*, showed that transplanted hMSCs promote functional improvement in a completely transected SCI animal assessed behaviourally and electrophysiologically and ascribed the results to neuronal differentiation of the transplanted cells (Kang *et al.*, 2012b). A recent study by Boido *et al* demonstrated improvements in several measurements of behavioural function including general posture, sensory functions and coordination (Boido *et al.*, 2012). In addition, there was also no allodynia-like hypersensitivity in their study, a complication which usually occurs following NSCs transplantation. Boido *et al* hypothesized that the improvement in functional outcome could be attributed to the reduction of the size of the cystic cavity (Boido *et al.*, 2012). However, another study reported that hMSC transplantation after SCI in rats was not sufficient to recover locomotor and bladder function despite evidence of a reduced inflammatory reaction (Park *et al.*, 2010b).

1.10.4 Modification of MSCs for treating SCI

1.10.4.1 Neurotrophic factor secretion:

One of the interesting features of stem cells, including MSCs is that they could be genetically modified to achieve a specific desired therapeutic action. Recent studies have shown that MSCs can be genetically modified to over-express or secrete neurotrophic factors like BDNF and GDNF which can promote better therapeutic effects including promoting cell survival and axonal regeneration. The fact that MSCs have a stable genetic background with exogenous genes which could be easily imported and transported make them suitable for gene therapy and modification (Liu *et al.*, 2011). In a study performed by Sasaki *et al*, the MSCs were genetically modified to secrete brain-derived neurotrophic factors (BDNF). These genetically modified (BDNF-hMSCs) cells were able to survive and demonstrate a better outcome in treating rats with SCI compared with non-genetically modified hMSCs (Sasaki *et al.*, 2009) both functionally and anatomically. In this study, these cells were shown to improve locomotor recovery and showed increased survival of CST neurons in the primary cortex at 5 weeks (Sasaki *et al.*, 2009). The ability of MSCs to secrete neurotrophic factors would be of great advantage as the efficacy of these neurotrophic factors depends on their continuous supply which could be offered by MSCs as opposed to treatment using neurotrophic factors alone which would necessitate periodic injection.

1.10.4.2 Differentiation/transdifferentiation ability:

Recent work also indicates that MSCs could be neurally induced or genetically modified to improve their therapeutic potential (Alexanian *et al.*, 2008b). These neurally-induced modified MSCs could be a potential and better source of cells to replace damaged neurons and glia in injured spinal cord and/or to promote axonal growth of host tissue as compared to naïve MSCs (unmodified MSCs). There have been several studies that have claimed that adult MSCs can differentiate into neurons or neuron-like cells in vitro (Black and Woodbury, 2001; Sanchez-Ramos *et al.*, 2000; Kim *et al.*, 2002; Long *et al.*, 2005) despite the absence of a neural phenotype in their undifferentiated state.

Studies have also reported that undifferentiated mesenchymal stem cells (MSCs) transplanted into the central nervous system (CNS) can survive and differentiate into neurons and glia (Thuret *et al.*, 2006; Phinney and Isakova, 2005; Coutts and Keirstead, 2008) but these findings also remain controversial. There has been a lively debate regarding the ability of MSCs to transdifferentiate into neurons with several studies strongly opposing the idea particularly of *in vivo* transdifferentiation. It is claimed that the appearance of cells with those characteristics is a tissue culture artefact (Phinney and Prockop, 2007) or a result of cell fusion (Terada *et al.*, 2002; Wumser and Gage 2002).

1.10.5 MSCs and clinical trials

The above mentioned properties of MSCs gathered from various clinical studies combined with long standing experience in the treatment of haemato-oncological diseases, has led to the use of MSCs in various clinical trials. The application of MSCs in treating CNS diseases has been progressively expanding and has moved into phase I/II clinical trials (Venkataramana *et al.*, 2010; Forostyak *et al.*, 2013). There are presently more than 200 clinical trials involving human MSCs for several different indications (National Institute of Health, 2013). MSCs have been thought to have a good translational potential into spinal cord injury based on the positive outcome from extensive animal studies (Tetzlaff *et al.*, 2011).

The safety of MSC transplantation in human SCI was demonstrated in one of the earliest clinical trials involving 42 patients in Prague in 2005 (Sykova *et al.*, 2006). The result of this trial also showed significant improvements in 10 patients. Results from other clinical trials are consistent with the idea that the procedure can be safe in both acute and chronic SCI and with some evidence of recovery (Park *et al.*, 2005; Cristante *et al.*, 2009).

1.10.6 Limitations and issues with MSC transplantation in SCI

There are several issues and concerns which need to be carefully addressed by current and future researchers in relation to the use of MSCs in SCI. Little is still known of how exactly the transplanted MSCs lead to functional recovery and how they interact with the host tissues. Despite a few demonstrable therapeutic effects and very few reports of adverse events, there have been large differences in outcomes and the treatment efficacy is yet to be established (Tetzlaff *et al.*, 2011; Harrop *et al.*, 2012; Amano *et al.*, 2009).

There is still limited knowledge on the exact mechanisms regarding how MSCs provide neuroprotection and improve behavioural outcomes as the histological data are highly variable (Tetzlaff *et al.*, 2011). Several studies involving MSCs transplantation in SCI have documented histological observations ranging from good survival of grafted cells, accompanied by a degree of MSCs differentiation into neural cells to poor survival and no convincing evidence to suggest a MSCs differentiation toward neural cells (Tetzlaff et al., 2011).

Additionally, human mesenchymal stem cells (hMSCs) from bone marrow have been reported to be associated with various disadvantages. They have been reported in various studies to be associated with poor proliferation capacity, limited life span and gradual loss of stemness during their expansion *in vitro* (Ringe *et al.*, 2002). Their properties also were shown to correlate negatively with age which implies that BM-MSCs from elderly people could be too inefficient to be used clinically. This is demonstrated by a study which shows that MSCs from old donors exhibited a reduced life span and increased numbers of senescent cells compared with MSCs from young donors (Stenderup *et al.*, 2003). In addition, their isolation requires invasive procedures which are associated with pain and morbidity and may only yield low cell numbers (Huang *et al.*, 2009). Some previous studies have also shown that MSCs derived from SCI donors can be of poor quality which further undermines the option of performing autologous cell transplants using the patient's own bone marrow derived MSCs (Minaire *et al.*, 1984; Wright *et al.*, 2011; Wright *et al.*, 2008; Klein-Nulend *et al.*, 2005; Hill *et al.*, 1991). Because of these limitations an alternate source is considered desirable and hESCs could be an excellent alternative from which to

derive MSCs. This source could circumvent some of the limitations of adult MSCs, while retaining the various therapeutic properties of their adult counterparts.

However, so far there have been no studies done on hESC-MSC transplantation in SCI despite numerous studies in which MSCs have been derived from hESCs. This study is therefore the first to assess the effect of hESC-MSCs transplanted into an animal model of SCI.

1.11 Summary of study aims

The general aims of this study were as follows:

1. The first aim of this thesis was to derive MSCs or mesenchymal like-stem cells from undifferentiated hESCs using a method suitable for generating large numbers of cells for testing in animal models of SCI.

2. The second aim of this thesis was to evaluate the ability of hESC-MSCs to promote the general/supporting therapeutic properties: survival, differentiation and ability to promote axonal regeneration and remyelination in the injured spinal cord using anatomical approaches.

Chapter 2

Derivation and characterization of MSCs from hESC

2 Derivation and characterization of MSCs from hESC

2.1 Introduction

The ease in isolating adult MSCs and their availability in most human tissues (da Silva Meirelles *et al.*, 2006; Mosna *et al.*, 2010) has lead to their frequent use in both basic scientific research and clinical applications. There are presently more than 200 clinical trials involving human MSCs in a variety of different conditions (National Institute of Health, 2013). Results vary but some promising outcomes have been reported. Mesenchymal stem cells (MSCs) are the main non-neural cells that have been extensively investigated in SCI research and are suggested to have translational potential based on various positive results in preclinical research (Tetzlaff *et al.*, 2011). MSCs have been reported to promote functional recovery by different mechanisms, such as axonal remyelination and regeneration, reducing neural inhibitory molecules, reducing the lesion volume and increasing the spared surviving tissues (Hofstetter *et al.*, 2002; Bizen *et al.*, 2003; Sasaki *et al.*, 2009; Gu *et al.*, 2010; Boido *et al.*, 2012). In addition, they are considered to have immunomodulatory effects (Hawryluk, 2012). MSCs derived from bone marrow are so far the most commonly used in the study of SCI with a more limited number of studies on cells derived from other sources such as adipose tissue and human umbilical cord. Apart from being the best characterized MSCs, evidence of safe and successful transplantation of bone marrow derived MSCs in other different diseases has led to them being considered attractive in the field of SCI research.

However, the use of adult MSCs has some limitations that limit their potential for clinical translation. Human mesenchymal stem cells (hMSCs) from adult sources have been reported to be associated with low proliferation, finite life span and gradual loss of stem cell-like properties during their in vitro expansion (Ringe *et al.*, 2002). Like other adult stem cells, the bone marrow derived MSCs (BM-MSCs) have been shown to decline in number and reduce in differentiation capacity as the cells age (Mueller & Glowacki, 2001). In addition, their isolation usually requires an invasive procedure which may be associated with pain and

morbidity and may yield only limited cell numbers (Huang *et al.*, 2009). Some previous studies have also shown that MSCs derived from spinal cord injured donors were of poorer quality than that from non-spinal cord injured donors and this may be a further problem which in particular, may limit autologous transplantation of bone marrow MSCs (Minaire *et al.*, 1984; Hill *et al.*, 1991; Klein-Nulend *et al.*, 2005; Wright *et al.*, 2008; Wright *et al.*, 2011). Because of these various limitations, an alternate source of MSCs could be a considerable advantage for clinical treatments. Derivation of MSCs from hESC is one potential source which might be developed to overcome some of the less desirable characteristics displayed by adult MSCs.

hESC-derived cells potentially offer several advantages over cells derived from adult sources. 1) hESCs avoid the need for harvesting cells from patients or donors using an invasive approach, 2) cells can be prepared from a single cell line with strict uniformity, thus avoiding the large degree of inter-sample variation seen when using primary material from human donors, 3) hESC derived cells show rapid proliferation and grow robustly and so can potentially be prepared on a large scale 4) hESC derived cells offer the potential for an 'off the shelf' product for acute transplantation. In comparison, autologous cells derived from adult tissues will require time for isolation and expansion in culture, 5) cells derived from hESCs could be engineered so that they combine optimal features tailored to the treatment of SCI.

Several different methods have now been successfully used to derive relatively homogenous populations of hESC-MSCs from hESC (Barberi *et al.*, 2005; Olivier *et al.*, 2006; Lian *et al.*, 2007; Trivedi & Hematti, 2008; Lee *et al.*, 2010; Gruenloh *et al.*, 2011; Wu *et al.*, 2013). However, MSCs derived using these methods have never been tested in SCI animal models so that the repair potential of hESC derived MSCs remains to be investigated.

2.2 Aims

The aim of this cell biology part of the study was to derive MSCs from hESCs using methods that could be shown to be reproducible and suitable for generating large numbers of cells for testing in animal models of SCI.

The first aim of this part of the study was to optimize a protocol for deriving MSCs or mesenchymal like-stem cells from undifferentiated hESCs. The starting point for this was a non embryiod body (EB) based protocol previously developed by Olivier *et al.* (2006) and Olivier & Bouhassira (2011). The H1 cell line (Thomson *et al.*, 1998) was chosen as the hESC line for the starting population. This cell line has been extensively studied and characterized by stem cell researchers worldwide and is regarded as one of the gold standard cell lines. This population was grown and maintained under feeder free condition in order to minimize the involvement of animal related products in the protocol. We also aimed to carefully characterize the MSCs–like cells prepared by this method by evaluating their morphology, adherence to a plastic surface, growth profile, surface markers and gene expression profile.

The second aim of this part of the study was to demonstrate the reproducibility of the optimized differentiation protocol through repeated derivation of MSCs from hESCs (i.e. by performing several different runs of differentiation in duplicate).

The third aim was to show that the derived MSCs could be stored in liquid nitrogen and that when later thawed and re-cultured, they would proliferate robustly and maintain similar MSC characteristics to those of cultures examined prior to cryopreservation. In addition, we aimed to show at this stage that the MSCs could be differentiated into bone and fat, as is characteristic of bone marrow MSCs.

2.3 Method and Material

2.3.1 Equipment

Standard laboratory equipment used included: water baths, vortex mixers, centrifuges, refrigerators:-4ºC, 20ºC, -80ºC, -180ºC liquid N_2 tank; tissue culture plastics, sterile and non-sterile glass pipettes, bottles and tubes (Corning Incorporated), flasks and 6-well plates (Corning Incorporated) and beakers; aluminium foil, cling film and plastic wrapping; laboratory digital balance and pH meters.

- Inverted light microscope (Olympus)
- Axiovert 200M fluorescent microscope with Axio Vision software (Carl zeiss)
- BD FACSCalibur™ flow cytometer with BD CellQuest Pro™ software-version (Becton Dickinson (BD) Ltd, Oxford, UK)
- 7300 Real-Time PCR system (Applied Biosystem Ltd, Warrington, UK)
- ND-1000 spectrophotometer with ND-1000 software-version (NanoDrop Technologies, Wilmington, USA)
- 2100 Bioanalyser and Expert 2100 software (Agilent Technologies Ltd, West Lothian, UK)
- Cryo 1ºC “Mr Frosty” freezing container

2.3.2 Cells lines and materials for hESC culture and hESC-MSC derivation and maintenance

- hESC: H1 cell line from Wicell which was grown in feeder free conditions.
- StemPro hESC SFM Growth supplement (Life Technologies)
- High Glucose Dulbeco Modiefied Eagles’s medium(DMEM) with L-Glutamine (Life technologies (Life Technologies)
- DMEM/F12 with L-Gutamine (Life Technologies)
- Bovine serum albumin (BSA) (Life Technologies)

- FGF-basic (Life Technologies)
- 2-mercaptorthanol (Life Technologies)
- Fetal bovine serum (FBS) Hyclone (Thermo Scientific)
- Non essential amino acid (NEAA) (Life Technologies)
- Penicillin and Streptomycin (Life Technologies)
- TrypLE Select (Invitrogen)
- PBS (with Mg2+ and Ca2+) (Life Technologies)
- PBS (without Mg2+ and Ca2+) (Life Technologies)

2.3.3 Media Formulations

2.3.3.1 hESC medium (StemPro hESC SFM complete medium)

Reagent	Amount	Concentration
DMEM/F12 +GlutaMAX (with Sodium Bicarbonate+ Sodium Pyruvate) (1X)	454ml	1X
StemPro® hESC SFM Growth Supplement (50X)	10ml	1X
BSA 25%	36ml	1.8%
FGF-basic (10µg/ml)	400µl	8ng/ml
2-mercaptoethanol (55mM)	909µl	0.1nM

2.3.3.2 MSC medium (D10 medium)

Reagent	Amount	Concentration
D-MEM high glucose, sodium pyruvate and GlutaMAX™	450ml	1X
FBS	50ml	10%
NEAA	5ml	1%
Penicillin+Streptomycin	5ml	1%

2.3.3.3 Adipogenic differentiation medium

Reagent for IBMX method	Amount	Concentration
DMEM/F12 +GlutaMAX (with Sodium Bicarbonate+ Sodium Pyruvate) supplemented with 10% FBS	200ml	1X
Dexamethasone (100µM)	2 ml	1µM
Indomethacin (140mM)	285.6µl	0.2mM
Insulin (10mg/ml)	200µl	10µg/ml
3-isobutyl-1-methylxanthine (500mM)	200µl	0.5mM

Reagent for SWH method	Amount	Concentration
DMEM/F12 +GlutaMAX (with Sodium Bicarbonate+ Sodium Pyruvate)	200ml	1X
Serum Replacer (KoSR)	40ml	20%

2.3.3.4 Osteogenic differentiation medium

Reagent	Amount	Concentration
D10 medium	200ml	1X
Dexamethasone (100µM)	200µl	100nM
Ascorbic acid-2-phosphatase (50mM)	200µl	50µM
B-glycerophosphate (1M)	2ml	10mM

2.3.3.5 MSC cryopreservation medium

Reagent	Amount	Concentration
DMEM/F12 +GlutaMAX (with Sodium Bicarbonate+ Sodium Pyruvate)	30ml	1X
Serum Replacer (KoSR)	10ml	20%
DMSO	10ml	20%

2.3.4 Flow Cytometry Reagents

- FITC-conjugated Mouse IgG1, k Monoclonal Isotype Control (**BD Bioscience, 55748)**
- R-PE-conjugated Mouse IgG1, k Monoclonal isotype Control (**BD Bioscience, 555398)**
- APC- conjugated Mouse IgG1 Monoclonal isotype Control (**BD Bioscience, 555751)**
- APC-Conjugated IgM Monoclonal Antibody (**BD Bioscience, F0117)**
- R-PE conjugated Mouse Anti-Human CD13 Monoclonal Antibody (**E-Bioscience, 12-0138-42)**
- FITC conjugated Mouse Anti-Human CD34 Monoclonal Antibody (**BD Bioscience, 555821)**
- FITC conjugated Mouse Anti-Human CD44 Monoclonal Antibody (**BD Bioscience-555478)**
- R-PE conjugated Mouse Anti-Human CD45 Monoclonal Antibody (**ebioscience, 12-0459**)
- FITC conjugated Mouse Anti-Human CD71 Monoclonal Antibody (**BD Bioscience, 555536)**
- R-PE conjugated Mouse Anti-Human CD73 Monoclonal Antibody (**BD Bioscience, 550257)**
- R-PE conjugated Mouse Anti-Human CD90 Monoclonal Antibody **(R&D system, 17-1057)**
- FITC conjugated Mouse Anti-Human CD106 Monoclonal Antibody (**BD Bioscience, 551146)**
- R-PE conjugated Mouse Anti-Human CD166 Monoclonal Antibody (**BD Bioscience, 559263)**
- R-PE conjugated Mouse Anti-Human CD271 Monoclonal Antibody (**BD Bioscience, 557196)**
- Purified Mouse Monoclonal IgM Clone STRO-1(anti-hSTRO-1) (**R&D system, MAB1038**)

2.3.5 MSC Differentiation Reagents and staining

- Dexamethasone (Sigma)
- Indomethacin (Sigma)
- Insulin (Sigma)
- 3-isobutyl-1-methylxanthine (Sigma)
- Knockout serum Replacer (KoSR) (Life Technologies)
- Ascorbic acid-2-phosphatase (Sigma)
- B-Glycerophosphate (Sigma)
- Alizarin Red S (Sigma)
- Oil Red O (Sigma)

2.3.6 Senescence Study

Senescence ß-Galactosidase Staining Kit: Fixative, Staining Solution, Solution A, Solution B, X-Gal (Cell Signalling TECHNOLOGY®, 9860)

2.3.7 Quantitative Real Time PCR

PCR Mastermix (Life Technologies)

Target primer/probe (Life Technologies):

Gene	Gene Name	Assay ID	Group
Oct-04	POU5F1	Hs04195369_s1	Class 5 homeobox 1
Nanog	Nanog homeobox	Hs02387400_g1	Homeobox transcription factor
T(Brachury)	Brachury	Hs00610080_m1	T-boxes
GSC	Gooseecoid homeobox	Hs00418279_m1	
Twist1	Twist homolog 1	Hs00361186_m1	Basic helix-loop-helix transcription factor
COL1A1	Collagen, type 1, alpha 1	Hs00164004_m1	Extracellular matrix structural protein
CD105	endoglin	Hs00923996_m1	Signalling molecule
CD31	endothelial cell adhesion	Hs00169777_m1	Cell adhesion molecule
CD45	Protein tyrosine phosphatise	Hs00236304_m1	receptor type C

2.3.8 Chemical

- Glycerol (Sigma)
- Isopropanol (Fisher Chemical)
- B-Mercaptoethanol (Life Technologies)
- Dimethyl sulfoxide (DMSO) (Sigma)
- Formalin solution (37% Formaldehyde)

2.3.9 Software

- Graphpad Prism® 4 for basic biostastistics and graphing
- BD FACSDiva version 6.1.3 for Flow Cytometry data analysis

2.3.10 hESC culture

The original Wisconsin hESC line H1 (Thomson *et al.*, 1998) was used as a starting population in all 20 different runs of the differentiation protocol. The hESCs were grown on murine embryonic fibroblast (MEF) cells when originally acquired. From passage 28 they were switched to feeder free conditions in which they were cultured on 6 well plates pre-coated with extracellular matrix (ECM; CellStart, Life Technologies) in StemPro hESC HFM media. The cells were passaged a further 10 to 20 times in feeder free conditions, in order to ensure the absence of MEF cells, before being used as a starting population for differentiation into MSCs. During this time the hESCs were fed daily with StemPro hESC HFM media until they attained confluency. When about 90% confluent the cells were mechanically detached using Stempro EZPassage disposable passage tool (Invitrogen) and vigorously pipetted in order to dissociate remaining cell clumps. The dissociated cells were then re-plated, cells from each well being split among 6 wells for maintenance and further expansion. All of the above cultures were maintained in an incubator at 37ºC and 5% CO_2.

2.3.11 Differentiation of hESCs to MSCs.

A concise diagram showing the differentiation protocol used is shown in figure 2-2 and the detail work flow is illustrated in figure 2-3. For each run of differentiation, 2 confluent wells of hESCs were selected from a 6 well-plate and used as the starting population for the differentiation. One of the 2 wells was labelled sample A and the other sample B. and a third well of cells was taken for RNA extraction in order to perform analysis using qRT PCR. The RNA extracted from this well was used to obtain data for day 0 of the differentiation protocol. The duplicate cell samples (A and B) selected for differentiation were mechanically detached from these wells (as described above in 2.3.10) and dissociated by pipetting vigorously. Cells from each well were divided into 4 equal portions. Each portion was transferred into a T25 flask to give 4 flasks each of sample A and sample B. The cells were then kept at 37ºC and 7.5% CO_2 incubator for approximately 28 days in D10 (DMEM+FBS 10%+NEAA+P/S) medium. The medium was changed every 7 days. After 28 days, the cells were dissociated

by adding TrypLE Select to the flasks and incubating for 2-4 hours. Subsequently, cells from one of the 4 flasks containing sample A and one of the 4 flasks containing sample B were re-plated into T25 flasks (usually 2). One flask from each of the replicates (A and B) was used for RNA extraction at day 5, day 10 and day 28 (see 2.3.15.4). However, qRT PCR analysis was subsequently performed only on the day 28 sample (i.e. corresponding to completion of the differentiation protocol.

2.3.12 Maintenance and expansion of hESC-MSCs

The MSC-like cells derived from the 28 day differentiation protocol were initially plated in 2 T25-cm2 flasks in D10 media and this was designated passage 0. Once they had attained 90% confluency (usually after 5-10 days in culture), the cells were again dissociated by adding 2ml of TrypLE Select and returning the flask to the incubator for 5 minutes and then replated at a density of $1X10^4$ cells/cm^2 in T25-cm^2 flask. They were maintained D10 (DMEM+FBS+NEAA+P/S) at 37ºC and 5% CO_2. This was designated passage 1. The flasks were observed daily under a light microscope and passaged when they attained 90% confluency, typically every 3 to 4 days. The cells were usually maintained in T25-cm^2 flasks except at passage 3, when T75-cm^2 flasks were used to obtain the larger numbers of cells required for characterization and to provide a stock of cells for cryopreservation (flow cytometry, qRT-PCR, see below). The media was changed every 2 -3 days with pre-warmed media (5 ml for T25-cm^2 flask, 12-15ml for T75-cm^2 flasks).

2.3.13 Cell counting and viability

At the end of every passage, a cell count was manually performed using a haemocytometer (Hawksley BS.748 improved Neubauer counting chamber). About 10µl of cell suspension which had been trypsinized and dissociated was collected and mixed with 10µl of Trypan Blue. The cells were then transferred to the haemocytometer and counted under an inverted phase contrast light microscope at X10 magnification. Viable cells were distinguished from non-viable cells by their bright appearance while non-viable cells stained blue. Viable cells were counted on 4 outer large squares and averaged. The volume within each

large square is 0.1mm^3 (each large square is 1mm X 1mm and the area between the slide and the coverslip is 0.1mm so the volume is 0.1mm^3). This gives an averaged cell count in a volume of 0.1mm^3. To obtain the number of cells in 1 ml, this value was multiplied by 10,000. This value was then multiplied by 2 to account for the dilution with the Trypan Blue solution. In summary, the total number of viable cells in 1 ml in this study was calculated using the formula: Average cells counted from 4 large square X 10,000 X 2 (dilution factor).

2.3.14 Cryopreservation protocol for hESC-MSCs

4-6 vials of hESC-MSCs from each different run (2-3 vials each of the A and B samples) were cryopreserved at passage 3. Cells were detached and re-suspended in MSC media at 2 X 10^6 cells per ml. An equal volume of freezing media was then added so that the final concentration of DMSO was 10%. After mixing, the 1 ml of cell suspension was transferred to a CryoTube™ and placed in a "Mr Frosty". These were stored overnight at -80ºC and subsequently transferred into a liquid nitrogen tank for long term storage.

2.3.15 Characterization of hESC-MSCs

The derived MSC-like cells were characterized using several of the standard approaches described in the literature (Olivier *et al.*, 2006; Chamberlain *et al.*, 2007; Uccelli *et al.*, 2008).

2.3.15.1 Morphology and adherence ability

Following the differentiation protocol, the cells were regularly checked under a phase contrast microscopy for the appearance of a spindle like and elongated morphology indicative of healthy cells of a mesenchymal lineage. The morphology of the cells was more carefully examined at passage 1 and passage 3 and images collected in order to compare the morphology with the classical appearance reported for MSCs.

2.3.15.2 Growth profiles

To analyse the growth profile of our hESC-MSCs, they were passaged each time they attained 90-100% confluency. At each passage they were re-plated at the

same initial density (1 x10^5 per cm^2) and at the end of each passage the cells were counted. These counts were used to calculate cumulative cell numbers. The cumulative cells numbers is a predicted cell doubling over a set period of time and was calculated by multiplying the end number of cells with the amplification fold of each passage. The growth profile was then determined from the cumulative growth chart which was established by series of cumulative cells numbers of each passage.

The growth profiles were further analysed by calculating the population doubling time using the online calculator: Roth V. 2006 <http://www.doubling-time.com/compute.php>

2.3.15.3 Flow cytometry analysis (surface marker expression)

This is a technique that uses detection of fluorescence to detect cell surface markers and thereby provide quantitative information on the combinations of markers and numbers of cells that express them. The first stage is to select the viable cell population. The equipment provides a plot in which each cell is represented by a dot. The position on the y axis is determined by cellular granularity and is referred to as side scatter (SSC). The position on the x axis is determined by cell size and referred to as forward scatter (FSC). The distribution of the cells on this scatter plot can be inspected and a gate placed around the main population of cells, excluding debris and dead cells that are usually seen in the lower left corner of the plot (Figure 2.1-A). The cells within the gate are those included in further analysis.

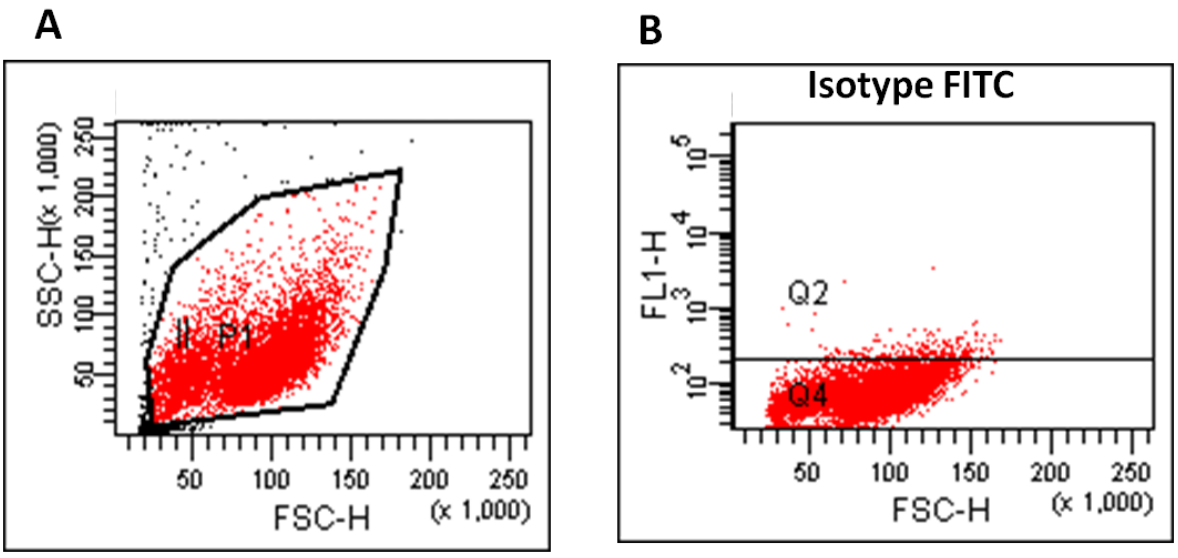

Figure 2-1.Example dot plots with gated population (A) and isotype control (B).

The red dots in plot A indicate viable cells to be included in the analysis. The red dots in graph B represent the isotype controls (including autofluorescence and non-specific background staining) which were placed in the first log. (SSC: side scatter intensity value which is proportional to flouresecent intensity; FSC: forward scatter which is proportional to the diameter of the cell).

The cells were then analysed by generating log scale dot plots for different combinations of surface markers included in the analysis. Initially, isotype controls were used to determine auto-fluorescence and other non-specific background staining and the cell population were positioned within the first log of the axis (Figure 2.1-B). In addition, positive controls were used to compensate for the overlapping emission spectra of different fluorochromes. Once the optimal compensation was achieved, the test cells were run and ten thousand gated events were collected for each different cell sample. All flow cytometry analysis in this study was performed on a BD FACSCalibur™.

A series of markers which have consistently been reported to be expressed by adult MSCs and other markers which are usually negative in MSCs populations were used to characterize our derived MSCs. The flow cytometry was performed at passage 1 and passage 3.

2.3.15.3.1 Preparation of cells for flow cytometry

Passaged cells were dissociated and re-suspended in DPBS+SR 5% at 1 X 10^6 cells per ml. Then, 100µl of the cell suspension was added to eppendorf tubes and mixed with different combinations of antibodies (1µl of each). The tubes were left for about 30 minutes in the dark environment at 4ºC. They were then

washed and subjected to 2 cycles of centrifugation and resuspension before finally being transferred into FACS tubes and loaded one by one in the FACSCalibur machine. The following antibodies were used:

Tube no.	FITC	Vol(µl)	PE	Vol(µl)	APC	Vol(µl)
1	IgG1	1	IgG1	1	IgG1	1
2	CD44	1	CD271	1		
3			CD73	1	CD105	1
4	HLA-ABC	1	CD13	1		
5	CD71	1	CD166	1		
6	CD106	1	CD90	1		
7	CD34	1	CD45	1		
8	Stro1 (unconjugated)	1			Goat antimouse Ig	1

Table 2-1-List of different antibody combinations used in flow cytometry

2.3.15.4 Quantitative real time-PCR (gene expression)

qRT-PCR was performed on samples obtained at 3 time points: 1) at the beginning of the differentiation protocol i.e undifferentiated hESCs which extracted on day 0; 2) on completion of the differentiation protocol i.e day 28 and 3) when the cells had acquired a homogenous mesenchymal-like morphology (i.e. at passage 3). This analysis was performed as part of the characterization process to compare the properties of hESC-MSCs with those of undifferentiated hESCs, as well as to analyze gene expression levels at different time points in the protocol. The mRNA expression level of different groups of genes typical of pluripotent stem cells, early mesodermal/epithelial-mesenchymal cells, MSCs and genes not expected to be present were quantified. The selected genes for pluripotency were *Nanog* and *Oct4* (Bhattacharya *et al.*, 2004; Hyslop *et al.*, 2005; Cai *et al.*, 2006; Adewumi *et al.*, 2007; Mountford, 2008) while *COL1A1* and *CD105* were selected to re-present genes highly expressed in adult MSCs (Silva *et al.*, 2003; Barry & Murphy, 2004; de Peppo *et al.*, 2010; Menicanin *et al.*, 2010). *Twist1* was chosen as an MSC/epithelial-mesenchymal transducing marker (Cakouros *et al.*, 2010) while *Brachury* (T) and *Goosecoid(GSC)* (Lee *et al.*, 2010) were selected for an early mesodermal lineage. Finally, *CD45* and *CD31* were selected as markers which should not be expressed in MSCs.

2.3.15.4.1 RNA extraction

Total RNA was extracted from cells using the Qiagen RNeasy mini kit according to manufacturers instructions. Cells were lysed directly in the flask by adding 700µl of RLT buffer to approximately 80% confluent T25 flasks. The lysates were then either directly processed or stored at -80ºC to be used later. Lysates were then homogenised by putting them through QIAshredder spin columns placed in a Heraeus BIOFUGE pico for 2 minutes at 13000 rpm. An equal volume of 70% ethanol was then added to the RNA and the sample was subsequently passed through an RNAeasy spin column for 15 seconds at 11000 rpm. The RNAeasy spin column contains a membrane that binds the RNA. Following this, 700µl RW1 buffer was added into the membrane bound RNA and spun for 15 second at 11000 rpm. The RNA was then washed twice with 500µl RPE buffer by spinning for 15 seconds at 11000 rpm for the first wash and 2 minutes at 11000 rpm for the second. Finally the RNA was eluted with 20-40µl of RNase free water passed through the spin column at 11000 rpm for 1 minute. The eluate was either immediately processed or frozen at -80ºC.

2.3.15.4.2 DNase treatment

Removing the contaminating DNA was done using the Ambion Turbo DNA free kit. 2µl buffer, 12µl water and 1µl DNase were added to 5µl RNA eluate and this mixture were incubated for 30 minutes at 37ºC. Following that, the mixture were briefly centrifuged and another 1 µl DNase added for another 30 minutes incubation at 37ºC. After that, 2µl stop solution was added to the samples and were placed at room temperature for 2 minutes. Samples were then centrifuged for 5 minutes at 11000 rpm. Subsequently, the supernatant which contains the DNased RNA was transferred into a new eppendorf and could either be processed to become cDNA or stored at -80ºC.

2.3.15.4.3 RNA quality control

RNA concentration and quality was assessed using the Nanodrop and Agilent®2100 bioanalyser respectively.

2.3.15.4.4 Nanodrop ND-1000 Spectrophotometer

The nanodrop measures RNA concentrations over a range of 2-3000ng per µl. The instrument automatically calculates the RNA concentration and absorbance. The instrument was calibrated with a blank (using RNAse free water) followed by 1.5µl of RNA sample. The absorbance spectrum ($OD_{260:280}$ ratio) and RNA

concentrations were measured and displayed. An absorbance between 2.0 and 2.2 was regarded as a measure of acceptable quantity of RNA to be used for further processing in this project.

2.3.15.4.5 Agilent 2100 Bio-analyser

The integrity of the RNA was assessed using an Agilent 2100 Bio-analyser and RNA 6000 LabChip™. The RNA is electrophoretically separated in the LabChip using strategically located electrodes. 1µl of DNased RNA sample per well is required for analysis of each different sample. The RNA components are detected by fluorescence and translated into virtual images, sized and quantified in relation to internal standards. The software will then analyse and generate an RNA integrity number (RIN). RIN values of more than 7 are regarded as indicating RNA of high quality.

2.3.15.4.6 cDNA synthesis

cDNA synthesis was performed by adding 10µl of DNase treated RNA into a reaction consisting of 1µ of 10mM dNTPs and 1µl of random hexamers(300ng/µl). The samples were then heated to 65ºC for 5 minutes followed chilling on ice and brief centrifugation. A mixture of 4µl of buffer, 2µl DTT and 1µ RNaseOUT were then added into the samples, which were then left at room temperature for 2 minutes. Finally, 1µl of superscript II (Invitrogen) was added to the samples before they were exposed to a temperature cycle of 25ºC for 10 minutes, 42ºC for 50 minutes and 70ºC for the remaining 15 minutes. The samples were either used immediately for analysis or frozen at -80ºC.

2.3.15.4.7 TaqMan qRT-PCR transcript analysis

TaqMan based qRT-PCR is an efficient and reproducible method of analysing gene expression. It uses small sequence specific probes for genes of interest that have a reporter fluorophore at the 5’ end and a quencher molecule at the 3’ end. If the target sequence is present during the amplification process, the probes anneal and the quencher is then cleaved by the enzyme Taq polymerase, functioning in the 5’ to 3’ direction. The cleavage of the quencher molecule allows the detection of the reported fluorophore. The signal intensity increases after every successful amplification cycle. The fluorescence signal can be normalised to a housekeeping gene expression levels of which are not affected by the procedures used to quantify the genes of interest. The housekeeper gene GAPDH was used throughout the procedure. Samples were prepared for analysis

by adding 5µl of a 1 in 64 dilution of cDNA into a reaction consisting of 2.2µl water, 7.5µl 2X Master Mix(Invitrogen) and 0.3µl primer. The reactions were performed in Optical 96-well Reaction plates with technical and biological replicates.

Data is analysed by comparing the cycle threshold (C_t) for each targeted probe to that of a housekeeper gene. C_t is measured as the reporter dye emission intensity rises above that of the background level which occurs during the exponential phase of the PCR. The C_t values are used to calculate ΔCt which is the difference between the target gene C_t and the housekeeper C_t. The mean ΔCt between technical replicates is calculated and used to calculate the expression value using the formula: $2^{\Delta Ct} \times 1000$. The expression values were plotted on graphs to illustrate the expression levels of the tested genes in different samples.

2.3.16 Senescence staining of hESC-MSCs

Senescence associated ß-galactosidase (SA ß-Gal) activity is a useful biomarker for detection of senescent cells in culture (Itahana *et al.*, 2007). SA ß-Gal is a lysosomal protein found predominantly in active fibroblasts and MSCs (Dimri *et al.*, 1995; Wagner *et al.*, 2008). It is the most widely used biomarker for senescent and aging cells because it is easily and rapidly detected. SA ß-Gal activity at pH 6 is regarded as indicative of senescent cells (Itahana *et al.*, 2007). The Senescent ß-Galactosidase Staining Kit (Cell Signalling) was used in this study according to the manufacturers instructions.

Passaged hESC-MSCs were re-plated at 2-5 X 10^4 cells in 35-mm dishes (6 well plate) and were cultured for 1-3 days. The media was then removed and the cells washed with D-PBS once and then fixed with 1X fixative solution for 10-15 minutes at room temperature. While waiting for the incubation, ß-Galactosidase staining solution was prepared. For each well of cells, a mixture containing 930µl 1X staining solution, 10µl Staining Supplement A, 10µl Staining Supplement B and 50µl 20mg/ml X-gal in DMF was prepared. The final pH of this solution has to be between 5.9-6.1. After removing the fixatives, the cells were rinsed twice with D-PBS and 1 ml of ß-Galactosidase staining solution was added to each well. The cells were incubated overnight in a dry incubator (no CO_2) at 37ºC. A blue

colour could be detected within 2 hours but was usually maximal in 12-16 hours. Blue cells representing senescent cells were viewed under an inverted light microscope at 10X magnification. For analysis purposes, at least 100 cells in 4 random fields were counted and the percentage of β-Galactosidase positive cells were calculated through the formula: (Total of positive cells/ Total cells) X 100

2.4 Expansion and preparation of cells for transplantation

2.4.1 Protocol for thawing hESC-MSCs

Cells were usually thawed approximately 3 weeks before they were required for transplantation. A cryotube containing around 1 X 10^6 cells was taken out of liquid nitrogen and placed in a water bath at 37ºC. Once most of the cells had thawed, the outside of the tube was disinfected with 70% ethanol and the cells were carefully transferred into a 15ml falcon tube followed by drop wise addition of 10ml of culture medium over 5 minutes to dilute residual DMSO. They were then centrifuged at 1200 rpm for 3 minutes to pellet the cells. Following that, the supernatant was discarded and the cells were resuspended in culture medium and divided equally between 2 T25 corning flasks. They were regarded as passage 3+1 at this point. They were kept in an incubator at 37ºC and 5% CO_2 and were repeatedly expanded, up to passage 3+5 to achieve the required number of cells for transplantation and re-characterisation.

2.4.2 Re-expansion of hESC-MSCs

After initial plating at passage 3+1 (see above), the cells were passaged each time they attained 80-90 % confluency. From this point onward (P3+2), cell numbers were carefully calculated at each passage in and a lower initial cell density (between 3500 and 4000 cells/cm^2) was used compared to that used prior to cryopreservation in order to maximise the proliferation capacity of the cells. The cells were passaged when approximately 80-90% confluent until passage 3+5. They were then prepared for transplantation. The growth profile of the cells was evaluated throughout this expansion process to compare it with the growth profile prior to cryopreservation.

2.4.3 GFP Labelling of hESC-MSCs

At 24 hours after the first passage i.e P3+2, the cells were infected with lentivirus expressing a gene that encodes the green fluorescent protein (GFP) to allow *in vivo* tracking after transplantation. In this study, three different lentiviruses were used at different stages of the study: 1) a Lentivirus donated by Dr George Smith from University of Kentucky, Titre: 5.72 X 10^8 IFU/ml), 2) GFP (Bsd) AMSBIO lentivirus (AMSBIO, LVP001, Titre: 1 X 10^8 IFU/ml) and 3) Null GFP lentivirus (was prepared by John McCabney in the Mountford Lab, using cDNA from Clontech, 631982, and 3rd generation lentivirus production plasmids, Titre: 8X10^8 IFU/ml). The virus infection was performed at a MOI (Multiplicity of Infection) of 50 for viruses 1 and 2 and a MOI of 20 for the third. The MOI was decided based on prior testing using 4 different MOIs: 10, 20, 50 and 100. The lowest MOI that resulted in 70-100% was chosen for the study i.e. to infect cells to be transplanted. The amount of virus (IFU=infectious units) needed to achieve the desired MOI was calculated by multiplying the number of cells to be infected by the desired MOI. The volume of virus required was then calculated by dividing the original titre of virus (available IFU in set volume) with the amount of virus needed (IFU needed). In this study, the infection was performed on approximately 130,000 cells in 2.5 ml D10 media in T25-cm2 flask. Another 2.5 ml of new media was added on the next day without removing the old media. The cultures were kept for 72 hours and then were dissociated for further expansion. The infection efficiency was checked by examining the presence of GFP positive cells using both fluorescent microscopy and flow cytometry.

2.4.4 Re-characterization of hESC-MSCs

At passage 3+5 cells were re-characterized using the same methods as was used to characterise the cells prior to the cryopreservation. These include 1) morphology and adherence to plastic (2.3.15.1), 2) growth kinetics/profile (2.3.15.2), 3) surface marker expression (2.3.15.3), 4) gene expression (2.3.15.4). This was done in order to confirm that the process of cryopreservation, thawing and repeated expansion did not affect their MSC-like properties (see above).

2.4.5 Functional differentiation into adipocytes and osteoblasts

Since the ability to form osteoblast and adipocytes is considered a characteristic of MSCs, the cultures prepared after cryopreservation were tested for this ability at P3+5, corresponding to the day of transplantation. This was performed using cells which were not infected with GFP lentivirus.

2.4.5.1 Adipogenic differentiation

Cells were re-suspended in D10 media and seeded at approximately 2.0 x 10^4 cells/cm^2 (about 2.0 x 10^5 cells/well of 6 well plate). One well of cells was prepared for differentiation and another prepared as a control. The cells were incubated until they were 90-100% confluent. They were then exposed to the differentiation medium while the control cells were kept in D10 media for 21 days and the media were replaced twice a week. Two different methods of adipogenic differentiation were used. The first, a commonly used method, used D10 medium supplemented with 1µM Dexamethasone, 0.2 mM Indomethacin, 10µg/ml insulin and 0.5mM 3-osobutyl-1-methyl-xanthine (Pittenger *et al.*, 1999; Sekiya *et al.*, 2004). The other, a serum withdrawal hypoxia method (SWH), used DMEM/F12 supplemented with knock out 10% serum replacer (KoSR) and incubation in partially hypoxic conditions (5% oxygen) (Olivier *et al.*, 2006). Both methods lasted for 21 days and cells were regularly observed for the appearance of lipid vacuoles in the cytoplasm. After 21 days, the media was aspirated and the cells were washed three times with D-PBS. The cells were then fixed by adding 0.5ml 10% formalin to each well and kept at room temperature for 1-2 hours. The cells were again washed 3 times with D-PBS followed by one wash with 70% ethanol. Afterwards, cells were stained with fresh Oil Red-O staining solution by adding 1ml of staining solution to each well. After approximately 15 minutes, the cells were further washed several times with 70% ethanol to clear excess dye and were covered with water to be viewed under the microscope.

2.4.5.2 Osteogenic differentiation

Cells were re-suspended in D10 media and seeded in 2 wells at 4 X 10^3 cells/ cm^2 (about 4 X 10^4 cells/well of 6 well plate). One well was used for differentiation and the other for control and tested when about 70% confluent. Cells for

differentiation were placed in D10 medium supplemented with 100 nM Dexamethasone, 50 µM Ascorbic Acid-2-phosphatase, and 10 mM ß-glycerophosphate (Colter *et al.*, 2001). The control cells were placed in D10 media. Both groups of cells were incubated at 37ºC in 5% CO_2 for 21 days. Media was replaced every 3-4 days and the cells were regularly inspected for increasing granularity in the cytoplasm. Upon 21 days, the media was aspirated and discarded. Each well of cells was washed 3 times with 0.5ml of D-PBS followed by fixation with ice cold 70% ethanol for about 1 hour. The cells were then washed 3 times and stained with 1 ml of 40mM Alizarin Red for 10 minutes. Finally the cells were again washed 2-3 times before being viewed under a light microscope.

2.5 Statistical analyses

When appropriate, numerical data is presented as mean ± standard error of the mean (SEM). Comparisons involving 2 groups were performed using Student's paired t-test and comparisons between multiple groups by one-way ANOVA. The statistical analysis was performed using GraphPad Prism software.

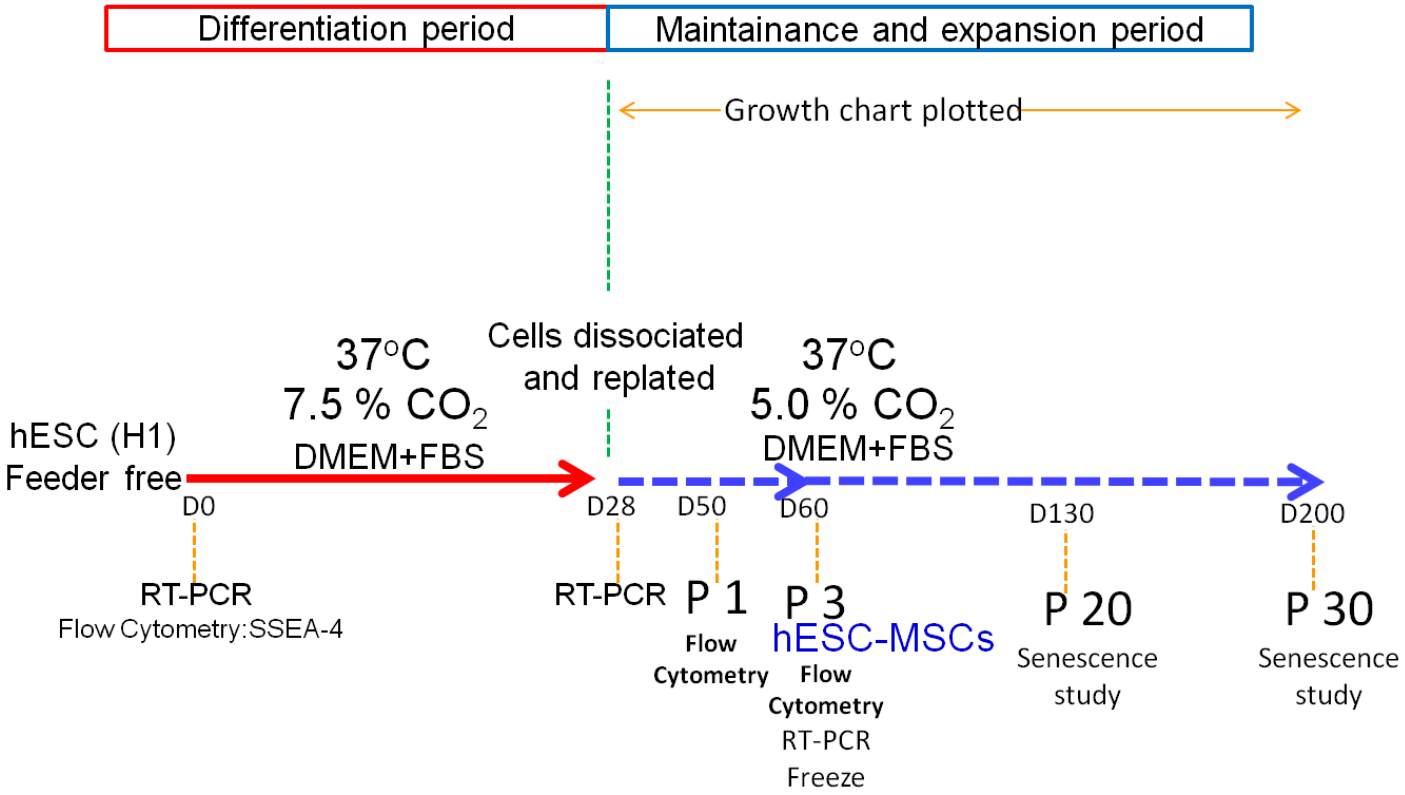

Figure 2-2. Diagram illustrating the optimized differentiation protocol and expansion protocol.

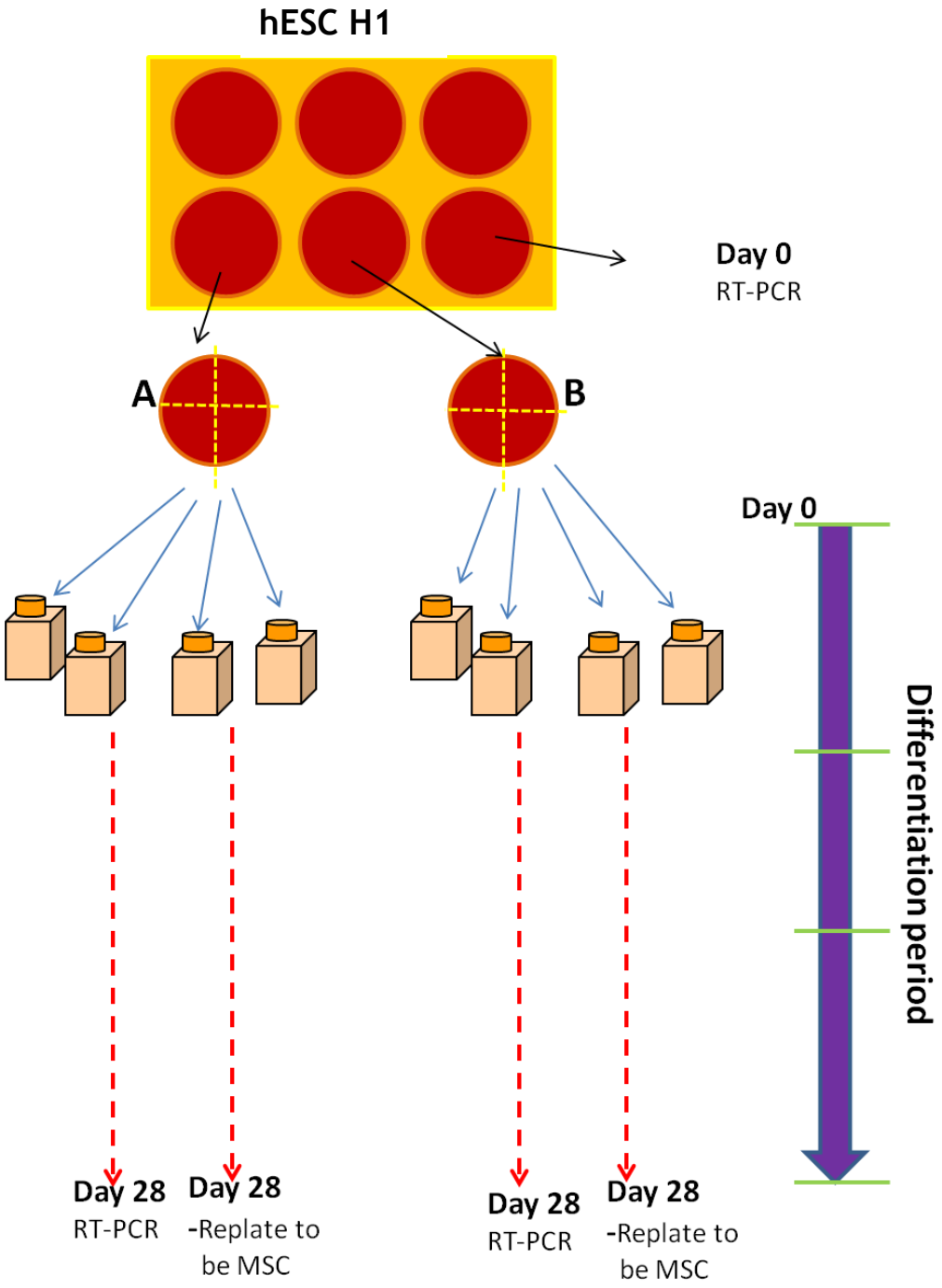

Figure 2-3. Detailed work flow for differentiation protocol (hESC to MSCs).

The dissociated H1 cells from the A and B wells were divided into 4 aliquots and each aliquot (a quarter well of cells) were switched to D10 media in new T25 flask. They were kept for 28 days in an acidic environment and then again dissociated and re-plated in D10 at 37ºC and 5% CO_2 during which they differentiate towards MSCs. RNA extraction was performed on day 0 (from one well of H1 cells) and from day 28 (from both samples A and B).

2.6 Results

2.6.1 SSEA-4 expression in hESCs (starting population)

In order to prove the effectiveness, consistency and reproducibility of the method for differentiation of hESCs into MSC-like cells, 20 independent runs of the protocol were performed and each run was performed in duplicate (labelled as A and B). Each run began with dissociation of the hESCs starting population and ended on day 28 of the differentiation protocol (Figure 2-2 and Figure 2-3). Each different run was performed in duplicates where 2 different replicates of the process were performed in parallel on the same cells which were divided into two samples: sample A and sample B. The starting populations of hESCs (Figure 2-5) were tested for the presence of SSEA-4, a marker for pluripotency, prior to the initiation of the differentiation protocol. All the starting populations were shown to be approximately 80-90% SSEA-4 positive (Figure 2-4).

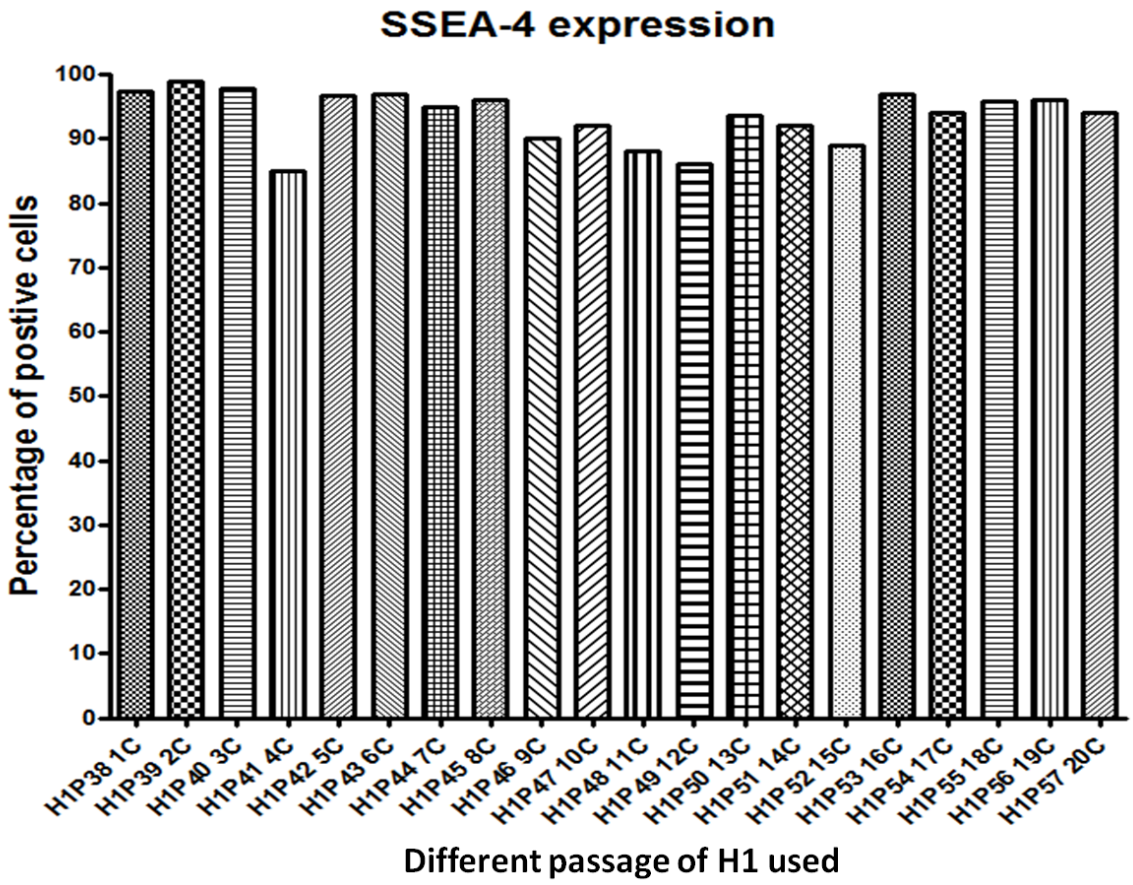

Figure 2-4. SSEA-4 expression in each population of H1 cells used as a starting population for the 20 differentiation runs.

The bar graph shows the consistently high percentage of cells stained for SSEA-4 in all starting populations used. hESCs ranging from passage 38 to passage 57 were used in different runs.

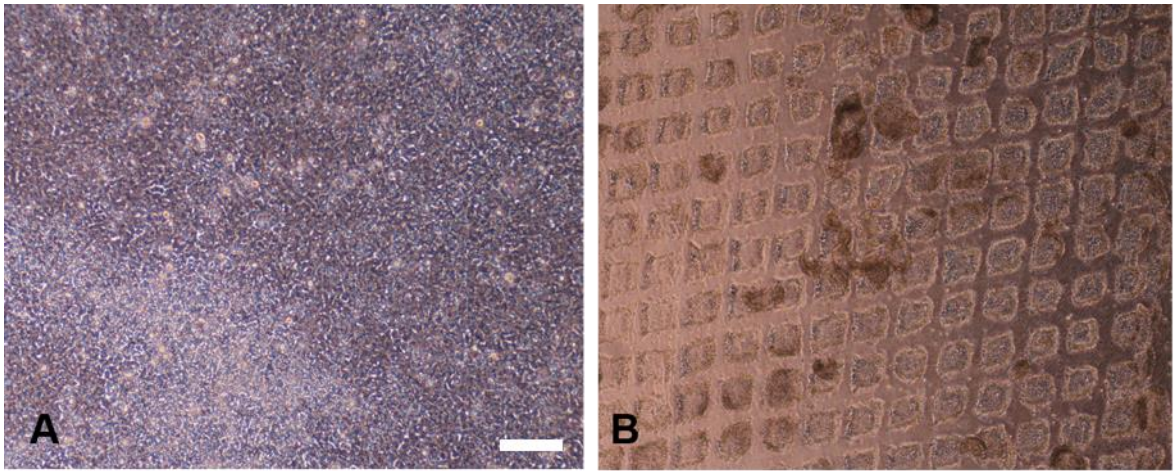

Figure 2-5. Images of hESC:

Image A shows an example of confluent undifferentiated H1 hESCs which were used as the starting population for the differentiation protocol. Image B shows hESCs that have been mechanically cut with the easytool in order to facilitate dissociation of the cells. (X10 magnification, both images, scale bar=100µm and applicable to both panels).

2.6.2 Successful runs of differentiation

A full list of the 20 differentiation runs performed is shown in table 2-2. Out of these, 12 runs were considered successful based on the following criteria: 1) cells of both replicates A and B demonstrated relatively similar morphology and grew almost equally robustly 2) the cells produced displayed the main surface markers considered characteristic for MSCs and 3) the cells produced exhibited a gene expression pattern consistent with that expected for MSCs. The other runs which did not fulfill these criteria were not included further in the study even though in some cases the cells had a morphology suggestive of MSCs. The cells from run 2C, 14C, 17C and 18C were excluded due to fungal contamination while cells from run 6C, 8C, 10C and 11C were excluded because the rate of growth of replicate A and B were significantly different.

Run	Included in the study
1C	√
2C	×
3C	√
4C	√
5C	√
6C	×
7C	√
8C	×
9C	√
10C	×
11C	×
12C	√
13C	√
14C	×
15C	√
16C	√
17C	×
18C	×
19C	√
20C	√

Table 2-2. List of 20 runs of differentiation performed and those selected for further study. Each run was coded from 1C to 20C. A tick indicates those runs selected for further study.

2.6.3 Morphology and ability to adhere to a plastic surface

The cell morphology was regularly checked and evaluated from the beginning of each differentiation protocol to gain an appreciation of the morphological change associated with differentiation from hESCs (Figure 2-5) into MSC-like cells. In all 12 successful runs, the cells display a mono-layered elongated

looking morphology (Figure 2-6) at the end of the differentiation period i.e. by day 28. At passage 1 (i.e. around day 40-45), the cells show a heterogeneous spindle shaped morphology which is characteristic of MSCs (Figure 2-7). At passage 3 (Figure 2-8), the cells have a similar appearance to passage 1.

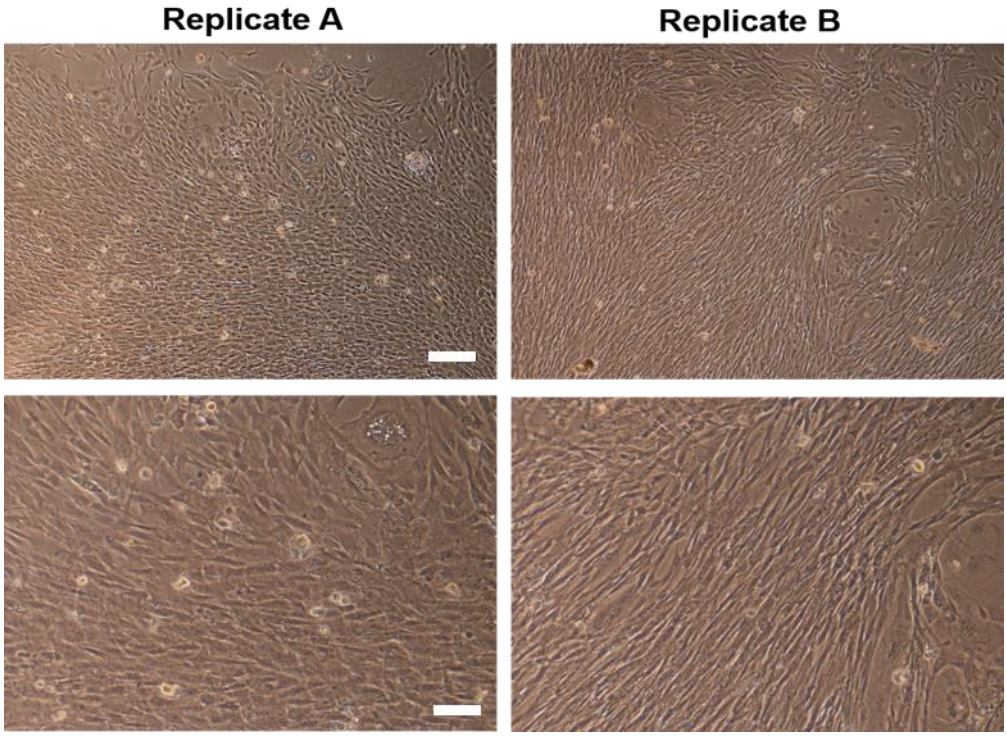

Figure 2-6. Morphology of cells at the end of the differentiation protocol (day 28):

Representative image from 2 replicates of run 1C. The images show a monolayer of elongated looking cells (Upper panel magnification: X4, scale bar=40µm; lower panel: X10, scale bar=100µm)

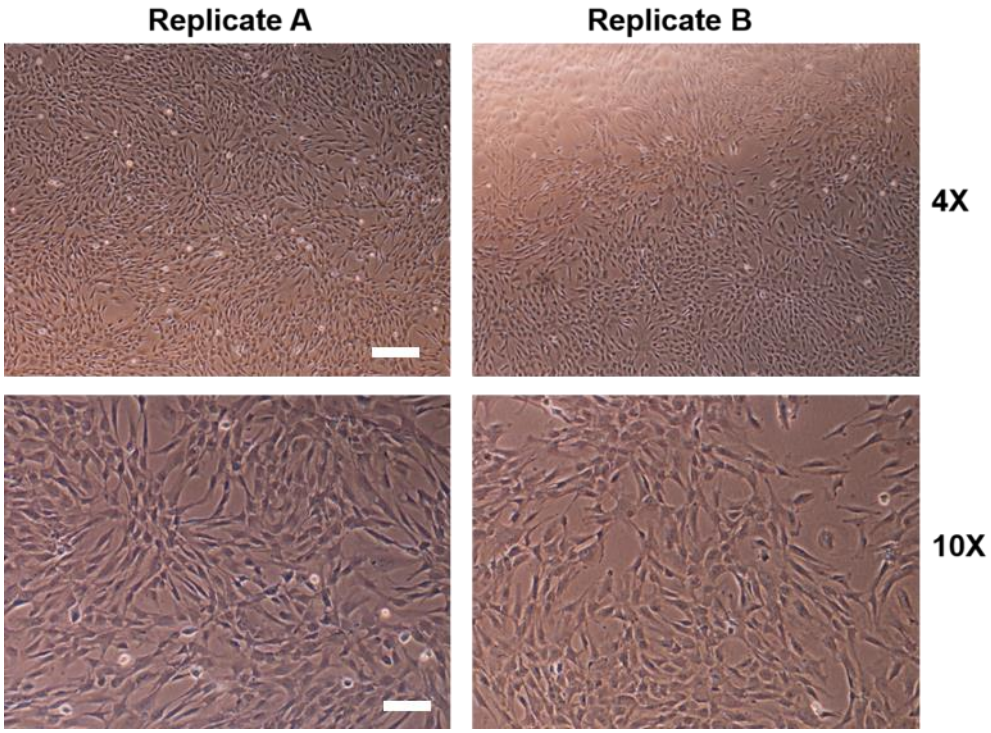

Figure 2-7. Morphology of hESC-MSCs at passage 1:

Representative image of hESC-MSCs from 2 replicates of run 1C at passage 1 before attain confluent. Both examples demonstrate a spindle shape and elongated morphology. (Upper panel magnification: X4, scale bar=40µm; lower panel: X10, scale bar=100µm)

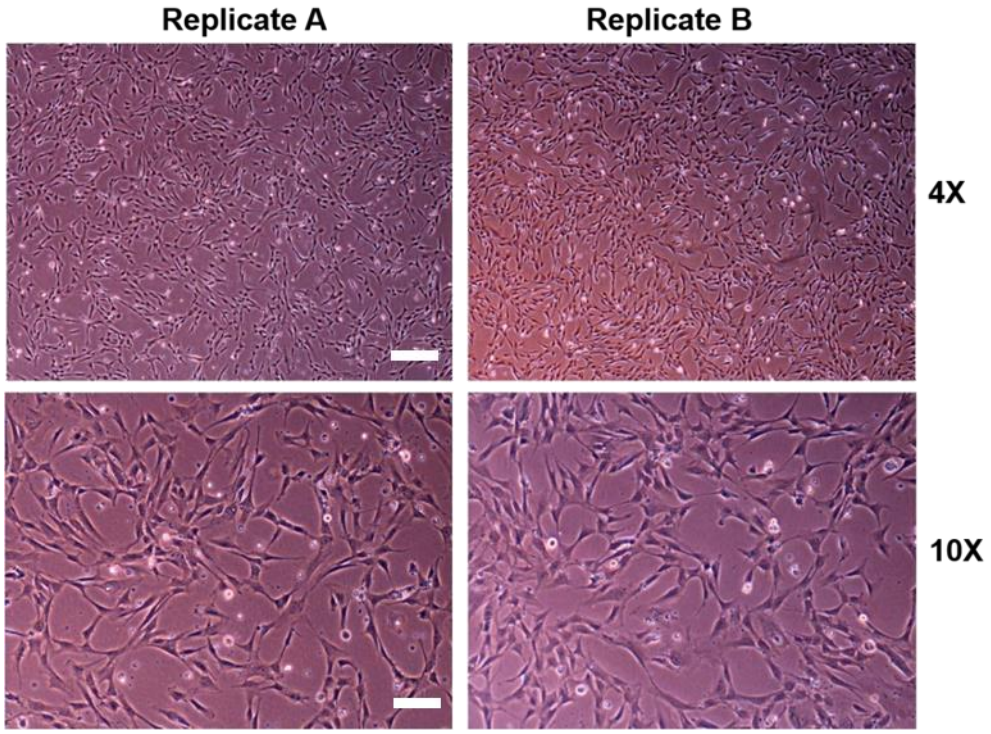

Figure 2-8. Morphology of hESC-MSCs at passage 3:

Representative image of hESC-MSCs from 2 replicates of run 1C at passage 3 before attain confluent. Both examples demonstrate a mesenchymal looking cells. Both images from replicate A and B display a characteristic of spindle shape and elongated morphology. (Upper panel magnification: X4, scale bar=40µm; lower panel: X10, scale bar=100µm)

The cells were strongly attached to the plastic surface of the culture flasks, which were not coated, by 3- 5 days after re-plating following the differentiation protocol.

2.6.4 Growth kinetics of hESC-MSCs

To determine the growth profiles of the cells derived in this experiment, cells from the 12 successful runs were counted each time they were passaged. The counts were used to produce cumulative growth charts from passage 1 to the maximum passage reached. The 12 cell cultures demonstrated a characteristic exponential growth pattern (Figure 2-9). Cells from 5 runs (1C, 4C, 5C, 15C and 16C) grew to passage 28 - 30 and the before the culture was intentionally brought to an end. The cultures of cells from other successful runs were terminated at earlier passages due to fungal contamination or other technical reasons. None of the runs were eliminated due to significant reduction in growth or significant numbers of senescent cells. The mean cumulative growth charts from the 12 successful runs demonstrated an exponential growth pattern up to passage 30 (Figure 2-10). Further analysis through calculation of the mean population doubling time (PDT) was also performed to objectively determine the changes in proliferation after prolonged culture and repeated passage. Graphs for the mean population doubling time (PDT) revealed a gradual small increment in doubling time with repeated passages and time in culture until passage 26. After passage 26 there was a steep increase in doubling time indicating a significant reduction in the cell's proliferative capacity (Figure 2-11). Additionally, the mean population doubling time for every five passages, beginning from passage 3 was also calculated in order to compare the PDT of the earlier passages to the later passages. This comparison was statistically tested using one way anova and the graph is shown in figure 2-12. The PDT significantly increased between passage 13 and 18 compared to the earlier passages (i.e passage 3 to 5).

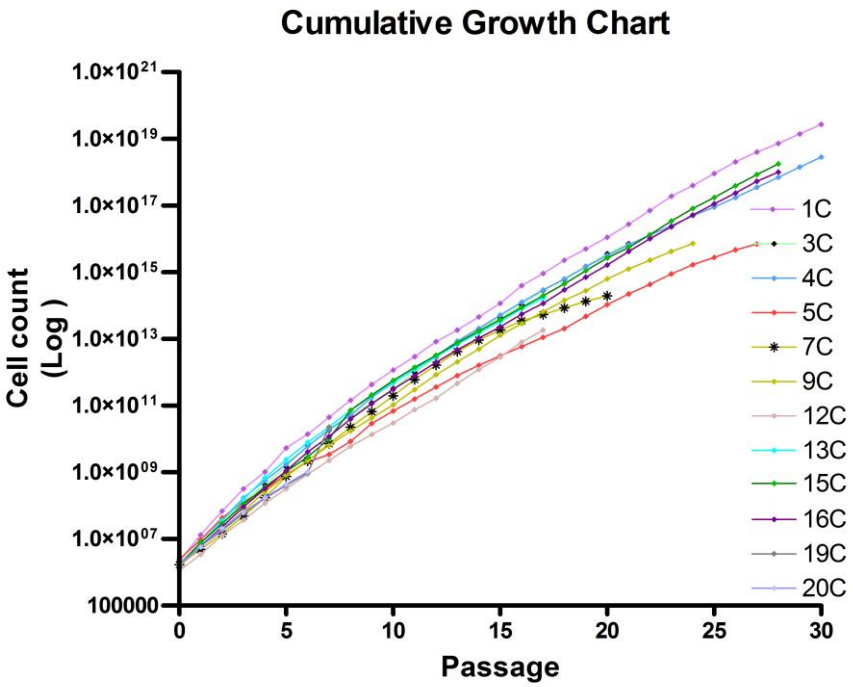

Figure 2-9. Cumulative growth chart for 12 successful differentiation runs:

The graphs represent the cumulative growth charts for each culture calculated from means of cell counts of samples A and B. Each of the cultures demonstrated an exponential growth pattern. The cumulative growth count is a prediction of cell doubling over a set period of time and is calculated by multiplying the end number of cells with the amplification fold of each passage.

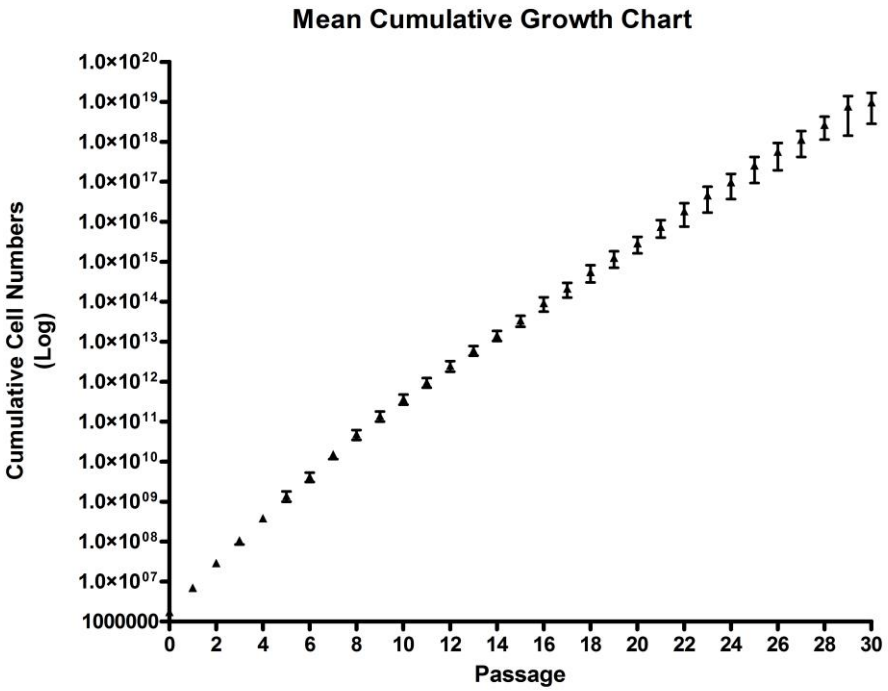

Figure 2-10. Mean Cumulative growth chart:

Mean Cumulative growth chart for 12 successful differentiation runs. The error bar shows the standard error**.**

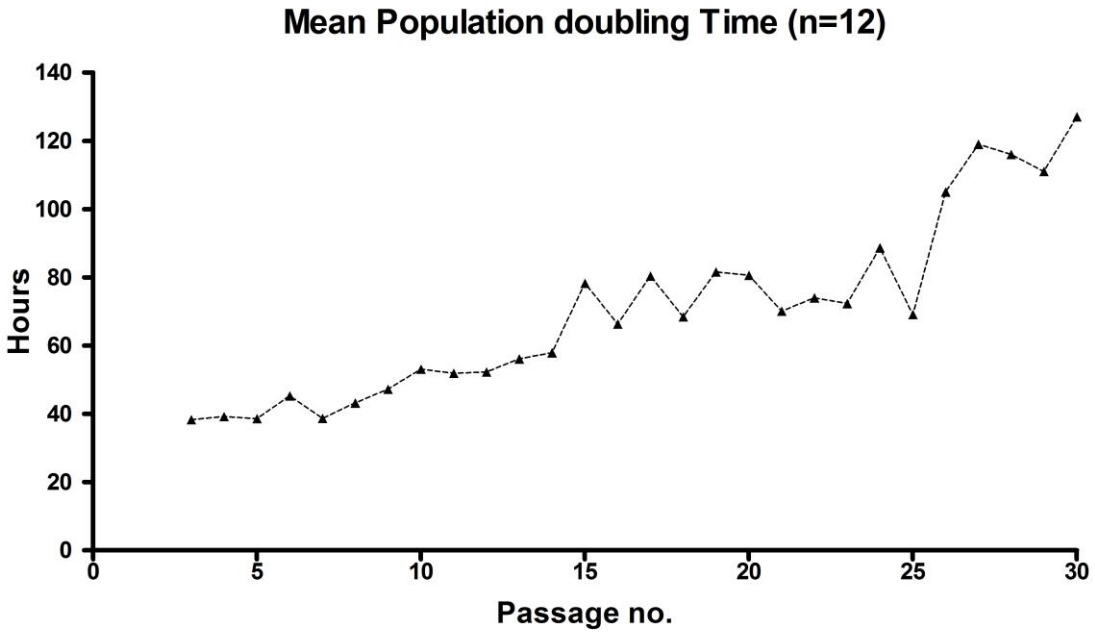

Figure 2-11. Population doubling time from passage 3 to passage 30:

The mean population doubling time from 12 different successful runs is plotted.

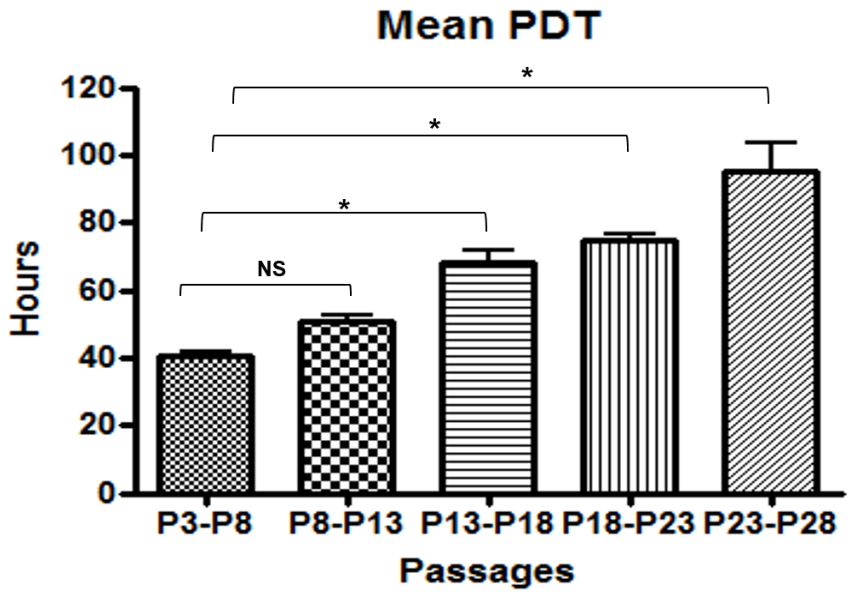

Figure 2-12. Mean population doubling (PDT) for every 5 passage:

The PDT from 12 runs are plotted in the chart (mean, standard error). (NS=not significant, *= P value <0.05).

2.6.5 Expression of Senescence Associated (SA) β-Galactosidase in hESC-MSCs

The presence of senescent cells in hESC-MSCs was determined using the Senescence ß-Galactosidase Staining Kit (Cell Signalling). The result was calculated from the mean percentage of 3 different samples collected from 1C, 4C and 5C. Enlarged cells with a blue stained cytoplasm were regard as positive for SA ß-Gal staining (Fig 2-13 top). The mean percentage of positive cells at passage 20 was 14.99% and this increased to around 27% at passage 3 (Figure 2-13 below).

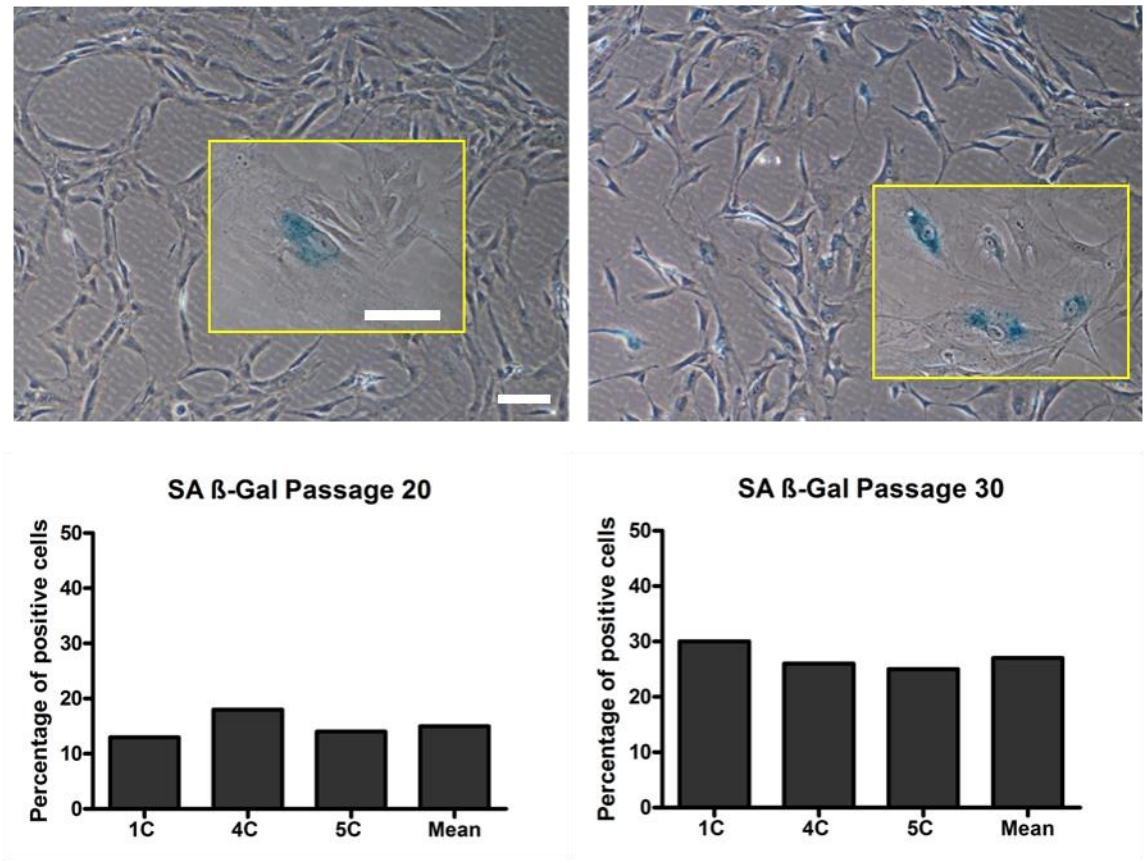

Figure 2-13. Senescence Associated β-Gal staining.

Representative images of positive SA-β gal staining of hESC-MSCs at passage 20 (upper left panel) and passage 30 (upper right panel, X10 magnification). The scale bar represent 100µm and applicable to both image of X10. The inset panels show cells with a large senescent morphology and peri-nuclear staining at X40 magnification. The scale bar represent 20µm and applicable to both inset panels. The lower panels show the percentage of positively stained cells in 3 different isolates of cells together with the mean of the 3. The bars represent the percentage of senescent cells

2.6.6 Surface Marker Profile

Surface marker expression expression was analysed using flow cytometry in order to determine the presence of MSC related markers as well the absence of the haematopoetic markers. This analysis was performed for each of the 12 successful differentiation runs at passage 1 and 3 using both replicates A and B. Passage 1 was chosen as this is the earliest point at which the cells are mesenchymal-like in appearance and an adequate number of cells are available to enable analysis with different combinations of markers. Analysis was performed at passage 3 to determine any change in surface marker expression

with time in culture and repeated passaging. In addition, passage 3 was chosen for qRT-PCR analysis as this is when the cells were cryopreserved for a later use.

The majority of surface markers tested were relatively consistently expressed by cells from each of the 12 successful runs, across both replicates. Most of the markers were also similarly expressed at passage 1 and 3, though with some changes which are detailed below. The percentage of cells positive for each surface marker, calculated as a mean of all 12 successful runs (including replicates A and B) and determined at passage 1 and 3 are shown in figure 2-17. The cells were highly positive (70-90 %) for CD44, CD73, CD105, HLA ABC, CD13 and CD166 which are markers characteristic of MSCs. They also expressed other MSC markers like CD71 and CD90 at lower levels (35-50 %). However, CD271, CD106 and Stro-1 were expressed by only 5-20% of cells. The haematopoietic markers CD45 and CD34 were expressed in no more than 2 % of cells tested. Figures 2-14 to 2-16 show representative dot plots from flow cytometry for each of the markers investigated (including the isotypes).

To determine the consistency in the surface marker profiles between passage 1 and passage 3, the mean percentages of positive cells at passage 1 and passage 3 were compared using Student's paired t-test (Table 2-3). This revealed a significant increase in the percentage of cells which expressed CD105 (P value:0.021) and CD13 (P value:0.014) at passage 3 compared to passage 1. In addition, there was a significant reduction in the cells that expressed CD271 (P value:0.034) at passage 3 compared to passage 1.

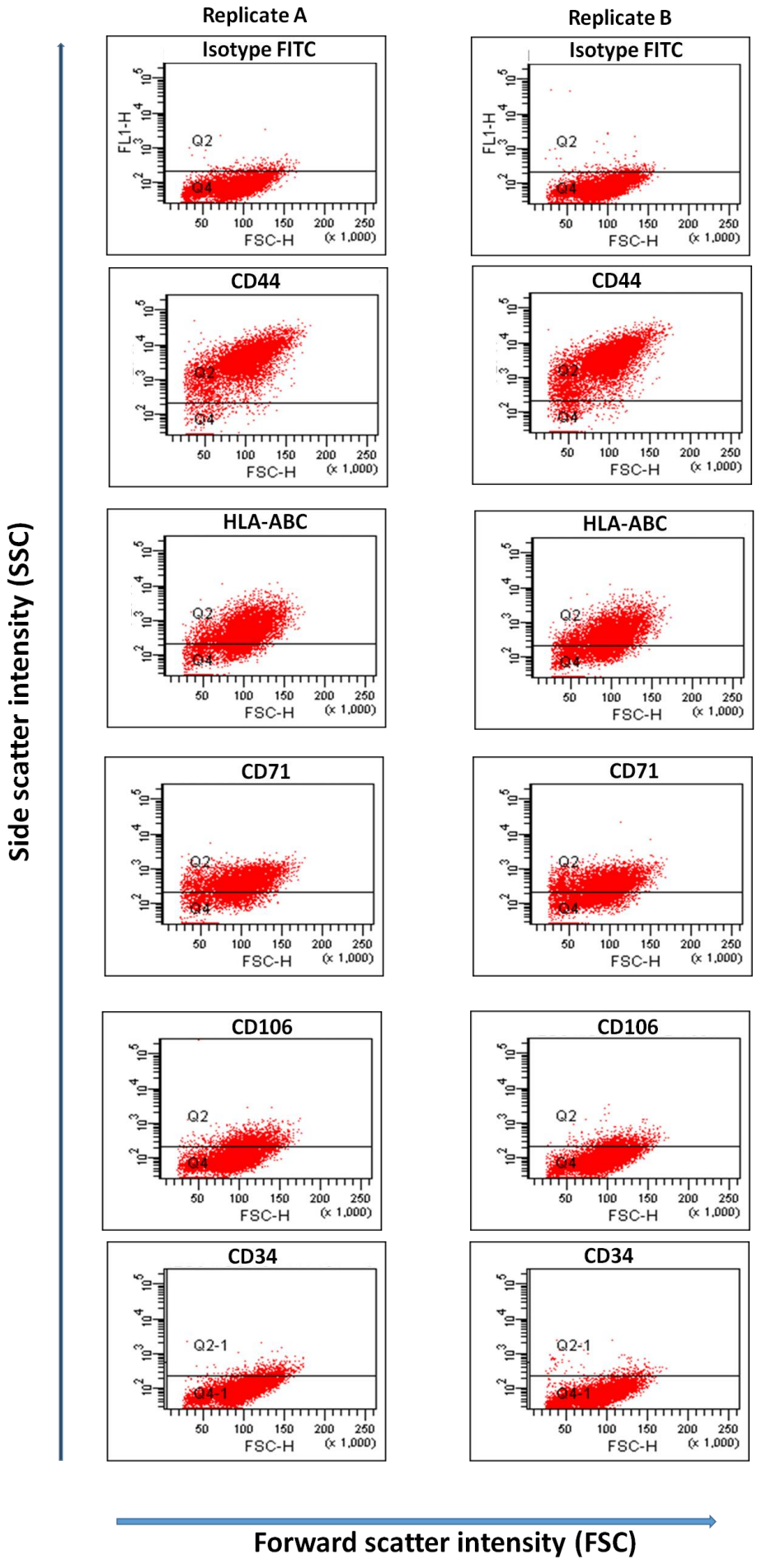
Replicate A
Replicate B
Isotype FITC
CD44
HLA-ABC
CD71
CD106
CD34
FL1-H
FSC-H
(x 1,000)
Q2
Q4
Q2-1
Q4-1
Side scatter intensity (SSC)
Forward scatter intensity (FSC)

Figure 2-14. Representative dot plots for flow cytometry analysis of different surface markers performed on hESC-MSCs at passage 3.

The majority of hESC-MSCs are positive (range between 70-90%) for important MSC markers: CD44, HLA-ABC (class 1). Dot plots for replicates A and B are similar in appearance. The red dots above the line represent the positively stained cells. (SSC: side scatter intensity value which proportional to fluorescent intensity; FSC: forward scatter is roughly proportional to the diameter of the cell). (Example from culture 1C; staining with FITC antibodies):

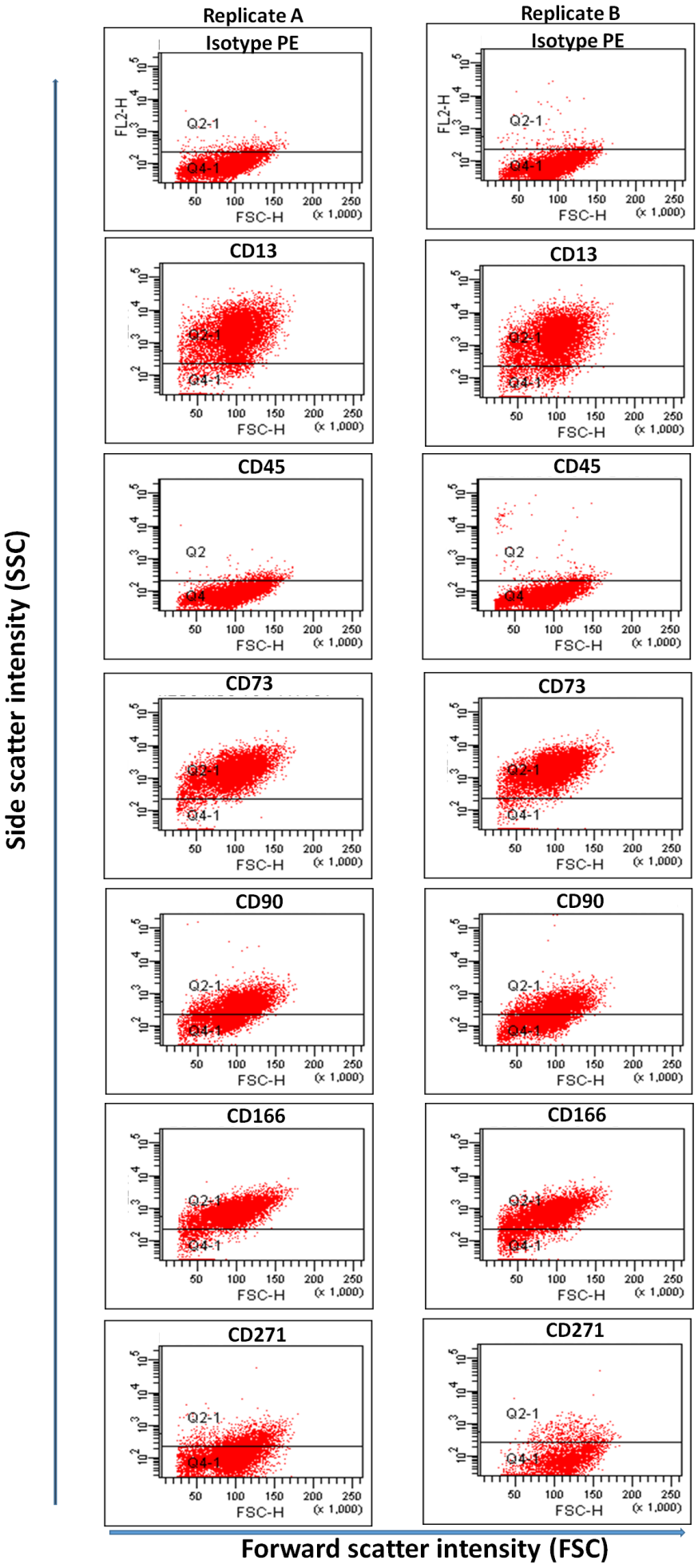
Replicate A
Replicate B
Isotype PE
CD13
CD45
CD73
CD90
CD166
CD271
FL2-H
FSC-H
(x 1,000)
Q2-1
Q4-1
Q2
Q4
Side scatter intensity (SSC)
Forward scatter intensity (FSC)

Figure 2-15. Representative dot plots for flow cytometry analysis of different surface markers performed on hESC-MSCs at passage 3.

The majority of hESC-MSCs are positive (range between 80-90%) for important MSC markers: CD73, CD13 and CD166 (80-90). Dot plots for replicates A and B are similar in appearance. The red dots above the line represent the positively stained cells. (SSC: side scatter intensity value which proportional to fluorescent intensity; FSC: forward scatter is roughly proportional to the diameter of the cell). (Example from culture 1C; staining with PE antibodies).

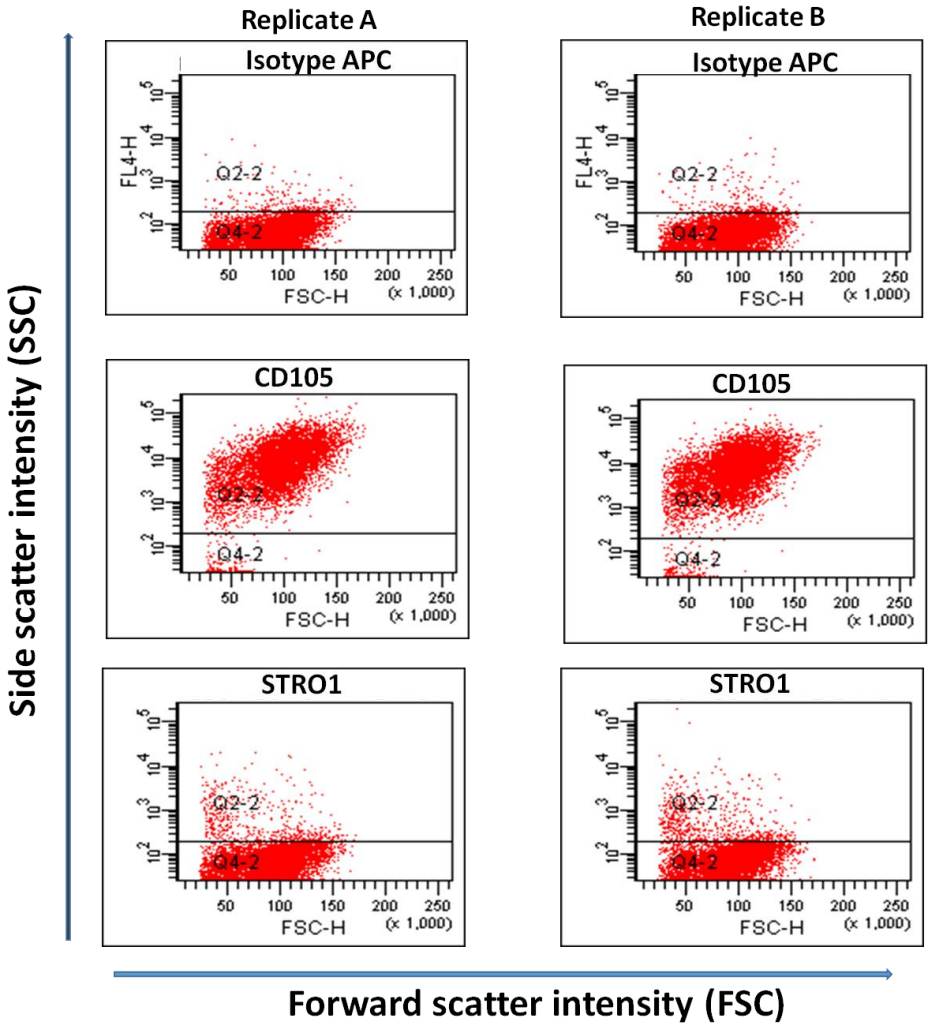

Figure 2-16. Representative dot plot for flow cytometry analysis of surface markers at passage 3.

The majority of hESC-MSCs express CD105 while only a small percentage express STRO 1. The red dots above the line represent the positively stained cells. (SSC: side scatter intensity value which is proportional to fluorescent intensity; FSC: forward scatter is roughly proportional to the diameter of the cell). (Example from 1C; staining with APC antibodies).

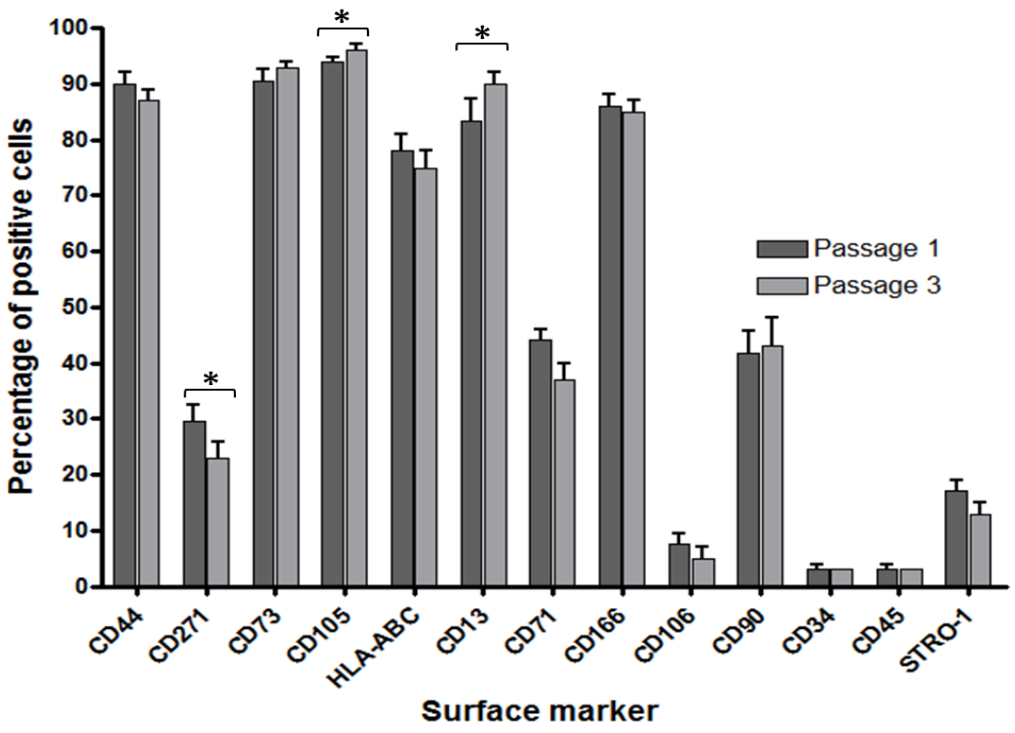

Figure 2-17. Surface marker expression at 2 different passages

Flow cytometry analysis performed at passage 1 and passage 3 demonstrated a consistent pattern of surface marker expression for most markers but some differences in CD13, CD105 and CD271. Mean and SEM, n=12. Statistical analysis was performed using students paired t-test. Asterisk (*) indicates p value <0.05 and is considered significant**.**

Surface Marker	Mean P1 (n=12)	S.D	Mean P3 (n=12)	S.D	P value
CD44	90.11%	2.18%	86.86%	1.89%	N.S
CD271	29.45%	3.00%	22.69%	3.43%	0.034
CD73	90.63%	1.80%	92.87%	1.09%	N.S
CD105	93.85%	1.41%	96.33%	1.13%	0.021
HLAABC	78.14%	2.55%	74.92%	2.59%	N.S
CD13	83.27%	3.75%	90.05%	2.31%	0.014
CD71	44.12%	2.49%	37.05%	3.19%	N.S
CD166	86.59%	1.76%	84.65%	2.16%	N.S
CD106	7.48%	1.87%	4.89%	1.54%	N.S
CD90	41.78%	3.53%	42.77%	4.70%	N.S
CD45	3.52%	0.79%	2.71%	0.31%	N.S
CD34	3.59%	1.10%	2.73%	0.27%	N.S
Stro 1	17.04%	2.90%	13.39%	1.89%	N.S

Table 2-3. Comparison of surface marker profile at passage 1 and passage 3:

The mean percentage and standard deviation calculated for the 12 different runs of cells is shown with P value for difference between passage 1 and passage 3. (N.S = not significant).

2.6.7 Gene expression profile

Quantitative real time PCR (RT-PCR) was performed in 11 successful runs using samples from day 0 and 28 (beginning and end of the differentiation protocol) and passage 3 of the expansion protocol. This was performed in order to look for changes in the mRNA expression levels of genes of interest, including those specific for MSCs at different stages of the protocol. In addition, this also allowed comparison of gene expression in hESC-MSCs compared to undifferentiated (day 0) hESCs. If the cycle threshold (Ct) of the targeted gene was more than 15 cycles greater than that for the housekeeper gene, then this was considered to represent no expression and the results were not included in further calculations and analysis. Results were normalised relative to expression of a housekeeper gene, GAPDH, using the formula: $2^{\Delta Ct}$ x 1000 (Schmittgen & Livak, 2008). Using this formula, a high value (e.g. 500) would indicate that the Ct for the targeted gene is within within 1 cycle of housekeeper gene whilst a low value (e.g. 0.1) would indicate that amplification of target gene required ≥ 15 cycles more than the housekeeper for signal detection and therefore equates to very low expression. ΔC_t values (C_t housekeeper gene – C_t target gene) from different time points were analysed statistically using one way anova. The results obtained are shown graphically in Figure 2-18.

The gene expression pattern at passage 3 was consistent with an MSCs phenotype. Both replicates of the 11 runs expressed relatively high levels of MSC related genes and low levels of pluripotent genes, compared with day 0 samples. Both *OCT4* and *Nanog* (pluripotency genes) were highly expressed at day 0 within the starting population of hESCs. Their expression levels were then significantly downregulated at later time points: by at least 40 fold at day 28 and more than 3000 fold at passage 3. The mesenchymal gene, *COL1A1* was significantly upregulated (by 35 fold) at day 28 and then slightly (but not significantly) downregulated at passage 3. *CD105* expression was upregulated at day 28 and further significantly upregulated (by 35 fold) at passage 3. Another potential mesenchymal gene, *Twist1* was significantly upregulated at day 28 compared with day 0. The *Twist1* expression was significantly downregulated at passage 3 compared with day 28 but was still significantly expressed compared with day 0. Additionally, there was either extremely low or no expression of *CD31* and *CD45*

genes in all samples tested and these data are not shown. Further analysis of mesodermal markers showed very minimal expression of *GSC* in all samples without any pattern to suggest any biological relevence. There was either extremely minimal expression or no expression of brachyury in all samples which were analyzed (data not shown).

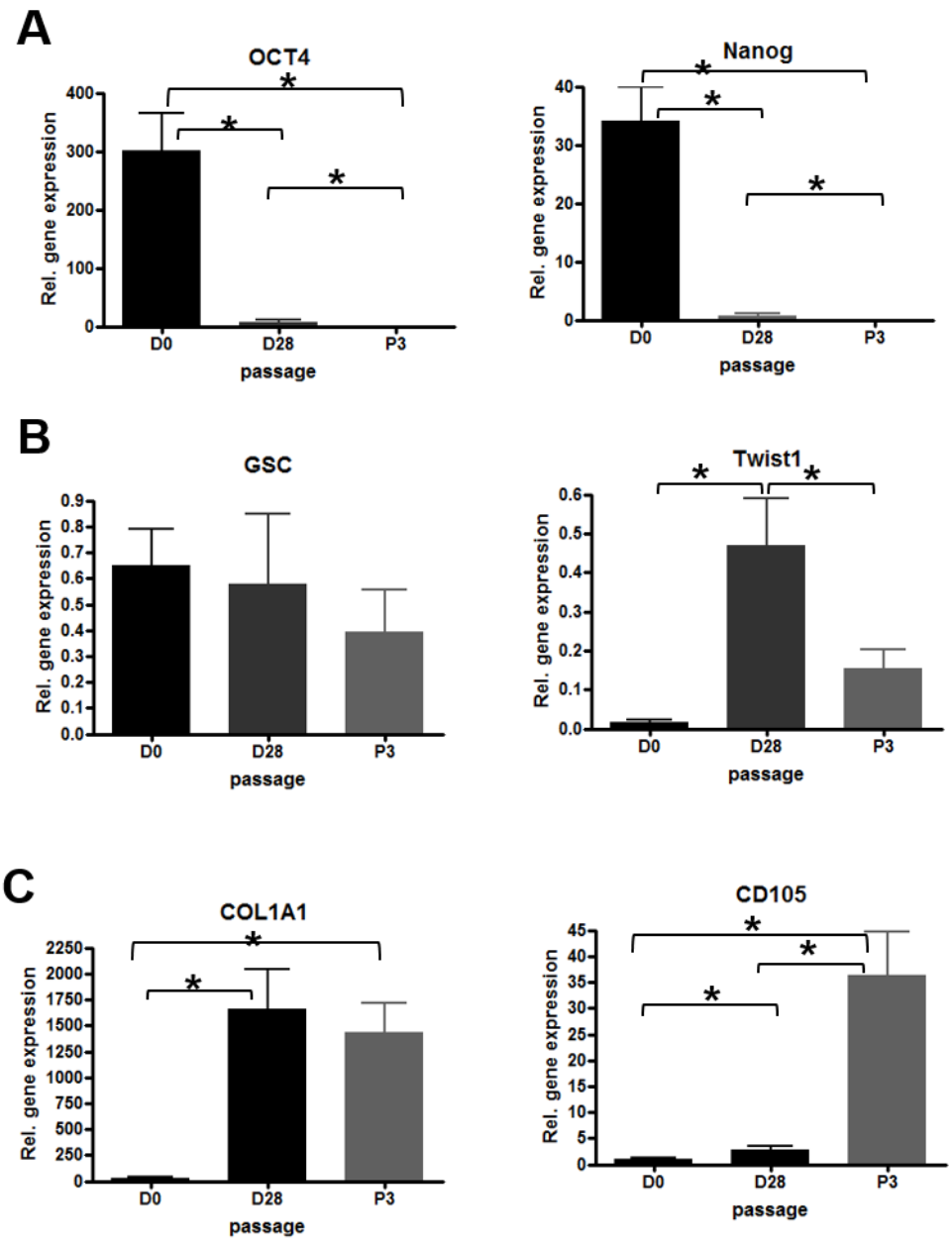

Figure 2-18. Gene expression analysis from qRT-PCR performed before cryopreservation. Gene expression calculated using the formula $2^{\Delta Ct}$ x 1000 and presented as mean and standard error calculated from 11 different isolates. The upper panels (A) show the downregulation of 2 pluripotency genes: OCT4 and Nanog. The middle panels (B) show 2 early mesodermal/epithelial-mesenchymal transition genes: GSC and Twist1. There is minimal expression of GSC at all time points. Twist1 is significantly upregulated at day 28 but subsequently decreased at passage 3. The lower panels (C) demonstrate the upregulation of 2 mesenchymal lineage genes: COL1A1 and CD105 at later time points. Statistical comparisons of ΔCt was performed using one way anova . Asterisks (*) indicate p values <0.05 which are considered significant.

2.6.8 Re-characterization

In order to determine whether the cells retain their properties following cryopreservation, the cells were re-characterized using the same methods as prior to cryopreservation. This was performed on cells from replicates A of 5 different runs (1C (A), 4C (A), 7C (A), 9C (A) and 13C (A)) at passage 3+5 (5 passages after they were recovered from liquid nitrogen). These are cells which were selected for transplanting into the animal model of SCI.

2.6.8.1 Morphology and adherence capacity

The cells showed a similar morphological appearance after they were recovered from liquid nitrogen and re-cultured under similar conditions to prior to cryopreservation. They displayed an elongated and spindle shaped morphology when regularly examined from passage 3+1 up to passage 3+5 (Figure 2-19). There were no noticeable cells of large size which would have suggested the development of senescence. In addition, all cell isolates retained the capacity to adhere to plastic surfaces.

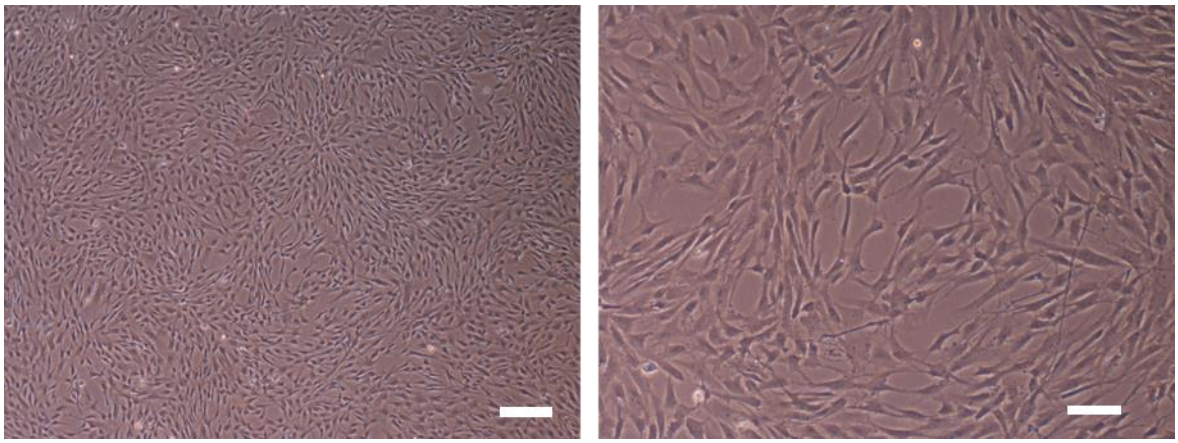

Figure 2-19. Image of hESC-MSC after cryopreserved and re-culture.

Representative image of hESC-MSCs from run 1C at passage 3+5. The cells display MSC-like features (elongated and spindle shaped) which are similar to earlier passages (Left image:X4, right image: X10).

2.6.8.2 Growth profile

Cell counts were performed at the end of every passage (passage 3+1 to passage 3+5) of all 5 isolates recovered from cryopreservation for transplantation (1C (A), 4C (A), 7C (A), 9C (A) and 13C (A)) in order to determine their growth profile following cryopreservation. The cumulative cell growth chart for the cryopreserved cultures demonstrated an exponential growth pattern which was either similar to or better than that for the cells not cryopreserved but maintained in culture to passages 4 to 8 (Figure 2-20). A comparison of the population doubling time of cryopreserved cells at passage 3+2 to passage 3+5 with cells grown on in culture to passage 5 to passage 8, revealed a shorter and more consistent doubling time than in the samples which were analysed before cryopreservation (Figure 2-21). A Student's paired t-test was performed to compare the mean population doubling time (calculated from passage 5 to passage 8 versus passage 3+2 to passage 3+5) of each cell isolate before and after cryopreservation. This revealed a significant reduction in the mean population doubling time of cryopreserved cells for 1C and 7C in comparison to none cryopreserved cells of the same populations (Figure 2-22). There was no significant difference in the mean population doubling time of 4C and 9C but the value tended to be lower for the cells which had been frozen (Figure 2-22). A Students paired t-test was used to compare the mean population doubling time of cryopreserved and non-cryopreserved cells of all four isolates and revealed a significant reduction for the mean PDT after cryopreservation (Figure 2-23). In summary, the results suggest that the proliferation capacity of hESC-MSCs does not deteriorate and in fact may improve following cryopreservation, although other factors such as potential differences in the initial density and final density when passaging need to be taken into consideration.

Cells from 13C (A) were not included in the above calculation as they were re-cultured using a higher cell density (10,000 cells/ cm^2) than the other cultures. In addition, cells from 13C (A) were only passaged up to passage 3+3 before they were then prepared for transplantation (see chapter 3). There was a slightly higher PDT displayed in 13C (A) after cryopreservation (Figure 2-24).

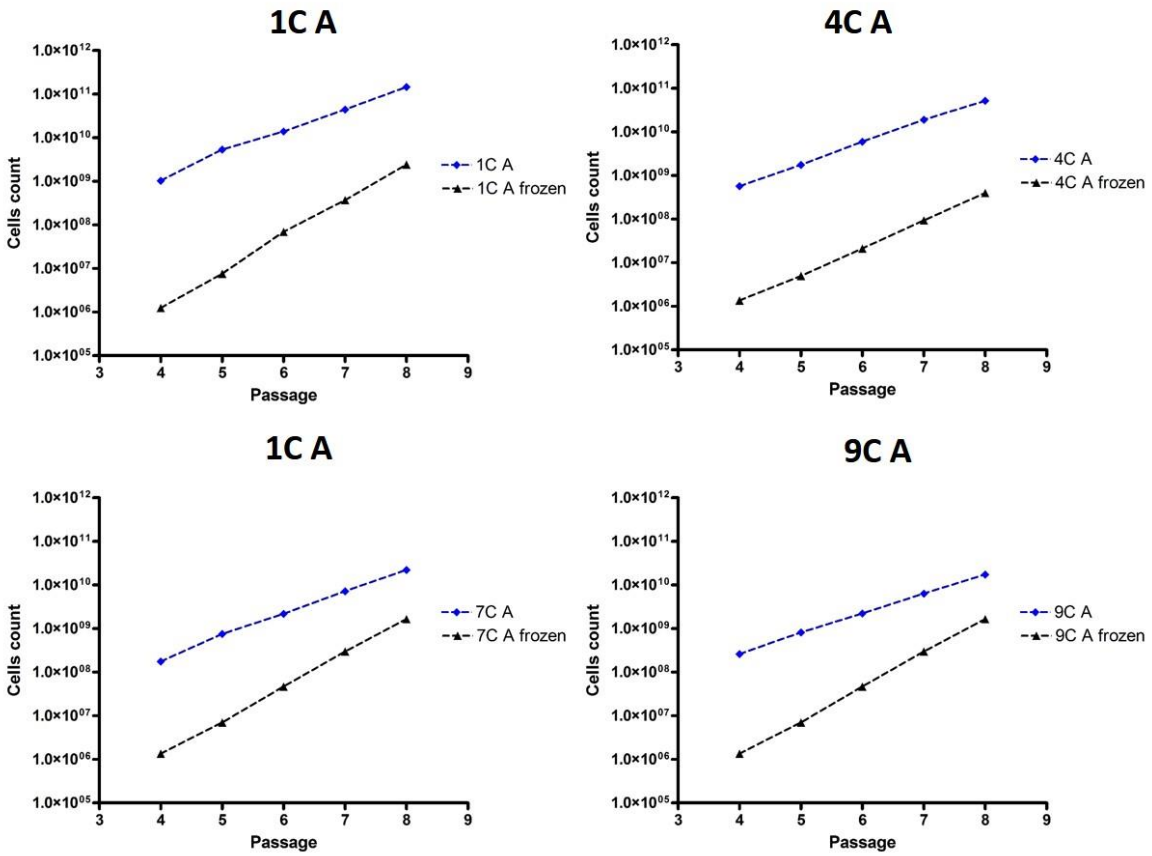

Figure 2-20. Cumulative growth chart (cryopreserved compared to non-cryopreserved).

Growth charts for 4 different cell isolates showing cumulative growth numbers over 5 different passages (from passage 4 to 8 versus passage 3+1 to 3+5).

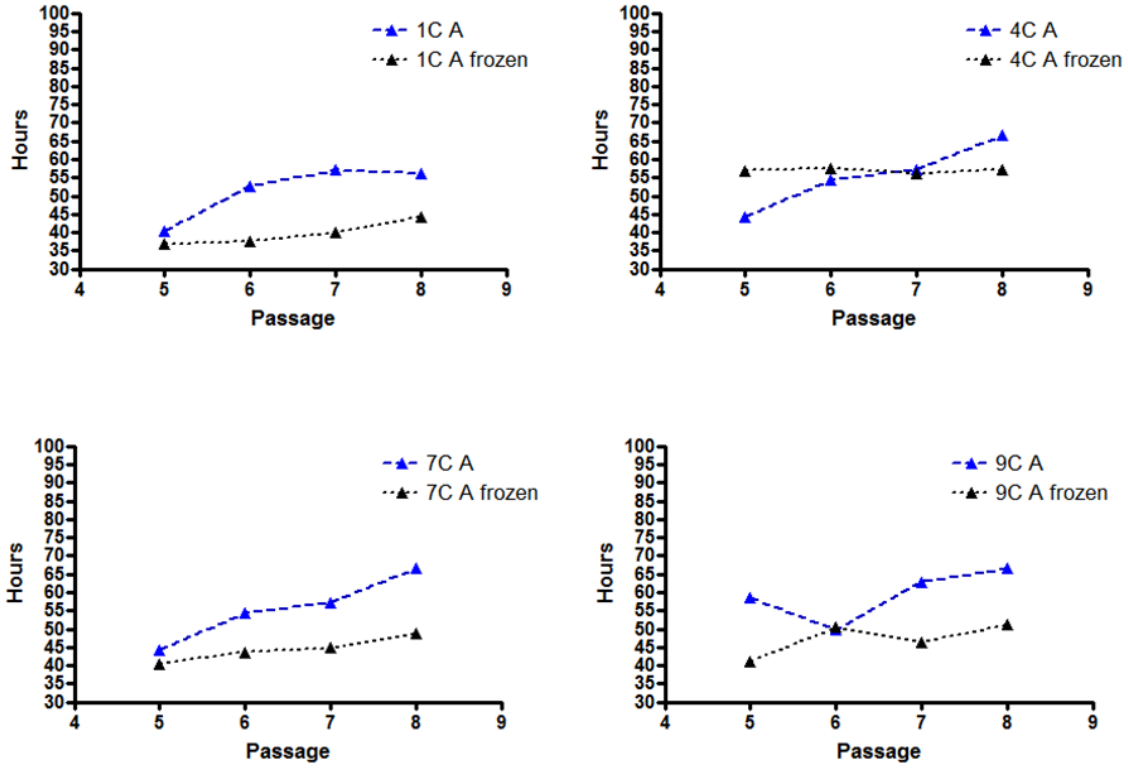

Figure 2-21. Population doubling time (PDT) chart (cryopreserved compared to non-cryopreserved).

Graphs of population doubling time for 4 different isolates comparing PDT for cryopreserved and non-cryopreserved cells over 4 different passages (from passage 5 to 8 versus passage 3+2 to 3+5).

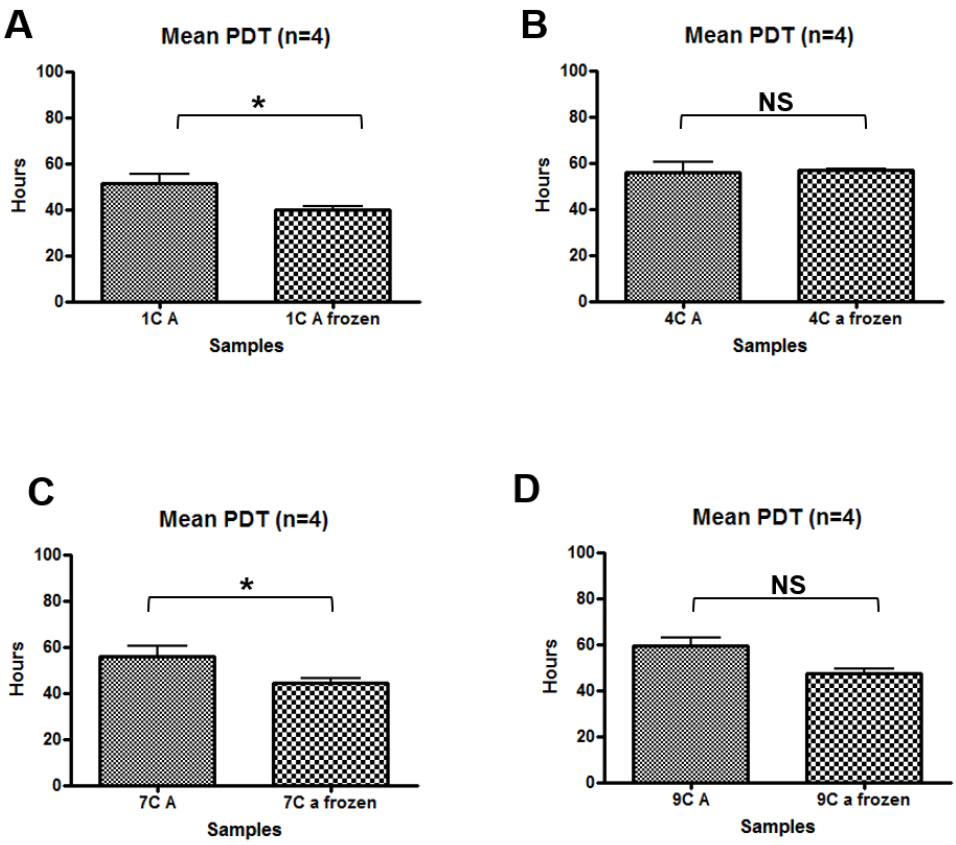

Figure 2-22. Mean population doubling time (PDT) calculated over 4 passages for 4 isolates of cryopreserved compared to non-cryopreserved cells.

Mean and standard error. NS= not significant, asterisk (*) indicates p value of <0.05.

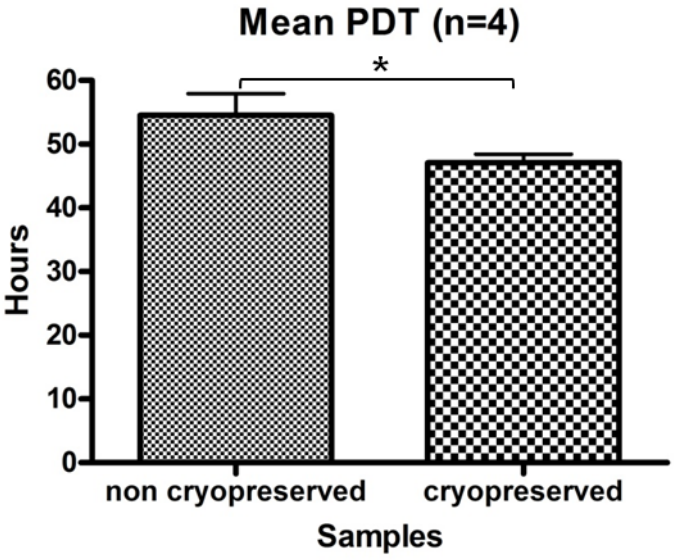

Figure 2-23. Comparison of population doubling time for cryopreserved compared to non-cryopreserved cells.

The values are a mean calculated for 4 isolates i.e. 1C-A, 4C-A, 7C-A and 9C-A over 4 passages. (Mean, standard error; NS= not significant, asterisk (*) indicates p value of <0.05).

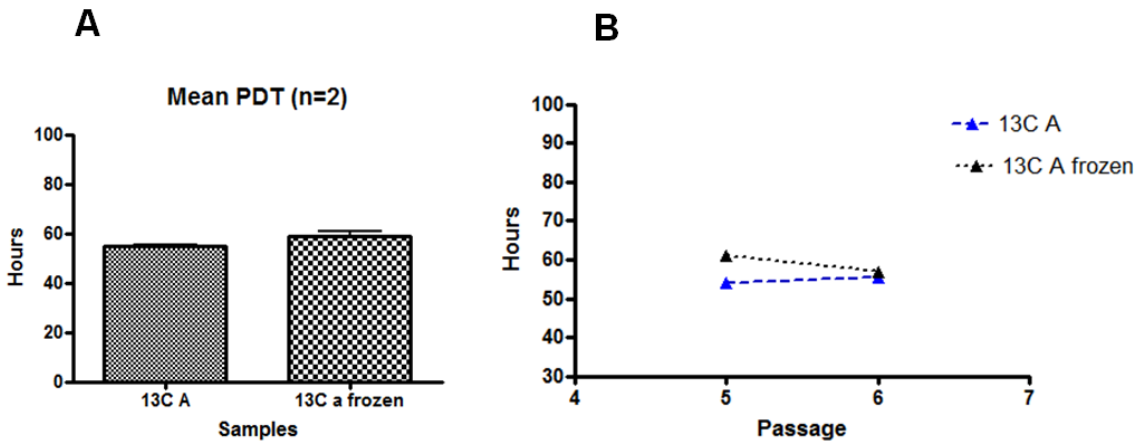

Figure 2-24. Population doubling time (PDT) of cell run 13C (cryopreserved compared to non-cryopreserved).

(A) Mean PDT calculated from passage 5 to passage 6 (non frozen) compared to mean from passage 3+2 to passage 3+3 (after freezing). (Mean, standard error). (B) Population doubling time over 2 passages

2.6.8.3 Surface marker expression

The flow cytometry analysis was performed on cells recovered from liquid nitrogen to determine the consistency of surface marker expression between cells at passage 3 (before cryopreservation) and cells at passage 3+5 (after cryopreservation) for the same set of surface markers. 5 different isolates of cells (replicate A) were tested and the results show a highly consistent marker expression at the 2 passages tested. The mean percentage positive cells for each marker at each passage is shown in in figure 2-25. Use of Student's paired t-test showed there was no significant difference between cryopreserved and non-cryopreserved cells except for CD34 which was significantly reduced after cryopreservation (table 2-3). But the percentage of cells positively stained for CD34 was in any case low in both passages, suggesting it may be of little biological significance.

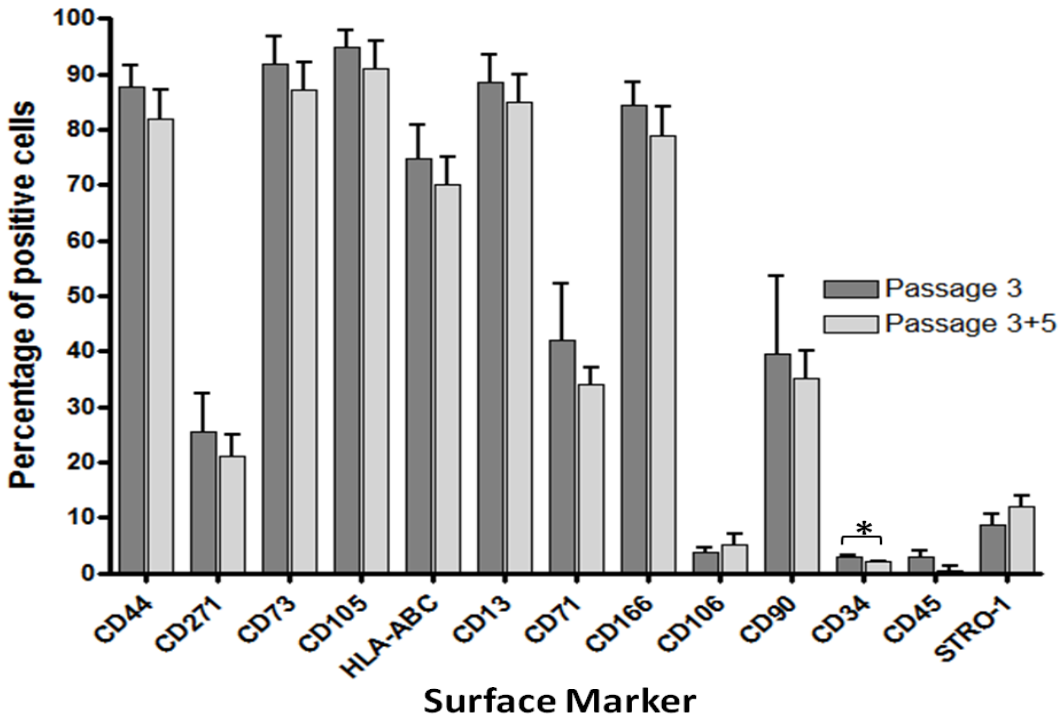

Figure 2-25. Surface marker expression at 2 different passages (passage 3 and passage 3+5).

Flow cytometry analysis performed at 2 different passages demonstrated a consistent pattern of surface marker expression with the only significant difference occurring for the non MSC marker CD34. (Mean, standard error, n=5. Statistical analysis was peformed using Student's paired t-test. An asterisk (*) indicates a p value <0.05.

Surface Marker	Mean P3 (n=5)	S.D	Mean P3+5 (n=5)	S.D	P value
CD44	87.62%	4.12%	94.15%	2.65%	N.S
CD271	25.46%	6.85%	24.43%	10.47%	N.S
CD73	91.80%	2.61%	92.24%	3.09%	N.S
CD105	94.86%	2.85%	96.30%	2.21%	N.S
HLAABC	74.76%	6.23%	59.62%	9.47%	N.S
CD13	88.56%	4.82%	92.46%	2.91%	N.S
CD71	42.06%	9.80%	42.12%	10.51%	N.S
CD166	84.44%	4.17%	71.72%	8.28%	N.S
CD106	3.68%	0.87%	5.90%	2.92%	N.S
CD90	39.48%	13.60%	41.89%	7.35%	N.S
CD45	3.12%	0.94%	1.97%	0.35%	N.S
CD34	3.12%	0.28%	2.00%	0.19%	0.009
Stro 1	8.76%	2.57%	3.83%	1.50%	N.S

Table 2-4. Comparison of surface marker profile at passage 3 and passage 3+5:

The mean percentage and standard deviation calculated for 5 different isolates of cells is shown with P the value for the difference between passage 3 and passage 3+5. (N.S = not significant).

2.6.8.4 Gene expression

Gene expression analysis for these 5 different isolates was performed in order to examine the effect of cryopreservation. This was performed by comparing the expression in samples at passage 3+5 (which had been extracted from thawed cryopreserved samples), with samples from passage 3 and day 0 which had not been subject to cryopreservation. To ensure better consistency for comparison, cDNA from cryopreserved and non-cryopreserved samples was prepared in parallel using the same stocks of reagents (e.g. mastermix and GAPDH). Mean gene expression levels were calculated for data from the 5 different samples and a one way ANOVA was performed in order to statistically compare the expression between the three different time points (Figure 2-26).

The MSC related genes *COL1A1* and *CD105* were significantly upregulated at both passage 3 and passage 3+5 compared to day 0 samples but were not significantly different from each other. The pluripotentency genes *OCT-4* and *Nanog* were significantly downregulated at both passage 3 and passage 3+5 compared to day 0. *Twist-1* was significantly upregulated at passage 3 compared with day 0. It was down-regulated at passage 3+5 compared to passage 3 but still significantly upregulated compared to day 0. This may suggest that the cells become more committed toward MSCs by passage 3+5. There was minimal expression of *GSC* in the samples and this showed a tendency for down-regulation at passage 3+5. In addition, there were no significant differences between the expression of genes tested in passage 3 and passage 3+5 samples except for *Twist1*. The other genes tested were either expressed at very low level or absent and these data are not shown. In summary, the gene expression level after cryopreservation at passage 3+5 demonstrate a pattern of expression consistent with passage 3 samples suggesting that cryopreservation does not affect gene expression at the transcription level in hESC-MSCs.

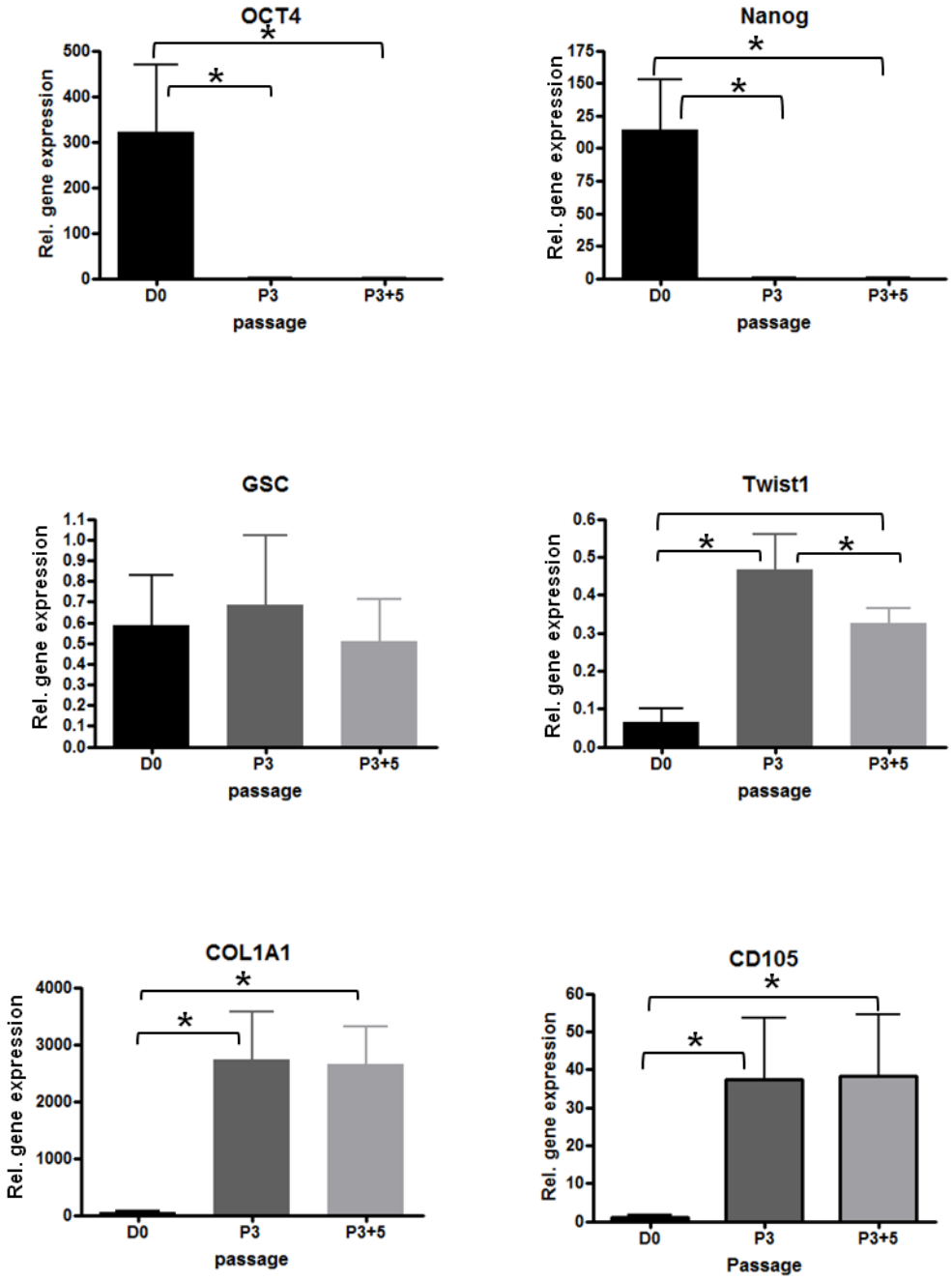

Figure 2-26. Gene expression analysis performed after cryopreservation.

Test performed using 5 different samples from passage 3+5 (extracted from samples which have been cryopreserved, thawed and re-cultured for transplantation) in comparison to samples from passage 3 and day 0 which were extracted prior to cryopreservation. Statistical analysis used is one way anova performed using the ΔCt value and asterisks (*) indicate p values of <0.05.

2.6.8.5 Functional differentiation

The differentiation ability of our hESC-MSCs following cryopreservation was determined by inducing some samples from all 5 different runs to form adipocytes and osteoblast. They were cultured at passage 3+5 in either

adipogenic or osteogenic medium for 21 days. Adipogenic differentiation was confirmed using both IBMX and SWH methods in all 5 samples by cytoplasmic lipid vacuoles staining red with Oil Red O (Figure 2-27). There were more and larger red stained vesicles using the SWH method. Osteogenic differentiation was also confirmed in all samples tested by the appearance of calcium deposits which stained red with Alizarin Red S (Figure 2-28). This staining was very homogenous and covered a very large area in contrast to the more heterogeneously and sparsely red stained cytoplasmic lipid vacuoles after adipogenic differentiation.

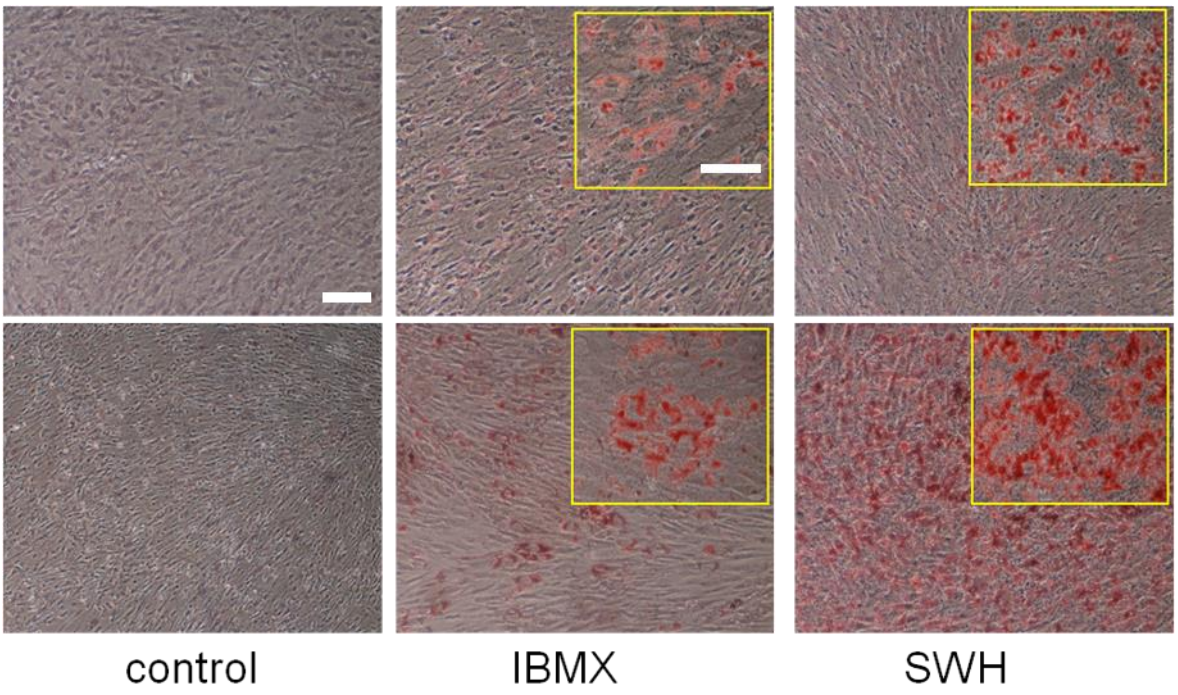

Figure 2-27. Adipogenic differentiation.

Representative Images at X10 magnification showing positively stained adipocytes in 2 different isolates of cells: 1C (A) upper panel and 4C (A) lower panels, after 3 weeks differentiation using the IBMX and SWH methods. The inset shows higher power (X40) images of adipocytes with red stained vesicles. The scale bar represent 100µm for all X10 images and 20µm for all inset images.

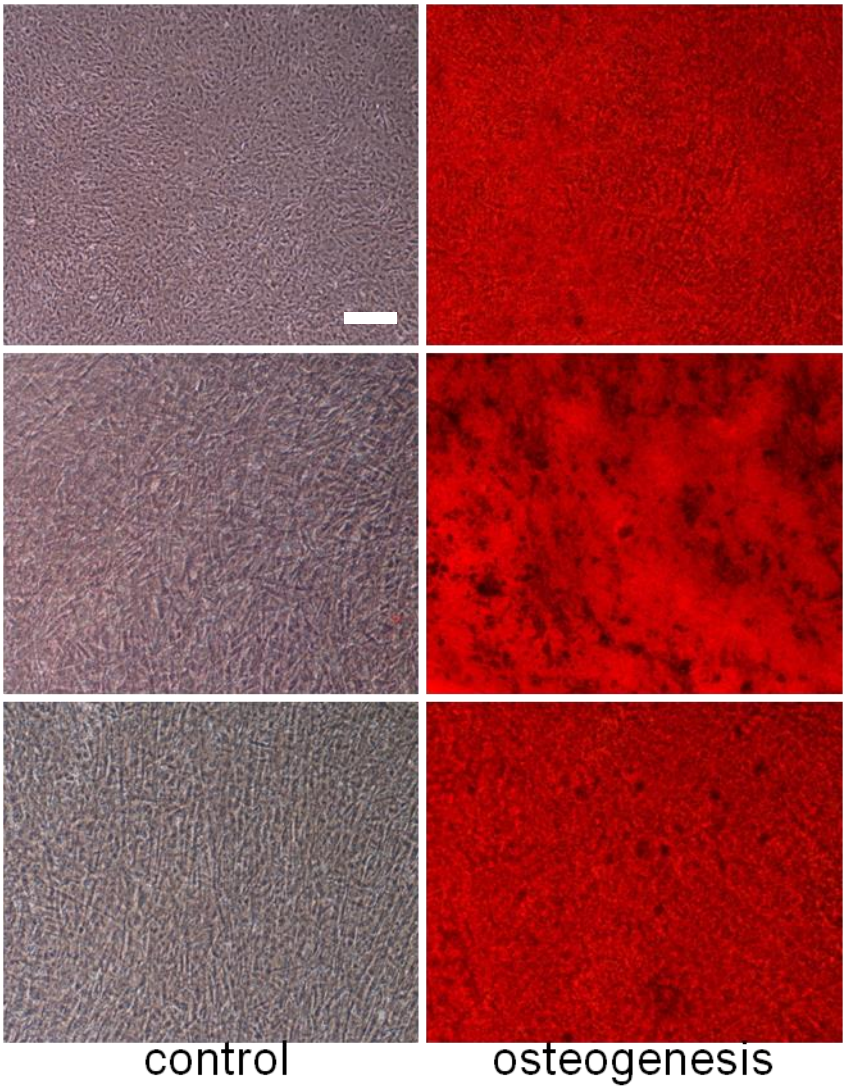

Figure 2-28. Osteogenic differentiation:

Representative images of cells from 3 different isolates: 1C (A) uppermost panels, 7C (A) middle panels and 9C (A) lower panels, positively stained by Alizarin Red S after 3 weeks differentiation period (X10 magnification, scale bar=100µm and applicable to all panels).

2.7 Discussion

There are various methods for the differentiation of MSCs from hESCs that have been reported in the literature by different groups (Barberi *et al.*, 2005; Olivier *et al.*, 2006; Lian *et al.*, 2007; Trivedi & Hematti, 2008; Lee *et al.*, 2010; Gruenloh *et al.*, 2011; Wu *et al.*, 2013). Among those reported are methods based on manual dissection of populations of cells in the culture, one version of which involves the formation of embroid bodies in the initial phase of the differentiation protocol (Bielby *et al.*, 2004; Lee *et al.*, 2010) and another version which omits this step (Olivier *et al.*, 2006). These two methods have been used successfully to derive MSCs from hESCs and have the advantage of being relatively simple compared to other established methods and also avoid using complicated techniques like fluorescence-activated cell sorting or extensive genetic manipulation which could potentially damage the cells. However neither of these 2 particular methods is free from animal products. The inclusion of animal products in the cell culture protocol risks contamination with animal pathogens and precludes the use of the cell product in humans. Lian and colleagues claim to have developed a protocol to derive clinical grade MSCs from undifferentiated hESCs which does not require serum, use of feeder cells of animal origin or genetic manipulation (Lian *et al.*, 2007). Another recent study by Wu *et al* also reported a successful derivation of MSCs from hESCs using chemically defined conditions without requiring any feeder layer, serum or SR of animal origin (Wu *et al.*, 2013). Such methods would be more clinically translatable but beyond the scope of this project due to time constraints and the desire to transition into the project's second phase which is transplanting the hESC derived MSCs into an animal model of spinal cord injury. Therefore a protocol developed by Olivier *et al.* (2006) the "raclure" method, was chosen owing to its relative simplicity, the cells obtained using this method still have a normal karyotype and can robustly grow up to 20-25 passages, while displaying MSC characteristics and not requiring any feeder layer. The "raclure" method was originally based on the mechanical dissection of a small population of spontaneously differentiated hESCs. These cells give rise to a homogenous culture of MSCs when placed in appropriate growth conditions (Olivier *et al.*, 2006). However, further observations (Olivier & Bouhassira, 2011) showed that

cells produced the same MSC populations as those from the raclure method, even if they were sourced from a confluent, undifferentiated hESC culture, as long as they were plated at low density. This relatively simple option of plating undifferentiated hESCs at low density was chosen in my experiment to avoid selective mechanical scraping, a difficult technique that requires considerable expertise to accomplish reliably. In this way, unnecessary damage to the cells was also avoided. The use of undifferentiated hESCs is also improves the uniformity of the starting cell population. DMEM+FBS+NEAA+P/S (D10) was used as the only differentiation medium as it is an established medium with proven effectiveness in differentiating hESCs to MSCs (Olivier *et al.*, 2006). Instead of using hESC cultured on MEF as my starting population, we used hESC which had been cultured on a feeder-free surface to further minimize the involvement of animal products. The starting populations of hESCs were tested for the presence of a pluripotency marker SSEA-4 prior to the initiation of the differentiation protocol to indicate their pluripotency. A high percentage (80-90%) of all the different starting populations expressed SSEA-4 indicating an ability to differentiate into any type of tissue.

Our derivation method appears to be consistent and reproducible as 12 independent runs yielded similar populations of MSC-like stem cells as judged by their morphology, surface marker expression and functional differentiation, as described in previous studies (Pittenger *et al.*, 1999; Olivier *et al.*, 2006; Pittenger, 2008). It is also supported by the analysis of gene expression in these cells (de Peppo *et al.*, 2010). In each successful run, both replicates (A and B) also showed a closely similar morphology and cell surface marker expression. The cells from other runs of differentiation were rejected due to either fungal contamination or significantly unequal proliferation of replicate A compared to B. This difference could be due to a difference in the number of cells used as the starting population, and these inconsistencies may have occurred particularly in the early phase of this study. In other words, the failure could be attributed to the contamination issue and my personal consistency rather than the method. The data obtained also supports the idea that the cells produced exhibit an MSC-like phenotype and could reasonably be categorized as MSCs. The evidence for this includes a cell morphology and ability to adhere to plastic in culture typical of MSCs, together with a characteristic surface marker and gene

expression profile and their ability to form osteoblast and adipocytes (discussed below; (Pittenger *et al.*, 1999; Dominici *et al.*, 2006; Olivier *et al.*, 2006; Pittenger, 2008).

2.7.1 Surface Marker expression

No single specific and definitive surface marker which defines MSCs and can be used to ensure their homogeneity has so far been described, even though a great number of surface markers have been investigated by different groups in an effort to define such markers (Beyer Nardi & Silva Meirelles, 2006). Deans and Moseley have documented a long list of candidate markers (Deans & Moseley, 2000) but none can be considered a single reliable marker of culture purity. Therefore characterization of cells as MSCs by surface marker depends on examining a combination of markers or a panel of markers selected from those that have been consistently reported to be present (positive markers) or absent (negative markers) in adult MSCs. It is widely accepted that MSCs do not express haematopoietic markers like CD34 and CD45 but that they do express markers like CD13, CD44, CD73, CD90, CD105 and CD166 (Uccelli *et al.*, 2008). The Mesenchymal and Tissue Stem Cells Committee of the International Society for Cellular Therapy (ISCT) has proposed three minimal criteria to define MSCs including certain specific surface markers (Dominici *et al.*, 2006). The committee proposed that the cells must express CD73, CD90 and CD105 and lack expression of CD14, CD34, CD45 or CD11b, CD79α or CD19 and HLA class II. The hESC-MSCs from this study were 70-90% positive for the majority of the proposed positive markers (CD44, CD73, CD105, CD166 and HLA-ABC) and approximately 40% positive for other markers like CD71 and CD90. In addition, they were less than 2% positive for the negative (hematopoietic) markers.

The relatively low population of CD90 (Thy-1; about 42%) suggested that the surface marker profile of hESC-MSCs in this study is not absolutely identical to that reported for MSCs from bone marrow which are usually more than 90% CD90 positive and do not therefore strictly fulfill all of the criteria from the ISCT that define MSCs. In addition, expression of some other markers was lower than in some previous reports on MSCs but these appear in any case to be more variably expressed and depend on the tissue of origin of the cells examined.

For example, CD271 has been found to be more specific to bone marrow derived cells (BÜHring *et al.*, 2007; Jarocha *et al.*, 2008) while CD106 is mix variably expressed in bone marrow derived MSCs, absent in MSC's derived from cord blood but highly expressed in MSCs from adipose tissue (Gronthos *et al.*, 2001; Gang *et al.*, 2004; Niehage *et al.*, 2011). In addition, only a small percentage of the hESC-MSCs population in this study expressed Stro-1. Stro-1 was one of the earliest markers suggested to be associated with MSCs (Simmons & Torok-Storb, 1991; Kolf *et al.*, 2007). It has been used in a very large number of studies on various types of MSCs but most do not report high proportions of Stro-1 positive cells (Lin *et al.*, 2011). So the low population of Stro-1 positive cells in this study is consistent with the majority of previous studies. In summary, since the classification of MSCs is based on a set of markers rather than a single definitive marker, the relatively low expression of certain markers does not necessarily preclude defining the cells produced here as hESC-MSCs.

There are variations in the expression of surface markers among MSCs from different sources (Strioga *et al.*, 2012) even though the main markers (e.g. CD73 and CD105) are relatively constantly expressed (Musina *et al.*, 2005). Differences in the methods used to derive and maintain hESC-MSCs in this study compared to others will contribute to inevitable differences in marker expression between studies (Terada *et al.*, 2002). This is because marker expression is readily influenced by the culture duration and environment. This is a well known issue affecting the comparability of data regarding MSCs between different labs. There are further variables that need also to be considered such as cell density, number of culture doublings, proliferative stage of the cells in culture and other factors that could affect the ability to compare MSCs from different laboratories (Katz *et al.*, 2005; Ho *et al.*, 2008; Pevsner-Fischer *et al.*, 2011; Lee *et al.*, 2013).

A comparison of the surface marker expression of hESC-MSCs tested at passage 1 and passage 3 reveal a highly consistent profile between these 2 different passages which indicates that repeated passaging does not significantly affect the surface marker expression of the cells in this study. There was however a significantly larger population which was positively stained for 2 important MSC markers, *CD13* and *CD105,* in passage 3 as compared to passage 1. This could reflect a larger and more purified MSC population at passage 3 as those cells

which did not acquire MSC features might have failed to attach themselves to the surface and subsequently died. *CD105* is one of the common surface markers for MSCs, and has been used in many studies that have successfully defined MSC populations which are able to form adipocytes, osteoblasts and chondrocytes (Haynesworth *et al.*, 1992; Majumdar *et al.*, 1998; Barry *et al.*, 1999; Pittenger *et al.*, 1999). On the other hand, there was a significant reduction in the population of cells positive for *CD271* at passage 3 compared to passage 1. This could just indicate that this marker is not sustained after repeated passaging rather than indicating any deterioration of MSC features.

2.7.2 Gene expression

Quantitative real time PCR was included as part of the characterization method in order to analyze changes in the expression of a set of genes, including MSC related genes, at a mRNA level at different stages of the protocol. RT-PCR is regard as a useful method for identifying markers for MSCs derived from different sources as they will most likely to exhibit unique genomic profiles (Tsai *et al.*, 2007). By examining the expression pattern of the selected gene markers, we also aimed to determine the effectiveness of our protocol in inducing a mesenchymal lineage specification at an earlier time point than cannot be determined using flow cytometry because of limited cell numbers. The results of the real time PCR demonstrate that the optimized protocol for derivation of MSCs from hESCs promotes a mesenchymal lineage specification pattern as early as day 28. There is significantly decreased transcription of *OCT4* and *NANOG* as the cells progress to become mesenchymal cells. Both are pluripotent genes which are known to be specifically expressed in hESCs (Bhattacharya *et al.*, 2004; Hyslop *et al.*, 2005; Adewumi *et al.*, 2007; Pan & Thomson, 2007). Therefore down regulation of these genes is part of the molecular evidence for commitment towards a mesnchymal lineage in cells of the day 28 and passage 3 samples compared with day 0 samples. Furthermore, *COL1A1* was shown to be significantly upregulated at day 28 and passage 3 which again supports the lineage commitment toward a mesenchymal phenotype which is consistent with a previous study (de Peppo *et al.*, 2010). *COL1A1* is a gene characteristic for mesodermal tissues and is highly abundant in MSCs (Silva *et al.*, 2003). In addition, *Twist1* and *CD105* were also upregulated in day 28 samples providing another sign of mesenchymal lineage commitment. Some studies have shown

that *Twist1* is highly expressed in adult MSCs and these studies also collectively suggested that this transcriptional regulator is a potential key molecular mediator of the maintenance, growth and development of MSCs from different sources (Menicanin *et al.*, 2010). In addition, *Twist1* is regarded as an epithelial-mesenchymal inducing transcription factor and this role is probably more consistent with our finding of a high expression on day 28 which was then downregulated at passage 3. The *twist-1* expression pattern in this experiment may demonstrate epithelial-mesenchymal transition (EMT) around day 28 followed by the appearance of more committed MSCs after repeated passaging and longer time in culture. However, further studies on *twist-1* expression at several time points (before day 28) are probably required before any conclusion can be drawn in relation to EMT in this study. Our test demonstrated that *CD105* is significantly upregulated at passage 3 which indicates a more committed population of MSCs. *CD105* (endoglin) is another consistent marker for MSCs from flow cytometry analysis but previous data at the mRNA level is very limited. *CD105* is a highly expressed surface antigen in MSCs with numerous flow cytometry analyses from several different studies of different types of MSCs in close agreement. This is the first data on *CD105* expression at the mRNA level in MSCs. There is no expression of *CD45* which suggests no undesired differentiation into haematopoetic cells (data not shown). The analysis on CD31 also showed extremely minimal expression at day 28 and passage 3, suggesting no significant endothelial differentiation (data not shown). The negative expression of *brachyury* and minimal expression of *GSC* indirectly support the MSC phenotype. In a previous study, both genes were shown to be raised at early time points i.e. day 7 to 10 of the differentiation period, rather than on day 28 (Lee *et al.*, 2010). Otherwise, further analysis of these early mesodermal genes at several earlier time points (before day 28) are required to determine their expression pattern. It is important to note that an absolute comparison between different genes is not possible due to the differences in efficiency of the respective primers and probes.

2.7.3 Cells growth kinetics

In practical terms, the ability of the cells to continue growing up to passage 20-30 is a vital property since it suggests that they could be produced in large amounts compared to MSCs from adult sources which are associated with low

numbers upon isolation and limited life span in culture. In general all cells from the 12 different runs in this study reached confluency after 3-4 days in culture with a starting density of 1 X 10^4 cells/cm^2 (plated in T-25 cm^2). This indicates that a starting population of 2.5 X 10^4 of hESC-MSCs could potentially generate up to 1 X 10^{16} cells and this quantity of cells would be much more difficult to attain from BM-MSCs as they can stop growing as early as passage 7 (Kern *et al.*, 2006). In another study on BM-MSCs it was reported that the same starting density i.e. 1 X 10^4 cells/cm^2, generated only between 1 X 10^8 to 1 x 10^{11} cells although since no information on flask size was given a direct comparison is not possible (Wagner *et al.*, 2008). A more careful analysis of proliferation capacity of the cells prepared in this study using the population doubling time demonstrated a fairly consistent and only very slowly increasing mean population doubling time up to around passage 26 when the time significantly increased, suggesting a significant reduction in proliferation (Figure 2-11). A serial comparison of mean PDT indicated a significant increase of PDT by passage 13 to 18 compared with passage 3 to 8 but the values were still relatively low in comparison to the BM-MSCs, which may to stop growing as early as passage 11-12 (Jin *et al.*, 2013). The hESC-MSCs derived in this study display a shorter and consistent population doubling time in the first 13 passages (40-50 hours and P value of mean P3-P8 vs P8-P13 was not significant) (Figure 2-12) compared with MSCs from bone marrow which has been shown to increase significantly after passage 6 (Lu *et al.*, 2006). This indicates a better preservation of proliferation capacity by hESC-MSCs. Several reports have highlighted the high proliferation potential and self renewal capacity of the MSCs as an important property for biomedical applications (Colter *et al.*, 2001; Lee *et al.*, 2006; Pricola *et al.*, 2009). In a recent study, the proliferation rate was reported to be associated with a better functional regenerative potential (Deskins *et al.*, 2013). Deskins *et al* claimed that when transplanted into a murine tissue wound model, cells with a better growth rate and cell viability in culture were able to create better vascularized granulation tissue and more longer graft survival. Therefore based on their proliferation capacities, hESC-MSCs offer better therapeutic potential compared to adult MSCs.

2.7.4 Senescence

Studies have shown that the biological properties of adult MSCs are not everlasting and will gradually diminish with time (Kretlow *et al.*, 2008). The deterioration is largely attributed to replicative senescence. Senescent cells are live cells which stop dividing in culture (Campisi & d'Adda di Fagagna, 2007). There are many factors which have been identified as a cause of senescence such as irreversible DNA damage, reactive oxygen species (ROS) and shortening of telomeres (Mamidi *et al.*, 2012). In our study, the hESC-MSCs could be passaged up to passage 20-30 before noticeable development of senescent features i.e relatively larger cells and positive staining for Senescence Associated ß-Galactosidase. As observed in this study, an increase in the percentage of cells positive for this marker was associated with a decrease in proliferation capacity (see section 2.6.4 and 2.6.5). However, the percentage of cells showing the senescence marker at late passages is relatively low in comparison to adult MSCs (Stenderup *et al.*, 2003; Wagner *et al.*, 2008; Heo *et al.*, 2009) suggesting a slower development of senescence in hESC-MSCs. In a study of MSCs from bone marrow, 20-30% of cells were found to be senescent as early as passage 6-10 (Stenderup *et al.*, 2003). Studies in adult MSCs at passage 9-10 have also revealed 50-80% senescent cells (Stenderup *et al.*, 2003; Wagner *et al.*, 2008; Heo *et al.*, 2009). The low percentage of senescent hESC-MSCs at late passages indicates a longer life span and is another advantage of these cells which may contribute to providing a better quality and higher volumes of cells for clinical application.

2.7.5 Re-characterization after cyropresevation

The future clinical application of hESC-MSCs would require expansion and cryopreservation before preparation for cell transplantation. Previous studies have demonstrated that cryopreservation for a single time using 10% DMSO, as in this study, should not affect the viability and functionality of MSCs from bone marrow and adipose tissues (Pittenger *et al.*, 1999; Kotobuki *et al.*, 2005; Liu *et al.*, 2008). This has not so far been studies for hESC-MSCs. When cryopreserving, the freezing solution is routinely supplemented with DMSO in order to protect the cells and their membranes from damage. In principle, the cryopreservation and thawing process may have important effects on all aspects of cellular

phenotype (the cell's morphology, viability, growth profile, gene expression and differentiation capabilities). Therefore, cells from 5 different runs which were selected to be used for transplantation were re-characterized in order to show that the onetime cryopreservation of hESC-MSCs does not affect their biological and functional properties.

2.7.5.1 Morphology

This study revealed that all hESC-MSCs which were examined after cryopreservation showed the typical elongated and spindle shaped morphology and strong adherence to plastic surfaces which is the most obvious evidence of retention of MSC-like features (Figure 2-19).

2.7.5.2 Surface marker expression

The pattern of expression of surface markers in the hESC-MSCs post-thawing was consistent to that before cryopreservation suggesting that repeated passaging and onetime cryopreservation does not affect these indicators of phenotype. Comparison of flow cytometry data for passage 3 (prior to cryopreservation) with that for passage 3+5 (5 passages after thawing) show fairly consistent expression of the positive cell surface markers tested (the only difference being for CD34) (Figure 2-25). In addition, the consistency of certain MSC markers like CD166 excludes the possibility of transformation into fibroblast as low CD166 expression has been associated with contamination with fibroblast like cells (Haflon *et al.*, 2011).

2.7.5.3 Growth kinetics

The hESC-MSCs derived in this study retain the ability to grow with an exponential growth pattern after being thawed and re-cultured (Figure 2-20). Analysis of population doubling time revealed a shorter and more consistent population doubling time in cells which had been cryopreserved (Figure 2-21, Figure 2-22, Figure 2-23). While the data confirm the ability of the hESC-MSCs to retain their growth capacity, other factors might have contributed to improving the population doubling time in the cryopreserved samples such as unintentional use of a lower initial plating density and final density when passaging the cells. Although it was not systematically investigated, it was observed that a higher

initial plating density and a more confluent state tended to reduce proliferation capacity and result in a relatively longer population doubling time for cells in culture. This is consistent with previous reports that MSCs in low density cultures contain a subpopulation of rapidly self-replicating cells that lead to a better capacity to generate more cells as compared to MSCs in high density cultures (Digirolamo *et al.*, 1999; Colter *et al.*, 2001; Smith *et al.*, 2004; Lee *et al.*, 2006).

2.7.5.4 Gene expression

Gene expression analysis was performed on samples collected from 5 different cells isolates, 1C, 4C, 7C, 9C and 13C, after they were recovered from liquid nitrogen and re-cultured up to passage 3+5 to be used in transplantation. This revealed results consistent with those seen at passage 3. The cryopreserved cells appear to retain the higher expression of MSC markers and lower expression of pluripotency markers that distinguish them from the hESCs. The consistent gene expression before and after cryopreservation shows it is not affected by the cryopreservation process and this is consistant with previous studies on adult MSCs (Mamidi *et al.*, 2012). Apart from suggesting maintainance of MSC-like features, the consistent expression of MSC-related genes in the cryopreserved cells may also be important for therapeutic application. For instance, the expression of CD105 is associated with a better healing performance in cardiac regeneration (Gaebel *et al.*, 2011). In this study, the transplantation of CD105 purified MSCs into an animal model of myocardial infarction resulted in significant preservation of left ventricular function compared with animals that received low CD105 MSCs.

2.7.5.5 Functional differentiation

In addition to other parameters like cell morphology and surface marker expression, functional differentiation remains as the gold standard for characterizing MSCs in culture. Many groups working on MSCs regard the ability of cells to differentiate into bone, fat and cartilage as necessary properties for defining the cells as MSCs (Bruder *et al.*, 1997; Digirolamo *et al.*, 1999; Pittenger *et al.*, 1999; Muraglia *et al.*, 2000; Barry *et al.*, 2001). Adipogenic and osteogenic differentiation were performed on 5 different isolates of our cells,

subsequently used for transplantation, in order to determine their differentiation potential. The tests were performed using samples at passage 3+5 (i.e. after being passaged 5 times following thawing). All tests showed a positive outcome with the formation of both adipocytes and osteoblast after induction in appropriate differentiation media for 3 weeks. This finding is consistent with the outcome of the functional differentiation study on hESC-MSCs derived by Olivier and colleagues (Olivier *et al.*, 2006), as well as other studies performed on adult MSCs (Pittenger *et al.*, 1999). Consistent with the report by Olivier et al (2006), the SWH method in our study seemed to promote better adipogenic differentiation with more and larger vesicles (Olivier *et al.*, 2006; Olivier & Bouhassira, 2011) compared to the classical IBMX method (Pittenger *et al.*, 1999; Colter *et al.*, 2001; Neubauer *et al.*, 2004; Sekiya *et al.*, 2004). The SWH method was developed based on the finding that hypoxia enhances lipid accumulation and FGF enhances PPAR-γ ligand-induced adipogenesis of MSCs (Wada *et al.*, 2002; Neubauer *et al.*, 2004). Following osteogenic differentiation, a large proportion of cells showed a homogenous red staining with Alizarin Red S indicated that osteoblasts were formed. In summary, our results show that hESC-MSCs can be differentiated into osteoblasts and adipocytes even after cryopreservation. Due to time limitations in our study, we could not explore the ability of our cells to form chondrocytes but there is a high possibility that they would form chondrocytes as there have been numerous studies describing the derivation of MSCs from hESCs with the ability to form chondrocytes (Barberi *et al.*, 2005; Boyd *et al.*, 2009; Gruenloh *et al.*, 2011; Wu *et al.*, 2013)

2.8 Conclusion

We were able to derive MSC-like cells from hESCs after 28 days of differentiation followed by repeated passaging for 10-15 days. The differentiation method used in this study is shown to be reproducible based on several successful runs of differentiation producing closely similar population cells in two replicates. The hESC-MSCs from this study grew very robustly, adhered to a plastic surface, have several MSC related surface markers including some of the main MSC markers like CD73 and CD105, express MSC-related genes and are able to form adipocytes and osteoblast. Re-characterization data indicate that our hESC-MSCs retain

their MSC properties and the ability to grow robustly after being cryopreserved which further enhances their potential for therapeutic application.

Chapter 3

Therapeutic effects of hESC-MSCs transplant following spinal cord injury

3 Therapeutic effects of hESC-MSCs transplant following spinal cord injury

3.1 Introduction

The use of MSCs in the treatment of SCI is considered promising because they have been reported to promote functional recovery by different mechanisms promoting axonal remyelination and regeneration, reducing neural inhibitory molecules, reducing the lesion volume and increasing the spared surviving tissues (Hofstetter *et al.*, 2002; Bizen *et al.*, 2003; Sasaki *et al.*, 2009; Boido *et al.*, 2012). Furthermore, MSCs are considered to have immunomodulatory effects which may contribute to an environment that is permissive for axonal extension and functional recovery (Hawryluk, 2012; Nakajima *et al.*, 2012). However, most studies have used MSCs from bone marrow which have some limitations that could limit their use in the clinical setting. They are reported to be associated with low proliferation, limited life span and gradual loss of stem-like properties during *in vitro* expansion (Ringe *et al.*, 2002) and other limitations which have been discussed previously (in Chapters 1 and 2). Because of these limitations other sources of MSCs may be more useful for clinical applications. Amongst the other potential sources of MSCs are hESCs and several studies have demonstrated successful derivation of MSCs from hESCs. These cells could circumvent some of the limitations of adult MSCs including variability, limited proliferation capacity and the need for invasive procedures. However, MSCs derived from hESCs have never been tested in animal models of SCI.

A cervical contusion injury model was chosen in this study as this model is the most clinically relevant (Zhang *et al.*, 2008; Anderson *et al.*, 2009), occurring most frequently in human injuries and closely reflecting the sequelae seen in clinical cases. At the experimental level, the Infinite Horizons device allowed the injury to be performed consistently and without the level of variation seen with other injury models. Additionally this type of injury has the added advantage of allowing the assessment of the corticospinal tract as it has been shown to completely interrupt the main dorsal column component of the corticospinal tract (Riddell and Toft, unpublished observations) when a force of 175 kdyn was applied to C6. As well as contusion injury, dorsal column lesions (wire-knife) were also performed in a small group of animals in order to

selectively examine the regeneration of primary sensory axons. This partial transection model is useful for the assessment of axonal regeneration across the lesion site (Martinez *et al.*, 2009).

The aim of the work in this chapter was to determine whether hESC-MSCs transplanted into an animal model of spinal cord injury could promote repair through different mechanisms reported in studies using adult MSCs. It was also hypothesized that based on a better proliferation capacity compared to BM-MSCs, that hESC-MSCs might even demonstrate additional properties.

3.2 Materials and Method

3.2.1 Cell preparation for transplantation

3.2.1.1 Preparing cells for surgery

On the day of transplantation, the cells to be transplanted were observed under the light microscope to assess the general appearance and confluency (80% confluency was expected and was achieved in all different sets of transplants). The cells were trypsinised according to the usual protocol where the old media was removed and the cells were washed with PBS. TrypLE Select (Life Technologies) was then added to the cells in the flask and the flask placed in the incubator at 37ºC and 5% CO_2 for 5-6 minutes. After 5-6 minutes, the flask was taken out and was gently tapped to detach the cells from the flask surface. Once the cells were detached and dissociated, they were filtered through a 70µm cell strainer into a 50ml falcon tube and were counted using a haemocytometer (see Chapter 2, section 3.2.4). The cells were then spun down at 1200 rpm for 3 minutes and the supernatant discarded. The cells were re-suspended in 100µl of fresh media and transferred into a small sterile 200µl eppendorf tube. The eppendorf was again centrifuged at 1200 rpm for 3 minutes. After re-centrifugation, the remaining supernatant was carefully removed from the cell pellet. Depending on the cell concentration (cells count), the cells were again re-suspended in 50-100 µl of fresh media. The cells in the tube were placed on ice and transported to the CRF for transplantation. The typical time from preparation of the cell suspension to transplantation ranged from 10-20 minutes.

3.2.2 Animal surgery

All experimental procedures carried out on animals were approved by the Ethical Review Panel of the University of Glasgow and performed in accordance with the UK Animals Scientific Procedures Act 1986 under the restrictions and regulations stipulated by the relevant Home Office personal, project and site licenses. All injury and transplantation surgery were performed by Dr John Riddell with the assistance of my colleagues Dr. Syed Hamid Syed Habib (PhD student) or Mr Andrew Toft (research assistant) or myself and the animal house technical staff. The observations reported in this chapter are based on investigation of 101 male Sprague Dawley rats. Of these 101 animals, 4 were non-lesioned animals from which normal data was obtained for comparison with lesioned and transplanted animals. 3 animals were non-lesioned and were transplanted with hESC-MSCs. 73 rats were subjected to a cervical contusion injury and were allowed to recover for 3 weeks. Of these, hESC-MSCs were transplanted into 49 animals. The remaining 24 contusion injury animals were not transplanted with cells. Finally, a further group of 21 animals were subjected to dorsal column lesions at L5/L6 with conditioning lesions being performed concurrently on 7 of them. All these 21 animals were acutely transplanted with hESC-MSCs into the lesion site.

All of the animals used were treated with daily cyclosporine from 2 days prior to transplant until the end of procedure, except the non-lesioned animals and a few animals that were subjected to contusion injury only.

3.2.3 Perioperative care

Animals subjected to surgery were administered 1ml/kg saline (Baxter Healthcare, UK) to prevent dehydration and 0.3mg/kg. Buprenorphin (vetergesic®; Alstoe Animal Health, UK) were given to control acute pain due to the surgical procedure. Lacrilube eye ointment was applied to prevent dryness during the procedure.

All the above mentioned drugs were administered in all operations: contusion injury, dorsal column injury, delayed cell transplantation and tracer injections.

3.2.4 Contusion injury

Rats were anaesthetised by induction with 5 % isofluorane in oxygen followed by 1-2% for maintenance. The fur overlying the target area was shaved and the skin was treated with 20% chlorhexidine solution (ECOLAB). For this particular type of injury, the contusion targeted the C6 segment. The overlying skin was then incised followed by dissection of the muscles to expose the cervical vertebra. A dorsal laminectomy was carefully performed by removing the C5 and C6 vertebrae to expose the spinal cord without damaging the dura layer. Subsequently, the vertebral column was held stable by clamping the C4 and C7 vertebrae using Adson's forceps. After C6 was identified, a 175 kilodyne contusion injury was performed using the Infinite Horizon (IH) impactor device (Precision System & Instrumentation, LLC, Nottinghill, US, Figure 3-1 and 3-2). This is a microprocessor controlled force feedback device which is capable of producing injuries at different levels of severity following the pre-set force combined with a high degree of consistency. When activated, the device lowered the impactor tip at approximately 120 m/s to contuse the spinal cord until the 175 kilodyne force was reached and it then immediately retracted.

A suture 10-0 (Ethicon) was then placed in the dura mater at the injury level to allow accurate identification during the subsequent cell transplantation three weeks later. Finally, wounds were closed in layers.

3.2.5 Delayed cell transplantation

49 animals underwent a further operation 3 weeks after the contusion injury was performed in order to transplant cells. 2 days prior to procedure, all the animals were started on cyclosporine (20mg/kg), subcutaneous, Norvartis) which was continued daily until the end of the procedure, except in 6 animals which were used to establish that immunosuppresion was required to promote survival of the transplanted hESC-MSCs.

Some degree of fibrous scar was usually observed over the contusion injury site but the surgeon was able to identify the injury location by localising the 10/0 non-absorbable (silk) sutures previously placed on either side of the lesion. In addition to that, the lesion site could also be identified from its visible relatively

darker area. Cell suspensions were concentrated to approximately 200,000 cells/µl and injected into the injury cavity site using a bevelled glass pipette of appropriate diameter (55µm-70µm) which was mounted on the microdrive of an arc manipulator and inserted into the lesion through a slit in the dura. The tip of the pipette was lowered to a depth of approximately 1000µm-1200µm. Cells were then carefully injected by applying brief (20-40 ms) pressure pulses (Picoinjector, WPI, Sarasota FL, USA) over several minutes as the pipette was gradually raised upward. The cells injection would be performed until they overflowed out of the lesion which usually required up to 40µl of suspension for each single animal, equivalent to approximately 8 $X10^6$ cells per animal. Wounds were closed in layers and analgesic was given.

3.2.6 Cortical tracer injection

4 weeks after cell transplantation (2 weeks prior to perfusion), 10 animals which had received C6 contusion injuries were then subjected to a tract tracer injection (BDA; 10,000 MW, product no. D-1956, Life Technologies) in order to label the corticospinal tract. The tracer was prepared by preparing a solution of 20% BDA in 0.1 M phosphate buffer (PB) with 2% fast green dye to detect spillage, (R.A. Lamb supplies, UK; product 42053). All of the cortical BDA tracer injections were performed by Mr. Andrew Toft with assistance from myself. The scalp was incised and a small window was drilled through the skull to expose the right sensorimotor cortex using bregma as an anatomical landmark for reference point (Figure 3-3). The BDA was injected using pressure injection through a fine glass pipette (tip diameter 30-40µm) into 10 injection sites in a grid pattern ranging from 1mm rostral of bregma to 2mm caudal and up to 4mm laterally. Approximately 300nl of BDA was delivered at each injection site. The pipettes were introduced in turn at each injection site to a depth of 1.8mm below the surface of the cortex and the BDA was continuously injected as the pipette was raised to 1.0 mm depth. The pipettes were then maintained at this depth for 1 minute before they were removed from the cortex. The scalp incision was then sutured and closed

3.2.7 Dorsal column lesion (wire-knife)

Animals were anaesthetised and maintained as described previously (see section 3.2.5). The lumbar spinal cord was exposed and a dorsal column lesion was made at the L3/L4 spinal segmental border. The location was identified based on the vicinity to the T13 and L1 vertebral junctions. The lesion was performed using a wire knife (David Kopf Instrument, Tujunga, USA; Figure 3-4(A)) made of a 100 µm diameter tungsten wire ensheathed within a Teflon cannula so that when the wire was protruded from the cannula, it coiled to form an arc. The wire knife was mounted on a manipulator arc fitted with a stepper motor and then inserted through a slit in the dura at approximately 700 µm to the left of the spinal cord midline and lowered to a depth of 950 µm. At that position, it was protruded to form a 1.5mm diameter arc under the dorsal columns. This was then raised against a glass rod placed on the surface of the cord to transect the dorsal columns without damaging the surface blood vessels (Figure 3-4 (B-C)). To ensure the most superficial fibres were transected while preserving the integrity of the dorsal vein, a pointed cotton bud or glass rod was pressed into the arc created by the wire knife for approximately 20 seconds. This manoeuvre was found to produce an accurate and reproducible lesion of the dorsal column white matter. After retracting the wire knife into its sheath and raising it out of the spinal cord tissue, it was rotated 180 degrees. The wire knife was re-inserted again into the spinal cord through the same slit in the dura to a depth of 850-900 µm and another lesion was performed extending the original dorsal column lesion to include the extreme left portions of the dorsal columns.

3.2.8 Conditioning lesions

Conditioning lesions were performed on 7 of the 15 animals subjected to dorsal column lesion. Immediately after the wire knife lesion was made at L3/L4, the left sciatic nerve was exposed at a mid-thigh level and isolated from surrounding tissues. The nerve was then ligated and cut at approximately 2-3mm distal to the ligature. The wounds at the thigh were closed with 3-0 vicryl.

3.2.9 Acute cell transplantation

Animals that received a dorsal column lesion were acutely injected with the cells into the lesion site using a glass pipette of appropriate diameter (55µm-

70µm). The glass pipette was filled with thick suspension of cells (100,000 cells/µl). It was then mounted on a stereotaxic arc and inserted into the lesion through a slit in the dura at 15° on each side. The tip of the pipette was lowered to a depth of approximately 1000µm-1200µm and the cells were then carefully injected by applying brief (20-40 ms) pressure pulses (Picoinjector, WPI, Sarasota FL, USA) over several minutes as the pipette was gradually raised upward. Cells were injected until they could be seen to overflow out of the lesion site which usually required between 30 to 36µl of cells suspension. Wounds were then closed in layers.

3.2.10 Spinal nerve tracer injection

4 weeks after cell transplantation (2 weeks prior to perfusion date), all the animals receiving dorsal column lesions were subjected to another operation to inject the tract tracer biotin dextran amine (BDA; 10,000 MW, product no. D-1956, Life Technologies) into L4 and L5 spinal nerves (Figure 3-5). Both targeted spinal nerves were exposed outside the vertebral column at the level of the tip of the iliac crest. Then the BDA was injected into each spinal nerve through a glass pipette with a bevelled tip (internal diameter around 50µm). Approximately, 3-4µl was injected using repeated 40 ms pressure pulses.

3.2.11 Cells transplantation into normal spinal cord

In addition to the injured animals, cells were also injected into the spinal cords of 3 uninjured animals to assess the interaction between the cells and host tissue in the absence of an injury. This group of animals was also treated with cyclosporine at 2 days prior to cell transplantation daily until the end of the procedure. The animals were anaesthetized and a laminectomy was performed (as described in 3.2.4). Cells were concentrated at approximately 100,000 cells/ µl and pressure injected using glass pipettes into 5-6 injection sites in the spinal cord (C5-C6). 1µl of cells were injected at each site and the injection sites were located lateral to the midline on the left and right sides of the cord at an angle 25° pointing medially (3 sites on left and 2-3 sites on right).

3.2.12 Perfusion and histological processing

In total 92 animals successfully reached the end of the procedure and were perfused and fixed, while 9 animals were perfused earlier due to autophagy of the hindlimb. These 9 animals were excluded from the study. The remaining animals were perfused at the following time points, depending on the experimental aims:

1. To assess the appearance of the spinal cord in normal animals, 4 non injured animals were perfused as normal controls.

2. To assess the direct interaction between the transplanted hESC-MSCs and host astrocytes, 3 uninjured animals that received cells were perfused at 1 week post transplant.

3. To assess the lesion cavity appearance corresponding to the post injury time at which cells were transplanted, 6 injured animals which did not receive any cells were perfused 3 weeks after the injury.

4. To assess the survival, migration and differentiation of transplanted cells- 3 animals were perfused at 5 days post-transplantation, 3 animals at 2 weeks post-transplantation, 3 animals at 4 weeks post-transplantation and 5 animals at 6 weeks post- transplantation. Additionally, in order to assess the effect of immunosuppression on cell survival, 6 animals which were not treated with cyclosporine were perfused at 3 different time points: 2 animals at 1 weeks post-transplantation, 2 animals at 2 weeks post-transplantation and 2 animals at 4 weeks post-transplantation.

5. To assess the proliferation of transplanted cells– 3 animals were perfused at 5 days post-transplantation, 2 animals were perfused at 2 weeks post transplantation and 1 animal at 6 weeks post transplantation.

6. The remaining animals were perfused for various other aims: the cells' ability to fill in the injury cavity, extracellular matrix formation, promotion of angiogenesis, and effects on astrogliosis in response to injury, promotion of

axonal regeneration and evidence of myelination. They were all perfused at 6 weeks post transplantation.

In order to avoid any potential problems associated with differences between cell isolates and the possibility that observation might be specific for one batch of cells, we attempted to examine each of the issues using transplants of at least 3 different cell isolates. The animals were anaesthetised and injected intraperitoneally with 300 mg sodium pentobarbital (Euthatal, 200mg/ml, Merial Animal Health Ltd, UK). They were perfused through the left ventricle with gravity fed mammalian Ringer's solution which contained 0.1% lidocaine until the liver became relatively clear. The animal was then immediately perfused with 1 l of 4% paraformaldehyde in 0.1 M phosphate buffer, pH 7.4. Subsequently, relevant parts of spinal cord were removed after identification of the injury site using the distinct brownish scar on the dorsal surface of the cord, as well as the 10/0 marking suture close to it. For the dorsal column lesioned animals, the lesion site was verified as being located at or just rostral to the L4 dorsal root entry zone. This was done by locating the L4 and L5 dorsal root ganglia and then following the L4 and L5 dorsal roots proximally to the L4 and L5 spinal cord segments.

From each animal, a portion of spinal cord of approximately 18 mm in length was extracted and immersed overnight in the same fixative solution with the addition of 30% sucrose for post-fixation and cryoprotection. The next day, the cord was prepared for cutting tissue sections. The cord would initially be segmented into approximately 6 mm length tissue blocks which spanned the lesion site. Whenever required, a 6mm tissue block rostral and caudal to the lesion block would also be prepared to provide more information on the extent of the transplanted cells distribution.

Tissue blocks were cut into 60 µm sagittal sections (transverse sections for normal transplanted animals) on a cryostat and washed in 0.1 M phosphate buffered saline before being incubated in 50% ethanol for 30 minutes. They were then washed 2-3 times in phosphate buffered saline 0.3 M (double salt PBS) followed by incubation at 4ºC for 72 hours in various combinations of the primary antibodies as listed in the table 3.1:

Antibody	Catalogue Number	Species	Specificity	Supplier	Concentration	function
GFP	AB13970	chicken	all fluorescent protein made by Aequorea victoria	Abcam	1:1000	to label transplanted cells
NF200	N0142	mouse	Human, monkey, pig,rabbit, hamster, rat, mouse	Sigma	1:1000	to label axon intermediate filaments
NF200	N4142	rabbit	wide species (including pig and rat)	Sigma	1:1000	to label axon intermediate filaments
GFAP	Z0334	rabbit	human, cow, cat, dog, mouse, rat, sheep	DAKO	1:1000	to label astrocyte intermediate filaments
GFAP	G3893	mouse	human, pig, rat	Sigma	1:1000	to label astrocyte intermediate filaments
Laminin	L9393	rabbit	human, mammal, avian, reptilian , amphibian source	Sigma	1:100	to label extracellular matrix basal lamina protein(laminin)
NeuN	MAB377	mouse	avian, salamander, chicken, ferret, human, mouse, porcine	Millipore	1:1000	to label neuronal nuclei
SMA	A5228	mouse	human, rabbit, rat, mouse, bovine, frog, goat, guinea pig, dog	Sigma	1:400	To label endothelial smooth muscle in blood vessels
ED1/CD68	MCA341R	mouse	rat	AbD Serotec	1:400	to label macrophages/microglia
Nestin	MAB358	mouse	mouse and rat (not human)	Millipore	1:400	to label reactive astrocytes
Ki67	ab15580	rabbit	mouse, rat, sheep, rabbit, horse, cow, dog, human	Abcam	1:500	to label proliferating cells
CASPR	ab34151	rabbit	mouse, rat, human	Abcam	1:500	to label paranodal junctions

Table 3-1. List of primary antibodies used to stain different targeted structures

The tissues from animals which were subjected to spinal nerve or cortical tracer injection were stained with streptavidin conjugated to the Alexa fluor 568 fluorophore (1:1000) which was substituted for one of the primary antibodies, in order to detect the BDA in traced axons.

After incubating for 72 hours, the tissue sections were again washed 3 times for about 10 minutes each in double salt PBS and incubated for 3-4 hours at room temperature with appropriate species specific secondary antibodies: Alexa 488 (1:500), Rhodamine (1:100), and Cy5 (1:500). All antibodies were diluted in PBS double salt with 0.3% Triton X-100. After incubation in secondary antibodies, sections were rinsed in PBS double salt 3 times for 10 minutes each to remove excess antibody. The sections were finally mounted on glass slides in anti-fade medium (Vectashield; Vector laboratories) to be observed under the microscope. For long term storage, all tissue slides were stored at -20ºC.

3.2.13 Post-processing analysis

3.2.13.1 Preliminary analysis on all sections

In general, all sections were examined using a Nikon Eclipse E600 epifluorescence microscope (Nikon, Japan) before selected sections were scanned using either a Bio-Rad Radiance 2100 or Zeiss LSM 710 confocal system using X20 or X40 (oil immersion) objective lenses. Laser excitation lines used for scanning included combinations of the following: 405 nm (blue diode, far violet), 488 nm (argon ion, blue), 543 nm (helium-neon, green) and 637 nm (red diode, red). Tissue was scanned as a single field of view or tiled composite of multiple fields depending on which features were to be illustrated. All sections were scanned through the full thickness of stained tissue, accumulating a series of z-section stacks with z spacing intervals from 0.5 to 2µm. Stacked images were projected into 2D builds using either Image J software (NIH, USA) or Zeiss Zen software (Zeiss, Germany). Images were exported to Adobe Photoshop CS6 (Adobe Systems, USA) and prepared for illustration by making minor changes to brightness and contrast.

3.2.14 Appearance in normal animals

Tissue sections were stained with 3 different combination of primary antibodies: GFAP and nestin, SMA and laminin, and ED1 and Ki67. 1 or 2 sections from close to the midline from these different combinations, were selected to be compared with injury sections at a similar location. The selected sections were then scanned using Zeiss LSM 710 confocal microscope.

3.2.15 Survival and distribution of transplanted cells

Cell survival was only assessed in animals receiving transplants in which GFP expression in the cells was 60-90% as determined prior to transplantation (see Chapter 2, section 2.4.3). Sections from animals perfused at different time points after transplantation were examined using a ZeissAxioplan 2 epifluoresce microscope to view GFP-Alexa488. Selected sections were scanned using confocal microscopy. Selected sections from animals that were not treated with cyclosporine were also examined to determine the survival of GPP labelled cells as well as to examine the co-localization of nestin and GFAP.

Additionally, all of the transplanted animals processed 6 weeks after transplantation (irrespective of GFP labelling level) were closely examined to document the distribution of the cells in relation to the injury area. A few sections from close to the midline and therefore also corresponding to the middle of the injury site were chosen from each animal. From observation of these sections the cell distribution within the injury was placed into three categories: 1) animals containing cells occupying most (>50%), of the injury area 2) animals in which cells partially occupied the injury area (25 - 50%) or 3) animals with a minimal region of cells (<25%). The presence of cells outside the injury area was also documented including whether they occurred rostrally and /or caudally and whether they formed solid tracks of cells or were scattered in distribution.

3.2.16 Proliferation and differentiation of transplanted cells in vivo

In order to determine whether the transplanted cells continue to proliferate in vivo, tissue sections stained with Ki67 were examined for any co-localization of Ki-67 labelling with the GFP labelled transplanted cells with particular emphasis on early time points after transplantation i.e. 5 days. The evidence for Ki-67 labelling in other types of cells was also determined by looking for co-localization with ED-1 (macrophage/microglia), GFAP (astrocyes) and NeuN (neurons). All sections from each animals were carefully reviewed under the fluorescence microscope and sections containing both GFP labelled cells and Ki67 immunoreactivity were selected for confocal microscopy (x20, multiple field views, 30-40 z sections). Areas of interest identified in these low power confocal images were then imaged at higher power (X40, 40-48 z sections). The area of interest was carefully scanned i.e. with spectral separation, at Z depth that would resolve multiple sections through to the structure of interest and without fluorescent flare. These aspects are very crucial to determine a potentially genuine co-localization if the labelled structures are in the same z-plane or not and was achieved by the assistance of more experienced operator, Andrew Toft. The extent of any co-localization was finally semiquantitatively determined by selecting multiple nuclei labelled with one fluorophore and the other colour channel was then checked to see if it also labelling the same structure of interest. This was performed using Zeiss Zen software. The co-labelling of colour channels on the same structure i.e. nuclei suggesting potential co-localization without depending on the number of pixels detected but would give a simple yes or no answer. The examination was further verified on the selected single z stack in the Image J software.

To examine the ability of transplanted hESC-MSCs to differentiate *in vivo*, the typical morphology of the GFP labelled cells were examined at different time points i.e. from 5 days post transplantation up to 6 weeks post transplantation. Any similarities or differences were determined using confocal microscopy at high power (X40 or greater). In addition, any similarities or differences were also determined between 3 different cells isolates of hESC-MSCs that were used for transplantation. The GFP labelled cells were also examined for any co-localization with other markers which are not typically expressed by MSCs such

as GFAP, NeuN, P75, Nestin, SMA, Laminin and NF200 which would suggest phenotypic changes and possible differentiation into other types of cells.

3.2.17 Secretion of extracellular matrix and promotion of angiogenesis

The ability of transplanted hESC-MSC to secrete extracellular matrix was examined using sections stained for laminin and were compared with tissues from non-transplanted animals. The laminin distribution within the cell-filled cavities was compared with the infilled cavities of non-transplanted animals.

The ability of the transplanted hESC-MSCs to promote angiogenesis was determined by examining the distribution of blood vessel (SMA) labelling within the transplant sites compared with the distribution within the matrix infilling of non-transplanted animals.

3.2.18 Effect of transplanted cells on host tissue astrocytosis

The glial reaction was assessed in normal (non-injured) transplanted with cells as a small bolus to determine the effect of transplanted cells with host astrocytes. This was assessed by examining the Nestin and GFAP appearance around the GFP labelled cell in normal animals so that the reaction to the injury did not complicate the assessment.

In addition, the glial scar surrounding the transplant area in sections from transplanted animals was compared with that around the injury in non-transplanted animals.

3.2.19 Quantitative analysis of injury/cavity

3.2.19.1 Measurement of the injury size

An attempt was made to quantify the injury dimensions of 3 week survival control animals (corresponding to the timing of cell transplants), 9 week survival control animals (corresponding the end of procedure for transplanted animals) and transplantated animals. Each section from each animal was observed using a fluorescence microscope and the section (near the midline) with the largest

injury site (i.e. cavity in case of non-transplanted animals and glial scar and/or other markers in case of transplanted animals) was selected for confocal imaging. The selected section was scanned as a tiled 2 field view (2 X 1) at X4 magnification through 1-3 z sections. The length of the injury/cavity was then measured in photoshop based on a known scale factor. The rostral and caudal margins of injury cavities and injured tissue (judged by GFAP immunolabelling or other markers and lack of normal tissue integrity) were drawn using the ruler facility in Photoshop. From this the length of the injury and the length of injury that had become a cavity were determined by multiplying with the known scale factor. In addition, the maximal width of the injury was calculated by counting the number of (sagittal) sections in which areas of injured tissue occurred and multiplying this by 60 (section thickness).

3.2.19.2 Measurement of the extent of glial reaction

To obtain an indication of the effect of cell transplants on the astroglial reaction, the thickness of the glial reaction (glial scar) surrounding the injury region in both transplanted and non transplanted animals was estimated. In addition the glial reaction in non-transplanted animals at the 3 week and 9 week postinjury time points was compared. This analysis was performed using the confocal images acquired to measure the injury cavity and transplanted injury site dimensions. However, further selection of these images was performed to exclude animals in which GFAP staining was not optimal and to select those animals where there were no cells or minimal numbers of cells extending out of the injury area. Animals with large numbers of cells immediately outside the injury were excluded because of the glial reaction that the cells were shown to produce whan injected into normal tissue. Measurements of the width of the glial reaction were made on 3 sides of the injury/cavity; rostrally, caudally and ventrally. The widest region of each of these sides was measured using the ruler in photoshop CS3 and multiplied with a known scale factor.

3.2.20 Interaction of transplanted cells with host tissues outside the injury site

Tissues with tracks of cells caudal or rostral to the injury were selected and examined to see whether the GFAP labelling suggested mingling of the

transplanted cells with host astrocytes or that the astrocytes were displaced and walled off from the transplanted cells.

3.2.21 The ability of cells to provide a substrate for regeneration of dorsal column axons

In order to determine the ability of transplanted cells to support axonal regeneration of ascending dorsal column fibres, sections from dorsal column lesioned animals were examined for evidence of axonal regeneration by observing the extent of BDA labelled fibres. Sections with good BDA labelling and close to the midline were chosen for further analysis with the confocal microscope at X20 (tile 6 X3 to 12 X6) to verify the extent of the axonal regeneration.

3.2.22 The ability of cells to provide a substrate for regeneration of CST axons

In order to determine the cells ability to support axonal regeneration of the cortico-spinal tract, sections from contusion injury animals that received cortical tracer injections of BDA were examined for evidence of axonal regeneration through the extent of the BDA labelled fibres. Sections with good BDA labelling close to the midline were chosen for further analysis with the confocal microscope at X40 (tile) to verify the extent of the axonal regeneration.The extent of axonal regeneration was also compared with that in non-transplanted animals.

3.2.23 Do regenerating axons become myelinated?

The ability of cells to promote axonal remyelination was determined by examining the evidence of myelination regenerating axons. This was performed by assessing the distribution of CASPR (paranodal junctions) and compared with the non-transplanted animals. The myelin markers were examined in relation to other co-labels: GFP (transplanted cells), NF200 (Axons) and P0 (peripheral myelin. This analysis need to be performed using the confocal microscope at low power X20 to determine the distribution of the myelin and at high power X40 for greater detail because one of the marker was detected using a fluorochrome outside the visible spectrum.

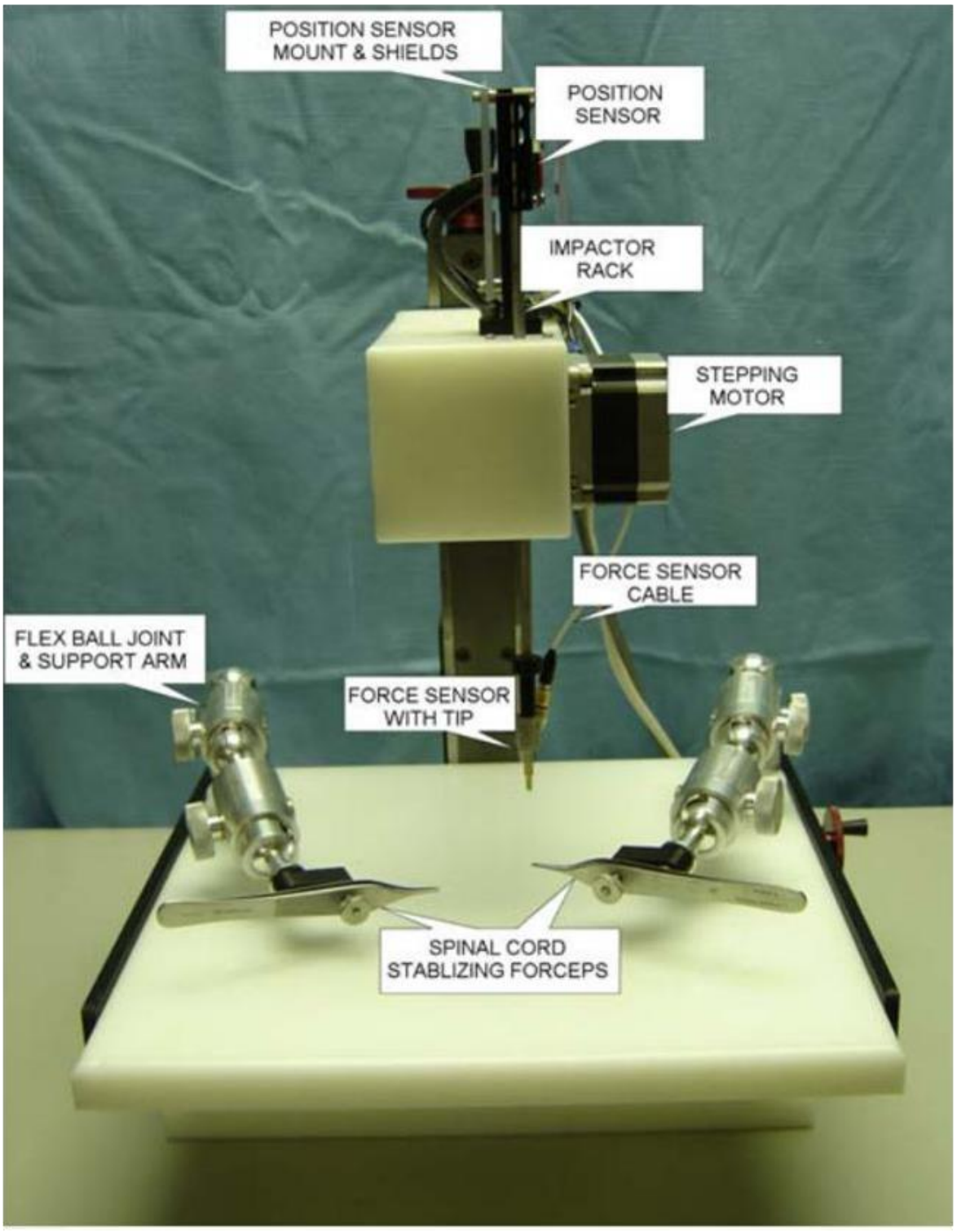

Figure 3-1. The Infinite Horizons Impactor.

The support arms were positioned and locked and forceps used to clamp the animal into position. The impactor tip was then moved and lowered into position just above the spinal cord. Once in position, the computer-controlled stepping motor is activated, driving the impactor downwards to hit the targeted area of the spinal cord. (Image taken from the PSI-IH Impactor user manual).

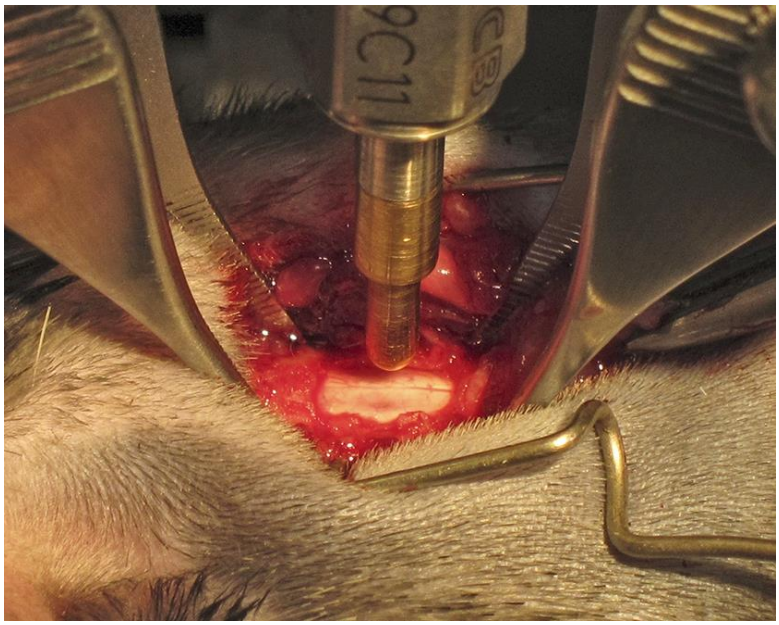

Figure 3-2. Contusion injury.

The injury procedure involved performing a dorsal laminectomy to remove the C5 and C6 vertebra to expose the spinal cord followed by fixing the C4 and C7 vertebrae using Adson forceps. Then, the impactor tip of the IH impactor was positioned over the exposed C6 and a computer-controlled contusion injury was performed.

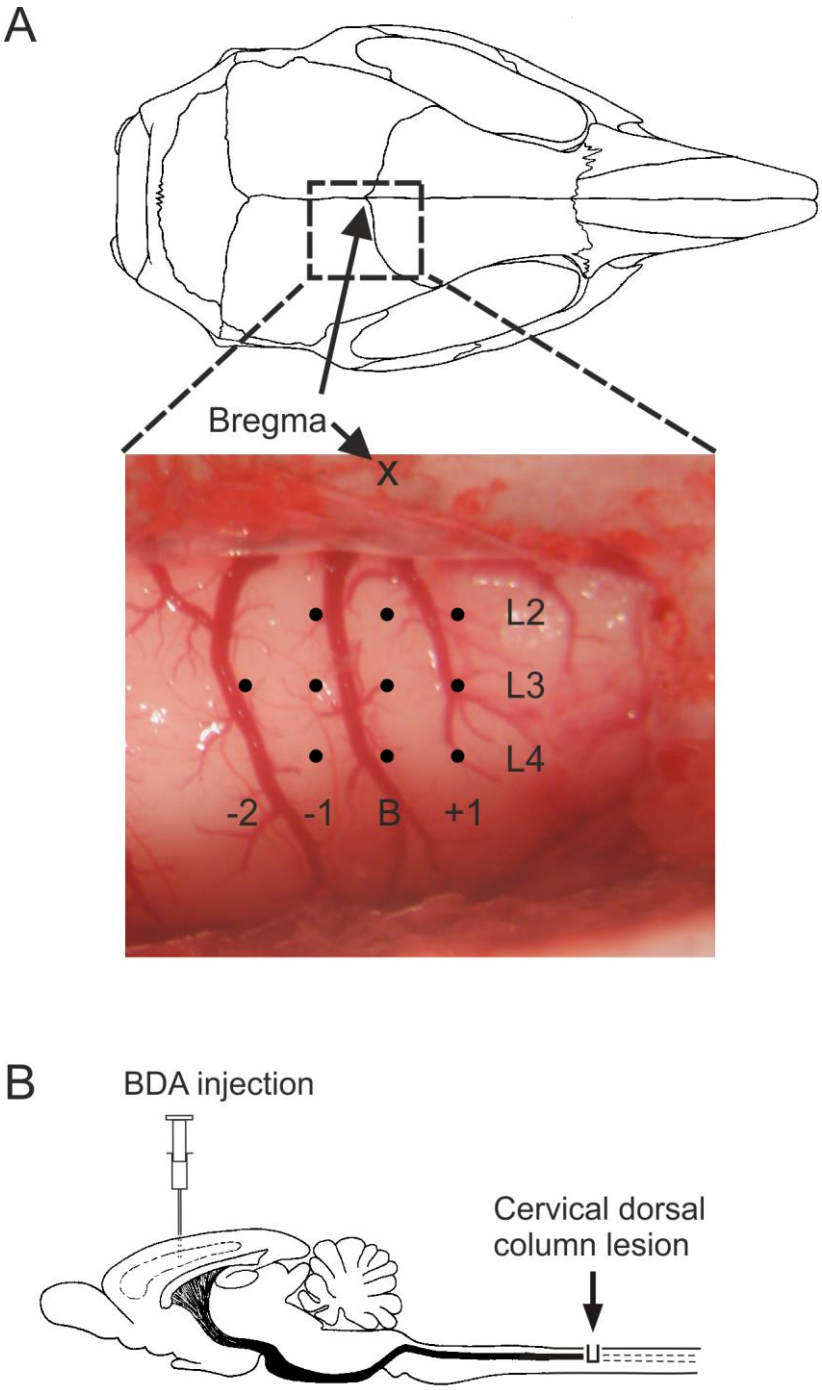

Figure 3-3. Location of cortical injection sites for BDA tracer delivery.

(A) A small window was drilled into the skull to expose the right sensorimotor cortex . The anatomical landmark bregma was used as a reference point from which each of 10 injection sites were measured. The injection sites (black dots) formed a grid, within the left cortex. (B) These injection sites encompass the main forelimb and hindlimb areas of the sensorimotor cortex.

Figure 3-4. Diagram to illustrate the procedure for making a wire knife lesion.

A) The wire knife protruded from the cannula and formed an arc. B) The wire knife in its cannula was inserted through a slit in the dura at left of the dorsal columns up to a depth of 950 µm. C) The wire knife was then protruded from the cannula which forming an arch encompassing the dorsal columns and raised against a glass rod. D) This procedure transect the dorsal column but preserve the dorsal vein. E) Finally, the wire knife was retracted in its ensheath and raised out of the cord. (Images B-E adapted from original images from Dr John Riddell).

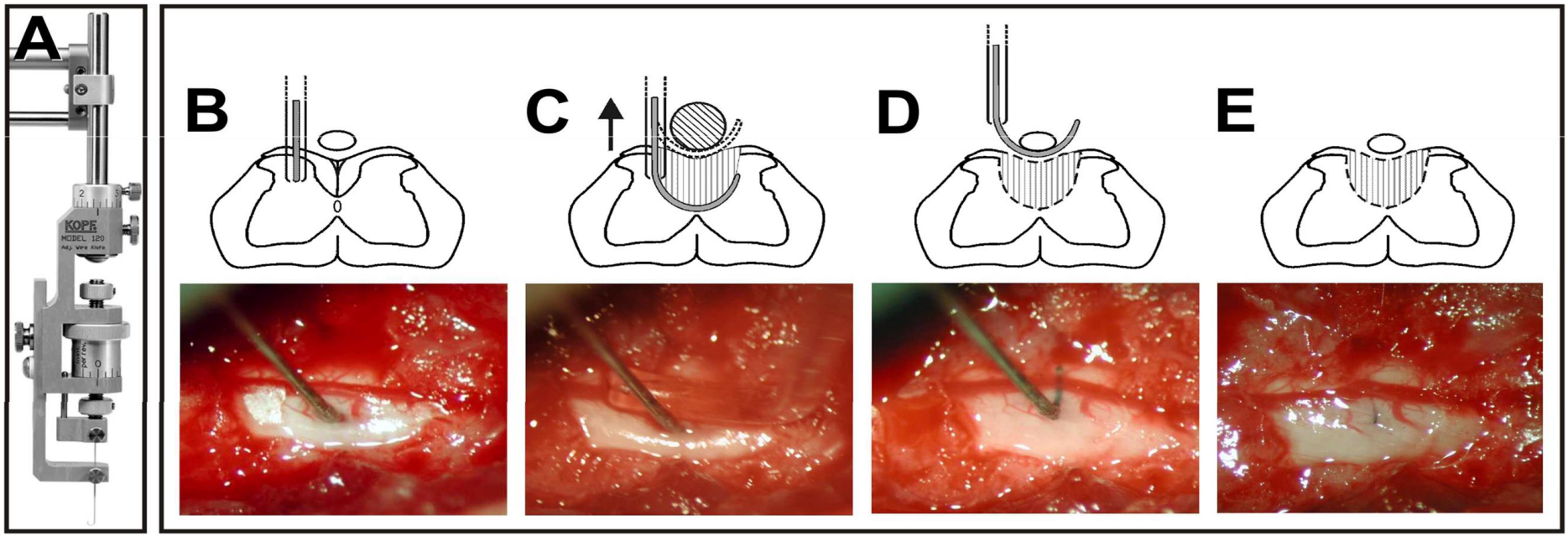
A
KOPF
MODEL 120
Adj. Wire Knife
B
C
D
E

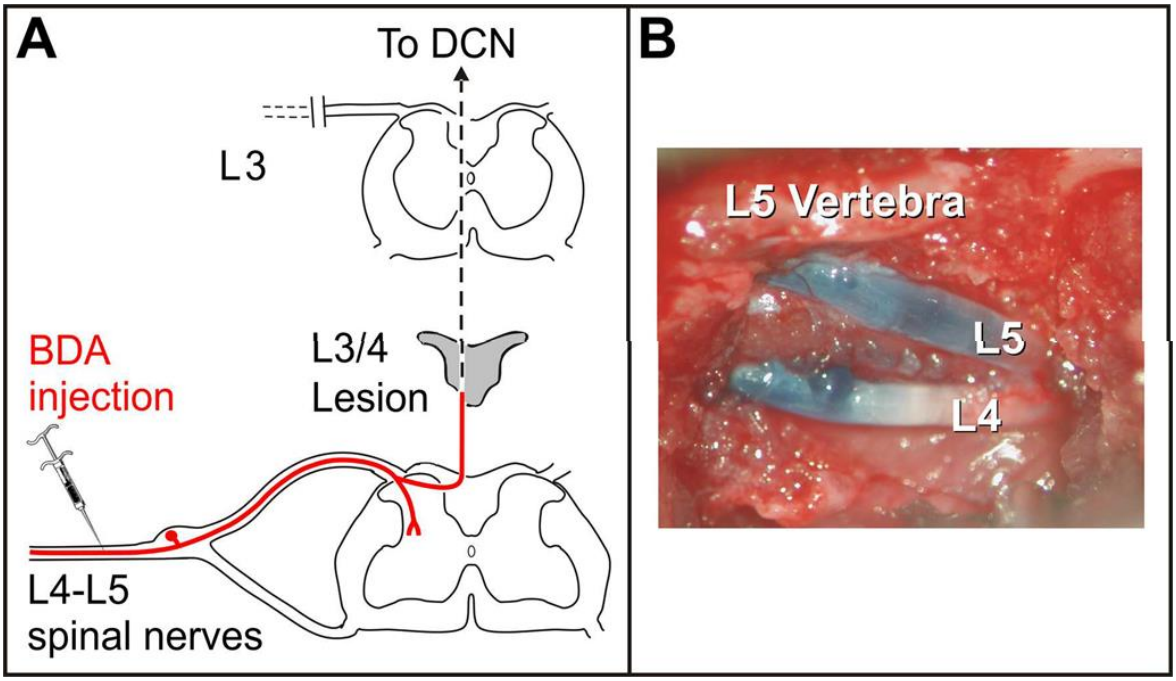

Figure 3-5. BDA tracer injection into spinal nerve.

Tracer was injected into the L4 and L5 spinal nerves and the tracer then travelled through to the dorsal root ganglion to label central branch. B) Image B shows the discoloration of the L4 and L5 after the injection. (Images modified from the original images prepared by Dr John Riddell).

3.3 Results

3.3.1 Injury characteristics at time of transplant

In order to obtain some understanding of the nature of the injury site into which transplants were made, 8 animals were perfused 3 weeks after the injury, which is equivalent to the delay between injury and transplantation. Spinal cords from these animals were processed with different combinations of antibodies. The combinations were chosen to show mainly the glial scar (GFAP and nestin), deposition of extracellular matrix (laminin) and blood vessels (SMA, laminin). The animals used in this part of the study are shown in Table 3-2.

No	Animal ID	Survival	Immunocytochemistry
1	R2412	3 weeks	GFAP+NF200 GFAP+ED1
2	R10413	3 weeks	GFAP+Nestin GFAP+Laminin
3	R16813	3 weeks	GFAP+Nestin GFAP+Laminin
4	R16913	3 weeks	GFAP+Nestin GFAP+Laminin
5	R17013	3 weeks	GFAP+Nestin GFAP+Laminin
6	R18013	3 weeks	GFAP+Nestin GFAP+Laminin
7	R9214	3 weeks	SMA+GFAP
8	R9314	3 weeks	SMA+GFAP

Table 3-2. Summary of animals used to investigate the injury site 3 weeks after contusion. This time point is equivalent to the time of delayed transplantation in animals receiving cells.

Representative examples of sections from these animals to illustrate the main features of the injury site are shown in Fig.3.8. The injury site in all animals was extensive and encompassed large parts of both the white and grey matter. It typically consisted of one or more fluid filled cavities. Where there was more than one cavity (i.e. the cavity was septated) these were generally divided by very strands of tissue (trebeculae) which could be very fragile and did not always survive the cutting and immunohistological processing. A glial scar formed around the cavities as indicated by denser immunolabelling for GFAP than areas

beyond the injury but nestin, which is co-localised with GFAP in reactive astrocytes, was only quite weakly and sparsley expressed (Fig 3.8 A and B).

There was deposition of a variable amount of extracellular matrix within areas of the injury. The distribution of this gave the impression that it may have been part of the cavity at one stage or destined to become cavity if the matrix had not formed. The matrix was very variable in extent (in Fig. 3.8 it increases for sections A to D) and was enriched for laminin (Fig 3.8 B and D). There was minimal SMA immunolabelling in the injury area and surrounding tissue (this was judged by eye to be less than in 9 week survival animals and transplanted animals, see below). Astrocytes (GFAP labelling) were rarely found within this matrix but regenerating axons revealed by neurofilament labelling (not illustrated) could be seen in the one animal in which this antibody was examined and this is consistant with this finding in longer survival animals without transplants which were investigated more fully. EDI labelling was also investigated in one animal (not illustrated) and ED1 labelled profiles were seen at two main locations. They formed a thin “layer” of cells around the rim of the cavity with a distribution which appeared to roughly correspond to the glial scar of reactive astrocytes. In addition, they were very extensively distributed throughout the extracellular matrix where this occupied part of the injury area. Expansion of the width of the central canal was also sometimes evident beyond the rostral and caudal margins of the injury. Information on the dimensions of the injury cavities is provided in Section 3.3.9

3.3.2 Testing the requirement for immunosuppression

In order to determine whether transplanted cells could survive in the injured spinal cord without any immunosuppressive treatment and if so, for how long, transplants were made into animals 3 weeks after a contusion injury and surviving cells looked for at 1, 2 and 4 weeks after transplantation. Two animals were examined at each time point and two different cell batches were used at each time point. GFP expression for most of the transplanted cells was 60 or 90 %. A summary of the animals used in this part of the study is shown in Table 3.3.

No	Animal ID	Cell batch	GFP %	ICC	Evidence of cells survival?	Post-transplant survival time
1	R11413	MSC 9C A(II)	60	GFP/Nestin/ GFAP	No (a few atypical GFP cells)	1 weeks
2	R19613	MSC 4C A(II)	90	GFP/Nestin/ GFAP	No (some amount of atypical GFP profile)	1 weeks
3	R11513	MSC 9C A(II)	60	GFP/Nestin/ GFAP	No GFP labelled cells	2 weeks
4	R19713	MSC 4C A(II)	90	GFP/Nestin/ GFAP	No GFP labelled cells	2 weeks
5	R4113	MSC 7C A(II)	22	GFP/Nestin/ GFAP	No GFP labelled cells	4 weeks
6	R11613	MSC 9C A(II)	60	GFP/Nestin/ GFAP	No GFP labelled cells	4 weeks

Table 3-3. Summary of animals used to assess the survival of transplanted cells without immunosuppression

The results indicated that there is dramatically poor survival of hESC-MSCs when they are transplanted 3 weeks after a contusion injury without any immunosuppressive treatment. Some GFP labelled profiles were seen in the one week survival animals but virtually none could be observed in the 2 week animals and they were completely absent at 4 weeks.

In one of the animals examined 1 week after transplantation GFP labelled profiles were extremely sparse and formed a small localised pocket of cells within the injury site (see Fig. 3.9 A). In the other animal the GFP labelled cells were more numerous and were located in two main regions. They formed a rim of cells around the perimeter of a small otherwise empty cavity (Fig. 3.9 B) and the also occurred as a small compact bolus of cells (see Fig. 3.9C). In both of these animals the GFP labelled cells had a very different appearance from that in culture (or in subsequent animals where immunosuppression was used), being rounded and devoid of any processes. Both the size and morphology of these GFP labelled profiles closely resemble that of macrophages that can be observed by their autofluorescence and by ED1 labelling, though this was not tested further. It is therefore possible that the GFP profiles are macrophages that have

phagocytosed the dead GFP expressing transplanted MSCs and therefore contain GFP. If this is the case then it is likely that virtually no cells survive by 7 days after transplantation without immunosuppression. Apart from a handful of GFP profiles of similar morphology seen in one of the 2 week animals, none of the animals examined at 2 and 4 weeks contained any GFP labelled cells (Fig. 3.10).

Although there was little if any survival of transplanted cells in these six animals without cyclosporine treatment, there was also less evidence of extensive fluid filled cavities at the injury (Fig. 3.9 and Fig 3.10). Most of the injury sites were filled with an extracellular matrix and only small occasional cavities were seen (e.g. Fig. 3.9 B). This was clearly different from most of the animals investigated at the 3 week post-injury time point equivalent to when the cells were transplanted. It is also in contrast to most of the 6 week survival cells which were treated with cyclosporine but were not transplanted with cells, many of which showed extensive cavitation (see below). This suggest that the transplanted cells or cells attracted to the area by the cells and perhaps part of the process by which the cells were killed and/or the cellular debris cleared from the site, may have produced an extracellular matrix.

In addition to examining GFP labelling, these animals were also immunolabelled for GFAP and nestin (Fig. 3.9 and 3.10). Nestin immunoreactivity, although not intense was more evident than in animals examined 6 weeks after injury, with or without cell transplants.

3.3.3 Testing the adequacy of immunosuppression

Having established that transplanted cells did not survive without immunosuppression, we next investigated whether an immunosuppression regime based on daily injections of cyclosporine (20mg/kg s.c.) would be adequate to prevent rejection of the transplanted cells and promote their survival for a duration sufficient to investigate their effect on the injured spinal cord. Animals were transplanted 3 weeks after a contusion injury but in this case cyclosporine administration was begun 2 days before the transplants and continued until the end of the procedure. Cell survival was assessed at 5 days, 2 weeks and 4 weeks in two animals at each time point transplanted with cells from different differentiation batches and the cells were 60 or 90% GFP

expressing. The animals used in this part of the study are summarised in Table 3.4.

No	Animal ID	Cell batch	GFP %	Surviving cells detected?	Post-transplant survival time
1	R11313	MSC 9C A(II)	60%	Many: in injury area, rostral and caudal	5 days
2	R18113	MSC 4C A(II)	90%	Many: in injury area, rostral and caudal	5 days
3	R2512	MSC 13C B	90%	Many: in injury area, rostral and caudal	2 weeks
4	R18213	MSC 4C A(II)	90%	Moderate numbers in injury area only	2 weeks
5	R2712	MSC 13C B	90%	Many: in injury area, rostral and caudal	4 weeks
6	R10613	MSC 9C A(II)	60%	Many: in injury area, rostral and caudal	4 weeks

Table 3-4. Summary of animals used to assess survival of transplanted cells in animals treated with daily injections of the immunosuppressant cyclosporin

Examination of sections from all of the animals investigated demonstrated excellent survival of GFP expressing transplanted cells at all time points. Examples of sections from these animals are shown in Fig. 3.11. Large numbers of GFP expressing cells were observed throughout the injury area and often beyond. Because of the small sample and considerable variability in the injury site morphology and pattern of distribution of labelled cells it was not possible to determine whether there were differences in the numbers of surviving cells at 2 weeks and 4 weeks. At both time points there were large numbers of cells which filled the injury site leaving no cavitation. However, gaps in the distribution of cells were evident but this was in cases where part of the injury site was occupied by extracellular matrix (Fig. 3.11 A and D).

3.3.4 Distribution of transplanted cells

Having established that good survival of cells could be obtained when cells were transplanted 3 weeks after an injury if cyclosporine treatment was provided through-out the survival period, further studies were conducted using a 6 week post-transplant survival time. Twenty-six animals were transplanted with hESC-derived MSCs. All of these were transplanted 3 weeks after the contusion injury

and were treated with cyclosporine. The transplanted animals received one of the 5 independently prepared batches of cells (i.e. from 5 different runs of the differentiation protocol) in order to avoid the possibility that use of a single batch differing from the rest could bias the results. The spinal cords from these animals were processed using different combinations of antibodies to investigate different aspects of the injury site but most sections were processed using antibodies to GFAP or NF200 in addition to GFP. These antibodies show the structure of the spinal cord and sections from these animals were used to examine the distribution of transplanted cells. The data is summarized in Table 3.5 (page 148-149).

No	ID	Cell batch	GFP(%)	Surviving cells	cells in the injury	Most or part	cells outside injury	cells rostral	cells caudal
1	R15312	MSC 4C A	90	yes	Yes	part	minimal	yes -scattered	yes -scattered
2	R15512	MSC 4C A	90	yes	Yes	most	many	yes -scattered	yes-scattered
3	R29412	MSC 1C A	74	yes	Yes	part	many	yes -scattered	yes-scattered
4	R34012	MSC 7C A	48	yes	Yes	minimal	minimal	yes-in track	yes-scattered
5	R29612	MSC 1C A	74	yes	Yes	part	many	yes-in large ball	yes-scattered
6	R33612	MSC 7C A	48	yes	Yes	minimal	minimal	no	yes-in track
7	R50512	MSC 1C A	74	yes	Yes	minimal	minimal	no	no
8	R29712	MSC 1C A	74	yes	Yes	most	many	yes-in track	yes-in track
9	R2913	MSC 7C A(II)	22	yes	Yes	part	no cells	no	no
10	R33912	MSC 7C A	48	yes	Yes	part	many	yes-scattered	yes-scattered
11	R10813	MSC 9C A (II)	60	yes	Yes	part	minimal	yes-scattered	yes-scattered
12	R33812	MSC 7C A	48	yes	Yes	part	many	outside the cord	outside the cord
13	R3013	MSC 7C A(II)	22	yes	Yes	minimal	no	no	no
14	R50612	MSC 1C A	74	yes	Yes	minimal	no	no	no
15	R2713	MSC 7C A(II)	22	yes	Yes	part	minimal	yes-scattered	yes-scattered
16	R3313	MSC 7C A(II)	22	yes	Yes	part	many	yes-in track	yes-in track
17	R33712	MSC 7C A	48	yes	Yes	part	many	yes-scattered	yes-scattered
18	R29212	MSC 1C A	74	yes	Yes	most	many	yes-in track	yes-in track
19	R50412	MSC 1C A (II)	90	yes	Yes	minimal	no	no	no

20	R50112	MSC 1C A(II)	34	yes	yes	part	minimal	no	no
21	R50212	MSC 1C A(II)	34	yes	Yes	part	many	yes-in track	yes-in track
22	R50312	MSC 1C A(II)	34	yes	Yes	part	many	yes-scattered	yes-scattered
23	R2413	MSC 7C A(II)	22	yes	Yes	part	many	yes-scattered	no
24	R2513	MSC 7C A(II)	22	yes	Yes	part	many	yes-scattered	yes-in track
25	R2613	MSC 7C A(II)	22	yes	Yes	part	minimal	yes-scattered	yes-scattered
26	R10513	MSC 9C A(II)	60	yes	Yes	part	minimal	yes-scattered	yes-scattered
						3 most	**13 many**	**4 in track**	**5 in track**
						17 part	**9 minimal**	**13 scattered**	**13 scattered**
						6 minimal	**4 no cells**	**1 in large ball**	**7 no cells**
								6 no cells	

Table 3-5. Summary of the distribution of cells in animals transplanted with hESC-MSCs three weeks after a contusion injury and investigated using immunocytochemistry 6 weeks after transplantation.

The data in Table 3-4 show that surviving GFP labelled cells were found in all animals (26 of 26 animals, 100%) and in all cases could be seen in the injury area. However, their distribution varied from animal to animal. Only a small proportion of animals had cells throughout the whole of the injury area (3 animals, 11%). Most animals (20 of 26; 74 %) had cells occupying approximately 25 to 50 % of the injury area with the remaining area occupied with extracellular matrix. In the few remaining animals (4 animals; 15%) GFP labelled cells occupied only a small area (less than 25%) of the injury site. Examples of sections from animals sacrificed 6 weeks after transplantation are shown in several figures which also illustrate other features of the investigation. See Figures 3-16, 3-17, 3-18 and 3-23. All animal was essentially devoid of cavities. Either the labelled cells or cells together with areas of extracellular matrix completely filled the injury area. In comparison, the injury sites of the 17 control animals showed extensive cavitation with varying amounts of infilling with extracellular matrix. Examples of the injury site in these control animals are shown in Fig. 3-12 and Fig. 3-22.

Cells were also seen distributed outside the injury area in most transplanted animals (23/26; 85%). Labelled cells could be observed in the host spinal cord rostral to the injury, caudal to the injury or on both sides of the injury. In the majority of animals (21/23 animals; 91%), cells were seen extending in both directions i.e. rostral and caudal to the injury site. The cells outside the injury site often formed continuous tracks of cells leading away from the injury (10/23 animals; 43%). These were typically close to the midline, just dorsal to the central canal. In the remaining animals, cells outside the injury site were seen to be scattered and dispersed rather than forming a track (13/23 animals; 48%). In the majority of these animals, the cells did not extend to the end of the section i.e. 3 mm rostral and caudal of the injury centre. For some animals sections were cut from blocks each side of the injury block. Cells were not seen in any of the 6 rostral blocks examined but a few cells were seen in 3 of 6 caudal blocks.

One interesting feature associated with the spread of cells beyond the lesion was clear evidence that the transplanted cells displaced host astrocytes. This was evident from the immunolabelling with GFAP, which in areas where GFP labelled cells were detected was largely absent (Fig. 3-11 D, Fig. 3-13, 3-31, 3-32, 3-33). This suggests that the transplanted cells interact with host astrocytes and this was confirmed in other sections of the study where cells were transplanted into normal non-injured spinal cord and into dorsal column injuries (see below,).

In 4 animals there was evidence of cells outside the spinal cord (on the dorsal surface) suggesting some leakage or overflow of cells.

3.3.5 Differentiation and proliferation of transplanted cells *in vivo*

In order to investigate whether the hESC-MSCs continue to proliferate *in vivo,* immunostaining for Ki67, a nuclear protein which is thought to be necessary for cellular proliferation and is widely considered a reliable marker for this process. It was assumed that proliferation, if it continued to occur, was most likely to be seen at an early time point after transplantation before other signalling potentially shut the process down. On the other hand, a few days are required for transplanted cells to be integrated and physically anchored within the tissue for processing. A survival period of 5 days was therefore chosen. Table 3.6 summarises the animals that were used in this part of the study.

No	Animal ID	Cell batch	GFP %	Immunocytochemistry	Time post-transplant
1	R2813	MSC 7C A(II)	22	GFP/Ki67/GFAP	5 days
2	R11313	MSC 9C A(II)	60	GFP/Ki67/GFAP	5 days
				GFP/Ki67/ED1	
				GFP/Ki67/NeuN	
3	R18113	MSC 4C A(II)	90	GFP/Ki67/GFAP	5 days
				GFP/Ki67/ED1	
				GFP/Ki67/NeuN	
4	R17613	None		GFP/Ki67/GFAP	5 days
				GFP/Ki67/ED1	
				GFP/NeuN/GFAP	
5	R17713	none		GFP/Ki67/GFAP	5 days

				GFP/Ki67/ED1	
				GFP/NeuN/GFAP	
6	R3313	MSC 7C A(II)	22	GFP/Ki67/GFAP	6 weeks

Table 3-6. Summary of animals used to investigate whether transplanted cells proliferate *in vivo.*

Ki67 immunolabelling was widespread throughout sections containing the transplanted injury sites. It was especially prevalent in areas of extracellular matrix surrounded by cells and at the edge of small cavities within the cell transplant (Fig. 3-13 A and B). However, it was less prevalent in areas where the transplanted cells were highest in density and it was not seen co-localised with GFP. This was confirmed by examining individual z sections in high power confocal images obtained from areas containing GFP and Ki67 immunolabelled structures of potential interest. Five fields of view, from 3 animals were examined and each of these contained multiple profiles. Only 2 z sections showed any potential co-localization and these examples were not convincing (Fig. 3-13 C, D, E, F and G). This suggests that hESC-MSCs do not proliferate *in vivo* but that other cell types within the injured spinal cord do.

The morphology of transplanted cells was investigated using confocal microscopy at 2 weeks and 4 weeks after transplantation. Examples of these observations are illustrated in Fig 3-14 and 3-15. Cells within the main area of the transplant showed a main spindle shaped simple morphology whereas cells which had spread out of the main injury site tended to develop a more complex morphology. This may reflect a mainly paracrine effect within the injury and a wider influence from host cells out-with the injury.

3.3.6 Extracellular matrix and blood vessel formation within the transplanted injury

In animals transplanted with cells, the injury site was remarkably well filled even when variable numbers of cells with varying distributions remained and this was in stark contrast to the extensive cavitation that typified the injury site of non-transplanted animals. Laminin is an extracellular matrix molecule commonly secreted by cells and immunocytochemistry was therefore used to investigate the extent to which laminin was a constituent of the tissue filling the injury site.

Table 3.7 summarises the animals used in this part of the study. All of the animals were investigated 9 weeks after the injury or 6 weeks after transplantation.

No	Animal ID	Cell batch	GFP %	Immunocytochemistry
1	R29312	MSC 1C A	74	GFP/Laminin/GFAP
2	R29412	MSC 1C A	74	GFP/Laminin/GFAP
3	R34012	MSC 7C A	48	GFP/Laminin/GFAP
4	R2313	no	-	GFP/Laminin/GFAP
5	R3113	no	-	GFP/Laminin/GFAP

Table 3-7. Table summarising the animals used to investigate laminin within the injury site of transplanted and control injured animals.

Fig. 3-16 shows examples of the distribution of laminin immunolabelling in two of the transplanted animals investigated. There was intense immunolabelling throughout the transplanted injury site in areas containing cells and those where cells were absent. The labelling was particularly intense where the transplanted cells were sparse or absent. In addition to a very dense labelling within the injury, where the labelling was lighter it was possible to see some of the details of labelled structures. This revealed numerous laminin positive blood vessels in and around the injury site. Examples of these are shown in Fig. 3-17.

Angiogenesis at the transplanted injury site was also investigated by performing immunocytochemistry for SMA which is a constituent of the walls of resistance vessels. For all animals the time point post-injury was nine weeks and 6 weeks after transplantation. Table 3.8 summarises the animals used for this purpose.

No	Animal ID	Cell batch	GFP %	Immunocytochemistry
1	R15412	MSC 4C A	90	SMA/GFAP/GFP
2	R29612	MSC 1C A	74	SMA/GFAP/GFP
3	R2713	MSC 7C A(II)	22	SMA/GFAP/GFP
4	R17213	None		GFP/SMA/GFAP
5	R19813	None		GFP/SMA/GFAP

Table 3-8. Table summarising the animals used to investigate angiogenesis using SMA immunolabelling.

Fig. 3-18 shows examples of the distribution of SMA immunolabelled blood vessels in sections from two animals. Numerous vessels were found in and around the injury site producing a network which appeared but developed at the injury site than in distant tissue. The vessels were not specifically associated with

regions containing transplanted cells but were also seen in extracellular matrix and beyond the borders of the injury. SMA labelled blood vessels were also seen in non-transplanted animals examined at an equivalent time point i.e. 9 weeks after injury (see Fig. 3-12 B and C) but they were fewer number and distributed mainly in the matrix deposited in the injury cavities.

3.3.7 Interaction between host glia and transplanted cells

To assess the integration of hESC-MSCs with spinal cord tissue and whether there is any reactivity between the cells and host glia, small bolus injections of cells were made into the spinal cords of normal non-injured animals so that the transplant-host interaction could be assessed without interference from the reaction to the injury. Immunoreactivity to GFAP and nestin which are upregulated in reactive astrocytes was used to assess glial reactivity 7 days after injection. Table 3.9 summarises the animals used to study this.

No	Animal ID	Cell batch	GFP %	Immuno-cytochemistry	Time post-transplant
1	R7013	MSC 7C A(II)	22	Nestin/GFAP/GFP	1 week
2	R22013	MSC 4C A (II)	90	Nestin/GFAP/GFP	1 week
3	R22113	MSC 4C A (II)	90	Nestin/GFAP/GFP	1 week

Table 3-9. Table summarising animals in which nestin was used in combination with GFAP to assess glial reactivity in response hESC-MSCs injected into normal non-injured spinal cord.

Fig. 3.19 shows examples of the results obtained. The small bolus of cells injected into the dorsal columns was surrounded by enhanced GFAP and nestin immunoreactivity while astrocytes were largely excluded from the area occupied by the transplanted cells. These observations suggest a significant interaction between the transplanted cells and host astrocytes.

3.3.8 The effect of transplants on the glial scar

To assess whether the transplanted cells had a similar effect to that indicated by bolus injections into normal animals, when transplanted into the injured spinal cord, GFAP and nestin immunoreactivity were observed in transplanted and control animals. The animals used in this part of the study are summarised in Table 3.10.

No	Animal ID	Cell batch	GFP %	Immunocytochem.	Time P-T
1	R3213	MSC 7C A(II)	22	GFP/Nestin/GFAP	2 weeks
2	R15212	MSC 4C A	95	GFP/Nestin/GFAP	6 weeks
3	R50612	MSC 1C A	74	GFP/Nestin/GFAP	6 weeks
4	R4413	None		GFP/Nestin/GFAP	2 weeks
5	R2113	None		GFP/Nestin/GFAP	6 weeks
6	R2213	none		GFP/Nestin/GFAP	6 weeks

Table 3-10. Summary of animals used to investigate glial activation in response to transplanted cells.

Fig. 3-20 shows examples from a transplanted and a control animal. Although a glial reaction around the injury site remained prevalent 9 weeks after the injury, there was very little nestin immunolabelling in either the control or transplanted animals and the two groups did not differ obviously in this respect. This suggests that the reaction of host glial cells to the transplanted cells may not persist at longer time points after transplantation or have little impact on the wider injury. The exclusion of astrocytes from the bolus injection site is, however, a feature that is equally obvious at the injury transplant site.

3.3.9 Quantification analysis of the injury

In order to carefully study the effect of hESC-MSCs on the morphology of the contusion injury, the injury dimensions and the thickness of the glial reaction (glial scar) surrounding the injury region of 3 week survival control animals (corresponding to the timing of cells transplant), 9 week survival control animals (corresponding the end of procedure for transplanted animals) and transplantated animals was measured and compared.

3.3.9.1 Injury size

Table 3.11 shows the results of the quantification analysis of the injury extent of these animals at 3 weeks after injury. The length of the injury area was usually 3mm or more (mean 3.68 mm ± 0.21) and most of this was occupied by a cavity and matrix in-filling. The width of the injury at epicentre of cavity was usually around 2mm (mean width 2.04 mm ± 0.06).

Animal ID	Length of Injury (mm)	Width of injury(mm)
R2412	3.62	2.04
R10413	3.32	2.04
R16813	3.24	2.10
R16913	3.69	2.04
R17013	3.16	2.10
R18013	3.29	1.62
R9214	4.75	2.22
R9314	4.39	2.16
mean	3.68	2.04

Table 3-11. Dimensions of the injury 3 weeks after contusion.

This time point is equivalent to the time of delayed transplantation in animals receiving cells and this information is presumed to be representative of the injury into which transplants were made in these animals. The table shows measurements of the maximal length of the injury area and the length occupied by cavity determined by inspection of saggital sections of the spinal cord at the injury site. The width of the injury was determined from the number of 60um sections containing injured tissue.

The 3 week post-injury time point examined here is equivalent to the time point at which transplants were made into animals receiving cells and the histology of the injury site is presumed to reflect the nature of the tissue into which the transplants were made. This indicates that transplants were made largely into fluid filled cavities but that in some cases the deposition of extracellular matrix will reduce the volume of cells required and prevent the spread of cells throughout the injury area. Representative images at 3 week post-injury which were used for measurements are shown in figure 3-21.

A similar approach was used to assess the dimensions of the injury sites (cavities, disrupted tissue, GFAP or other marker enhancement) in both transplanted and control non-transplanted animals. This data is shown in table 3.12 and table 3.13 respectively with representative images of the injury site shown in figure 3-22 and 3-23. The dimensions of the injury in control animals at 9 weeks after the injury were very similar to those of animals examined 3 weeks after the injury suggesting that the injury site is already at its greatest extent by 3 weeks. The slight reduction in cavity length at 9 weeks compared to 3 week post-injury animals may reflect increased infilling and accumulation at the injury site of extracellular matrix at the later time point. Further comparison of these control animals with transplanted animals revealed a significant reduction of the injury extent (length and width) in the transplanted animals. The data from these 3 different groups of animals were compared and tested statistically using

one way anova with post-hoc turkey comparison test and is illustrated in figure 3-6 (A) and (B). The length of the injury area in control animals was usually 3mm or more (mean 3.57mm ±0.07) compared with the transplanted animals which ranged between 1.47-2.99 (mean 2.15mm ±0.11) (p value=<0.001). The width of the injury in control animals was around 1.6 to 2.1mm (mean 1.9mm ±0.04) while in transplanted animals was between 0.8 to 1.8mm (mean width 1.34mm±0.05) (p value=<0.001). In comparison, the injury sites of the 17 control animals showed extensive cavitation with varying amounts of infilling with extracellular matrix. Examples of the injury site in these control animals are shown in Fig. 3.12.

The injury area of the control animals was either occupied by a single large cavity, multiple small cavities and/or matrix infilling. On the other hand, the injury area of the transplanted animals was either completely filled with cells, partially filled with cells or a mixture of cells and matrix with almost no visible cavities in any of the animals. Further calculation on the aspect ratio of the injury sites (length/width) reveal a relatively smaller aspect ratio for the transplant (mean 1.60 ±0.11) compared with the control animals at 9 weeks post injury (mean 1.81 ±0.05) and 3 weeks post injury (mean 1.60 ±0.09) but not significantly different (p value>0.05 for transplanted versus 3 week and transplanted versus 9 week) upon tested using one way anova with post-hoc turkey comparison test. The data was illustrated in figure 3-6. The smaller aspect ratio for the transplanted animals suggest that the injury is not the same proportional shape as the injury in 3 and 9 week post injury eventhough the injury is shorter and less wide in transplanted animals. The larger aspect ratio of the 3 and 9 weeks control animals may suggest that rostro-caudal elongation is a greater contributor to cavity volume than medio-lateral and the cell transplant inhibit this elongation and lead to the overall outcome of the injury volume. Apart from figure 3-23, examples of the injury site in transplanted animals are also shown in many other figures: figure 3-16, 3-18. 3-20, 3-27, 3-28 and 3-30.

No	Animal ID	Length of injury (mm)	Width of injury
1	R2313	3.42	1.68
2	R3113	3.47	2.28
3	R17213	4.09	1.98
4	R19813	3.82	1.86
5	R19913	3.98	1.86
6	R11013	3.21	1.98
7	R18913	3.21	1.80
8	R17113	3.66	1.98
9	R19413	3.31	1.68
11	R2113	3.57	1.80
12	R2213	3.69	2.10
13	R3413	3.96	2.04
14	R4213	3.04	1.68
15	R17313	3.56	1.86
16	R17413	3.59	1.92
17	R17513	3.87	1.68
18	R33512	3.60	2.16
	Mean	3.57	1.9

Table 3-12. Quantification of injury/cavity dimensions (maximal length and width of the injury area) in control animals 9 weeks after contusion injury

No	ID	Length (mm)	width (mm)
1	R15312	1.57	0.84
2	R15512	1.73	1.14
3	R29412	1.84	1.32
4	R34012	1.95	1.20
6	R29612	2.76	1.62
7	R33612	2.27	1.56
8	R50512	1.97	1.44
9	R29712	2.43	1.68
10	R2913	2.73	1.68
11	R33912	1.80	1.50
12	R10813	2.70	1.44
13	R33812	1.48	1.62
14	R3013	2.00	1.26
15	R50612	2.33	1.80
16	R2713	2.92	1.14
17	R3313	2.91	1.08
18	R33712	2.30	1.14
19	R29212	1.47	1.80
20	R50412	2.99	1.26
21	R50112	1.82	1.32
22	R50212	2.10	1.08
23	R50312	1.76	0.96
24	R2413	1.93	1.38
25	R2513	2.00	0.96
26	R2613	1.68	1.20
27	R10513	2.63	1.44
	Mean	2.15	1.34

Table 3-13. Quantification of injury/cavity dimensions (maximal length and width of the injury area) in transplanted animals 6 weeks after transplantation

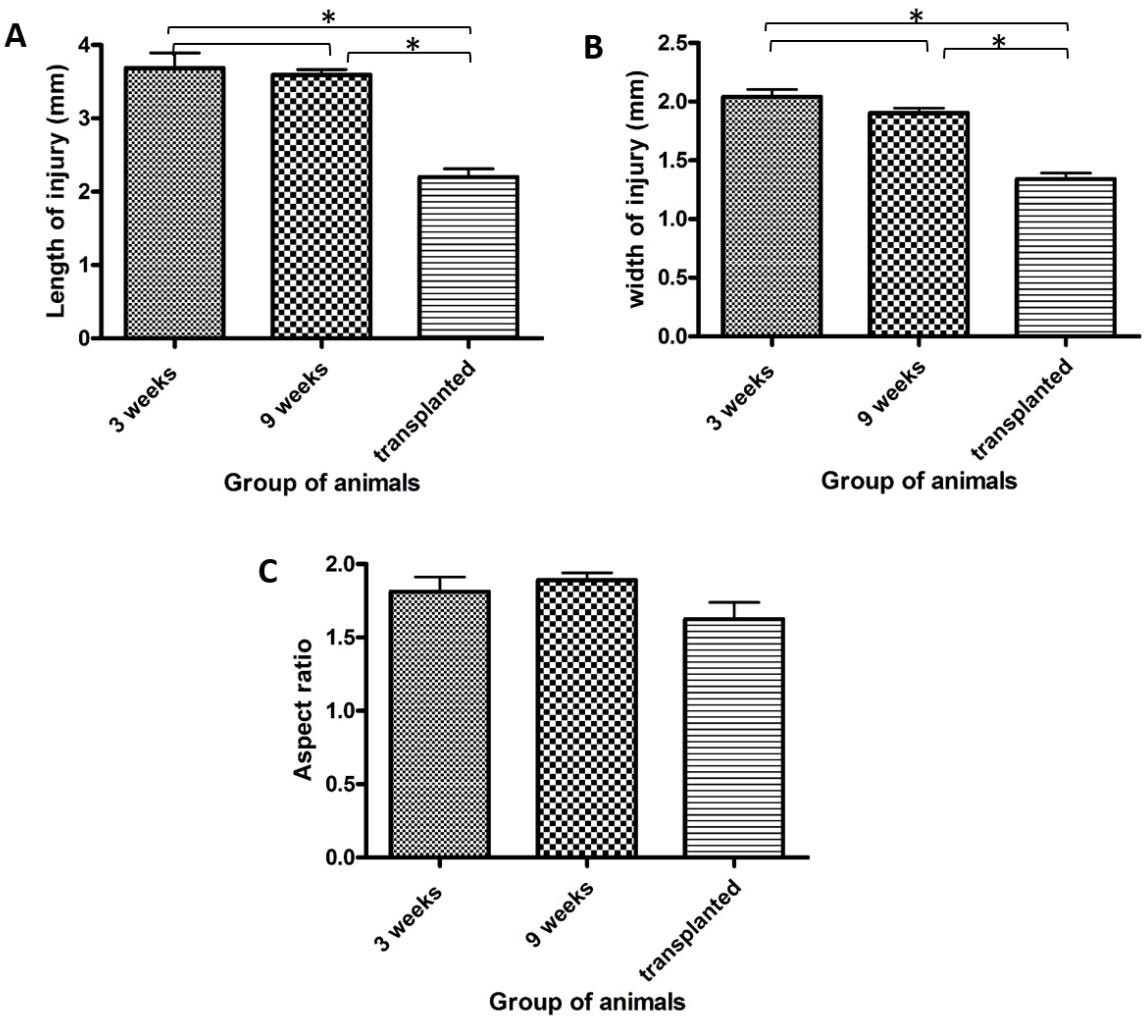

Figure 3-6. Comparison of length, width and aspect ratio of injury region.
Bar chart represent the length of the injury region taken from control animals (3 weeks and 9 weeks survival) and transplanted animals (A, right). The left bar chart represent the width of the injury region (B) and another bar chart represent the aspect ratio of the injury region. The error bars represent standard error of mean (SEM). Statistical analysis used is one way anova and asterisks (*) indicate p values of <0.05.

3.3.9.2 Dimension of glial scar

Tables 3-14, 3-15 and 3-16 show measurements of glial scar thickness/width based on GFAP immunolabelling which identifies the astroglial reaction to the injury, and possibly to the cells transplantated cells. Representative images of astroglial reaction in these 3 different groups (i.e. 3 weeks control, 9 weeks control and transplanted animals) are shown in the figures 3-24, 3-25 and 3-26. The width of the glial extent in control animals was 0.4mm or more (mean 0.49mm ±0.04) 3 weeks after injury (Table 3-14) and reduced to approximately 0.30 to 0.48mm (mean 0.35 ±0.03) at 9 weeks after injury (Table 3-15).

No	ID	Treatment	rostral	caudal	ventral	Mean (um)	mean (mm)
1	R2412	no	793.19	669.68	229.25	564.04	0.56
2	R10413	no	512.96	968.91	209.60	563.83	0.56
3	R16813	no	451.22	531.94	176.85	386.67	0.38
4	R16913	no	375.23	572.33	216.15	387.90	0.38
5	R17013	no	493.96	512.96	176.85	394.59	0.39
6	R18013	no	721.94	911.92	271.64	635.17	0.63
7	R9314	no	598.44	517.71	311.13	475.76	0.47
			563.85	669.35	227.35	**Mean(um)**	**0.49**

Table 3-14. Thickness of glial scar in control animals 3 weeks after injury

No	ID	Cell batch	rostral	caudal	ventral	Mean(um)	mean (mm)
1	**R2313**	no	470.20	156.03	157.20	261.14	0.26
2	**R17213**	no	797.94	479.63	153.93	477.17	0.48
3	**R19813**	no	289.73	246.97	134.28	223.66	0.22
4	**R2113**	no	408.46	489.21	286.56	394.74	0.40
5	**R17313**	no	470.20	531.94	248.90	417.02	0.42
6	**R17413**	no	479.70	379.98	160.36	340.01	0.34
7	**R17513**	no	332.47	408.46	189.95	310.29	0.31
			464.10	384.60	190.17	**Mean (um)**	0.35

Table 3-15. Thickness of glial scar in control animals 9 weeks after the injury

The data from these 3 groups of animals was compared using one way anova, illustrated in figure 3-7. There was a significant increase in glial thickness surrounding the injury region of the transplanted animals, ranging from 0.54 to 1.04 (mean 0.72mm ±0.04) (p value<0.001 for transplants versus 3 week and transplant versus 9 week)(Table 3-16) compared with both group of control animals. This finding suggests a strong glial reaction of the host tissue toward the transplanted cells which supports the previous finding with cell injections into non-injured (see section 3.3.7).

No	ID	Cell batch	rostral	caudal	ventral	Mean (um)	mean (mm)
1	**R34012**	MSC 7C A	1505.63	1320.38	291.48	1039.16	1.04
2	**R29612**	MSC 1C A	1106.65	1099.90	304.58	837.04	0.84
3	**R33612**	MSC 7C A	1142.66	915.96	370.08	809.57	0.81
4	**R50612**	MSC 1C A	926.48	997.42	298.03	740.64	0.74
5	**R2713**	MSC 7C A(II)	854.93	945.18	517.11	772.41	0.77
6	**R33712**	MSC 7C A	1011.67	1059.16	271.83	780.89	0.78
7	**R29212**	MSC 1C A	845.43	643.79	307.64	598.95	0.60
8	**R50412**	MSC 1C A (II)	702.94	916.67	343.88	654.50	0.65
9	**R50112**	MSC 1C A(II)	598.44	717.19	301.30	538.98	0.54
10	**R2413**	MSC 7C A(II)	631.70	774.18	209.45	538.44	0.54
11	**R2513**	MSC 7C A(II)	1111.40	869.18	238.91	739.83	0.74
12	**R2613**	MSC 7C A(II)	1068.66	717.19	265.09	683.65	0.68
13	**R10513**	MSC 9C A(II)	755.18	997.42	212.09	654.90	0.66
			943.21	921.05	302.42	**Mean (um)**	**0.72**

Table 3-16. Thickness of glial scar in transplanted animals 6 weeks after transplantation

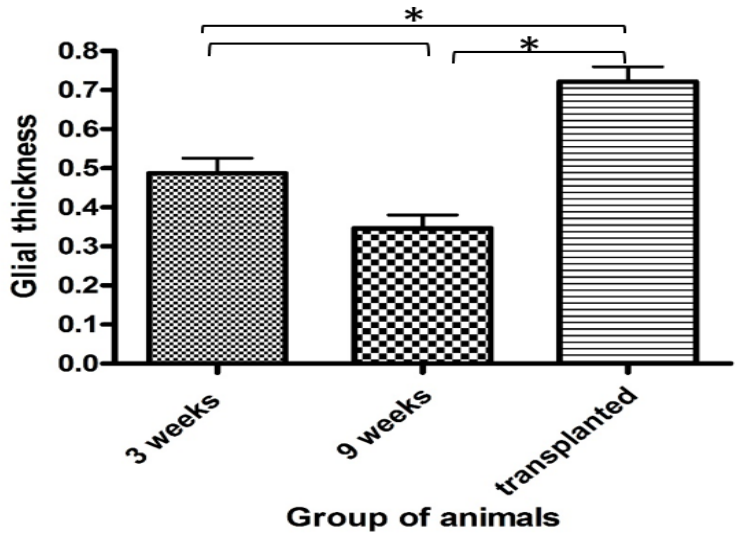

Figure 3-7. Comparison of the glial reaction surrounding the injury region.
Bar chart showing the thickness of the glial reaction surrounding the injury site of control animals (3 weeks and 9 weeks survival) and transplanted animals (A). Error bars represent standard error of mean (SEM). Statistical analysis used is one way anova and asterisks (*) indicate p values of <0.05.

3.3.10 Axonal regeneration promoted by cell transplants

Axonal regeneration within transplants of hESC-MSCs was investigated by using NF200 immunolabelling which reveals the neurofilament within myelinated fibres. When this is detected at the centre of a transplanted injury site which would otherwise be cavity or extracellular matrix deposited after tissue necrosis, this labelling can reliably be interpreted as representing regenerating fibres. Table 3.14 summarises the animals in which this approach was taken.

3.3.11 Neurofilament immunolabelling of axons

No	Rat No	Cell Batch	GFP%	Markers	Post-transplant
1	**R2512**	MSC 13C	90	GFP/NF200/GFAP	2 weeks
2	**R2712**	MSC 13C	90	GFP/NF200/GFAP	4 weeks
3	**R18213**	MSC 4C A (II)	90%	GFP/NF200/GFAP	4 weeks
4	**R33912**	MSC 7C A	48	GFP/NF200	6 weeks
5	**R10813**	MSC 9C A (II)	60	GFP/NF200	6 weeks
6	**R18413**	MSC 4C A (II)	90	GFP/NF200	6 weeks
7	**R33812**	MSC 7C A	48	GFP/NF200	6 weeks
8	R10613	MSC 9C A(II)	60	GFP/NF200	4 weeks
9	**R15312**	MSC 4C A	90	GFP/NF200/GFAP	6 weeks
10	**R15512**	MSC 4C A	90	GFP/NF200/GFAP	6 weeks
11	**R29712**	MSC 1C A	74	GFP/NF200/GFAP	6 weeks
12	**R2913**	MSC 7C A(II)	22	GFP/NF200/GFAP	6 weeks
13	**R19213**	MSC 4C A(II)	90%	GFP/NF200/GFAP	6 weeks
14	**R3413**	no		GFP/NF200/GFAP	9 weeks
15	**R4213**	no		GFP/NF200/GFAP	9 weeks
16	**R11013**	no		GFP/NF200	6 weeks
17	**R18913**	no		GFP/NF200	6 weeks
18	**R17113**	no		GFP/NF200	6 weeks
19	**R19413**	no		GFP/NF200	6 weeks

Table 3-14 Table summarising the animals used to investigate regenerating fibres in hESC-MSC transplants using NF200 immunoreactivity.

An example of neurofilament labelling in a transplanted injury site is shown in Fig. 3-27. In this example transplanted cells are distributed throughout the injury site which is delineated by the GFAP immunolabelling. There is, however, no obvious gap in the NF200 immunolabelling demonstrating the density of

regeneration within the transplant. Since regenerating axons can enter the transplant from all directions and are numerous, single axons cannot be followed for any appreciable length, but there is clear evidence that NF200 immunolabelled axons infiltrated the region inside the injury cavity associated with transplanted cells. This feature is shown in figure 3-28. In non-transplanted animals, there was also some evidence of NF200 immunolabelled axons entering the matrix filled area but not the injury area devoid of matrix as shown in figure 3-29. It is not possible using this immunocytochemical approach to determine whether fibres cross from one side of an injury to another. This information can only be obtained using a tract-tracing approach.

3.3.12 Investigation of corticospinal tract axons by tract tracing

Contusion injuries at C6 using 175 kdyn force results in injuries which completely interrupt the main component of the corticospinal tract (Riddell and Toft, unpublished observations) which travels in the ventromedial aspect of the dorsal columns. Injection of BDA into the sensorimotor cortex was therefore used to label corticospinal fibres and investigate their regenerative response to hESC-MSC transplants. Table 3.15 summarises the animals used in this part of the study.

No	Animal ID	Cell batch	GFP %	Markers
1	R50112	MSC 1C A(II)	34	GFP/BDA/GFAP
2	R50212	MSC 1C A(II)	34	GFP/BDA/GFAP
3	R50312	MSC 1C A(II)	34	GFP/BDA/GFAP
4	R2413	MSC 7C A(II)	22	GFP/BDA/GFAP
5	R2513	MSC 7C A(II)	22	GFP/BDA/GFAP
6	R2613	MSC 7C A(II)	22	GFP/BDA/GFAP
7	R10513	MSC 9C A(II)	60	GFP/BDA/GFAP
8	R17313	None		GFP/BDA/GFAP
9	R17413	None		GFP/BDA/GFAP
10	R17513	None		GFP/BDA/GFAP

Table 3-15 Summary of animals used for tract tracing of corticospinal fibres.

The results from all 7 animals were consistant and unequivocal. In all of the animals fibres belonging to the main component of the corticospinal tract approached the transplanted injury sites. Typically these axons reached the interface of the transplant but only very rarely did axons overlap with the cells. In no case was there any appreciable regeneration within the transplant (Fig 3-30 A-F). There was also no evidence that transplantation reduced the die back of corticospinal fibres. In control injured animals without a transplant, corticospinal fibres approached the rim of the injury cavity with equal proximity and in at least equal numbers (Fig 3-30 G-L).

3.3.13 Investigation of ascending dorsal column fibres by tract tracing

The ability of hESC-MSCs to support and promote the regeneration of dorsal column axons was investigated in 7 animals in which the dorsal columns were injured using a wire knife device. Transplants were made into these animals acutely and regenerating fibres were visualised using tract racing with BDA. A further 5 animals were investigated in the same way but also received conditioning injuries which were produced by sectioning the sciatic nerve. A summary of the animals used to study dorsal column axonal regeneration is shown in Tables 3.16 (no conditioning injury) and 3.17 (transplants combined with conditioning injury).

No	Animal ID	Cell batch	GFP %	Markers
1	R23612	MSC 4C A	90%	GFP/BDA/GFAP
2	R23712	MSC 4C A	90%	GFP/BDA/GFAP
3	R31412	MSC 1C A	74%	GFP/BDA/GFAP
4	R31512	MSC 1C A	74%	GFP/BDA/GFAP
5	R35612	MSC 7C A	48%	GFP/BDA/GFAP
6	R35712	MSC 7C A	48%	GFP/BDA/GFAP
7	R35812	MSC 7C A	48%	GFP/BDA/GFAP

Table 3-16 Summary of animals used to investigate dorsal column axon regeneration through hSEC-MSC transplants.

No	Animal ID	Cell batch	GFP %	Markers
1	R23512	MSC 4C A	90%	GFP/BDA/GFAP
2	R31212	MSC 1C A	74%	GFP/BDA/GFAP
3	R1113	MSC 1C A (II)	60%	GFP/BDA/GFAP
4	R1413	MSC 1C A (II)	60%	GFP/BDA/GFAP
5	R1513	MSC 1C A (II)	60%	GFP/BDA/GFAP

Table 3-17. Summary of animals used to investigate dorsal column axon regeneration through hSEC-MSC transplants combined with a conditioning injury.

Six of the 7 animals without a conditioning lesion showed good BDA labelling of sensory fibres allowing assessment of axonal regeneration but one animal was excluded from further analysis because the BDA labelling of sensory fibres was too poor. In all of the 6 animals with good BDA labelling the transplanted cells filled the lesion site and in 5 of these animals, variable numbers of cells formed a track extending rostral of the injury site. These cells were typically distributed near the midline in an area dorsal to the central canal. In all 6 animals analysed BDA labelled fibres could be seen within the transplanted lesion site (Figs. 3.31, 3.32 and 3.33). In each case the fibre growth was disorganised and rather than being directed across the lesion site in an ordered fashion. Fibres were often tortuous and clearly different from normal dorsal column axons and they penetrated the transplant region for varying distances with some fibres reaching the rostral margins of the injury site. However, despite the presence of a rostral track of cells in 5 of the animals, in 4 of the 5, none of the fibres projected rostral of the injury site even within this cellular track. An example of regenerating fibres in one of these animals in shown in Fig. 3.31. Despite numerous regenerating axons at the rostral injury margin, none entered the densely populated track of transplanted cells leading rostral to the injury. However, for one of the animals (R23612) conditions appeared to combine particularly favourably. A broad rostrally directed track of cells provided a path leading away from the transplanted injury site and in this animal numerous fibres could be seen within the transplanted injury and some could also be seen within the cell track rostral to the injury. Regenerating fibres were measured extending up to 1.06mm from the rostral edge of the injury region (measured from a section with the most rostral regenerating axons seen). An example section from this animal is shown in Fig. 3.32. This however, was the only animal

in which there was any significant degree of axonal regeneration beyond the injury in animals without conditioning lesions.

Of the five animals in which transplants were combined with conditioning injuries to the sciatic nerve, one was excluded due to poor BDA labelling. The remaining 4 animals all had cells which spread rostral to the injury site but only one showed clear regeneration of fibres rostral to the injury (R1413). In this animal, the regenerating fibres (also measured from the section with the most rostral regenerating axons) was seen to be extending up to 0.69mm from the rostral edge of the injury region. The regeneration observed in this animal is illustrated in Fig. 3.33.

A noticeable feature of each of the animals with rostrally directed cell tracks, which was seen when confocal microscopy was performed to reveal GFAP immunolabelling, was that astrocytes were largely absent from an area corresponding to the distribution of GFAP labelled cells. This suggests that transplanted cells spreading beyond the injury into the host spinal cord tissue may exclude host astrocytes. This can be seen in Figs. 3.31, 3.32 and 3.33, where axons also appear to be displaced from the caudal cell track where BDA labelled fibres would be expected.

3.3.14 Myelination at transplanted injury sites

To investigate whether regenerating fibres become myelinated sections from the transplanted injury site of 5 animals were immunoreacted with antibodies to CASPR which is a contactin-associaed protein found at the paranodal secions of myelin sheaths. This was used to look for evidence of Nodes of Ranvier within the centre of transplants indicative of myelination of regenerating fibres within the transplant. Neurofilament immunolabelling was also used to label regenerating fibres and look for associations with CASPR. Most of the animals were processed 6 weeks following transplantation. Table 3.18 summarises the animals used to investigate myelination using CASPR.

No	Animal No	Cell batch	GFP %	Immunocytochem.	Post-transplant
1	R33812	MSC 7C A	48	GFP/CASPR/NF200/ P0	6 weeks
2	R10613	MSC 9C A(II)	60	GFP/CASPR/NF200/ P0	4 weeks
3	R10313	MSC 9C A(II)	60	GFP/CASPR/NF200/ P0	6 weeks
4	R10713	MSC 9C A(II)	60	GFP/CASPR/NF200/ P0	6 weeks
5	R17113	None		GFP/CASPR/NF200/ P0	6 weeks
6	R19413	None		GFP/CASPR/NF200/ P0	6 weeks

Table 3-18. Summary of animals used for investigating myelination of regenerating fibres using the expression of the paranodal protein CASPR

Sections from all of the animals examined showed evidence of numerous nodes of Ranvier in the centre of transplanted injury sites. Fig. 3.34 shows examples from one of the animals. The axons on which these nodes are located cannot be spared fibres since they are in the middle of the injury and the presence of CASPR therefore indicates that these regenerating fibres have acquired a myelin sheath. The presence of a paranodal protein such as CASPR further indicates that this myelination is functional and the fibres could be expected to propagate impulses. Some of the CASPR immunolabelling was associated with NF200 positive fibres but, interestingly, much of it was not.

Figure 3-8. Injury site appearance 3 weeks after contusion.
The injury site was examined three weeks after contusion to assess tissue reactivity and cavity morphology at the time of cell transplantation. All sections showed a strong gliotic reaction to injury, evidenced by intense astrocyte labelling with GFAP (A-D, green). There was also some expression of nestin but this was not co-localised to astrocytes (A & D, red). The appearance of the injury site depended on the extent to which it was occupied by endogenous matrix (which was enriched for laminin, red in B & C). The sequence of examples from A to D show examples that range from a large single cavity (A) though multiple cavities (B) to those partly filled (C) or largely filled (D) by extracellular matrix. All images represent composites of multiple x20 fields of view from 60 µm thick tissue sections and projected from 15-20 z-sections. Scale bar = 500 µm, applicable to all panels.

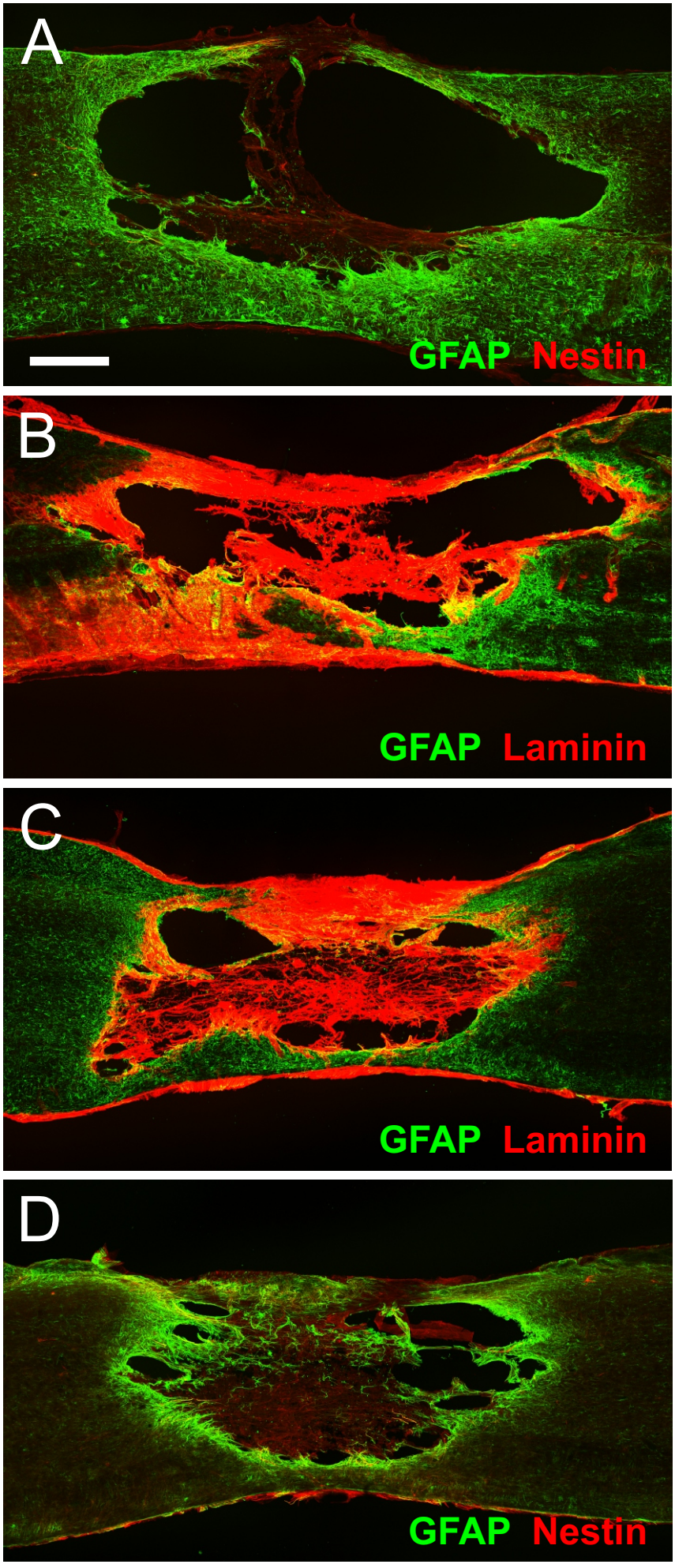
A
GFAP Nestin
B
GFAP Laminin
C
GFAP Laminin
D
GFAP Nestin

Figure 3-9. Cell survival at one week post-transplant in animals without immunosuppression.
Saggital sections showing examples of the GFP labelled profiles seen in animals one week after injury. A, a small pocket of GFP labelled cells and scattered cells within the injury site. B, GFP labelled cells forming a rim around around a moderately sized injury cavity. C, a small area of cells within the extracellular matrix filling the injury site. Note that the cells are rounded in morphology. All sections show a strong gliotic reaction (GFAP, blue A-D) and some expression of nestin (A-D, red). Despite the poor survival of cells there is minimal cavitation due to extensive matrix infilling of the injury site (A-D). All images represent composites of multiple x20 fields of view from 60 µm thick tissue sections and projected from 15-20 z-sections. Scale bar (A) = 500 µm, applicable to all panels.

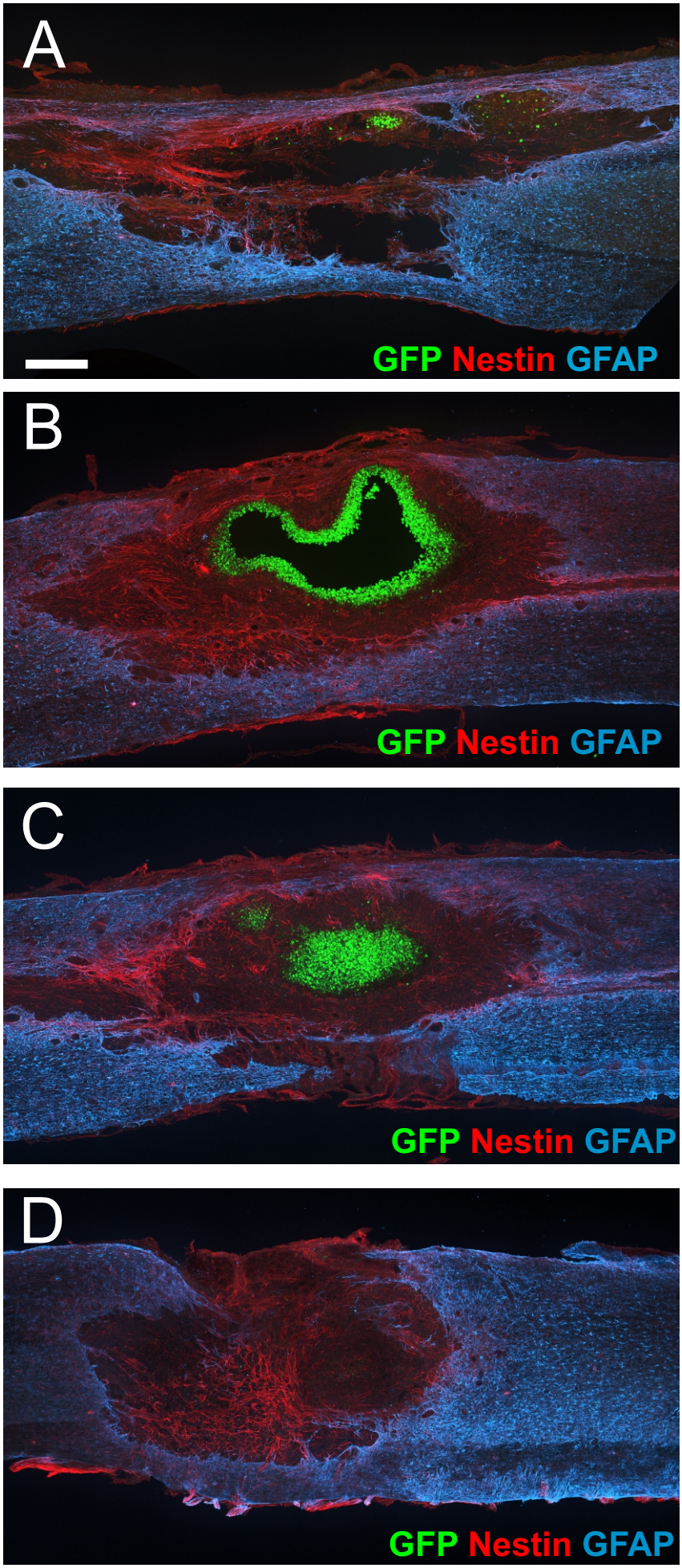
A
GFP Nestin GFAP
B
GFP Nestin GFAP
C
GFP Nestin GFAP
D
GFP Nestin GFAP

Figure 3-10. Absence of surviving cells at 2 and 4 weeks post-transplant in animals without immunosuppression.
GFP labelled cells were virtually absent from sections from 2 week (A and B) and 4 week (C and D) animals. All sections showed a strong gliotic reaction to injury as showed by intense astrocyte labelling with GFAP (A-D, blue) and expression of nestin (A-D, red). There was extensive matrix infilling of the injury site in all animals (A-D). All images represent composites of multiple x20 fields of view from 60 µm thick tissue sections and projected from 15-20 z-sections. Scale bar (A) = 500 µm, applicable to all panels.

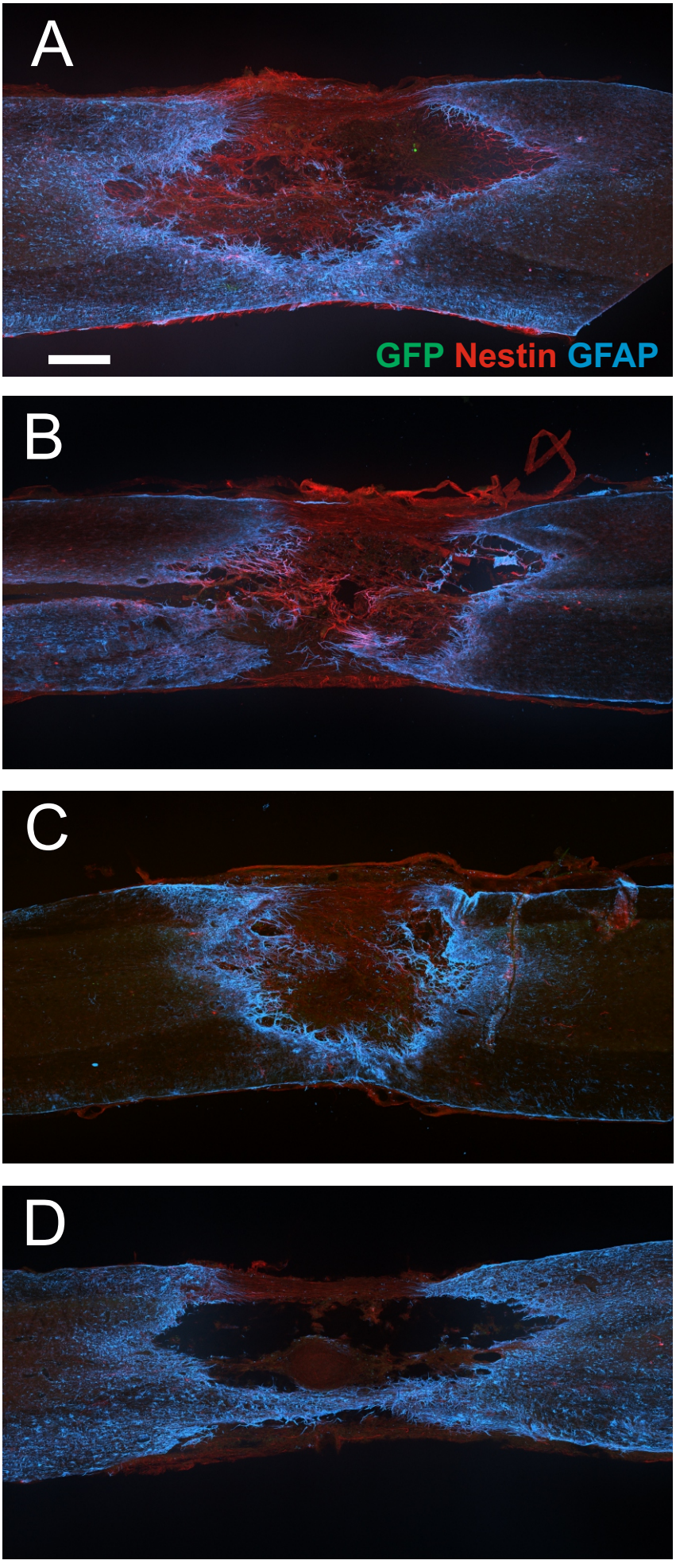
A
GFP Nestin GFAP
B
C
D

Figure 3-11. Cell survival in immunosuppressed animals at different time points. Sections from the transplant site of immunosuppressed animals 5days after transplantation (A, 60% GFP) two weeks after transplantation (B; 90% GFP) and 4 weeks after transplantation (C and D, 90% and 74% GFP). Numerous surviving cells are seen widely distributed within the injury site and over varying distances beyond the injury. In A and D cells are absent from some areas of the injury site occupied by extracellular matrix. All images represent composites of multiple x20 fields of view from 60 µm thick tissue sections and projected from 14-18 z-sections. Scale bar = 500 µm.

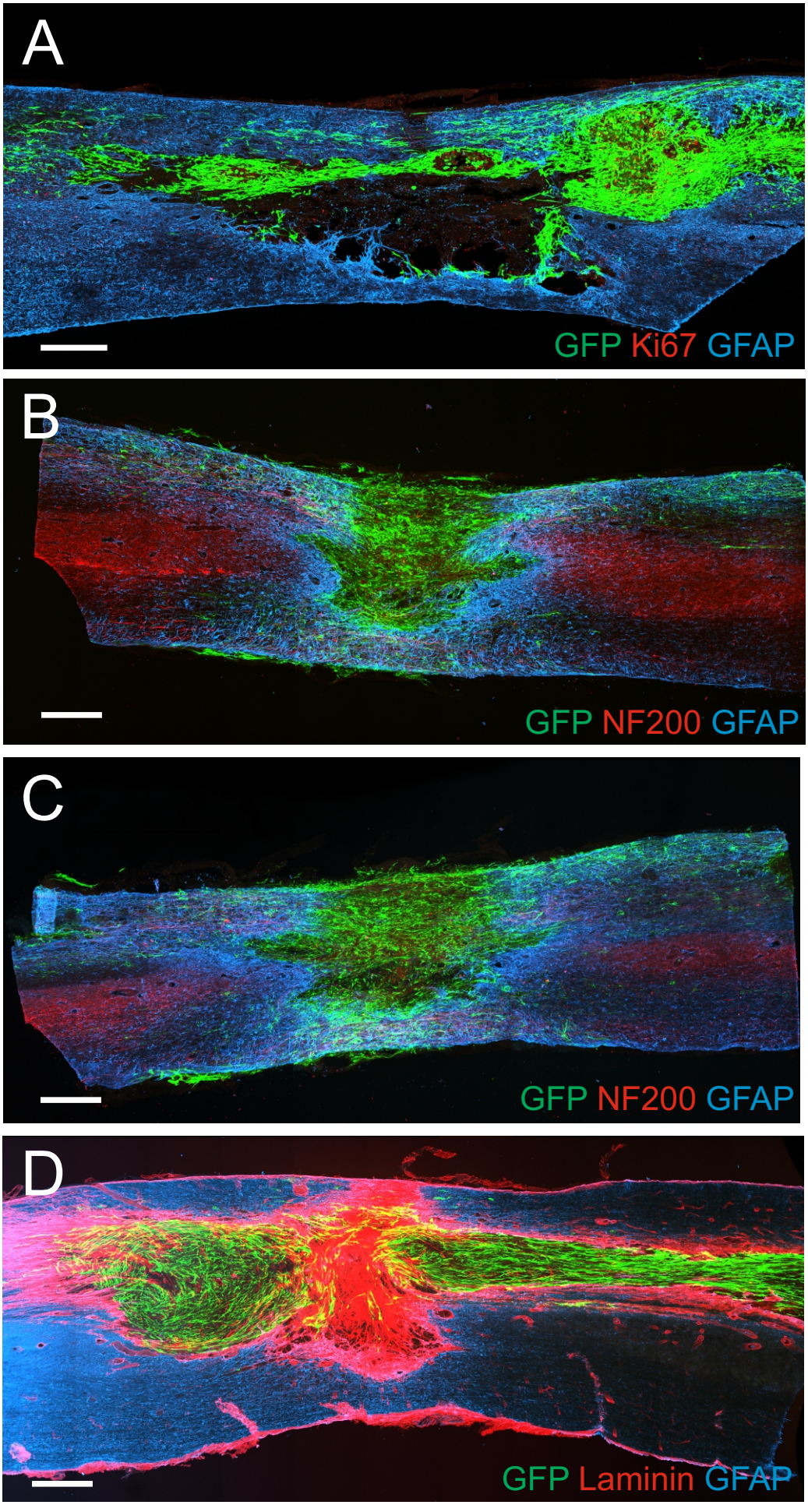
A
GFP Ki67 GFAP
B
GFP NF200 GFAP
C
GFP NF200 GFAP
D
GFP Laminin GFAP

Figure 3-12. Characteristics of contusion injury sites 9 weeks after injury in immunosuppressed animals.

A, B and C show three examples of parasaggital sections through the injury site of control non-transplanted animals at a 9 week post-injury survival time equivalent to the animals examined 6 weeks after transplantation. The sections illustrate the extensive cavitation shown by these animals with varying degrees of matrix infilling. An intense glial scar remains around the injury cavities (GFAP, blue). All images represent composites of multiple x20 fields of view from 60 µm thick tissue sections projected from 16-24 z-sections. Scale bar = 500 µm, applicable to all panels.

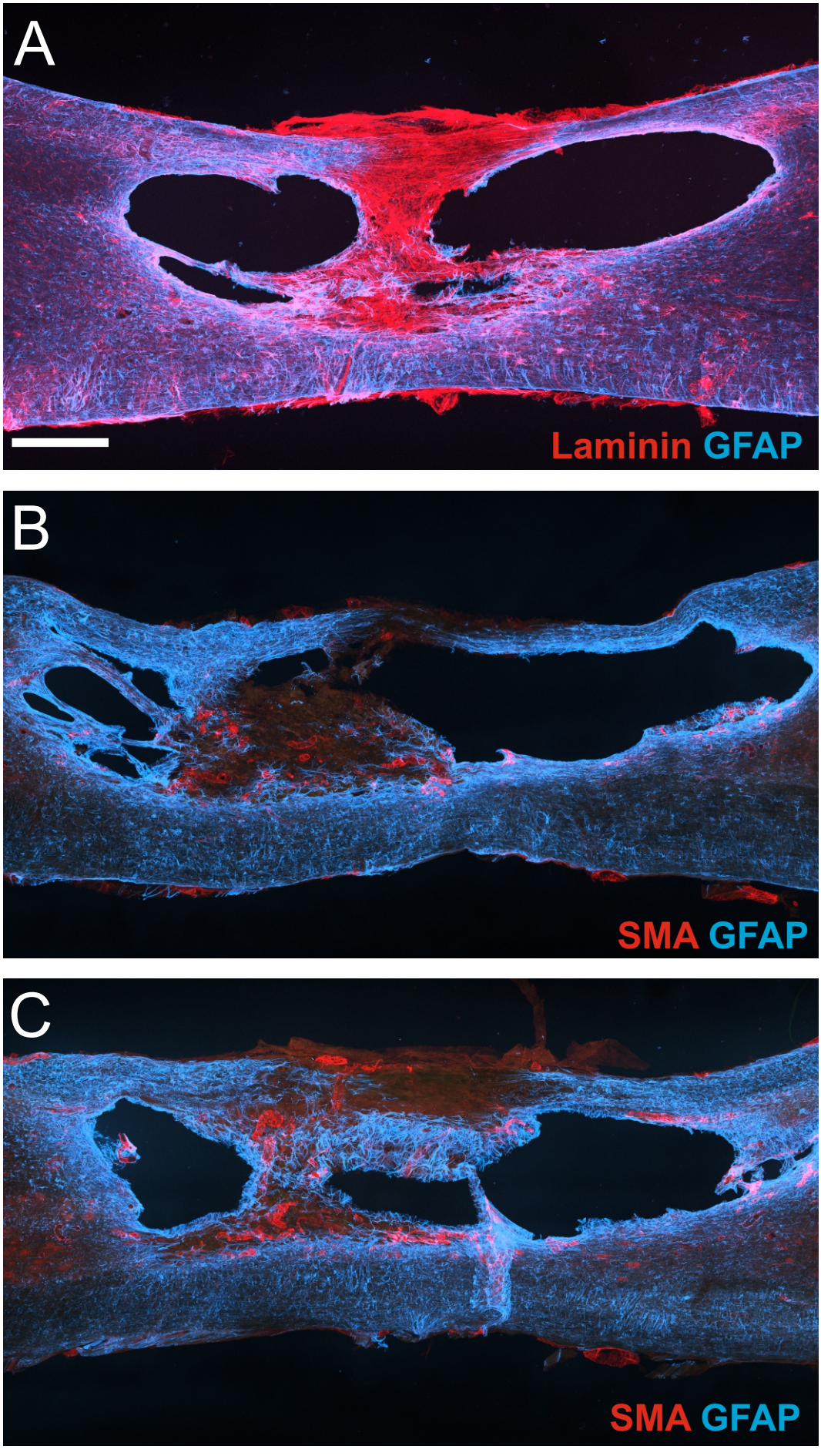
A
Laminin GFAP
B
SMA GFAP
C
SMA GFAP

Figure 3-13. Ki67 immunolabelling at a transplanted injury site 5 days after transplantation.

A and B, parasaggital section through an injury site transplanted with hESC-MSCs five days earlier showing the distribution of Ki67 immunolabelling. Labelled profiles were concentrated in areas occupied by extracellular matrix rather than cells. High power confocal scanning of areas containing transplanted cells (C and D) showed that Ki67 immunoreactivity never colocalised with GFP. A further analysis on single z stack images from 3 different animals (E, F and G) also revealled no genuine evidence of co-localization. Images A and B represent composites of multiple x20 fields of view from 60 µm thick sections projected from 16-20 z-sections. Scale bar = 500 µm. Images C and D represent single field views projected from 35-39 z sections. Images E, F and G represent a single field of view in single z sections. Scale bar = 100 µm.

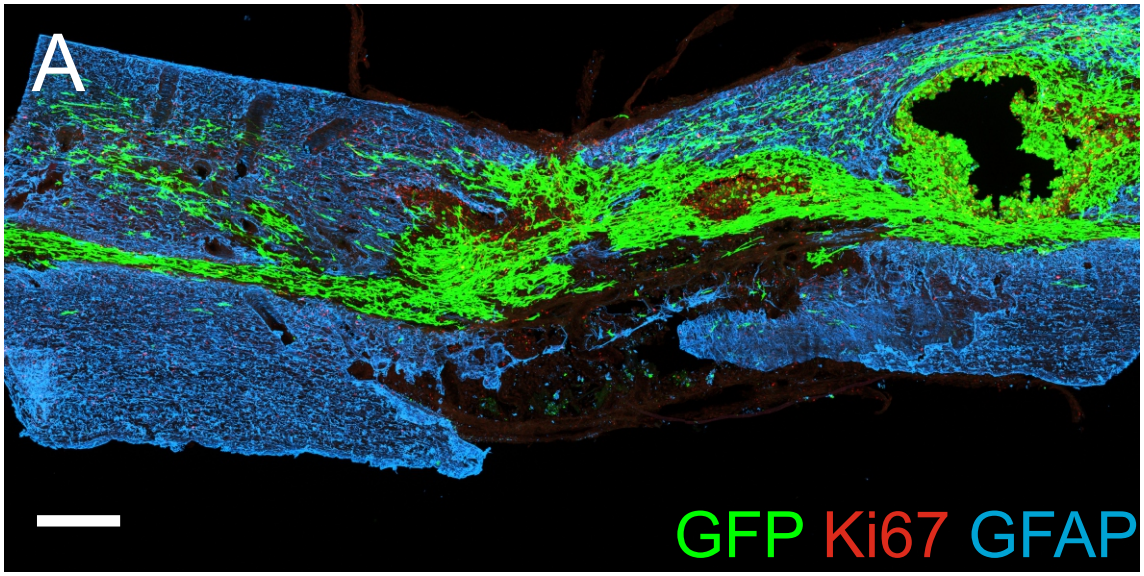
A
GFP Ki67 GFAP

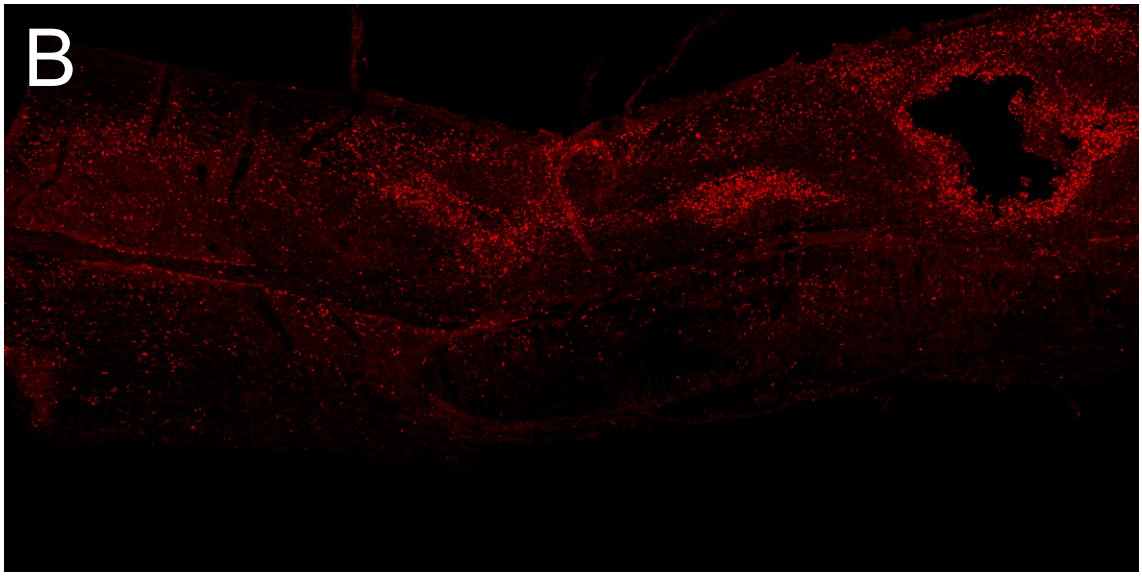
B

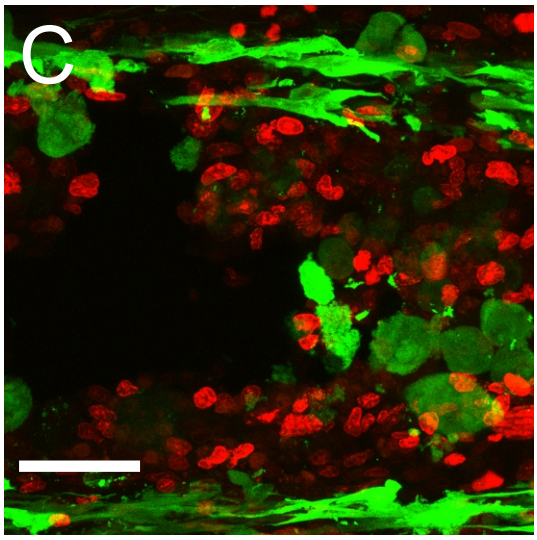
C

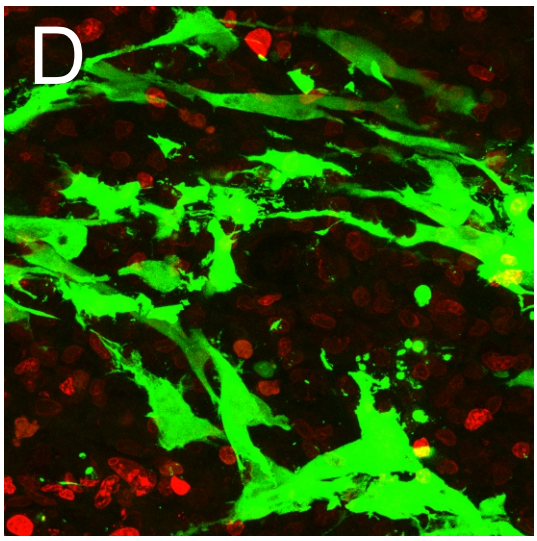
D

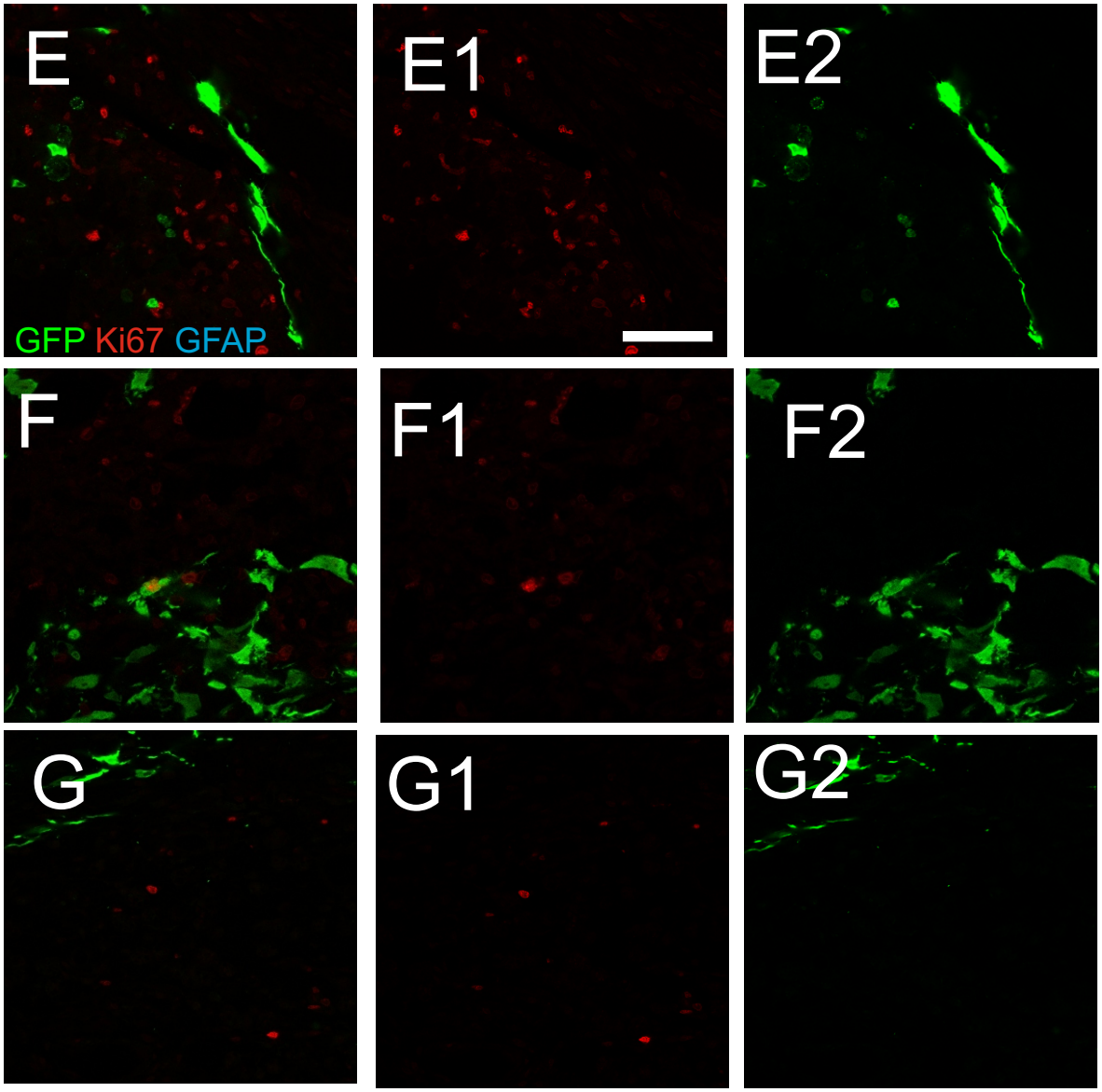
E
E1
E2
GFP Ki67 GFAP
F
F1
F2
G
G1
G2

Figure 3-14. Cell morphology 2 weeks after transplant into the injured spinal cord

A and D show two different parasagittal sections from the same animal. The boxed area indicated on each is shown at high magnification in B-C and E-F respectively. B-C shows the morphology of cells located outside the main transplant area while E-F shows the morphology of cells at the centre of the transplant. Images A and D represent composites of multiple x20 fields of view and images B-C and E-F represent one field view from 60 µm thick tissue sections and are projected from 30-35 z-sections. Scale bar = 500 µm (A and D) 200µm (B-C and E-F). GFP expression=90%.

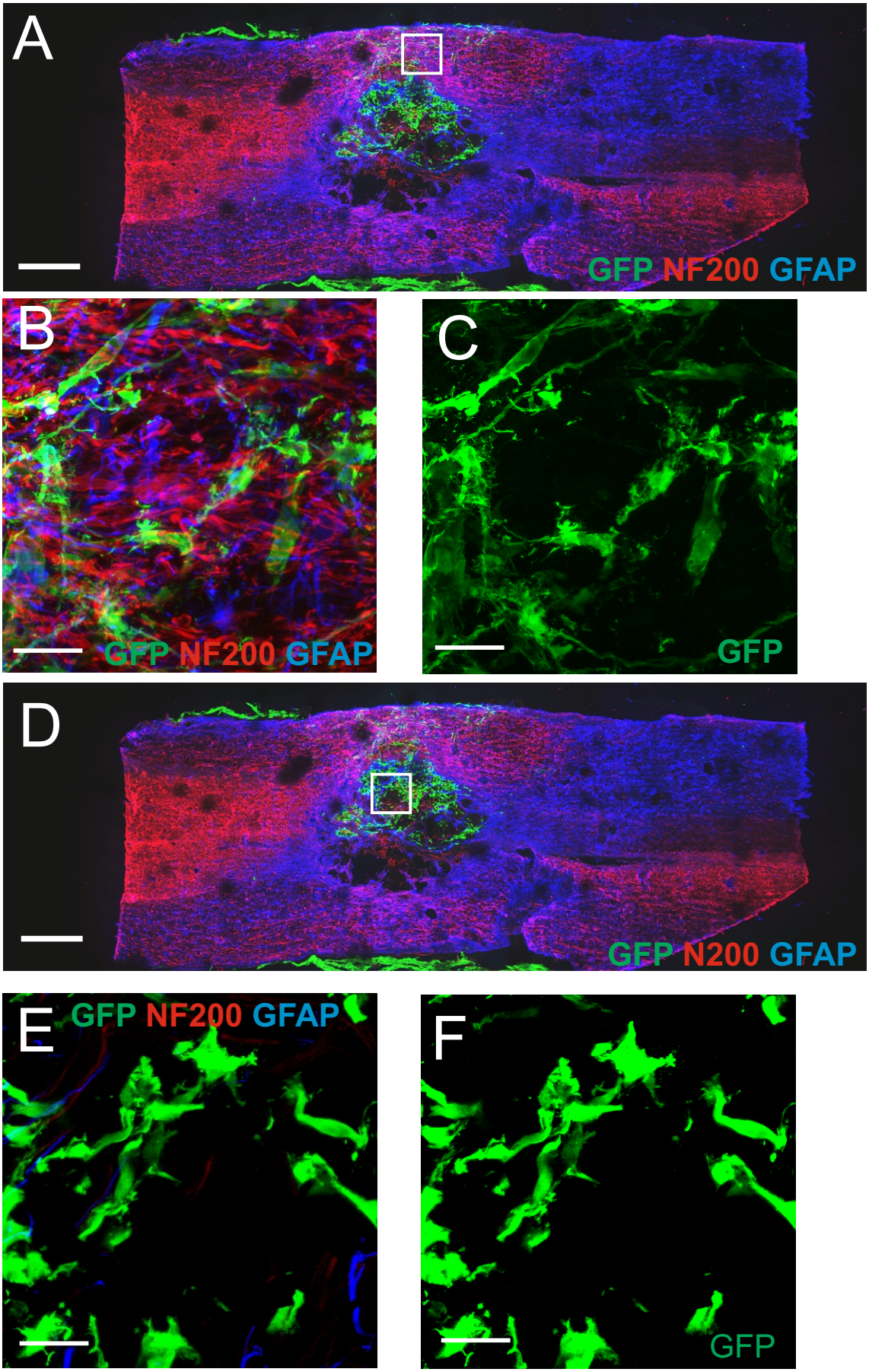
A
GFP NF200 GFAP
B
GFP NF200 GFAP
C
GFP
D
GFP N200 GFAP
E
GFP NF200 GFAP
F
GFP

Figure 3-15. Cell morphology 4 weeks after transplantation into the injured spinal cord

A and D show two different parasagittal sections from the same animal. The boxed area indicated on each is shown at high magnification in B-C and E-F respectively. B-C shows the morphology of cells located outside the main transplant area while E-F shows the morphology of cells at the centre of the transplant. Images A and D represent composites of multiple x20 fields of view and images B-C and E-F represent one field view from 60 µm thick tissue sections and are projected from 30-35 z-sections. Scale bar = 500 µm (A and D) 200µm (B-C and E-F). GFP expression=90%.

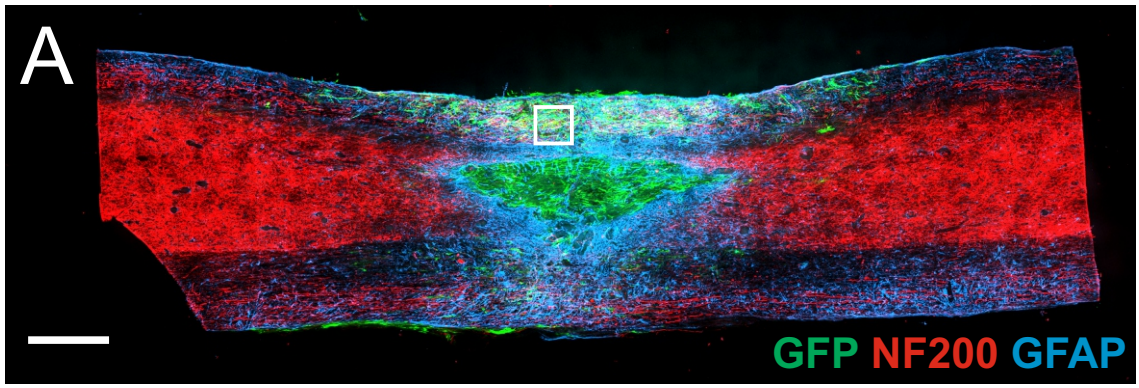
A
GFP NF200 GFAP

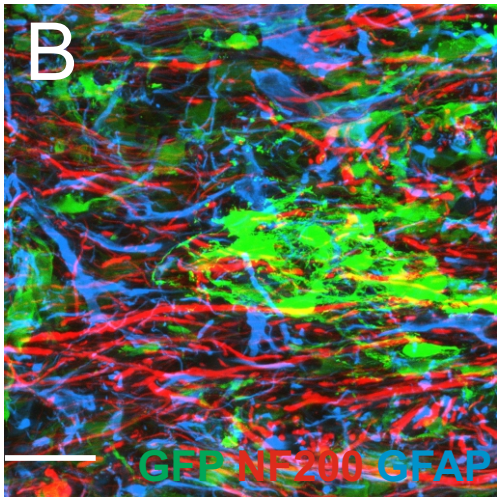
B
GFP NF200 GFAP

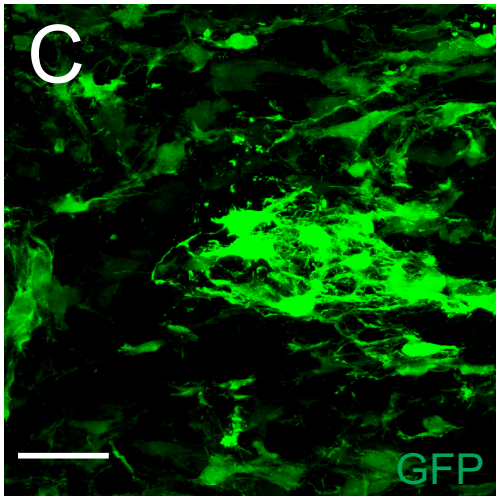
C
GFP

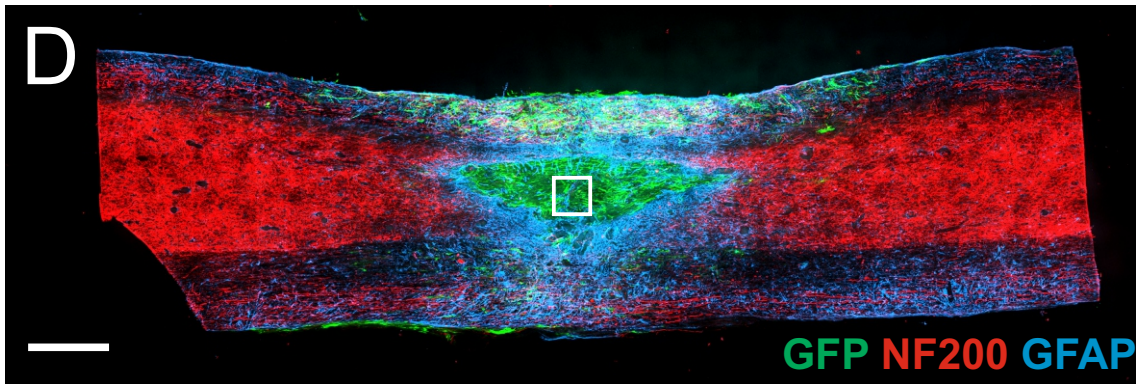
D
GFP NF200 GFAP

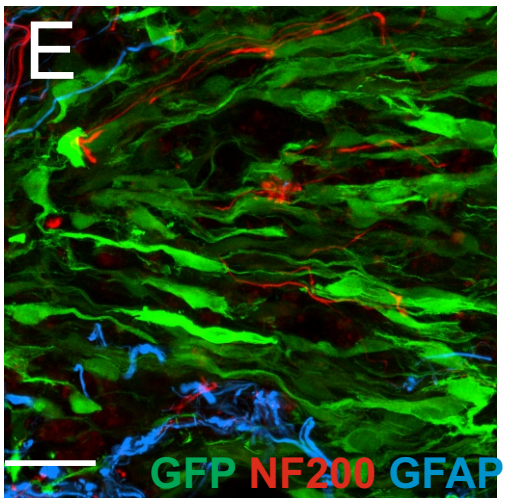
E
GFP NF200 GFAP

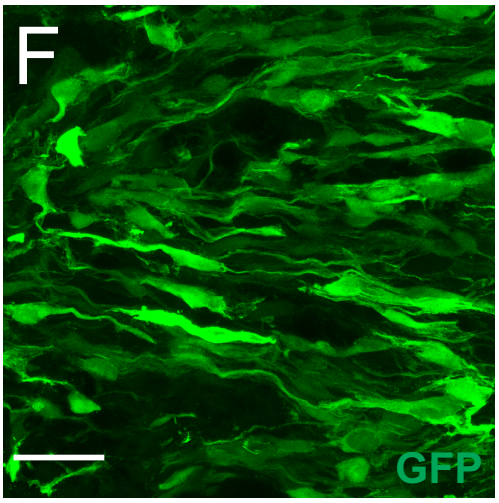
F
GFP

Figure 3-16. Extracellular matrix distribution in the injured spinal cord at 6 weeks after transplantation.

A and B are parasaggital sections through the injuries transplanted with hESC-MSCs 6 weeks earlier. The images show the very dense distribution of laminin (red) which is especially intense in regions of the injury where cells (green) are absent. All images represent composites of multiple x20 fields of view from 60 um thick tissue sections and projected from 18-20 z-sections. Scale bar = 500 µm, applicable to all panels. (GFP expression; A 48%, B 74%)

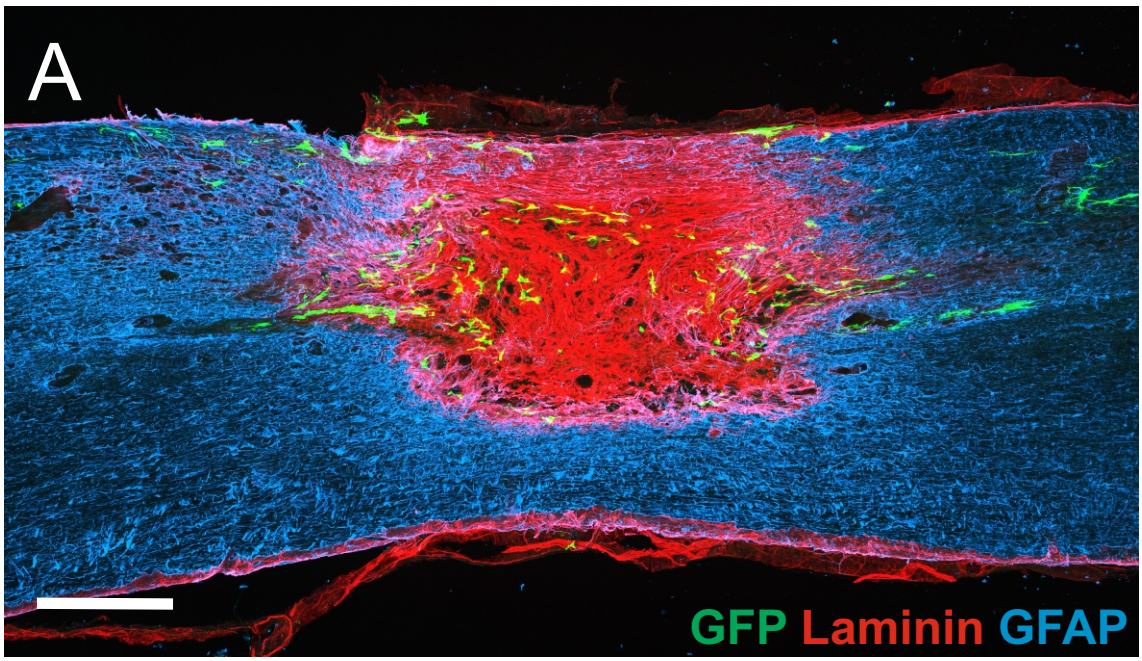
A
GFP Laminin GFAP

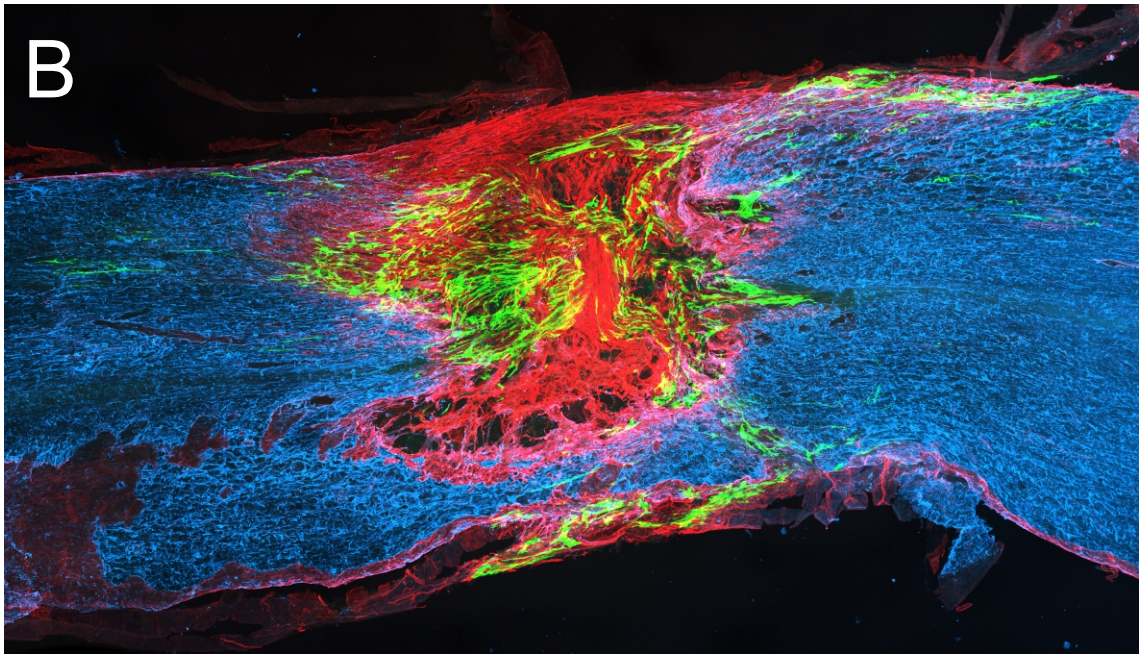
B

Figure 3-17. Immunolabelling with laminin showing blood vessels around the injury site.

A and B show parasaggital sections through a transplanted cord. The sections are lateral to the main injury and transplant site where the laminin staining is less dense. This enables visualization of some of the details of the laminin immunolabelling which includes numerous blood vessels which are particularly numerous at a level equivalent to the injury. Both images represent composites of multiple x20 fields of view from 60 um thick tissue sections and projected from 15-16 z-sections. Scale bar = 500 μm, applicable to all panels. (GFP expression 60%)

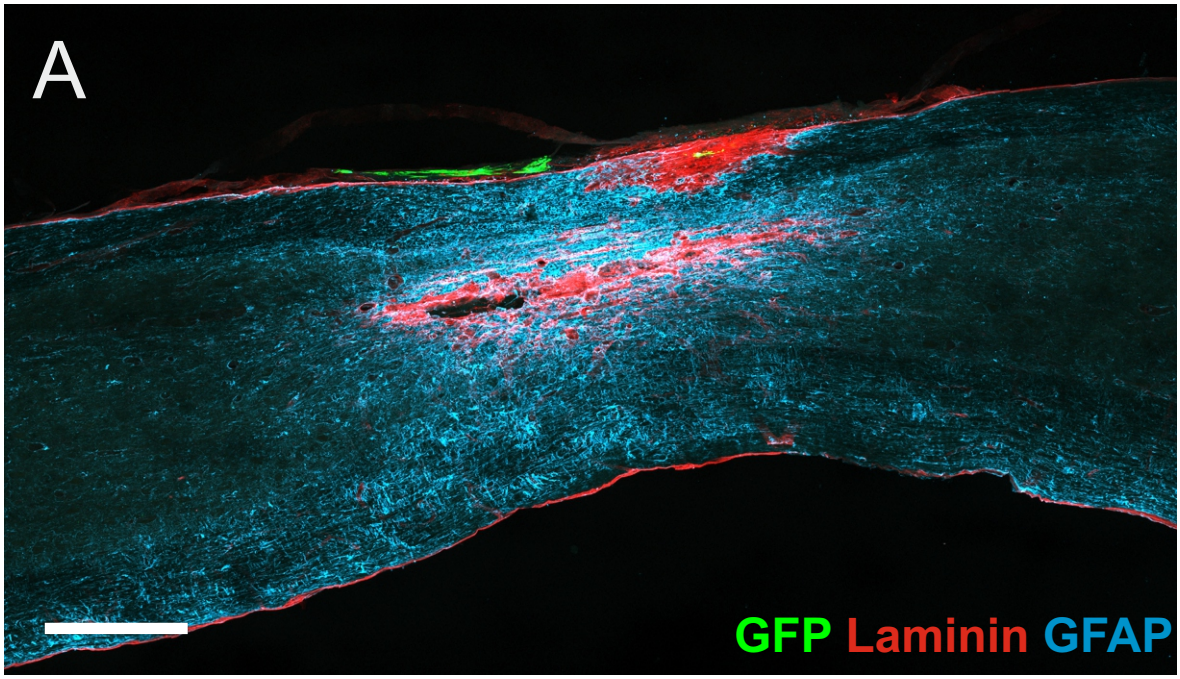
A
GFP Laminin GFAP

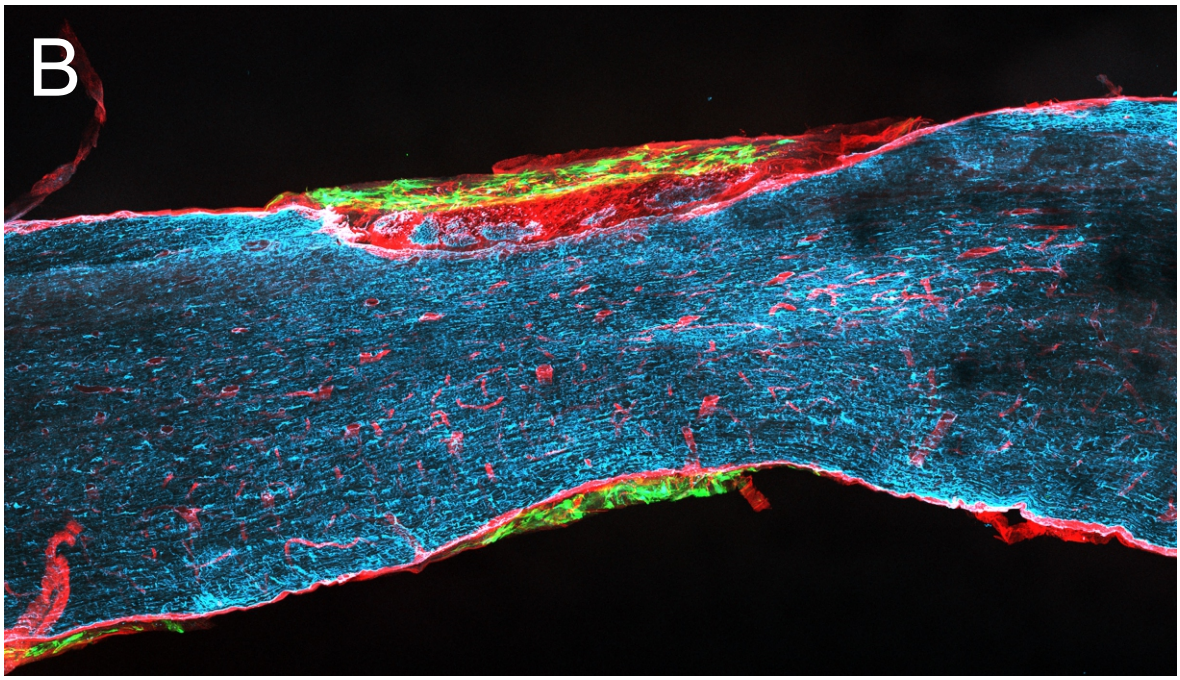
B

Figure 3-18. Distribution of blood vessels immunolabelled with SMA in the injured spinal cord 6 weeks after transplantation.

1 A,B and 2,A,B show two examples of saggital sections through transplanted injuries where SMA (red) reveals development of a profuse network of resistance vessels at the injury site. The vessels are distributed in and around the injury site and are not associated specifically with transplanted cells. All images represent composites of multiple x20 fields of view from 60 µm thick tissue sections and projected from 18-20 z-sections. Scale bar = 500 µm, applicable to all panels. (GFP expression 74%)

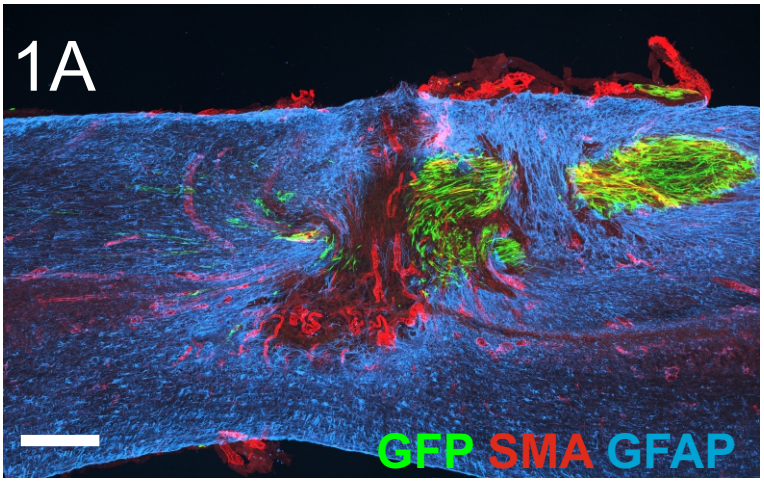
1A
GFP SMA GFAP

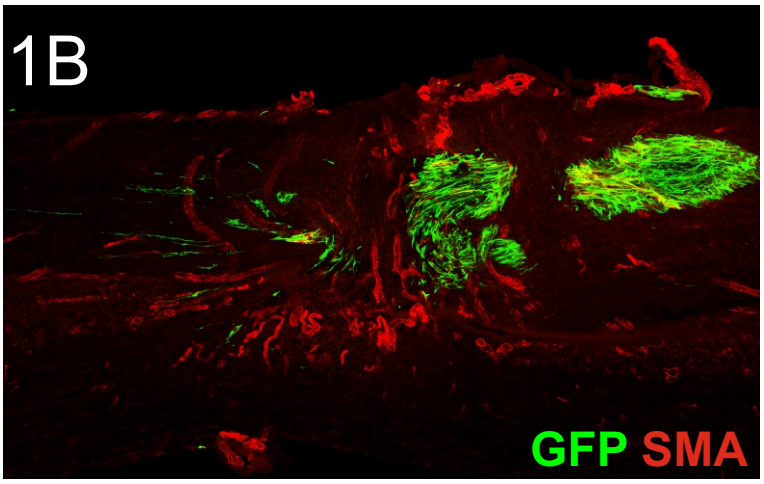
1B
GFP SMA

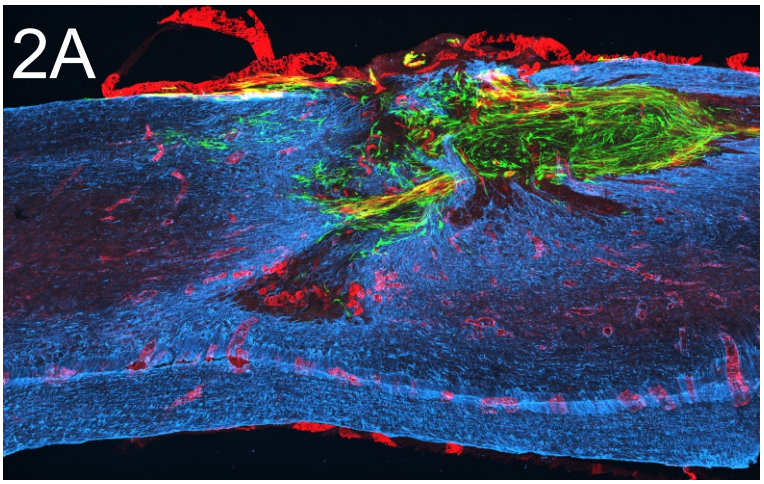
2A

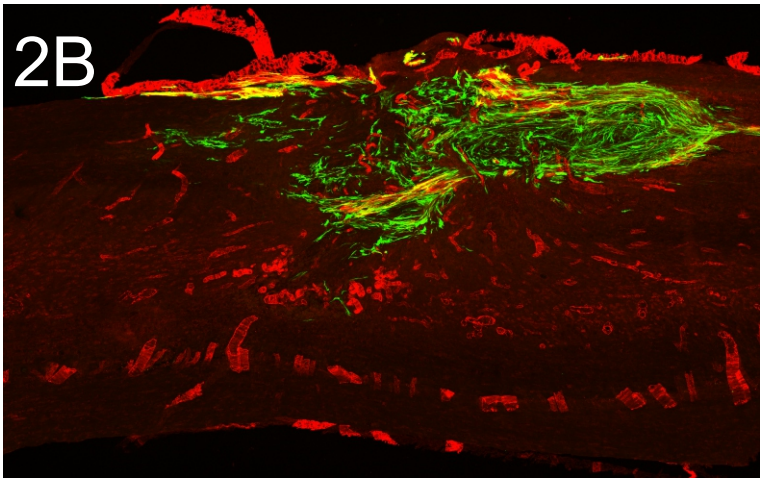
2B

Figure 3-19. Assessment of the reaction of host glial cells to hESC-MSCs injected into the non-injured spinal cord.
Each row of images illustrates the astroglial reaction (nestin in red, GFAP in blue) surrounding a small bolus injection of cells made into the dorsal columns in normal animals. The images in column 1 A to 4A were taken at X10 magnification while all remaining images are X20 magnification. Column 1B to 4B illustrates the relationship of injected cells to the glial cells. Column 1C to 4C illustrates the nestin immunoreactivity surrounding the transplanted cells. Column 1D to 4D illustrates the glial reaction around the transplanted cells and the exclusion of glial cells from the cell bolus. All images represent one field of view from 60 µm thick tissue sections and are projected from 30-40 z-sections. Scale bars: 1A-4A = 200 µm, note scale bar in 1A applicable to 2A and 4A. 1B-D to 4B-D = 100 µm, note scale bar in 3B applicable to 3B-D and scale bar in 1B applicable to all others. Row 3 field of view digital zoom set to a factor of 0.7. (GFP expression=90 %)

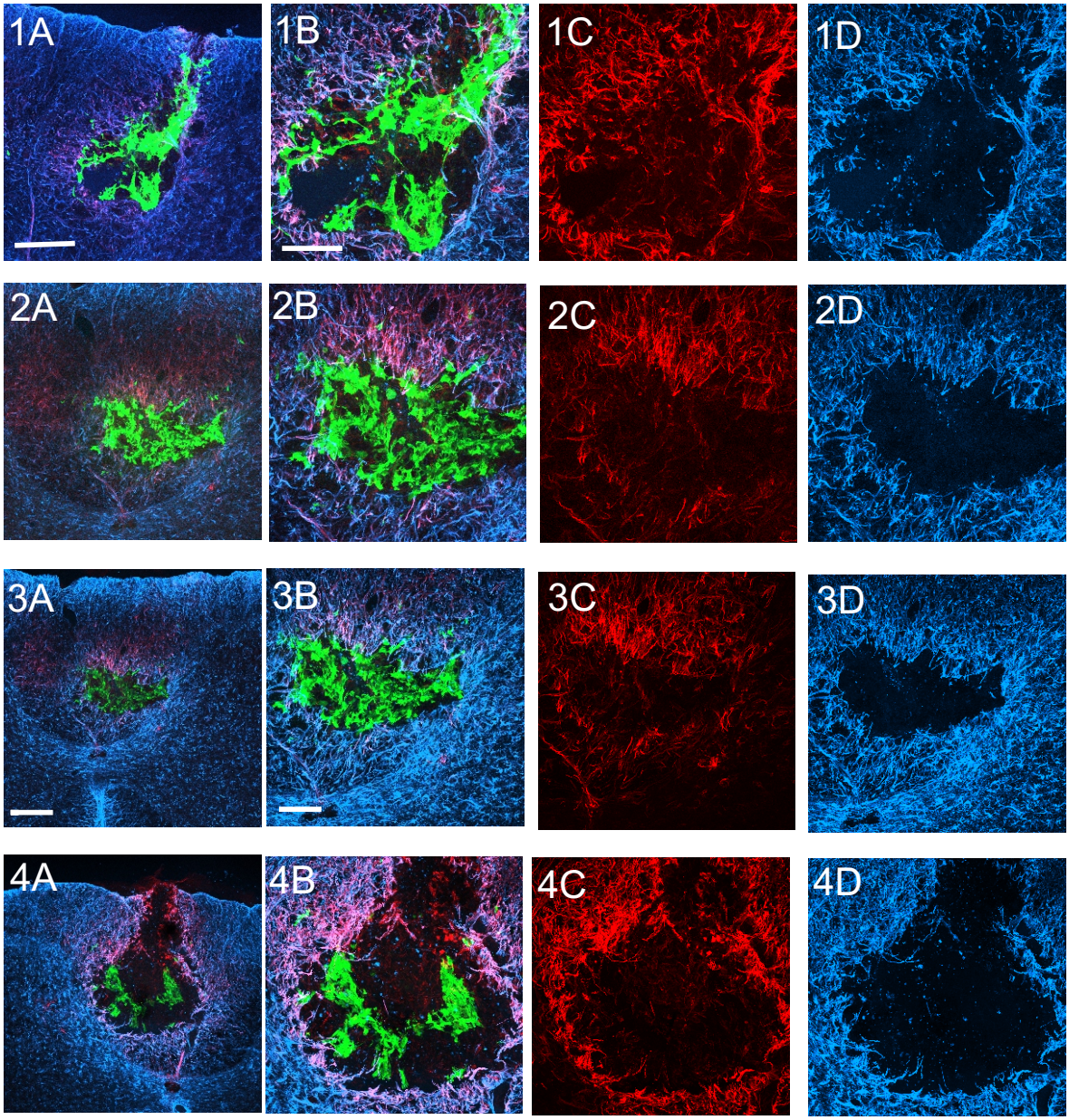
1A
1B
1C
1D
2A
2B
2C
2D
3A
3B
3C
3D
4A
4B
4C
4D

Figure 3-20. Nestin & GFAP for glial reaction.

A and B, parasaggital sections through the injury site in a transplanted and control non-injured animal processed using immunocytochemistry for GFAP (blue) and nestin (red). Neither section shows much nestin immunoreactivity which would be indicative of glial activation although GFAP remains upregulated around both injury sites. All images represent composites of multiple x20 fields of view from 60 µm thick tissue sections and projected from 14-16 z-sections. Scale bar = 500 µm, applicable to all panels. (GFP expression 60%)

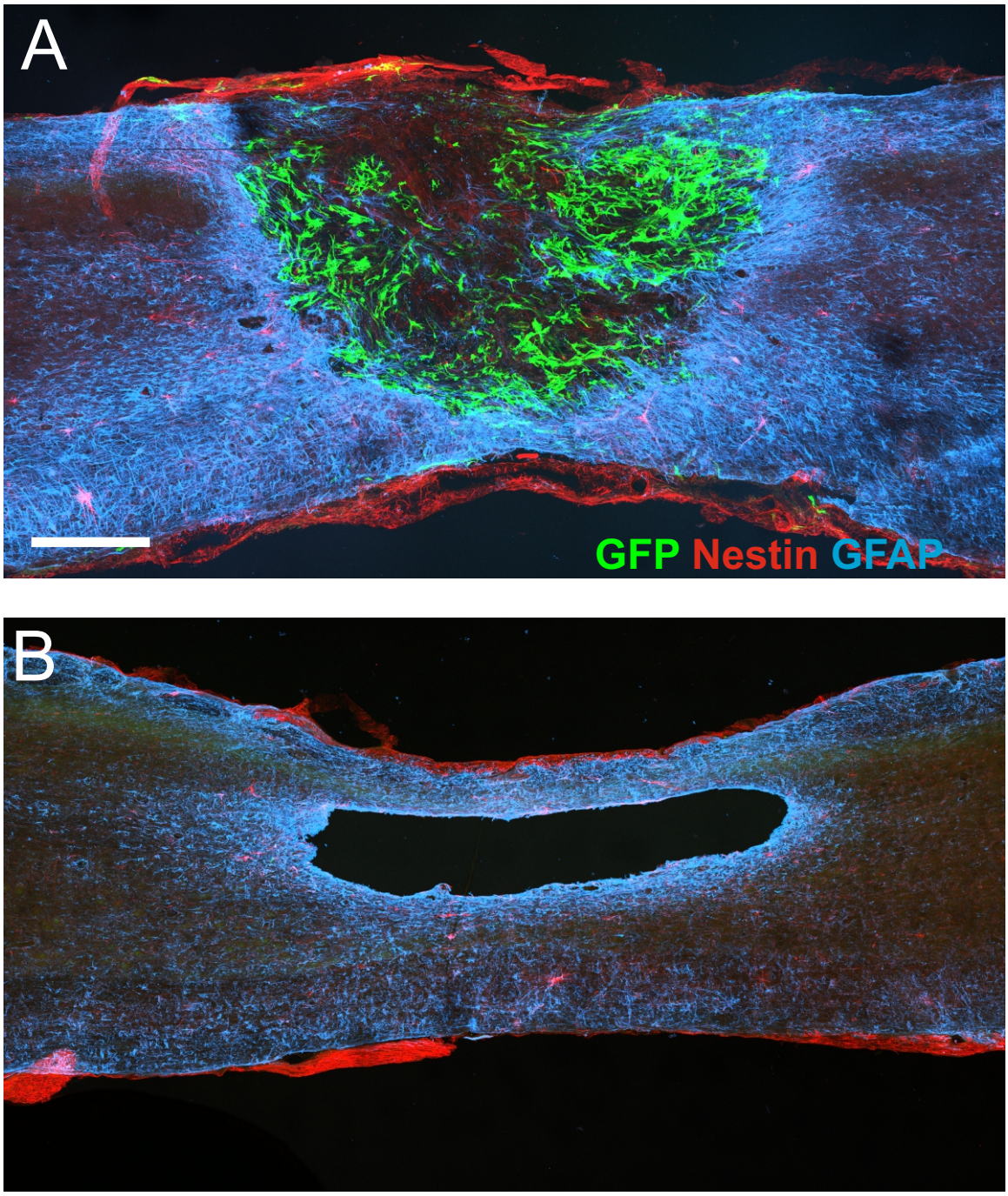
A
GFP Nestin GFAP
B

Figure 3-21. Quantitative analysis of the Injury dimensions 3 weeks after contusion.
The figure shows measurements (indicated by the white line) of the maximal length of the injury area for the lesion sites of 8 different animals. The sequence of images illustrate examples of the range of injury site types, from large single cavities with minimal extracellular matrix(A-D) to relatively small multiple cavities, more significantly filled with extracellular matrix (E-H). All images represent composites of 2 fields of view at X4 magnification from 60 µm thick tissue sections and are projections of from 1-3 z-sections. Scale bar = 600µm, applicable to all panels.

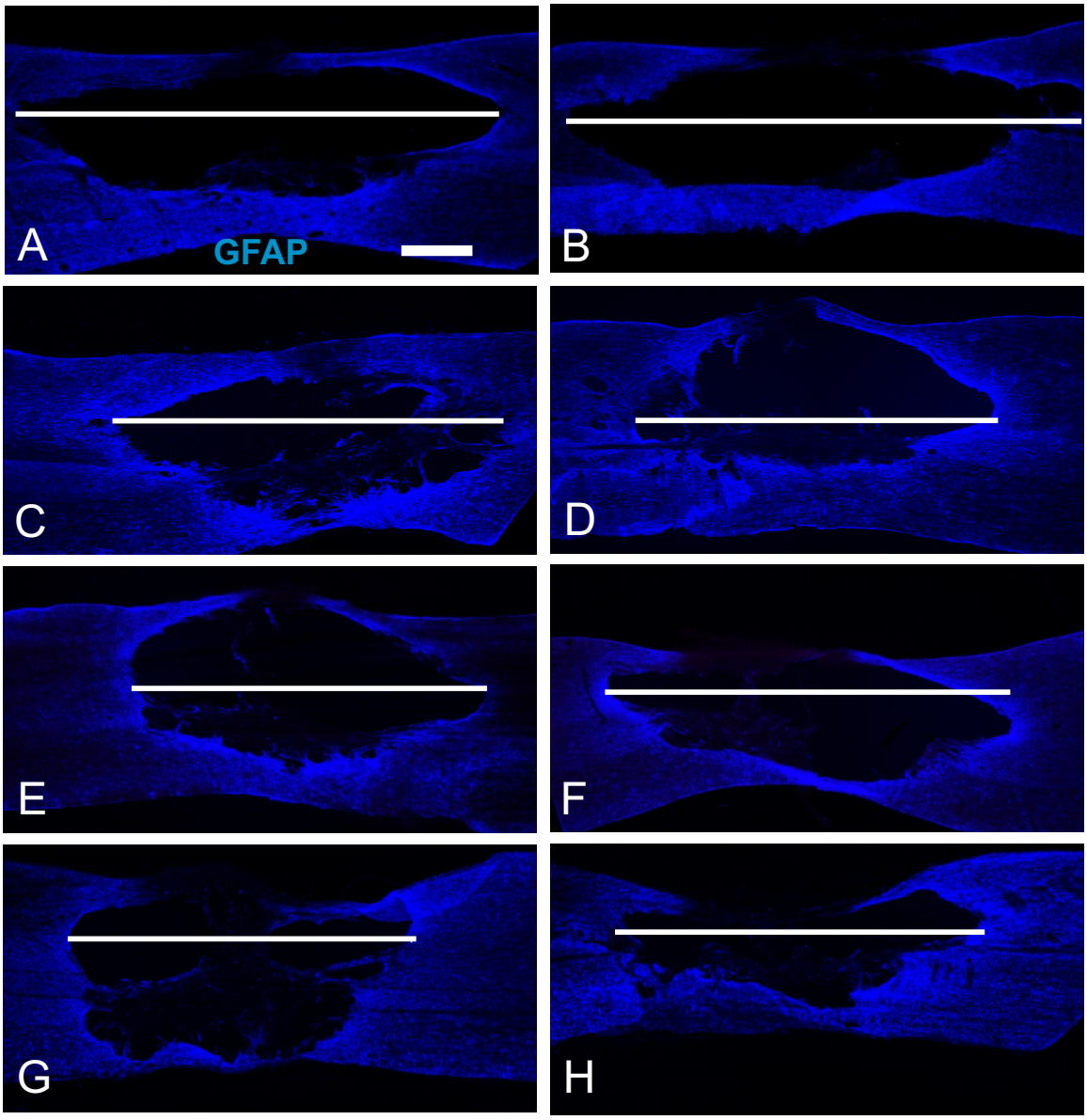
A
GFAP
B
C
D
E
F
G
H

Figure 3-22. Quantitative analysis of the Injury dimensions 9 weeks after contusion (corresponding to 6 weeks after transplantation).
The figure show measurements (indicated by the white line) of the maximal length of the injury area for the lesion sites of 10 different animals. The sequence of images demonstrated an examples of the of injury site types, from large single cavity without noticeable extracellular matrix (A-B) and with minimal extracellular matrix(C-D) to relatively smaller and multiple cavities and more occupied by extracellular matrix (E-J). All images represent composites of 2 fields view of X4 objective from 60 µm thick tissue sections and projected from 1-3 z-sections. Scale bar = 600 µm, applicable to all panels.

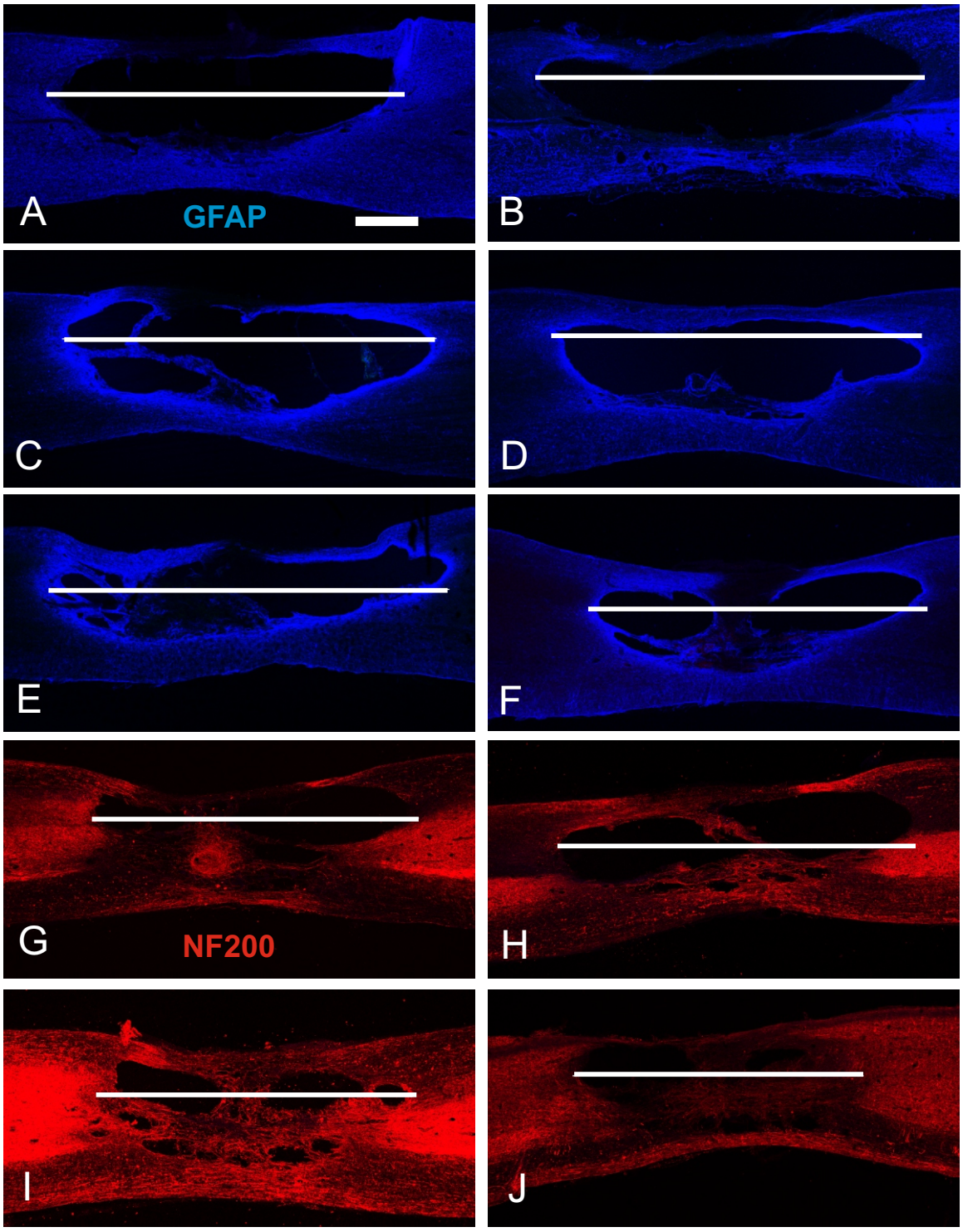
A
GFAP
B
C
D
E
F
G
NF200
H
I
J

Figure 3-23. Quantification analysis of the Injury dimensions 6 weeks after transplantation.
The figure show shows measurements of the maximal length of the injury area (as indicated by the white line) of 20 different transplanted animals. The various examples demonstrated a fairly consistent size of injury region that ranging from relatively larger and filled with less cells and extracellular matrix to smaller extent of injury and filled with more cells and extracellular matrix (A-T) and ingrowth axons (M-T). All images represent composites of 2 fields view of X4 objective from 60 µm thick tissue sections and projected from 1-3 z-sections. Scale bar = 600 µm, applicable to all panels.

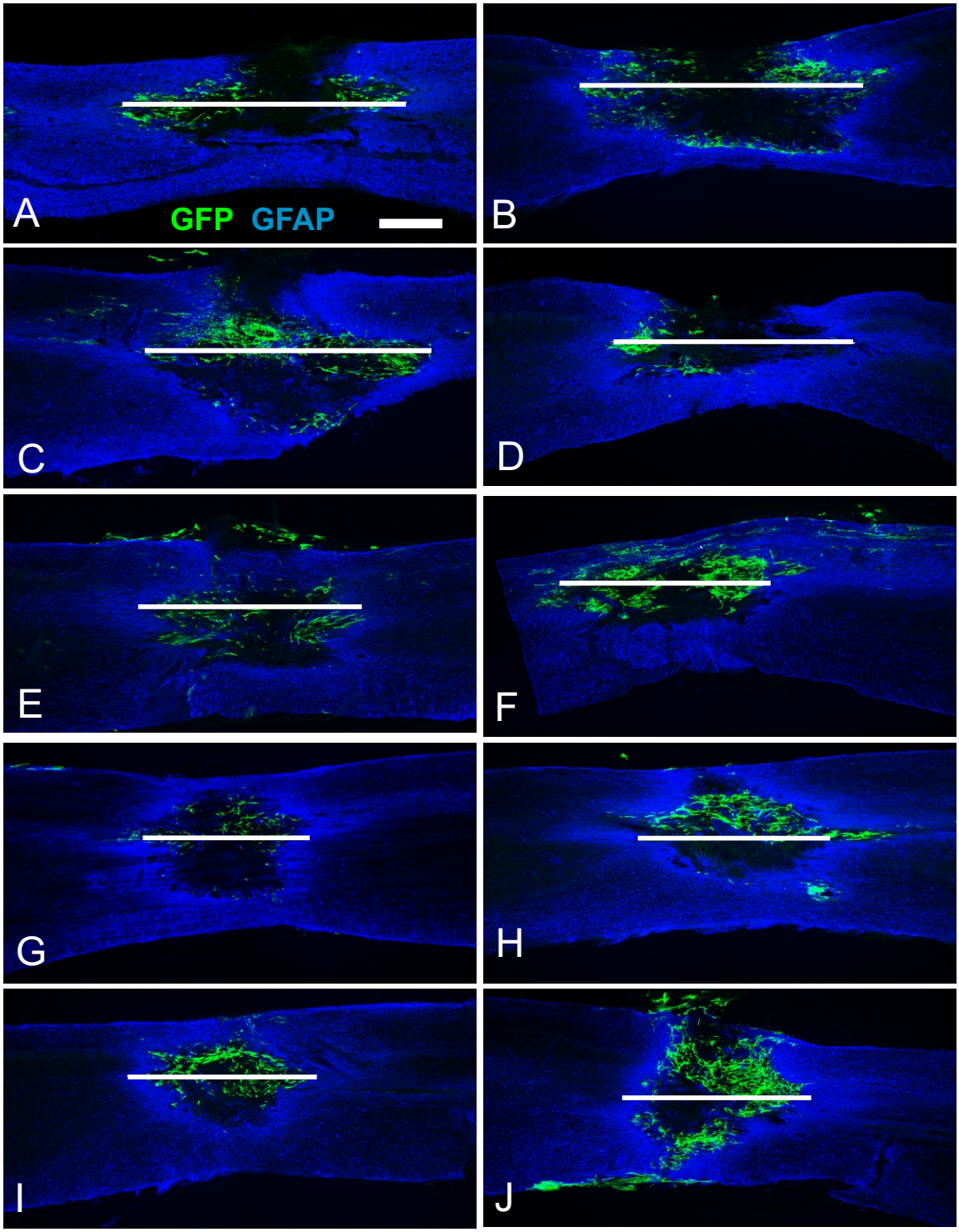
A
GFP GFAP
B
C
D
E
F
G
H
I
J

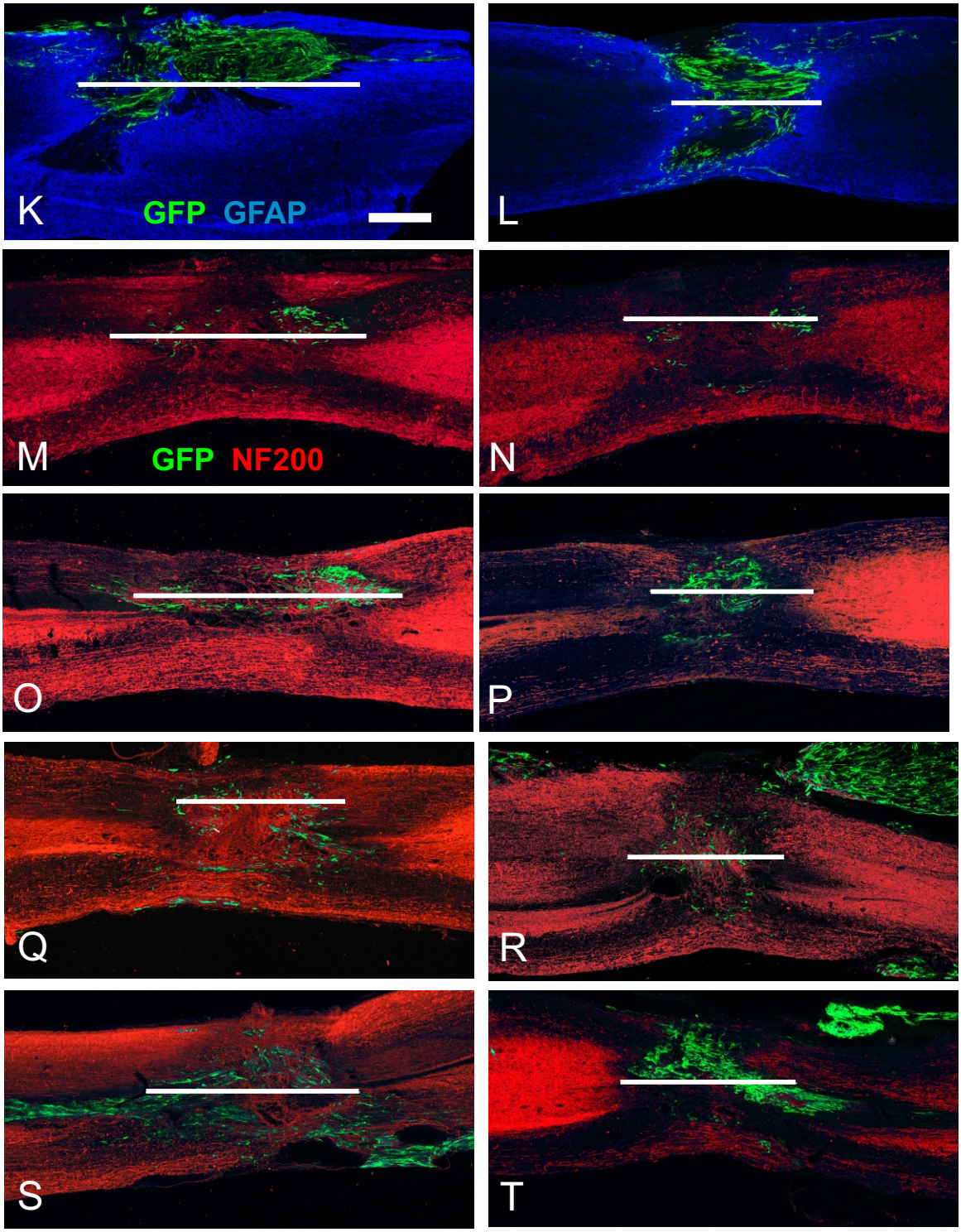
K
GFP GFAP
L
M
GFP NF200
N
O
P
Q
R
S
T

Figure 3-24. Quantitative assessment of the exent of the glial scar 3 weeks after injury

Confocal micrographs of parasagittal sections (A-G, taken from 7 different animals) showing the extent of the glial reaction to injury as assessed using the GFAP immunoreactivity (blue) surrounding the injury cavity/area. The dotted white line indicates an estimate of the outer border of the glial thickening. Measurements were made between this line and the inner border of the injury at three positions (red arrows) corresponding to the thickest regions of the rostral, caudal and ventral edges of the injury. All images represent composites of 2 fields view of X4 magnification from 60 µm thick tissue sections and are projections of 1-3 z-sections. Scale bar = 600 µm, applicable to all panels.

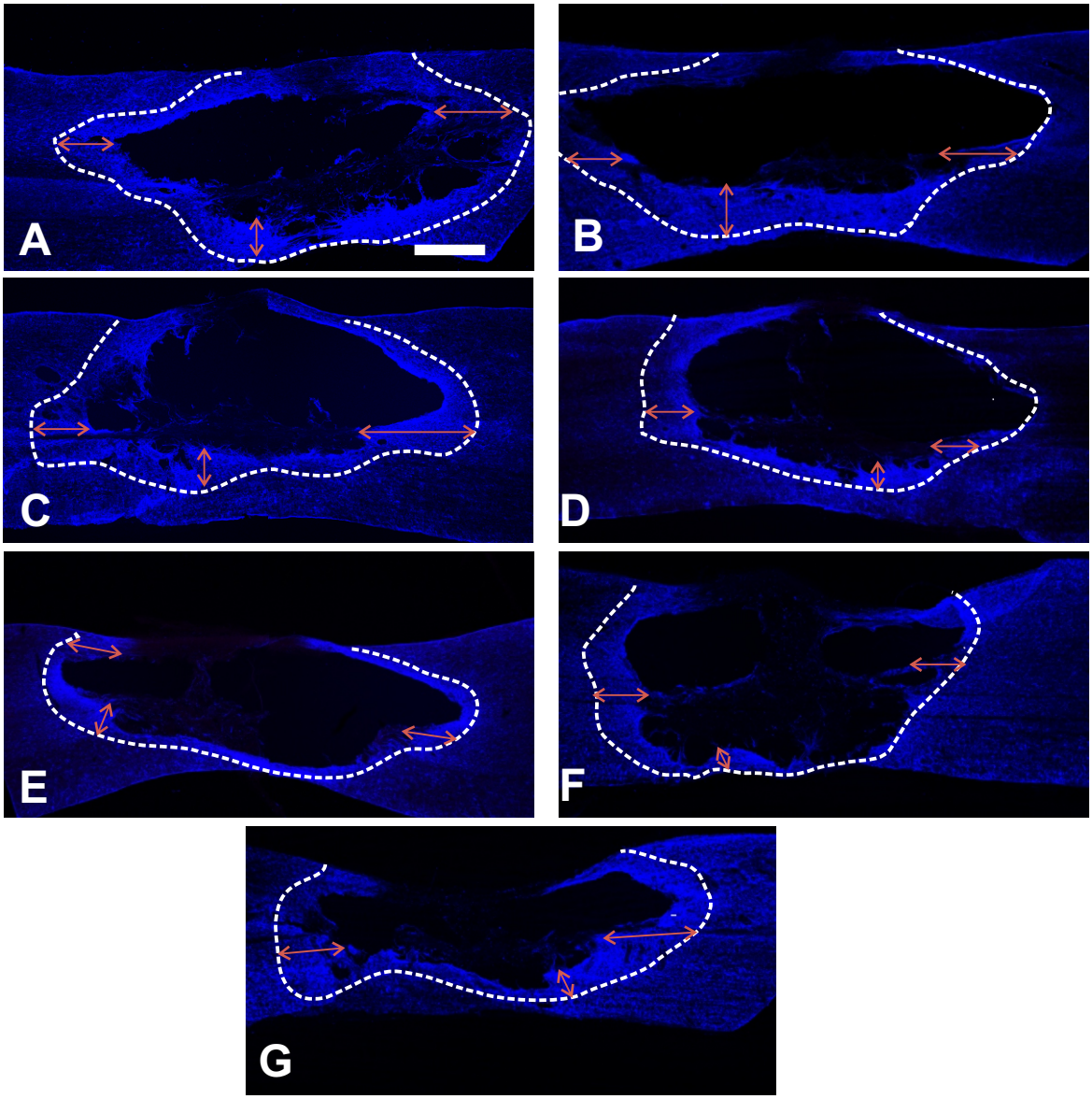
A
B
C
D
E
F
G

Figure 3-25. Quantitative assessment of the extent of the glial scar 9 weeks after injury

Confocal micropgraphs of parasagittal sections (A-G, taken from 7 different animals) showing the extent of the glial reaction to injury as assessed using the GFAP immunoreactivity (blue) surrounding the injury cavity/area as seen previous images i.e. of 3 weeks animals. The dotted white line indicates an estimate of the outer border of the glial thickening. Measurements were made between this line and the inner border at three positions (red arrows) corresponding to the thickest region of the rostral, caudal and ventral edges of the injury. All images represent composites of 2 fields view of X4 magnification from 60 µm thick tissue sections and are projections of 1-3 z-sections. Scale bar = 600 µm, applicable to all panels.

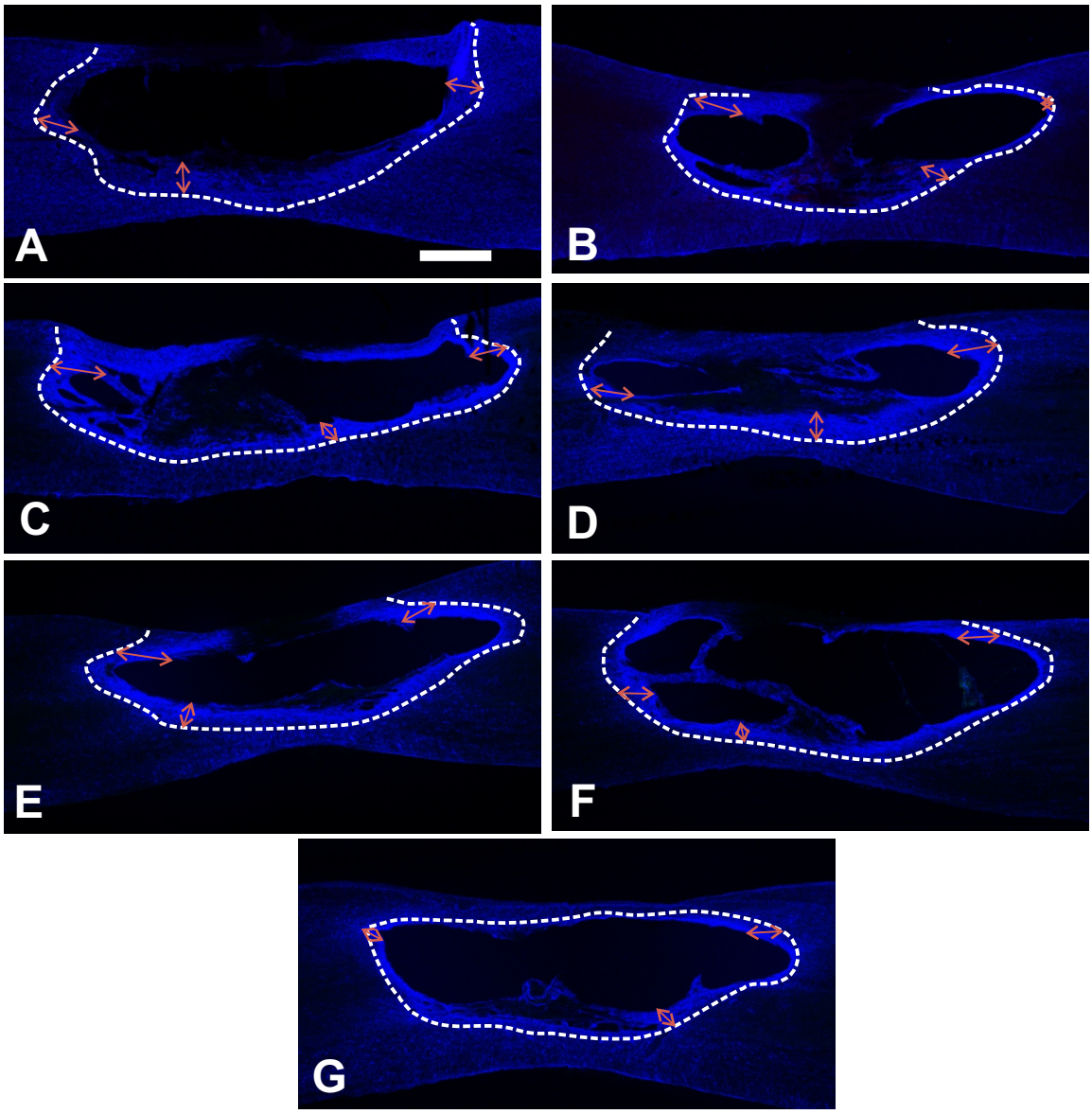
A
B
C
D
E
F
G

Figure 3-26. Quantitative assessment of the extent of the glial scar 6 weeks after transplantation

Confocal micropgraphs of parasagittal sections (A-M, taken from 13 different animals) showing the extent of the glial reaction to injury. There was a greater glial reaction seen in each images based on the GFAP (blue) immunoreactivity surrounding the injury cavity/area compared with both group of previous images i.e. of 3 week and 9 week after injury of control animals. The dotted white line indicate an estimate of the outer border of the glial thickening. Measurements were made between this line and the inner border at three positions (red arrows) corresponding to the thickest region of the rostral, caudal and ventral edges of the injury. All images represent composites of 2 fields view of X4 magnification from 60 µm thick tissue sections and are projection of 1-3 z-sections. Scale bar = 600 µm, applicable to all panels. (GFP expression=22%-90%)

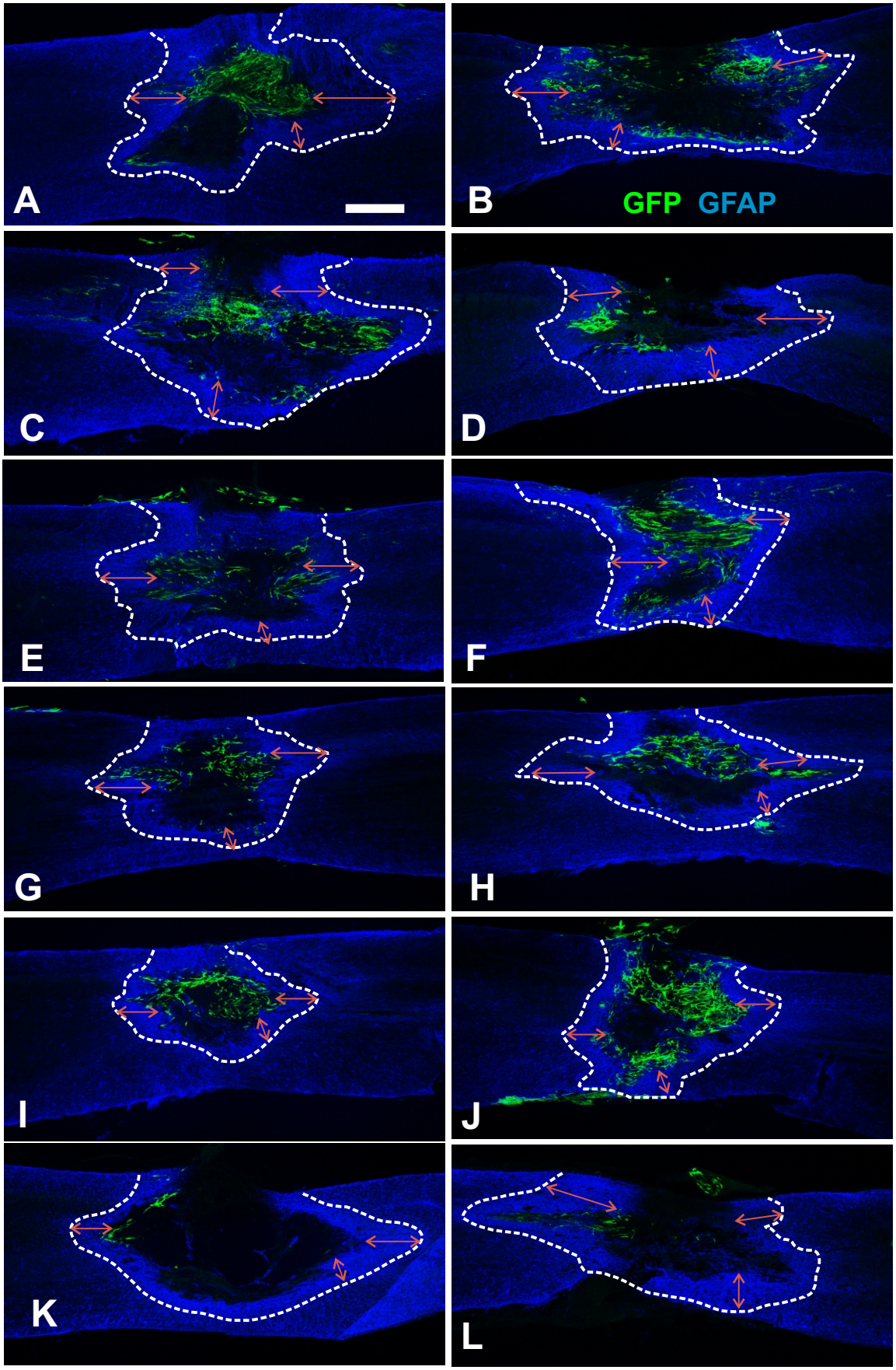
A
B
GFP GFAP
C
D
E
F
G
H
I
J
K
L
M

Figure 3-27. Neurofilament immunolabelling of regenerating axons in hESC-MSC transplants.

A, B and C, parasaggital section through a transplanted injury site 4 weeks after transplantation showing the distribution of transplanted cells (GFP, A), glial cells (GFAP, A and B) and axons (NF200, A and C). Note that NF200 immunolabelling (C) is virtually uninterrupted at the injury site reflecting dense axonal regeneration. D and E show a higher power scan of the boxed area in A to illustrate the detail of regenerating fibres (D) growing amongst the transplanted cells (E). Images A, B and C represent composites of multiple x20 fields of view and images D and E represent one field view from 40 µm thick tissue sections and projected from 30-35 z-sections. Scale bar = 500 µm (A,B and C) ,50 µm (D and E). GFP expression=90%

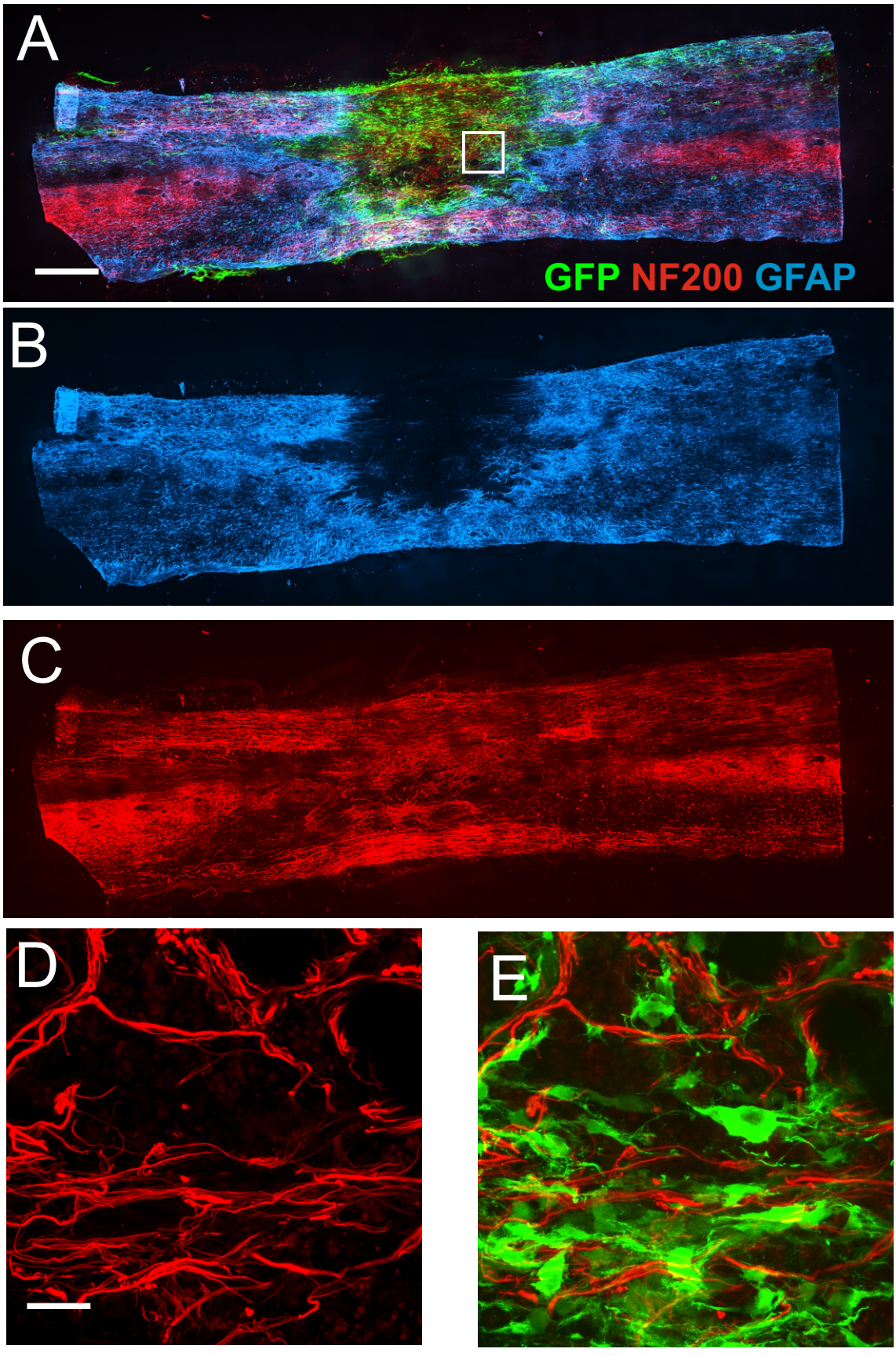
A
GFP NF200 GFAP
B
C
D
E

Figure 3-28. Neurofilament immunolabelling of regenerating axons entering matrix/cell filled area in hESC-MSC transplanted animal.

A-D, parasaggital sections through a transplanted injury site 6 weeks after transplantation showing the axons clearly entering the injury area filled with either matrix or cells. A1, A2, B1, B2, C1, C2, D1 and D2 show a higher power scan of the boxed area to illustrate the detail of regenerating fibres (D) growing amongst the transplanted cells and matrix. Images A ,B, C and D represent composites of multiple x20 fields of view and images A1, A2, B1, B2, C1, C2, D1 and D2 represent one field view from 40 µm thick tissue sections, projected from 30-35 z-sections. Scale bar = 500 µm (A,B, C and D) ,50 µm (A1, A2, B1, B2, C1, C2, D1 and D2). GFP expression=90%

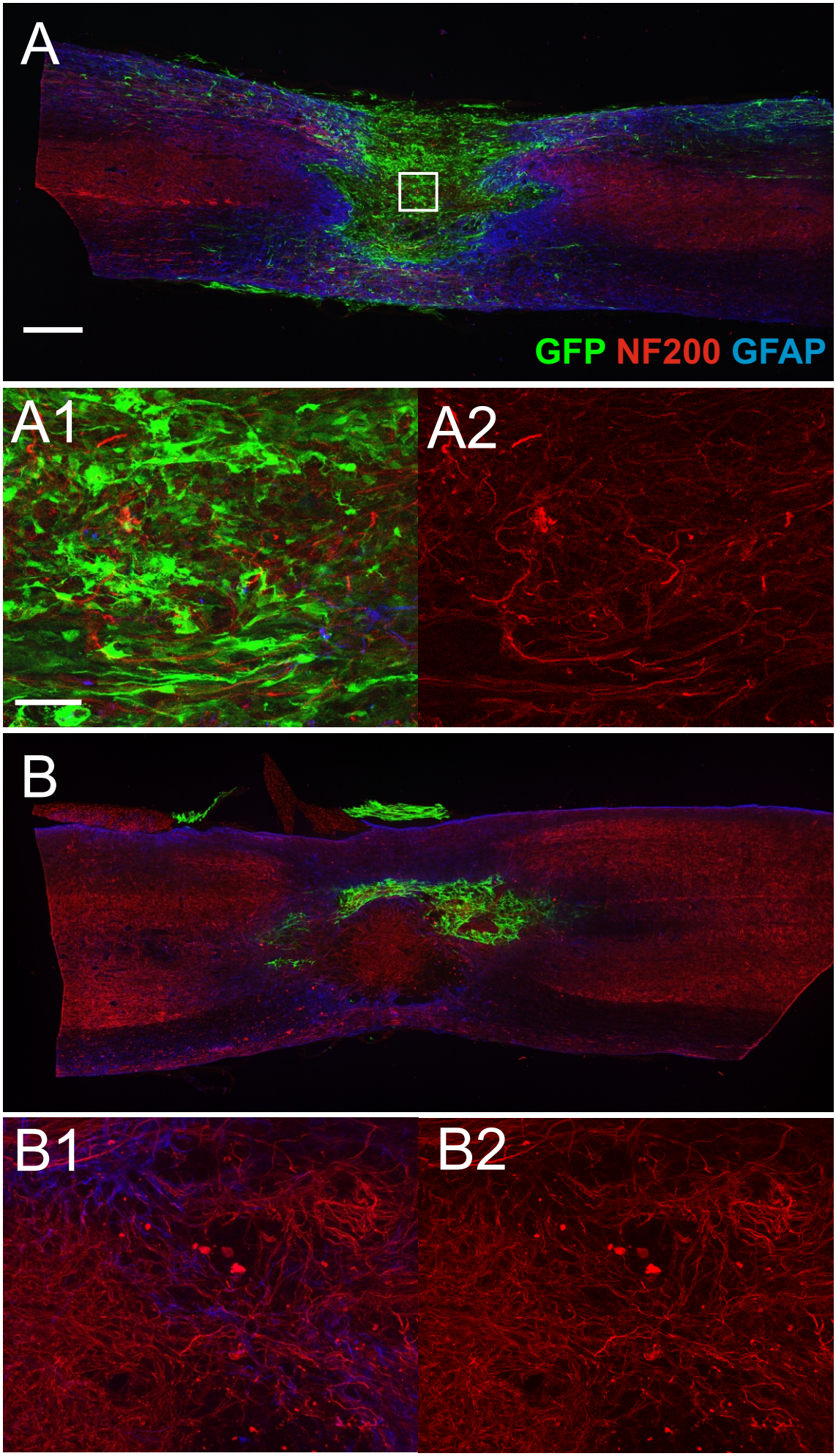
A
GFP NF200 GFAP
A1
A2
B
B1
B2

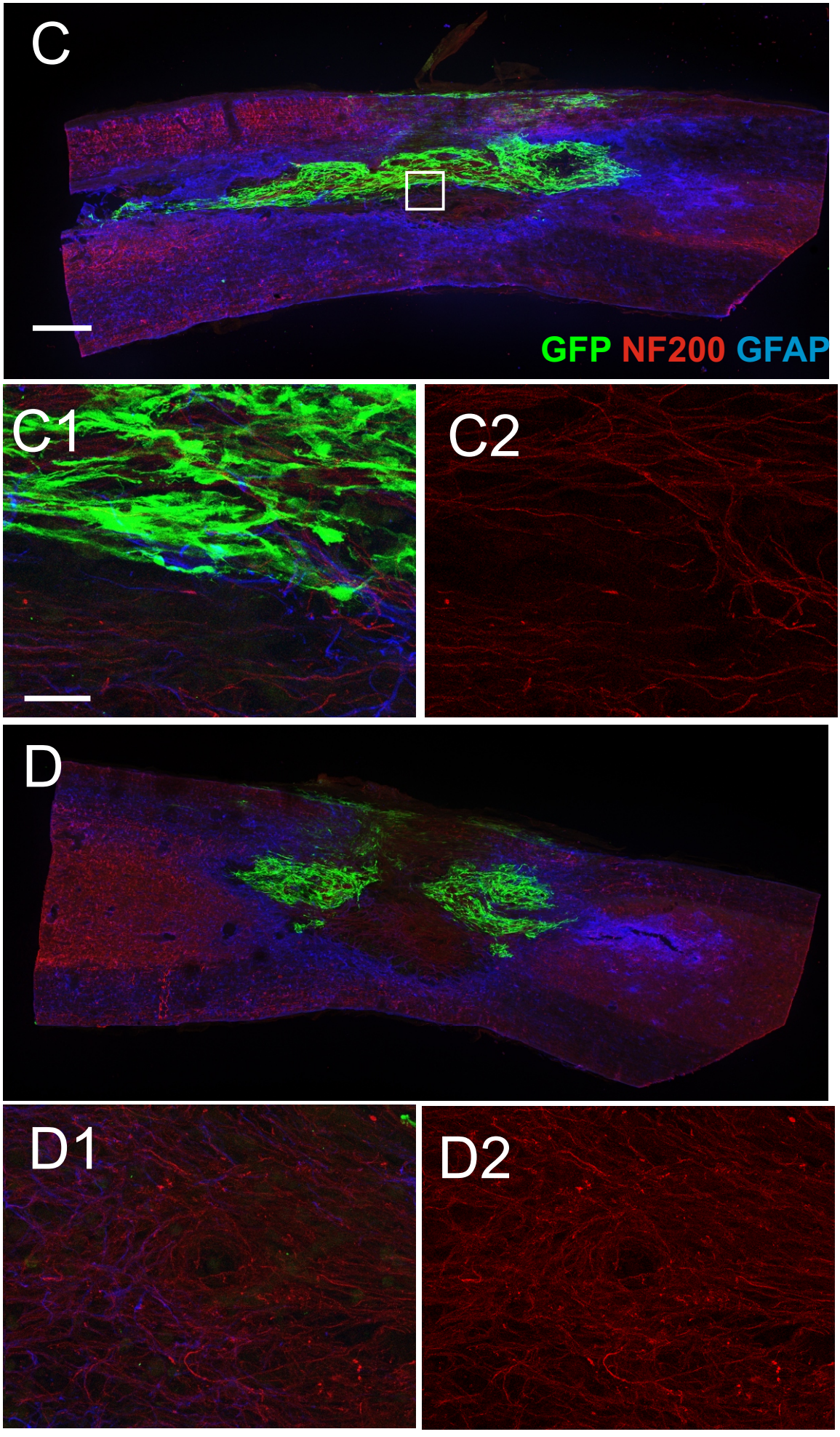
C
GFP NF200 GFAP
C1
C2
D
D1
D2

Figure 3-29. Neurofilament immunolabelling of regenerating axons only entering matrix filled area in non transplanted animals.
A and B , parasaggital section through an injury site 9 weeks after injury showing the axons fail to enter an injury area without matrix (A) but do enter the injury area filled with matrix (B). A1, A2, B1, and B2 show a higher power scan of the boxed area to illustrate the detail of regenerating fibres (D) growing amongst the matrix and not to the area without matrix (A1 And A2). Images A and B represent composites of multiple x20 fields of view and images A1, A2, B1, and B2 represent one field view from 40 µm thick tissue sections, projected from 30-35 z-sections. Scale bar = 500 µm (A, B, C and D), 50 µm (A1, A2, B1, B2, C1, C2, D1 and D2).

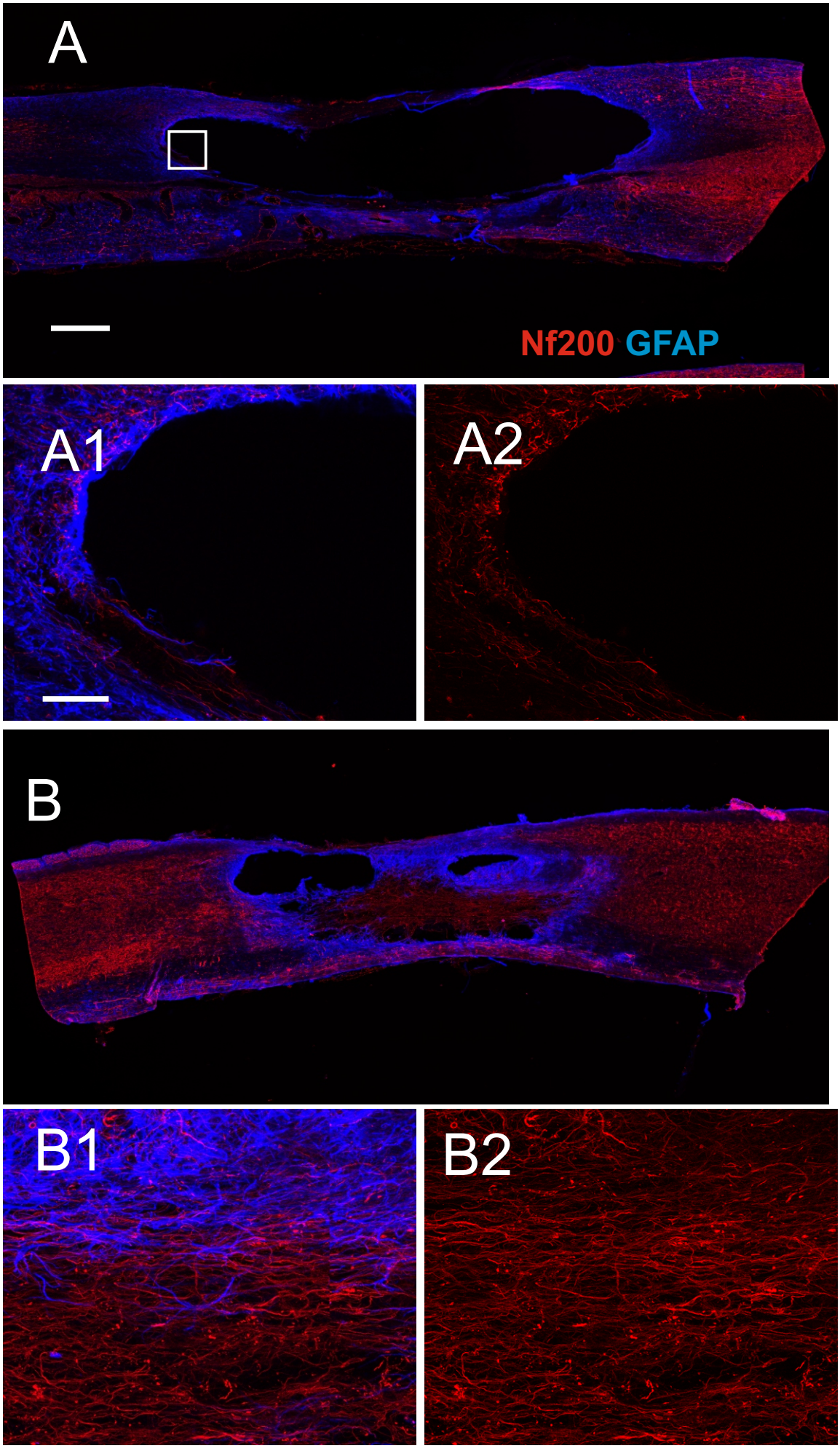
A
Nf200 GFAP
A1
A2
B
B1
B2

Figure 3-30. Corticospinal tract axons fail to regenerate in hESC-MSC transplants.
A-L, parasaggital sections from close to the midline in two animals transplanted with hESC-MSCS (A-C and D-F) and two control injured but non-transplanted animals (G-I and J-L). The sections show corticospinal fibres of the main component anterogradely labelled with BDA (red). Axons either stop short of the GFP labelled cells in the injury site, or grow as far as the cells but do not grow into them. The image in D shows the density of corticospinal fibres a few mm rostral to the injury site for comparison. Corticospinal fibres in non-transplanted animals (G-L and J-K) approached cavities in similar numbers and with similar proximity to the fibres approaching transplants (A-D and D-E).
Images A, G and J represent composites of multiple X20 fields while all other images are composites of multiple X40 views. The images are projections of 26-34 z-sections. Scale bar = 500 μm for A and applies to all X20 panels, 200μm for B and applies to all X40 panels. (GFP expression=34% for A, B, C and 22% for E and F).

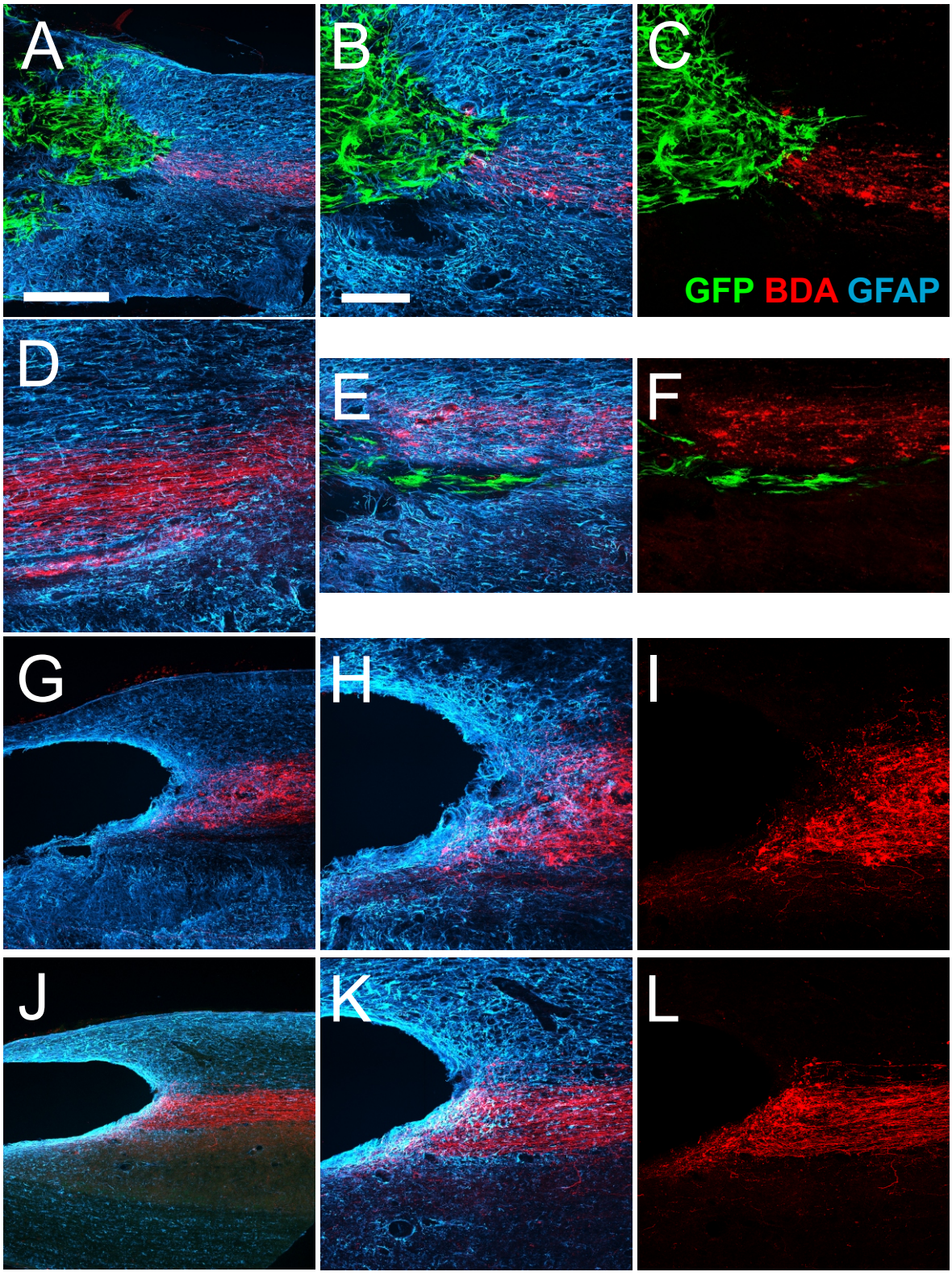
A
B
C
GFP BDA GFAP
D
E
F
G
H
I
J
K
L

Figure 3-31. Axonal regeneration of dorsal column fibres in a transplanted animal without a conditioning injury.

Parasagittal section from an animal in which the transplanted cells filled the injury and formed a track of cells extending rostral to the injury site. Despite the presence of this track of cells and numerous regenerating fibres within the injury site, none of the fibres projected rostral to the injury. Note the absence of GFAP immunolabelling in a region corresponding to the transplant and also the cells that have become distributed rostral to the injury. All images represent composites of multiple x20 fields of view from 60 µm thick tissue sections and projections from 20 z-sections. Scale bar = 500 µm, applicable to all panels (GFP expression 48%).

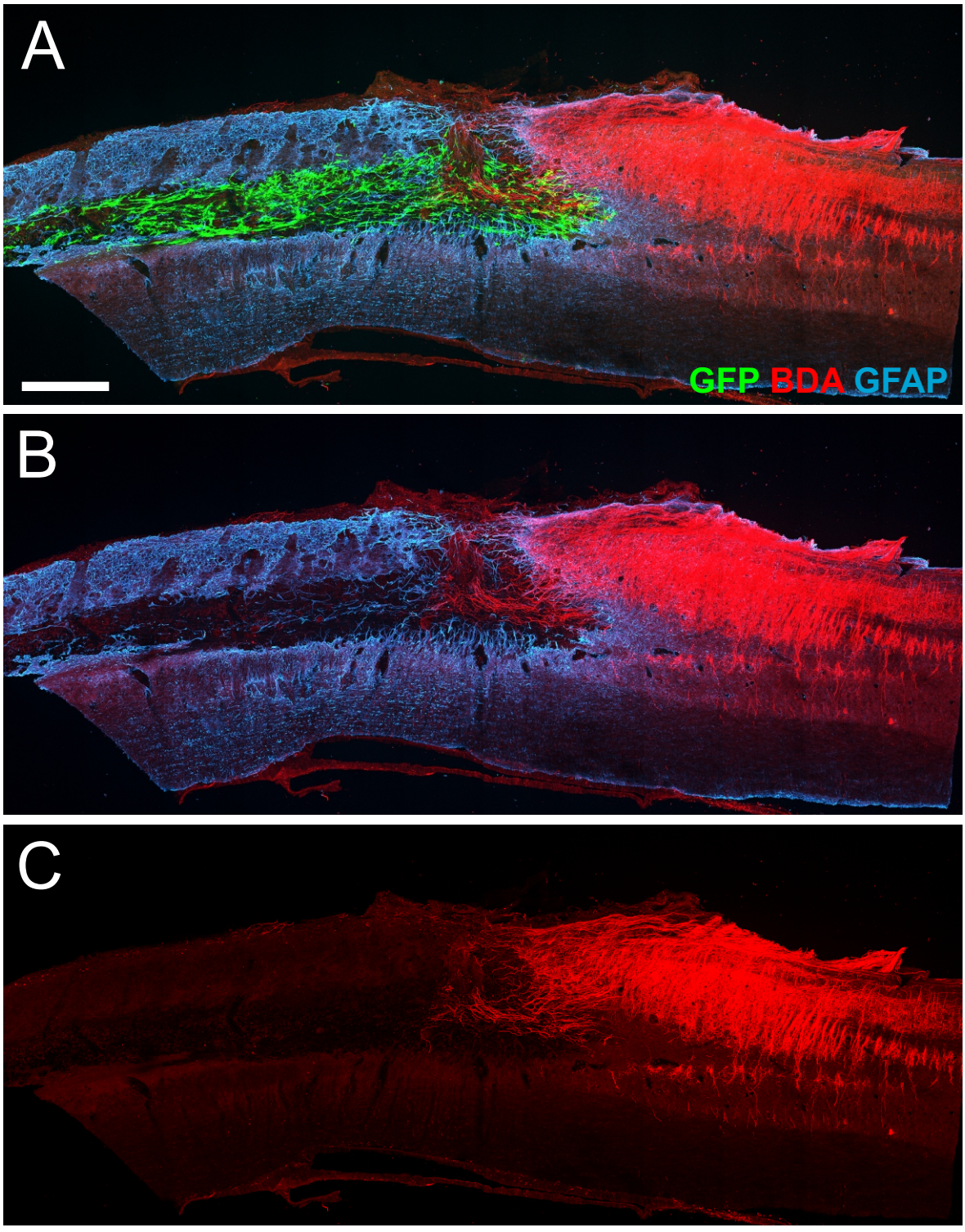
A
GFP BDA GFAP
B
C

Figure 3-32. Axonal regeneration of dorsal column fibres in a transplanted animal without a conditioning injury.

Parasagittal section from an animal in which the transplanted cells filled the injury and formed a track of cells extending rostral to the injury site. In this case, regenerating fibres do project into the rostral cell track, extending several 100s of microns beyond the injury site. Note the absence of GFAP immunolabelling in a region corresponding to the transplant and also the cells that have become distributed rostral to the injury. All images represent composites of multiple x20 fields of view from 60 µm thick tissue sections and projected from 16 z-sections. Scale bar = 500 µm, applicable to all panels (GFP expression 90%).

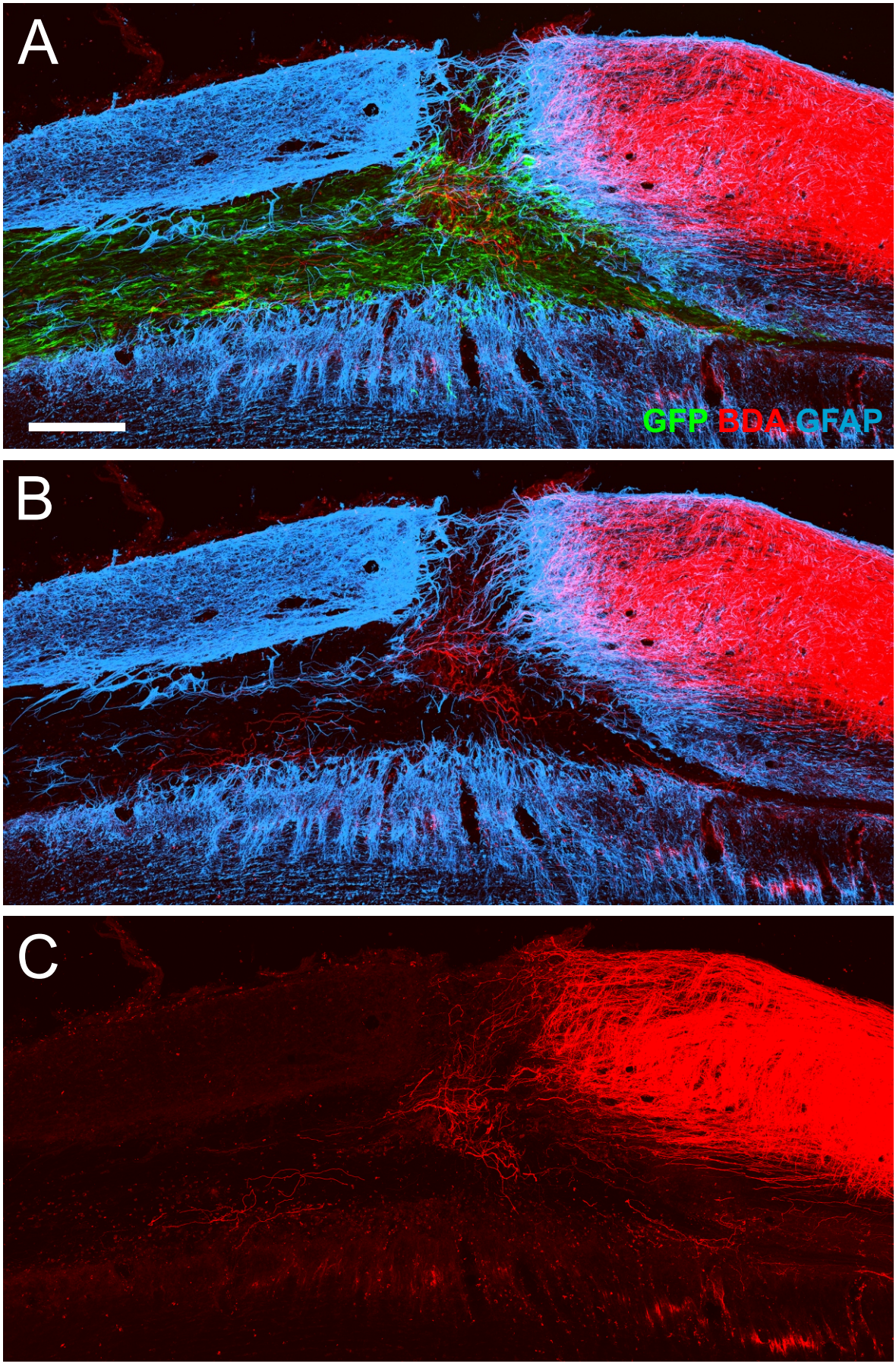
A
GFP BDA GFAP
B
C

Figure 3-33. Axonal regeneration of dorsal column fibres in a transplanted animal with a conditioning injury.

Parasagittal section from an animal in which the transplanted cells filled the injury and formed a track of cells extending both rostral and caudal to the injury site. In this case, regenerating fibres project into the rostral cell track, extending several 100s of microns beyond the injury site. Note the absence of GFAP immunolabelling in a region corresponding to the transplant and also the cells that have become distributed rostral and caudal to the injury. Note also the absence of BDA labelled fibres in the cell track caudal to the injury despite numerous labelled fibres immediately dorsal to the cells. Images A and B represent composites of multiple x20 fields of view from 60 µm thick tissue sections and projected from 16 z-sections. Scale bar A and B = 500 µm. C and D are enlarged images of the boxed areas. Scale bars = 200 µm (GFP expression 60%).

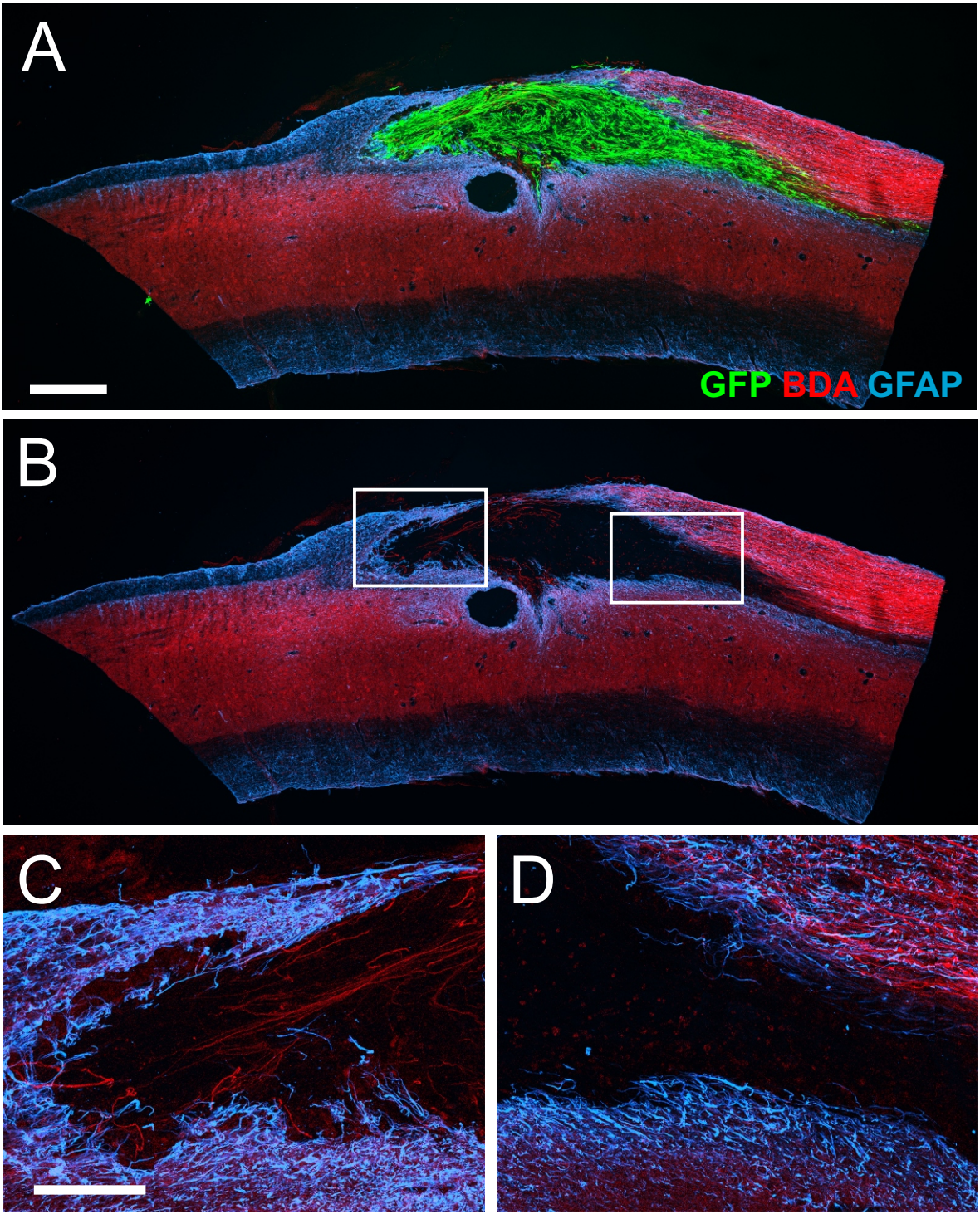
A
GFP BDA GFAP
B
C
D

Figure 3-34. Immunolabelling for CASPR within a transplanted injury site indicative of myelination of regenerating fibres.

A and B show high power scans of an area of the dorsal columns above an injury site while C and D shows an area within the centre of a transplanted injury. Both regions contain numerous CASPR immunoreactive profiles but those in the dorsal columns are much more numerous as would be expected as this is outside the injury area and will contain many spared fibres. The CASPR labelled paranodal regions in C and D will be on regenerating fibres. Some of the CASPR is associated with NF200 positive fibres. All images represent composites of multiple x40 fields of view from 60 µm thick tissue sections and projected from 25-30 z-sections. Scale bar = 50 µm, applicable to all panels.

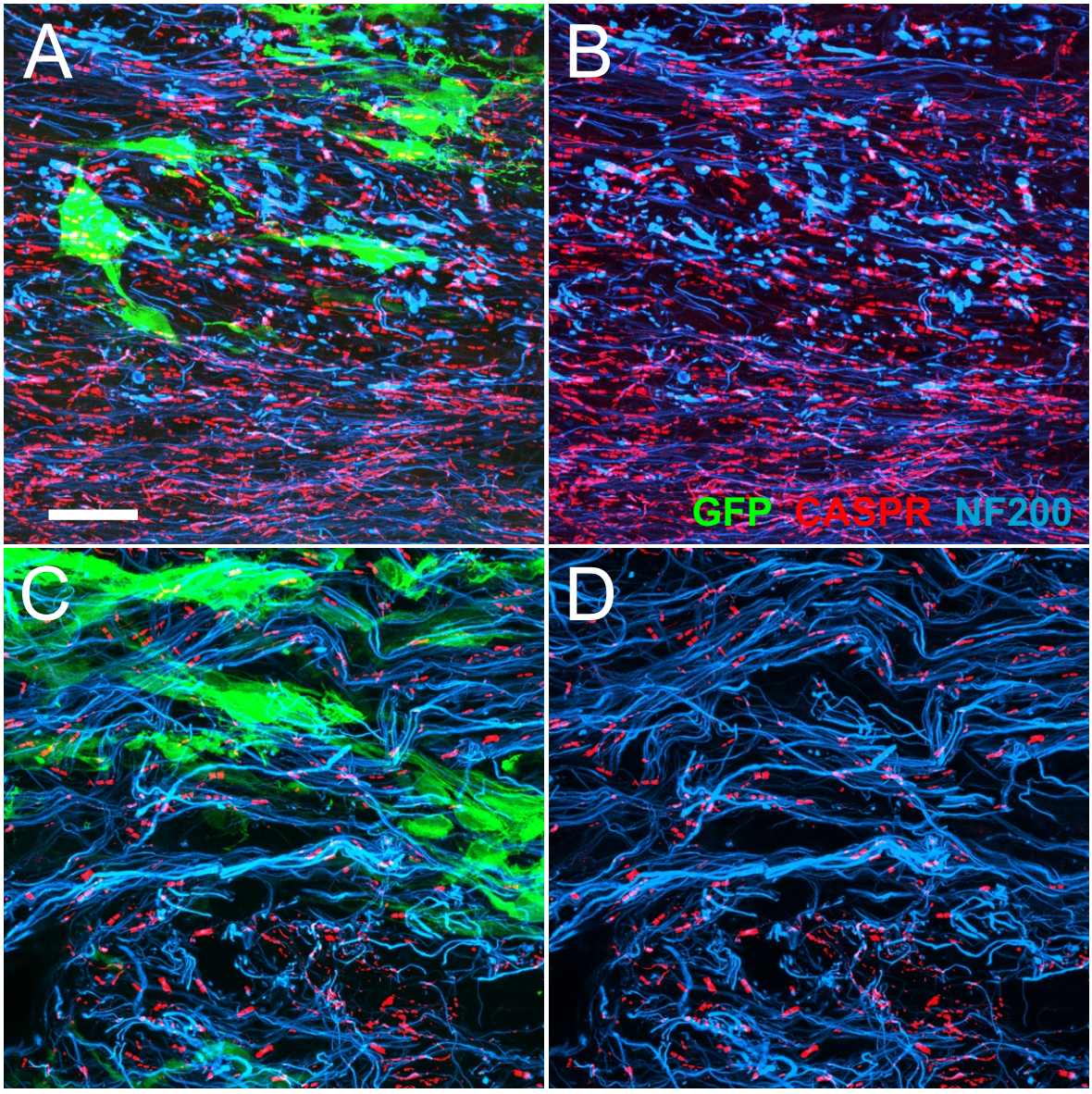
A
B
GFP CASPR NF200
C
D

3.4 Discussion

3.4.1 Injury model

A contusion injury model is the most clinically relevant (Zhang et al., 2008; Anderson et al., 2009) and the Infinite Horizons device is recognised as a state of the art device providing the best level of consistency. Nevertheless there is a large degree of variation in the morphology of the injury sites that are produced and this is probably due to biological factors such as the pattern of the blood supply as much as operator variability. The variation on the injury site morphology, does however mean that relatively large group sizes are required to make meaningful observations. This together with the limit to the number of antibodies which can be used at one time and the need for a three dimensional picture of the pattern of immunolabelling from sections throughout the whole cord means that to obtain a detailed picture over several issues requires a large number of animals and is highly labour intensive.

Although there is variability in the histological picture, a clear feature of the injuries is that by 3 weeks after a C6 175 kdyn contusion injury damage extends throughout the grey and white mater of the spinal cord. There is the formation of one or more fluid cavities which extend for more than 3mm longitudinally, and occupy some 2/3rds of the width of the spinal cord at that level. Although not quantified it also extends more than 2/3rds of the dorso-ventral height of the cord. A further common feature is that a variable degree of matrix infilling occupies part of the injury area and this rich in laminin. A comparison of the dimensions of the injury site at 3 weeks compared with 9 weeks post-injury suggests that the injury site and cavity is already at is greatest extent by this 3 week time point and this time point can probably be considered a chronic injury.

The existence of large cavities means that cell transplants at this time point are often made into fluid filled spaces of considerable volume and his explains why large numbers of cells could often be injected before any evidence of overflow from the injection site could be seen. Because of the variable degree of infilling with extracellular matrix, the volume of cavity within the cord available to accommodate transplanted cells will vary from one animal to another and cannot be readily judged or predicted. Our strategy to overcome this difficulty

was to avoid transplanting a fixed “dose” of cells but to inject what appeared to the required to fill the injury site (the point at which overflow was seen) at the time of transplantation. This will inevitably lead to variation in the numbers of cells that are seen at the end point of the experiments. There are two further sources of variability regarding the distribution of the cells which will arise from the variable nature of the injury site. One is that in some animals multiple cavities rather than a single unified cavity occur and it is possible that if the septa dividing the cavities are robust enough, cells may enter one cavity but not another, especially since cells were usually injected at a single point. The other is that cells will not be able to occupy areas already occupied by extracellular matrix and this will mean that there will be areas of the injury site which will be devoid of cells for this reason.

3.4.2 hESC-MSC transplants require immunosuppression for survival in rodent models

A common problem in preclinical studies of transplant therapies in SCI is graft survival. Many studies have reported limited survival of transplanted cells and the factors that may influence this have been widely debated (Patel et al., 2010). The problem is exacerbated when human cells are transplanted into rodent models (i.e. by xenografting). Investigation of animals transplanted with hESC-MSCs without any form of immunosuppression showed that the cells die within days of being transplanted. Although various factors may influence the survival of cells including the immune response to the injury itself and the inhospitable environment created by the injury this is unlikely to be the major factor here as the transplants were made at a delayed time point when some of the hostile conditions will have abated. The much better survival seen with subsequent transplants performed with immunosuppression tends to confirm this. The rapid death of the cells is probably mainly attributable to that fact that the transplanted cells represent a xenograft and will therefore elicit an immune response resulting in transplant rejection. It is nevertheless, notable that their demise is so spectacularly rapid occurring within just days and these observations may have implications for other studies since immunosuppression or use of immunocompromised animals has not been universally employed even when transplanting human cells into animals in preclinical studies of MSC transplantation. This is likely to complicate interpretation of outcome in such

studies and leads to some doubt regarding some of the positive outcomes reported, especially where cell survival was not well monitored. In subsequent experiments, daily injections of 20mg/kg cyclosporine s.c. promoted much improved survival. It may not however, be an entirely adequate level of immunosuppression for longer term studies since the cell numbers a 6 weeks appeared to be reduced compared to the few animals investigated at shorter time points.

The regime used for immunosuppression though adequate may not be ideal. The requirement for daily injections is labour intensive and the plasma levels of cyclosporine are likely to fluctuate considerably with 24 hourly administration. However, this is a compromise between maintaining adequate plasma levels to provide immunosuppressive cover and not inflicting stress on the animals with more frequent injections. In general this regime appeared to be well tolerated by the animals and there was no incidence of animals becoming sick as a result of the cyclosporine treatment. The use of cyclosporine is realistic in the sense that immunosuppression is likely to be required in any clinical translation. In further preclinical studies the use of nude rats would be an alternative but then the injury would not be realistically modelled as there would not be the usual immune response. In our experiments cyclosporine treatment was started well after the injury pathology had developed. Other immunosuppression regimes involving slow release pellets or microspheres may be developed in future and might provide more stable plasma levels that would further improve survival of the cells (Sevc et al., 2013).

3.4.3 Transplanted cells fill the injury site and significantly reduce the extent of the injury

One of the most dramatic outcomes of the transplantation was the consistency with which transplantation lead to solid filling of the injury site and the contrast between this and the extensive tissue disruption and cavitation seen in control non-transplanted animals. The injury site in the transplanted animals in this study tended to consist of a combination of both cells and matrix, with few lesions fully occupied by GFP labelled hESC-MSCs. The areas where cells were absent could represent areas already filled with endogenous matrix at the time of transplantation or also be as a result of cell migration or cell death, leaving

spaces in which extracellular matrix could form. Additionally, the transplanted cells themselves could further promote extracellular matrix formation. Otherwise, this filling of the injury site is consistent with other reports using transplants of bone marrow derived MSCs, though generally performed acutely or with shorter delays after injury (Wu et al., 2003; Ankeny et al., 2004). In agreement with the data from previous studies which have used adult MSCs, our data also show a significant injury size reduction in the animals that received different batches of hESC-MSCs (Ankeny et al., 2004; Boido et al., 2012; Gu et al., 2010). This could potentially be attributed to a neuroprotective effect of the transplanted cells, preventing further damage to spared tissue following the injury, as suggested by Ankeny et al (2004). Apart from that, it could also be due to the modest axonal growth promoting effect which may further reduce the injury extent. Additionally, this data could also be a good indicator of the consistency of different batches of hESC-MSCs prepared in this study to consistently provide a neuroprotective and modest growth promoting effect leading to a meaningful therapeutic outcome.

In addition the cells frequently spread variable distances from the injury site. There was no fixed pattern to this but the cells tended to be distributed close to the midline and around or above the central canal and rarely extended beyond 3mm from the midsagittal line of the section. Although not systematically investigated, this spread of cells was also seen at early time points (e.g. 5 days two animals) so that it may be an artefact of the transplant process rather than migration of the cells. As has been discussed previously (Lu et al., 2006) injected cells tend to move through tissues down a pressure gradient (Lu et al., 2006). It is possible that the cells may, for example track down the central canal, especially if this is broadened following injury.

Where the cells had spread in appreciable numbers beyond the injury site, it was notable that they displaced resident glial cells. This is a behaviour that has been noted before for bone marrow MSCs in rodent models (Lu et al., 2006). A similar behaviour was observed when bolus injections of cells were made into normal cord and under these conditions an intense glial reaction to the transplanted cells was also revealed. This sort of glial reaction has been noted before (Toft et al., 2013) for different cell types even when transplants were syngeneic so that it is unlikely to be a result of xenografting. This property could be considered

undesirable in a cell intended for transplantation in the context of a spinal cord injury therapy though it may be possible to control this by engineering in the longer term (Santos-Silva et al., 2007).

The transplanted cells clearly produced or encouraged the production of an extracellular matrix throughout the injury site which was rich in laminin. This is known to be a good substrate for axonal regeneration. There was also evidence from both laminin and SMA immunolabelling of the development of a profuse network of blood vessels in the transplant and surrounding the injury site. This may be important in ensuring the survival of the grafted cells and indeed the size of the cavities that need to be filled by the transplanted cells is likely to pose a significant problem in terms of sustain the transplanted cells. Angiogenesis must be an important factor in this process but may also contribute to a general improvement in the vascularisation of the spinal cord in the vicinity of the injury which could aid repair (Fassbender et al., 2011). There was no clear evidence that the cells continued to proliferate or differentiate in vivo and there was no evidence of any teratogenic effects.

3.4.4 Transplants support regeneration of some fibre types

Tract tracing of corticospinal fibres showed no evidence that hESC-MSCs could support regeneration of this type of fibre. The fibres did not enter the transplanted injury area and there was no indication when compared to non-transplanted animals that the cells reduced die back of the coricospinal fibres. This is consistant with other reports using bone marrow MSCs (Lu et al., 2006). Corticospinal fibres have proved in general to be poor at regenerating within cell transplants, possibly because they have a low intrinsic growth capacity. The ability of hESC-MSCs to support or indeed promote regeneration of ascending dorsal column fibres was investigated because these fibres have greater capacity for regeneration than corticospinal fibres. Their regeneration can also be boosted by carrying out a conditioning injury to the peripheral branch of the axons by sectioning the appropriate peripheral nerve. Sensory axons are less easily visualised than corticospinal fibres because BDA labelling does not work well when injections are made into peripheral nerve such as the sciatic nerve. Ctb is often used as an alternative tract tracer but while it efficiently labels the terminals of sensory fibres it is only weakly seen in the parent axons. For this

reason, a new technique has been developed in the lab which involves the injection of BDA into the spinal nerves and making the injury at a lumbar rather than the more usual cervical level. The combined effect of injecting closer to the spinal cord and making the injury close to where the labelled fibres enter the spinal cord is that the BDA present in the dorsal column fibres is strong enough to provide very clear labelling of the dorsal column fibres at the injury site. The injury to the lumbar dorsal columns was made using a wire knife device. This method ensures that all axons projecting rostral to the injury which would be labelled by the tracer injections are interrupted and that spared fibres cannot therefore be confused with regenerating fibres. This was a common problem in early studies of axonal regeneration and lead to several false reports of bridging axonal regeneration (Steward et al., 2003). The wire knife was used in such a way that not only axons in the dorsal columns but also the dorsal roots entering immediately above the injury site were transected so that any fibres in these roots which were inadvertantly labelled would not be confused with regenerating fibres. Consistant with the evidence from neurofilament labelling and from previous studies, numerous regenerating dorsal column fibres were seen within hESC-MSC transplants. However, in most cases, even where a track of transplanted cells extended rostrally from the injury site, there was no regeneration beyond the injury site. That is the axons did not cross from one side to another – so called bridging axonal regeneration. However, in two of the animals examined one with a conditioning injury and one without, there was clear evidence of fibres crossing the injury site. Whether this can be considered true bridging regeneration, however, is debatable. A consistant feature associated with the distribution of cells outwith the injury area was the absence of immunolabelling for GFAP. This suggests that the transplanted cells had in effect replaced astrocytes so that the environment within the cord within the cell tracks may then be an extension of the environment within the transplanted injury site where the axons regenerate successfully rather than an essentially host environment within which transplanted cells have integrated and mingled. The rostral cell tracks then simply become an extension to the cell transplant. This may be less useful than if the presence of the cells modified the host environment since the axons ma then simply be trapped within the rostral cell track rather than at the transplant site.

3.4.5 Regenerating fibres acquire a myelin sheath

Myelination of regenerating fibres will be an important aspect of ensuring they are functionally useful if they can negotiate the hostile environment of the injury site to reach the opposite side and form useful connections. Evidence for myelination of the regenerating fibres within hESC-MSC transplants was obtained by showing that the paranodal protein CASPR is found in the centre of hESC-MC transplants. In the middle of the transplanted injury site these can only represent regenerating fibres and this can therefore confidently be considered evidence for myelination of these fibres. Interestingly not all of this CASPR immunolabelling was association with neurofilament immunolabelling and this might be a technical issue or it may suggest that not all regenerating myelinated fibres contain neurofilaments. The myelination will be of little functional consequence in the current study because the regenerating fibres are “blind” and end largely within the transplanted injury (in the case of dorsal column fibres at least). The cells responsible for this myelination could be Schwann cells dedifferentiated rom the dorsal roots or arising from OPC progenitors (Zawadzka et al., 2010) or they could be oligodendrocytes. This could potentially be investigated using immunocytochemistry for P0 (peripheral type myelin formed by Schwann cells) or MBP (central type myelin). Remyelination of spared but demyelinated fibres was not investigated in this project. P0 immunolabelling could again be used to obtain evidence of peripheral type myelin which if around central axons would indicate remyelination. Remyelination with central type myelin is more difficult to detect but this could be investigated using Electron Microscopy and examination of thickness and nature of myelin sheaths (Totoiu and Keirstead, 2005)

Chapter4

General discussion and conclusion

4 General discussion and conclusion

4.1 Discussions

4.1.1 Implications of cell biology results for use of MSCs in cell transplantation

In this present study, we have reproducibly differentiated MSC like cells from hESCs and expanded these cells efficiently to produce large volumes of cells of fairly similar phenotype. These hESC-MSCs closely resemble adult MSCs that were obtained from tissues such as bone marrow according to a number of criteria which include morphology, adherence, cell surface markers, gene expression and ability to differentiate into osteoblasts and adipocytes. Although MSCs have been derived from hESCs previously this is the first time that it has been shown that cryopreservation has minimal effect on the properties of the cells. The ability to generate large number of cells of reproducible phenotype with minimal effect after cryopreservation provide proof of principle that it should be possible to produce an “off the shelf” MSC cell for therapeutic interventions. Additionally, cryopreserved cells would offer several advantages for clinical applications such as easier transportation compared to cells in culture.

4.1.2 Advantages of hESC-MSCs over adult MSCs

hESC-MSCs offer several advantages over MSCs from adult sources such as bone marrow and adipose tissues. Firstly, hESC-MSCs can be prepared in greater consistency compared with those from adult sources such as derivation of cells from the patient themselves. This is because MSCs from patients have been shown to vary in quality and therapeutic properties (Minaire *et al.*, 1984, Klein-Nulend *et al.*, 2005, Wright *et al.*, 2008). Secondly, hESC-MSCs also have the benefit over the autologus strategies by facilitating early intervention which may be beneficial (see below). An autologous transplantation strategy would require the cells to be harvested from the patient themselves and there is likely to be some delay in deciding whether this is an appropriate treatment as this would involve obtaining patient consent and then arranging for the tissue harvesting operation. There would also be delay while the cells were expanded up to the point where there were sufficient for transplantation. The longer the delay, the more cells are likely to be required as cystic cavities form and need to be filled.

Early intervention may be important in maximising the benefits of transplantation of these cells in the context of an application in the treatment of spinal cord injury. There is evidence that two main therapeutic mechanisms of MSC cells transplants include a neuroprotective effect and an immunomodulatory (Abrams *et al.*, 2009, Ankeny *et al.*, 2004)(see below). However, the neuroprotective mechanism is likely to be of decreasing value with time after injury as the pathological processes triggered by the injury progress. Similarly, the immune response to traumatic injury develops over the first few days of injury and peaks within 2 weeks of the injury. This means that the benefit to be derived from a transplant of MSCs in terms of modifying the immune response in a therapeutically beneficial way may also decline with time after this point as the damage and secondary injury processes as well as the block on regeneration may already be largely established and irreversible. Although early intervention may be desirable and would be facilitated by the availability of an "off the shelf" cell product there are likely to be formidable problems associated with early transplantation of cells. It will be necessary to assess the patients suitability for treatment using a cellular therapy, to allow them time to consider whether they wished to have this treatment and then to wait until they were fit enough (i.e. had recovered from other injuries which may have been sustained) until transplantation could be performed.

It is likely that the transplant would need to be performed by an invasive surgical process. Although there have been studies in which cells have been injected systemically into the vascular system and some of these have claimed that cells reach the injury site and have a therapeutic effect (Osaka *et al.*, 2010), the evidence that that this would be a successful approach is not yet very compelling. A further advantage of the use of hESC derived MSCs over adult stem cells in therapeutic application would be the avoidance of an invasive procedure which would be required to harvest the cells. In the case of an autologous transplantation strategy, this would be an invasive procedure that would need to be performed on the patient themselves as soon feasible after the injury.

4.1.3 Disadvantages of hESC-MSCs and iPSCs as a potential alternative cell source

One potential disadvantage of the use of hESC-MSCs is that they will require use of immune suppression. Although there has been some discussion of hESCs being immune privileged this is controversial and the differentiation process might also affect the expression of antigens. We found that when transplanted into the spinal cord of our animal model, treatment with immunosuppressive drugs was essential to the survival of the transplanted cells. However, the complicating factor here is that these transplants are xenograft (i.e. human cells into the rat) and this alone is likely to result in an immune response. Therefore producing MSCs from induced pluripotent stem cells (iPSCs) may offer another alternative. This alternative source of stem cells from which to derive MSCs has the advantage over hESCs as immunesuppression may not be required since such cells could be obtained from the patient. Use of these cells as a starting population, as for hESCs should have the advantage that a consistent product can be produced. Additionally, the use of iPSCs would avoid the ethical issues that are associated with hESC. This is because hESCs are obtained from human embryos, although usually they are derived from excess eggs from *in vitro* fertilization clinics. iPSCs have also been shown to differentiate into functional neurons, astrocytes and oligodendrocytes (Miura *et al.*, 2009) and were recently reported able to support the reconstruction of CST pathways, promote endogenous neuron survival and promote functional recovery of hind limbs in animal study(Fujimoto *et al.*, 2012). However, in comparison to hESCs it would not have the advantage of avoiding an invasive procedure to obtain the cells (though this may be less invasive than for adult cells) and it would also not have the advantage of an “off the shelf” product in terms of allowing an early intervention since the cells would need to be re-programmed to iPSCs, differentiated to MSCs and then expanded.

4.1.4 Implications of in vivo testing of hESC-MSCs

Mesenchymal stem cells obtained from bone marrow are extensively investigated in animal models of SCI and have now even been used in clinical trials (Tetzlaff *et al.*, 2011, Harrop *et al.*, 2012, Forostyak *et al.*, 2013). The results from pre-clinical work are variable but a number of reports claim functional benefits

especially following transplantation at acute time points and a number of different mechanisms which may contribute to these beneficial effects have been reported. However this is the very first time to our knowledge that hESC derived MSCs have been investigated. Consistent with the fact that the hESC-MSCs cultured and characterised in the first part of this study have many properties as bone marrow derived MSCs, we found that when transplanted *in vivo* hESC-MSCs showed many of repair properties of adult MSCs. hESC-MSCs in this study were shown to have good survival in the immunosuppressed animals, filling the injury area, supporting angiogenesis and promoting axonal regeneration. However it is notable that hESC-MSCs did not appear to have any clear advantage in terms of promoting axonal regeneration. Consistent with observations made in studies using MSCs from other sources, numerous regenerating axons were observed within the transplant environment and some of these could be shown by tract tracing to originate from sensory fibres travelling in the dorsal columns. However, there was little evidence of genuine bridging axonal regeneration. Also consistent with previous observations, corticospinal tract axons did not grow into the transplant environment. These observations suggest that in principle hESC derived MSCs should be at least as therapeutically beneficial as adult MSCs but as with other cells, their main mechanism of action when transplanted alone will not be through promotion of bridging axonal regeneration. However the functional benefits of hESC-MSCs transplant have not yet been investigated.

4.2 Future work

4.2.1 A GMP grade cell product

There are several aspects of the current work which it would be useful to follow up in future studies. Firstly, although the works in this thesis provide proof of principle that it should be possible to produce an “off the shelf” MSC cell for therapy in SCI, the current cell culture method is not entirely free of the use of animal products. Clinical application of the use of hESC derived MSCs would require that the whole process is made free from the use of animal products including culturing of hESCs, differentiation into MSCs and maintenance of hESC-MSCs. This could potentially be achieved by performing a serum free differentiation method as reported by Lian *et al* and Wu *et al* (Lian *et al* 2007;

Wu *et al*, 2013) or by replacing the animal serum with human serum. In addition, the cells could then be maintained and expanded in GMP media rather than using media supplemented with animal serum. The MSCs derived using this method would be more clinically translatable but beyond the scope of this project due to time limitations.

4.2.2 Potential anti-inflammatory actions of hESC-MSCs

MSCs of bone marrow origin are reported to have an immune modulator effect and this may be an important mechanism contributing to their potential beneficial therapeutic actions in spinal cord injury. There is some evidence that MSCs transplant can influence the population of macrophages at the site of a spinal cord injury (Nakajima *et al*., 2012). It has been shown that when transplanted into animal models, bone marrow derived MSCs (from human) skew the phenotype of MSCs towards the pro-reparative M2 rather than the harmful M1 phenotype. In the current study, we did not investigate this potential effect of hESC-MSCs and this is something that could be investigated in future work. One complication with the assessment of this mechanism of human cells using *in vivo* transplantation in animals is the need for immunosuppression in order to prevent immune rejection of the cells. This could potentially interfere with reliable investigation of this mechanism. It is possible that an *in vitro* approach could be used as an alternative.

4.2.3 Mechanisms of actions of hESC-MSCs at a cellular and molecular level

Although there is a body of work that suggests various mechanisms of repair are promoted by MSCs transplants and that functional outcome can be improved as a result, the precise cellular properties that are important in providing this therapeutic effect are not understood. It is known that MSCs from adult sources produce a large number of secreted factors *in vitro* and it is likely that they do so *in vivo* although information on this is much less clear because of the technical difficulty of examining this question. The *in vitro* secretome of MSCs has been most extensively studied for bone marrow MSCs (BM-MSCs) which have been shown to produce various cytokines and growth factors, some of the main ones being BDNF, VEGF and IL-6 (Seo *et al*., 2011, Wilkins *et al*., 2009, Kinnaird

et al., 2004). Some of these factors are likely to be involved in the beneficial repair properties of MSC although some of the cytokines might be expected to have a detrimental effect since they are pro-inflammatory. There is some variability in reports on the factors produced by BM-MSCs and this likely reflects differences in the precise cell populations in different studies in different labs because of the differences in cell donors and preparation methods. It is quite likely that there will be differences between the secretome of MSCs from different tissues. For example, it has been reported that MSCs from human lamina propria in the nose produce a cytokine which enhances myelination in vitro but this factor is not produced by BM-MSCs (Lindsay *et al.*, 2013). An important area for future study will therefore be one directed at gaining a better understanding of the properties of transplanted cells which are important for the their positive repair effects. A better understanding of the factors secreted by cells may be a contribution towards this process. At present it is not clear what factors are produced by hESC-MSCs and how they compare to those produced by adult cells and this would therefore be a useful area to investigate. For example, a comparative study on the factors that are produced by BM-MSCs and hESC-MSCs could be performed in vitro using microarray or quantitative RT-PCR (Kwan Sze et al, 2007). The study would reveal whether hESC-MSCs also produce secretomes that are potentially useful for spinal cord injury repair and the data could give indications of how they might affect the SCI environment. Should the study reveal that hESC-MSCs do not produce any useful factors for SCI repair compared to BM-MSCs, the option to genetically modifiy the hESC-MSCs to over-express or secrete neurotrophic factors like BDNF and GDNF could be considered. These 2 factors were shown to promote better therapeutic effects including promoting cell survival and axonal regeneration in SCI (Sasaki et al 2009). The ability of MSCs to secrete neurotrophic factors would be of great advantage as the efficacy of these neurotrophic factors depends on their continuous supply which could be offered by transplanted cells.

4.3 Conclusion

In conclusion, the first section of this work in this thesis indicates that it should be possible to produce MSC-like cells from hESC that sharing many properties of bone marrow derived MSCs (BM-MSCs) on a consistent and reliable basis and in large quantities. The second section of this work in this project shows that when

transplanted into animal models of spinal cord injury, hESC-MSCs can survive and fill the injury site. They also appear to have most of the beneficial actions previously reported for MSCs of bone marrow origin.

The fact that hESC-MSCs appear very similar in effect to bone marrow derived cells is promising but their actions have yet to be investigated using functional outcome measures and this is the next important area of investigation that should be addressed in future work. However, like MSCs and cells from other sources, hESC-MSCs are not able to promote bridging axonal regeneration. The implications of this are that when MSCs are transplanted alone with the aim of treating spinal cord injury, any beneficial effects they have will not be due to functional axonal regeneration but will be due to other mechanisms such as improved blood supply, neuroprotection, immune modulation and perhaps promotion of remyelination and plasticity. This has implications for the degree of functional recovery that can be expected, the type of patient that might benefit and potentially also practical aspects of any therapy. Without the promotion of axonal regeneration, functional benefits arising from the alternative mechanisms are likely to be quite modest. Without axonal regeneration, only those with incomplete spinal cord injuries are likely to benefit from the treatment. The timing of the treatment may also be an important issue as the neuroprotective and immune modulatory mechanisms may be of greatest benefit in the early stages after injury.

Bibliography

ABRAMS, M. B., DOMINGUEZ, C., PERNOLD, K., REGERA, R., WIESENFELD-HALLIN, Z., OLSON, L. & PROCKOP, D. 2009. Multipotent mesenchymal stromal cells attenuate chronic inflammation and injury-induced sensitivity to mechanical stimuli in experimental spinal cord injury. *Restorative Neurology and Neuroscience,* 27**,** 307-321.

ADEWUMI, O., AFLATOONIAN, B., AHRLUND-RICHTER, L., AMIT, M., ANDREWS, P. W., BEIGHTON, G., BELLO, P. A., BENVENISTY, N., BERRY, L. S., BEVAN, S., BLUM, B., BROOKING, J., CHEN, K. G., CHOO, A. B., CHURCHILL, G. A., CORBEL, M., DAMJANOV, I., DRAPER, J. S., DVORAK, P., EMANUELSSON, K., FLECK, R. A., FORD, A., GERTOW, K., GERTSENSTEIN, M., GOKHALE, P. J., HAMILTON, R. S., HAMPL, A., HEALY, L. E., HOVATTA, O., HYLLNER, J., IMREH, M. P., ITSKOVITZ-ELDOR, J., JACKSON, J., JOHNSON, J. L., JONES, M., KEE, K., KING, B. L., KNOWLES, B. B., LAKO, M., LEBRIN, F., MALLON, B. S., MANNING, D., MAYSHAR, Y., MCKAY, R. D., MICHALSKA, A. E., MIKKOLA, M., MILEIKOVSKY, M., MINGER, S. L., MOORE, H. D., MUMMERY, C. L., NAGY, A., NAKATSUJI, N., O'BRIEN, C. M., OH, S. K., OLSSON, C., OTONKOSKI, T., PARK, K. Y., PASSIER, R., PATEL, H., PATEL, M., PEDERSEN, R., PERA, M. F., PIEKARCZYK, M. S., PERA, R. A., REUBINOFF, B. E., ROBINS, A. J., ROSSANT, J., RUGG-GUNN, P., SCHULZ, T. C., SEMB, H., SHERRER, E. S., SIEMEN, H., STACEY, G. N., STOJKOVIC, M., SUEMORI, H., SZATKIEWICZ, J., TURETSKY, T., TUURI, T., VAN DEN BRINK, S., VINTERSTEN, K., VUORISTO, S., WARD, D., WEAVER, T. A., YOUNG, L. A. & ZHANG, W. 2007. Characterization of human embryonic stem cell lines by the International Stem Cell Initiative. *Nat Biotechnol,* 25**,** 803-16.

AFIFI, A. & BERGMAN, R. 2005. *Functional Neuroanatomy,* United States of America, Lange Medical Books/McGraw-Hill.

AGGARWAL, S. & PITTENGER, M. 2005. Human mesenchymal stem cells modulate allogeneic immune cell responses. *Blood,* 105**,** 1815 - 1822.

ALEXANIAN, A. R., FEHLINGS, M. G., ZHANG, Z. & MAIMAN, D. J. 2011. Transplanted neurally modified bone marrow-derived mesenchymal stem cells promote tissue protection and locomotor recovery in spinal cord injured rats. *Neurorehabil Neural Repair,* 25**,** 873-80.

ALEXANIAN, A. R., MAIMAN, D. J., KURPAD, S. N. & GENNARELLI, T. A. 2008. In vitro and in vivo characterization of neurally modified mesenchymal stem cells induced by epigenetic modifiers and neural stem cell environment. *Stem Cells Dev,* 17**,** 1123-30.

ALEXANIAN, A. R., SVENDSEN, C. N., CROWE, M. J. & KURPAD, S. N. 2011. Transplantation of human glial-restricted neural precursors into injured spinal cord promotes functional and sensory recovery without causing allodynia. *Cytotherapy,* 13**,** 61-8.

ALMON, R. R., DUBOIS, D. C., BRANDENBURG, E. H., SHI, W., ZHANG, S., STRAUBINGER, R. M. & JUSKO, W. J. 2002. Pharmacodynamics and pharmacogenomics of diverse receptor-mediated effects of methylprednisolone in rats using microarray analysis. *J Pharmacokinet Pharmacodyn,* 29**,** 103-29.

AMANO, S., LI, S., GU, C., GAO, Y., KOIZUMI, S., YAMAMOTO, S., TERAKAWA, S. & NAMBA, H. 2009. Use of genetically engineered bone marrow-derived mesenchymal stem cells for glioma gene therapy. *Int J Oncol,* 35**,** 1265-70.

ANKENY, D. P., MCTIGUE, D. M. & JAKEMAN, L. B. 2004. Bone marrow transplants provide tissue protection and directional guidance for axons after contusive spinal cord injury in rats. *Experimental Neurology,* 190**,** 17-31.

ASHER, R. A., MORGENSTERN, D. A., SHEARER, M. C., ADCOCK, K. H., PESHEVA, P. & FAWCETT, J. W. 2002. Versican is upregulated in CNS injury and is a product of oligodendrocyte lineage cells. *J Neurosci,* 22**,** 2225-36.

BACH, F., ALBERTINI, R., JOO, P., ANDERSON, J. & BORTIN, M. 1968. BONE-MARROW TRANSPLANTATION IN A PATIENT WITH THE WISKOTT-ALDRICH SYNDROME. *The Lancet,* 292**,** 1364-1366.

BALENTINE, J. D. 1978. Pathology of experimental spinal cord trauma. II. Ultrastructure of axons and myelin. *Lab Invest,* 39**,** 254-66.

BAPTISTE, D. C., FEHLINGS, M. G., JOHN, T. W. & ANDREW, I. R. M. 2007. Update on the treatment of spinal cord injury. *Progress in Brain Research*. Elsevier.

BARBERI, T., STUDER, L., IRINA, K. & ROBERT, L. 2006. Mesenchymal Cells. *Methods in Enzymology*. Academic Press.

BARBERI, T., WILLIS, L. M., SOCCI, N. D. & STUDER, L. 2005. Derivation of multipotent mesenchymal precursors from human embryonic stem cells. *PLoS Med,* 2**,** e161.

BARON-VAN EVERCOOREN, A., GANSMULLER, A., DUHAMEL, E., PASCAL, F. & GUMPEL, M. 1992. Repair of a myelin lesion by Schwann cells transplanted in the adult mouse spinal cord. *J Neuroimmunol,* 40**,** 235-42.

BARRY, F., BOYNTON, R. E., LIU, B. & MURPHY, J. M. 2001. Chondrogenic differentiation of mesenchymal stem cells from bone marrow: differentiation-dependent gene expression of matrix components. *Exp Cell Res,* 268**,** 189-200.

BARRY, F. P., BOYNTON, R. E., HAYNESWORTH, S., MURPHY, J. M. & ZAIA, J. 1999. The monoclonal antibody SH-2, raised against human mesenchymal stem cells, recognizes an epitope on endoglin (CD105). *Biochem Biophys Res Commun,* 265**,** 134-9.

BARRY, F. P. & MURPHY, J. M. 2004. Mesenchymal stem cells: clinical applications and biological characterization. *Int J Biochem Cell Biol,* 36**,** 568-84.

BEYER NARDI, N. & SILVA MEIRELLES, L. 2006. Mesenchymal Stem Cells: Isolation, In Vitro Expansion and Characterization. *In:* WOBUS, A. & BOHELER, K. (eds.) *Stem Cells*. Springer Berlin Heidelberg.

BHATTACHARYA, B., MIURA, T., BRANDENBERGER, R., MEJIDO, J., LUO, Y., YANG, A. X., JOSHI, B. H., GINIS, I., THIES, R. S., AMIT, M., LYONS, I., CONDIE,

B. G., ITSKOVITZ-ELDOR, J., RAO, M. S. & PURI, R. K. 2004. Gene expression in human embryonic stem cell lines: unique molecular signature. *Blood,* 103**,** 2956-64.

BIELBY, R. C., BOCCACCINI, A. R., POLAK, J. M. & BUTTERY, L. D. 2004. In vitro differentiation and in vivo mineralization of osteogenic cells derived from human embryonic stem cells. *Tissue Eng,* 10**,** 1518-25.

BIERNASKIE, J., SPARLING, J. S., LIU, J., SHANNON, C. P., PLEMEL, J. R., XIE, Y., MILLER, F. D. & TETZLAFF, W. 2007. Skin-derived precursors generate myelinating Schwann cells that promote remyelination and functional recovery after contusion spinal cord injury. *J Neurosci,* 27**,** 9545-59.

BILLON, N., JOLICOEUR, C. & RAFF, M. 2006. Generation and characterization of oligodendrocytes from lineage-selectable embryonic stem cells in vitro. *Methods Mol Biol,* 330**,** 15-32.

BIZEN, A., HONMOU, O., INOUE, M., IIHOSHI, S., HOUKIN, K. & HASHI, K. 2003. Transplantation of mesenchymal stem cells derived from the bone marrow into the demyelinated spinal cord. *International Congress Series,* 1252**,** 471-475.

BLACK, I. B. & WOODBURY, D. 2001. Adult Rat and Human Bone Marrow Stromal Stem Cells Differentiate into Neurons. *Blood Cells, Molecules, and Diseases,* 27**,** 632-636.

BOIDO, M., GARBOSSA, D., FONTANELLA, M., DUCATI, A. & VERCELLI, A. 2012. Mesenchymal stem cell transplantation reduces glial cyst and improves functional outcome following spinal cord compression. *World Neurosurgery*.

BONNER, J. F., BLESCH, A., NEUHUBER, B. & FISCHER, I. 2010. Promoting directional axon growth from neural progenitors grafted into the injured spinal cord. *Journal of Neuroscience Research,* 88**,** 1182-1192.

BOYD, N. L., ROBBINS, K. R., DHARA, S. K., WEST, F. D. & STICE, S. L. 2009. Human embryonic stem cell-derived mesoderm-like epithelium transitions to mesenchymal progenitor cells. *Tissue Eng Part A,* 15**,** 1897-907.

BRADBURY, E. J., MOON, L. D., POPAT, R. J., KING, V. R., BENNETT, G. S., PATEL, P. N., FAWCETT, J. W. & MCMAHON, S. B. 2002. Chondroitinase ABC promotes functional recovery after spinal cord injury. *Nature,* 416**,** 636-40.

BREGMAN, B. S., KUNKEL-BAGDEN, E., REIER, P. J., DAI, H. N., MCATEE, M. & GAO, D. 1993. Recovery of Function after Spinal Cord Injury: Mechanisms Underlying Transplant-Mediated Recovery of Function Differ after Spinal Cord Injury in Newborn and Adult Rats. *Experimental Neurology,* 123**,** 3-16.

BREGMAN, B. S., KUNKEL-BAGDEN, E., SCHNELL, L., DAI, H. N., GAO, D. & SCHWAB, M. E. 1995. Recovery from spinal cord injury mediated by antibodies to neurite growth inhibitors. *Nature,* 378**,** 498-501.

BROSAMLE, C. & SCHWAB, M. E. 1997. Cells of origin, course, and termination patterns of the ventral, uncrossed component of the mature rat corticospinal tract. *J Comp Neurol,* 386**,** 293-303.

BRUDER, S. P., JAISWAL, N. & HAYNESWORTH, S. E. 1997. Growth kinetics, self-renewal, and the osteogenic potential of purified human mesenchymal stem cells during extensive subcultivation and following cryopreservation. *J Cell Biochem,* 64**,** 278-94.

BÜHRING, H.-J., BATTULA, V. L., TREML, S., SCHEWE, B., KANZ, L. & VOGEL, W. 2007. Novel Markers for the Prospective Isolation of Human MSC. *Annals of the New York Academy of Sciences,* 1106**,** 262-271.

CAI, J., CHEN, J., LIU, Y., MIURA, T., LUO, Y., LORING, J. F., FREED, W. J., RAO, M. S. & ZENG, X. 2006. Assessing Self-Renewal and Differentiation in Human Embryonic Stem Cell Lines. *STEM CELLS,* 24**,** 516-530.

CAKOUROS, D., RAICES, R. M., GRONTHOS, S. & GLACKIN, C. A. 2010. Twist-ing cell fate: Mechanistic insights into the role of twist in lineage specification/differentiation and tumorigenesis. *Journal of Cellular Biochemistry,* 110**,** 1288-1298.

CALDWELL, M. A., HE, X., WILKIE, N., POLLACK, S., MARSHALL, G., WAFFORD, K. A. & SVENDSEN, C. N. 2001. Growth factors regulate the survival and fate of cells derived from human neurospheres. *Nat Biotechnol,* 19**,** 475-9.

CAMPISI, J. & D'ADDA DI FAGAGNA, F. 2007. Cellular senescence: when bad things happen to good cells. *Nat Rev Mol Cell Biol,* 8**,** 729-40.

Canadian Association of Emergency Physicians 2009, *A Position Statement: methylprednidolone is not a standard of care*. Available from http://caep.ca/resources/position-statements-and-guidelines/steroids-acute-spinal-cord-injury (28 January 2013)

CAO, Q., ZHANG, Y. P., IANNOTTI, C., DEVRIES, W. H., XU, X. M., SHIELDS, C. B. & WHITTEMORE, S. R. 2005. Functional and electrophysiological changes after graded traumatic spinal cord injury in adult rat. *Exp Neurol,* 191 Suppl 1**,** S3-S16.

CAO, Q. L., ZHANG, Y. P., HOWARD, R. M., WALTERS, W. M., TSOULFAS, P. & WHITTEMORE, S. R. 2001. Pluripotent stem cells engrafted into the normal or lesioned adult rat spinal cord are restricted to a glial lineage. *Exp Neurol,* 167**,** 48-58.

CAO, Q.-L., HOWARD, R. M., DENNISON, J. B. & WHITTEMORE, S. R. 2002. Differentiation of Engrafted Neuronal-Restricted Precursor Cells Is Inhibited in the Traumatically Injured Spinal Cord. *Experimental Neurology,* 177**,** 349-359.

CARPENTER, M., FREY-VASCONCELLS, J. & RAO, M. 2009. Developing safe therapies from human pluripotent stem cells. *nature biotechnology,* 27**,** 606-613.

CARPENTER, M. K., INOKUMA, M. S., DENHAM, J., MUJTABA, T., CHIU, C. P. & RAO, M. S. 2001. Enrichment of neurons and neural precursors from human embryonic stem cells. *Exp Neurol,* 172**,** 383-97.

CASALE, E. J., LIGHT, A. R. & RUSTIONI, A. 1988. Direct projection of the corticospinal tract to the superficial laminae of the spinal cord in the rat. *The Journal of Comparative Neurology,* 278**,** 275-286.

CHAMBERLAIN, G., FOX, J., ASHTON, B. & MIDDLETON, J. 2007. Concise review: mesenchymal stem cells: their phenotype, differentiation capacity, immunological features, and potential for homing. *Stem Cells,* 25**,** 2739-49.

CHEN, J., LI, Y. & CHOPP, M. 2000. Intracerebral transplantation of bone marrow with BDNF after MCAo in rat. *Neuropharmacology,* 39**,** 711-716.

CHIBA, Y., KURODA, S., MARUICHI, K., OSANAI, T., HOKARI, M., YANO, S., SHICHINOHE, H., HIDA, K. & IWASAKI, Y. 2009. Transplanted bone marrow stromal cells promote axonal regeneration and improve motor function in a rat spinal cord injury model. *Neurosurgery,* 64**,** 991-9; discussion 999-1000.

CHOPP, M., ZHANG, X. H., LI, Y., WANG, L., CHEN, J., LU, D., LU, M. & ROSENBLUM, M. 2000. Spinal cord injury in rat: treatment with bone marrow stromal cell transplantation. *Neuroreport,* 11**,** 3001-5.

CHRISTENSEN, M. D., EVERHART, A. W., PICKELMAN, J. T. & HULSEBOSCH, C. E. 1996. Mechanical and thermal allodynia in chronic central pain following spinal cord injury. *Pain,* 68**,** 97-107.

CHRISTENSEN, M. D. & HULSEBOSCH, C. E. 1997. Chronic central pain after spinal cord injury. *J Neurotrauma,* 14**,** 517-37.

CHUAH, M. I. & AU, C. 1991. Olfactory Schwann cells are derived from precursor cells in the olfactory epithelium. *Journal of Neuroscience Research,* 29**,** 172-180.

CHUNG, K., LANGFORD, L. A. & COGGESHALL, R. E. 1987. Primary afferent and propriospinal fibers in the rat dorsal and dorsolateral funiculi. *J Comp Neurol,* 263**,** 68-75.

COHEN, J. J. 1993. Apoptosis. *Immunol Today,* 14**,** 126-30.

COLTER, D., SEKIYA, I. & PROCKOP, D. 2001. Identification of a subpopulation of rapidly self-renewing and multipotential adult stem cells in colonies of human marrow stromal cells. *Proc Natl Acad Sci USA,* 98**,** 7841 - 7845.

COUTTS, M. & KEIRSTEAD, H. S. 2008. Stem cells for the treatment of spinal cord injury. *Exp Neurol,* 209**,** 368-77.

CRISTANTE, A. F., BARROS-FILHO, T. E. P., TATSUI, N., MENDRONE, A., CALDAS, J. G., CAMARGO, A., ALEXANDRE, A., J TEIXEIRA, W. G., OLIVEIRA, R. P. & MARCON, R. M. 2009. Stem cells in the treatment of chronic spinal cord injury: evaluation of somatosensitive evoked potentials in 39 patients. *Spinal Cord,* 47**,** 733-738.

CROWE, M. J., BRESNAHAN, J. C., SHUMAN, S. L., MASTERS, J. N. & BEATTIE, M. S. 1997. Apoptosis and delayed degeneration after spinal cord injury in rats and monkeys. *Nat Med,* 3**,** 73-6.

CUMMINGS, B. J., UCHIDA, N., TAMAKI, S. J. & ANDERSON, A. J. 2006. Human neural stem cell differentiation following transplantation into spinal cord injured mice: association with recovery of locomotor function. *Neurol Res,* 28**,** 474-81.

DA SILVA MEIRELLES, L., CHAGASTELLES, P. & NARDI, N. 2006. Mesenchymal stem cells reside in virtually all post-natal organs and tissues. *J Cell Sci,* 119**,** 2204 - 2213.

DA SILVA MEIRELLES, L., FONTES, A. M., COVAS, D. T. & CAPLAN, A. I. 2009. Mechanisms involved in the therapeutic properties of mesenchymal stem cells. *Cytokine & Growth Factor Reviews,* 20**,** 419-427.

DAVIES, S. J., FITCH, M. T., MEMBERG, S. P., HALL, A. K., RAISMAN, G. & SILVER, J. 1997. Regeneration of adult axons in white matter tracts of the central nervous system. *Nature,* 390**,** 680-3.

DAVIES, S. J., GOUCHER, D. R., DOLLER, C. & SILVER, J. 1999. Robust regeneration of adult sensory axons in degenerating white matter of the adult rat spinal cord. *J Neurosci,* 19**,** 5810-22.

DE PEPPO, G. M., SVENSSON, S., LENNERAS, M., SYNNERGREN, J., STENBERG, J., STREHL, R., HYLLNER, J., THOMSEN, P. & KARLSSON, C. 2010. Human embryonic mesodermal progenitors highly resemble human mesenchymal stem cells and

display high potential for tissue engineering applications. *Tissue Eng Part A,* 16**,** 2161-82.

DE POMMERY, J., ROUDIER, F. & MENÉTREY, D. 1984. Postsynaptic fibers reaching the dorsal column nuclei in the rat. *Neuroscience Letters,* 50**,** 319-323.

DEANS, R. J. & MOSELEY, A. B. 2000. Mesenchymal stem cells: biology and potential clinical uses. *Exp Hematol,* 28**,** 875-84.

DESKINS, D. L., BASTAKOTY, D., SARASWATI, S., SHINAR, A., HOLT, G. E. & YOUNG, P. P. 2013. Human Mesenchymal Stromal Cells: Identifying Assays to Predict Potency for Therapeutic Selection. *Stem Cells Translational Medicine,* 2**,** 151-158.

DI GIOVANNI, S. 2006. Regeneration following spinal cord injury, from experimental models to humans: where are we? *Expert Opinion on Therapeutic Targets,* 10**,** 363-376.

DIGIROLAMO, C. M., STOKES, D., COLTER, D., PHINNEY, D. G., CLASS, R. & PROCKOP, D. J. 1999. Propagation and senescence of human marrow stromal cells in culture: a simple colony-forming assay identifies samples with the greatest potential to propagate and differentiate. *Br J Haematol,* 107**,** 275-81.

DIMRI, G. P., LEE, X., BASILE, G., ACOSTA, M., SCOTT, G., ROSKELLEY, C., MEDRANO, E. E., LINSKENS, M., RUBELJ, I., PEREIRA-SMITH, O. & ET AL. 1995. A biomarker that identifies senescent human cells in culture and in aging skin in vivo. *Proc Natl Acad Sci U S A,* 92**,** 9363-7.

DOETSCH, F., CAILLE, I., LIM, D. A., GARCIA-VERDUGO, J. M. & ALVAREZ-BUYLLA, A. 1999. Subventricular zone astrocytes are neural stem cells in the adult mammalian brain. *Cell,* 97**,** 703-16.

DOMINICI, M., LE BLANC, K., MUELLER, I., SLAPER-CORTENBACH, I., MARINI, F., KRAUSE, D., DEANS, R., KEATING, A., PROCKOP, D. & HORWITZ, E. 2006. Minimal criteria for defining multipotent mesenchymal stromal cells. The International Society for Cellular Therapy position statement. *Cytotherapy,* 8**,** 315-7.

DOU, C. L. & LEVINE, J. M. 1994. Inhibition of neurite growth by the NG2 chondroitin sulfate proteoglycan. *J Neurosci,* 14**,** 7616-28.

DOUGHERTY, K. D., DREYFUS, C. F. & BLACK, I. B. 2000. Brain-derived neurotrophic factor in astrocytes, oligodendrocytes, and microglia/macrophages after spinal cord injury. *Neurobiol Dis,* 7**,** 574-85.

DREYFUS, C. F., DAI, X., LERCHER, L. D., RACEY, B. R., FRIEDMAN, W. J. & BLACK, I. B. 1999. Expression of neurotrophins in the adult spinal cord in vivo. *Journal of Neuroscience Research,* 56**,** 1-7.

EFTEKHARPOUR, E., KARIMI-ABDOLRAZAE, S. & FEHLINGS, M. G. 2008. Current status of experimental cell replacement approaches to spinal cord injury. *Neurosurgery Focus,* 24**,** 1-13.

EVANS, M. J. & KAUFMAN, M. H. 1981. Establishment in culture of pluripotential cells from mouse embryos. *Nature,* 292**,** 154-6.

FAWCETT, J. W. & ASHER, R. A. 1999. The glial scar and central nervous system repair. *Brain Res Bull,* 49**,** 377-91.

FILBIN, M. T. 2003. Myelin-associated inhibitors of axonal regeneration in the adult mammalian CNS. *Nat Rev Neurosci,* 4**,** 703-13.

FINKLESTEIN, S. P., APOSTOLIDES, P. J., CADAY, C. G., PROSSER, J., PHILIPS, M. F. & KLAGSBRUN, M. 1988. Increased basic fibroblast growth factor (bFGF) immunoreactivity at the site of focal brain wounds. *Brain Res,* 460**,** 253-9.

FINLEY, M. F., KULKARNI, N. & HUETTNER, J. E. 1996. Synapse formation and establishment of neuronal polarity by P19 embryonic carcinoma cells and embryonic stem cells. *J Neurosci,* 16**,** 1056-65.

FORET, A., QUERTAINMONT, R., BOTMAN, O., BOUHY, D., AMABILI, P., BROOK, G., SCHOENEN, J. & FRANZEN, R. 2010. Stem cells in the adult rat spinal cord: plasticity after injury and treadmill training exercise. *Journal of Neurochemistry,* 112**,** 762-772.

FOROSTYAK, S., JENDELOVA, P. & SYKOVA, E. 2013. The role of mesenchymal stromal cells in spinal cord injury, regenerative medicine and possible clinical applications. *Biochimie*.

FU, E. S. & SAPORTA, S. 2005. Methylprednisolone inhibits production of interleukin-1beta and interleukin-6 in the spinal cord following compression injury in rats. *J Neurosurg Anesthesiol,* 17**,** 82-5.

FUJIMOTO, Y., ABEMATSU, M., FALK, A., TSUJIMURA, K., SANOSAKA, T., JULIANDI, B., SEMI, K., NAMIHIRA, M., KOMIYA, S., SMITH, A. & NAKASHIMA, K. 2012. Treatment of a mouse model of spinal cord injury by transplantation of human induced pluripotent stem cell-derived long-term self-renewing neuroepithelial-like stem cells. *Stem Cells,* 30**,** 1163-73.

FURLAN, J. C., NOONAN, V., CADOTTE, D. W. & FEHLINGS, M. G. 2011. Timing of decompressive surgery of spinal cord after traumatic spinal cord injury: an evidence-based examination of pre-clinical and clinical studies. *J Neurotrauma,* 28**,** 1371-99.

GAEBEL, R., FURLANI, D., SORG, H., POLCHOW, B., FRANK, J., BIEBACK, K., WANG, W., KLOPSCH, C., ONG, L.-L., LI, W., MA, N. & STEINHOFF, G. 2011. Cell Origin of Human Mesenchymal Stem Cells Determines a Different Healing Performance in Cardiac Regeneration. *PLoS ONE,* 6**,** e15652.

GANG, E. J., HONG, S. H., JEONG, J. A., HWANG, S. H., KIM, S. W., YANG, I. H., AHN, C., HAN, H. & KIM, H. 2004. In vitro mesengenic potential of human umbilical cord blood-derived mesenchymal stem cells. *Biochem Biophys Res Commun,* 321**,** 102-8.

GARDINER, P., BEAUMONT, E. & CORMERY, B. 2005. Motoneurones "learn" and "forget" physical activity. *Can J Appl Physiol,* 30**,** 352-70.

GATTI, R., MEUWISSEN, H., ALLEN, H., HONG, R. & GOOD, R. 1968. IMMUNOLOGICAL RECONSTITUTION OF SEX-LINKED LYMPHOPENIC IMMUNOLOGICAL DEFICIENCY. *The Lancet,* 292**,** 1366-1369.

GEFFNER, L., SANTACRUZ, P., IZUIRETA, M., LFLOR, L., MALDONADO, B., AUAD, A., MONTENEGRO, X., GONZLEZ, R. & SILVA, F. 2008. Administration of autologous bone marrow stem cells into spinal cord injury patients via multiple routes is safe and improves their quality of life: Comprehensive case studies. *Cell transplantation,* 17**,** 1277-1293.

GHOSH, M., TUESTA, L. M., PUENTES, R., PATEL, S., MELENDEZ, K., EL MAAROUF, A., RUTISHAUSER, U. & PEARSE, D. D. 2012. Extensive cell migration, axon regeneration, and improved function with polysialic acid-modified Schwann cells after spinal cord injury. *Glia,* 60**,** 979-92.

GIESLER, G. J., JR., NAHIN, R. L. & MADSEN, A. M. 1984. Postsynaptic dorsal column pathway of the rat. I. Anatomical studies. *J Neurophysiol,* 51**,** 260-75.

GIUFFRIDA, R. & RUSTIONI, A. 1992. Dorsal root ganglion neurons projecting to the dorsal column nuclei of rats. *J Comp Neurol,* 316**,** 206-20.

GRIMPE, B. & SILVER, J. 2002. The extracellular matrix in axon regeneration. *Prog Brain Res,* 137**,** 333-49.

GRONTHOS, S., FRANKLIN, D. M., LEDDY, H. A., ROBEY, P. G., STORMS, R. W. & GIMBLE, J. M. 2001. Surface protein characterization of human adipose tissue-derived stromal cells. *J Cell Physiol,* 189**,** 54-63.

GRUENLOH, W., KAMBAL, A., SONDERGAARD, C., MCGEE, J., NACEY, C., KALOMOIRIS, S., PEPPER, K., OLSON, S., FIERRO, F. & NOLTA, J. A. 2011. Characterization and in vivo testing of mesenchymal stem cells derived from human embryonic stem cells. *Tissue Eng Part A,* 17**,** 1517-25.

GU, W., ZHANG, F., XUE, Q., MA, Z., LU, P. & YU, B. 2010. Transplantation of bone marrow mesenchymal stem cells reduces lesion volume and induces axonal regrowth of injured spinal cord. *Neuropathology,* 30**,** 205-17.

HAFLON, S., ABRAMOV, N., GRINBLAT, B. & GINIS, I. 2011. Markers distinguishing mesenchymal stem cells from fibroblasts are downregulated with passaging. *Stem Cells and Development,* 20**,** 53-66.

HALL, E. D. 1992. The neuroprotective pharmacology of methylprednisolone. *J Neurosurg,* 76**,** 13-22.

HARDY, S. A., MALTMAN, D. J. & PRZYBORSKI, S. A. 2008. Mesenchymal stem cells as mediators of neural differentiation. *Curr Stem Cell Res Ther,* 3**,** 43-52.

HARROP, J. S., HASHIMOTO, R., NORVELL, D., RAICH, A., AARABI, B., GROSSMAN, R. G., GUEST, J. D., TATOR, C. H., CHAPMAN, J. & FEHLINGS, M. G. 2012. Evaluation of clinical experience using cell-based therapies in patients with spinal cord injury: a systematic review. *Journal of Neurosurgery: Spine,* 17**,** 230-246.

HAWRYLUK, G. W., SPANO, S., CHEW, D., WANG, S., ERWIN, M., CHAMANKHAH, M., FORGIONE, N. & FEHLINGS, M. G. 2013. An Examination of The Mechanisms by Which Neural Precursors Augment Recovery Following Spinal Cord Injury: A Key Role for Remyelination. *Cell Transplant*.

HAWRYLUK, G. W. J. M., A; WANG, J; WANG, S; TATOR, C; FEHLINGS, M.G 2012. An in Vivo Characterization of Trophic Factor production following neural precursor cell or bone marrow stromal cell transplantation for spinal cord injury. *Stem Cells and Development,* 00.

HAY, E. D. 2005. The mesenchymal cell, its role in the embryo, and the remarkable signaling mechanisms that create it. *Developmental Dynamics,* 233**,** 706-720.

HAYNESWORTH, S. E., BABER, M. A. & CAPLAN, A. I. 1992. Cell surface antigens on human marrow-derived mesenchymal cells are detected by monoclonal antibodies. *Bone,* 13**,** 69-80.

HEO, J. Y., JING, K., SONG, K. S., SEO, K. S., PARK, J. H., KIM, J. S., JUNG, Y. J., HUR, G. M., JO, D. Y., KWEON, G. R., YOON, W. H., LIM, K., HWANG, B. D., JEON, B. H. & PARK, J. I. 2009. Downregulation of APE1/Ref-1 is involved in the senescence of mesenchymal stem cells. *Stem Cells,* 27**,** 1455-62.

HICKS, S. & D'AMATO, C. 1975. Motor-sensory cortex-corticospinal system and developing locomotion and placing rats. *AM. J. Anat.*, 143, 1-42.

HILL, E. L., TURNER, R. & ELDE, R. 1991. Effects of neonatal sympathectomy and capsaicin treatment on bone remodeling in rats. *Neuroscience,* 44, 747-755.

HIMES, B., NEUHUBER, B., COLEMAN, C., KUSHNER, R., SWANGER, S., KOPEN, G., WAGNER, J., SHUMSKY, J. & FISCHER, I. 2006. Recovery of function following grafting of human bone marrow-derived stromal cells into the injured spinal cord. *Neurorehabil Neural Repair,* 20, 278 - 296.

HO, A. D., WAGNER, W. & FRANKE, W. 2008. Heterogeneity of mesenchymal stromal cell preparations. *Cytotherapy,* 10, 320-30.

HOFSTETTER, C. P., SCHWARZ, E. J., HESS, D., WIDENFALK, J., EL MANIRA, A., PROCKOP, D. J. & OLSON, L. 2002. Marrow stromal cells form guiding strands in the injured spinal cord and promote recovery. *Proc Natl Acad Sci U S A,* 99, 2199-204.

HORKY, L. L., GALIMI, F., GAGE, F. H. & HORNER, P. J. 2006. Fate of endogenous stem/progenitor cells following spinal cord injury. *J Comp Neurol,* 498, 525-38.

HORWITZ, E., LE BLANC, K., DOMINICI, M., MUELLER, I., SLAPER-CORTENBACH, MARINI, F., DEANS, R., KRAUSE, D. & KEATING, A. 2005. Clarification of the nomenclature for MSC: The International Society for Cellular Therapy position statement. *Cytotherapy,* 7, 393-395.

HUANG, G. T., GRONTHOS, S. & SHI, S. 2009. Mesenchymal stem cells derived from dental tissues vs. those from other sources: their biology and role in regenerative medicine. *J Dent Res,* 88, 792-806.

HULSEBOSCH, C. E. 2002. RECENT ADVANCES IN PATHOPHYSIOLOGY AND TREATMENT OF SPINAL CORD INJURY. *Advances in Physiology Education,* 26, 238-255.

HWANG, D. H., KIM, B. G., KIM, E. J., LEE, S. I., JOO, I. S., SUH-KIM, H., SOHN, S. & KIM, S. U. 2009. Transplantation of human neural stem cells transduced with Olig2 transcription factor improves locomotor recovery and enhances myelination in the white matter of rat spinal cord following contusive injury. *BMC Neurosci,* 10**,** 117.

HYSLOP, L., STOJKOVIC, M., ARMSTRONG, L., WALTER, T., STOJKOVIC, P., PRZYBORSKI, S., HERBERT, M., MURDOCH, A., STRACHAN, T. & LAKO, M. 2005. Downregulation of NANOG induces differentiation of human embryonic stem cells to extraembryonic lineages. *Stem Cells,* 23**,** 1035-43.

IKEDA, O., MURAKAMI, M., INO, H., YAMAZAKI, M., NEMOTO, T., KODA, M., NAKAYAMA, C. & MORIYA, H. 2001. Acute up-regulation of brain-derived neurotrophic factor expression resulting from experimentally induced injury in the rat spinal cord. *Acta Neuropathol,* 102**,** 239-45.

ILLES, J., REIMER, J. & KWON, B. 2011. Stem Cell Clinical Trials for Spinal Cord Injury: Readiness, Reluctance, Redefinition. *Stem Cell Reviews and Reports,* 7**,** 997-1005.

ITAHANA, K., CAMPISI, J. & DIMRI, G. P. 2007. Methods to detect biomarkers of cellular senescence: the senescence-associated beta-galactosidase assay. *Methods Mol Biol,* 371**,** 21-31.

IWANAMI, A., KANEKO, S., NAKAMURA, M., KANEMURA, Y., MORI, H., KOBAYASHI, S., YAMASAKI, M., MOMOSHIMA, S., ISHII, H., ANDO, K., TANIOKA, Y., TAMAOKI, N., NOMURA, T., TOYAMA, Y. & OKANO, H. 2005. Transplantation of human neural stem cells for spinal cord injury in primates. *J Neurosci Res,* 80**,** 182-90.

IZRAEL, M., ZHANG, P., KAUFMAN, R., SHINDER, V., ELLA, R., AMIT, M., ITSKOVITZ-ELDOR, J., CHEBATH, J. & REVEL, M. 2007. Human oligodendrocytes derived from embryonic stem cells: Effect of noggin on phenotypic differentiation in vitro and on myelination in vivo. *Mol Cell Neurosci,* 34**,** 310-23.

JAROCHA, D., LUKASIEWICZ, E. & MAJKA, M. 2008. Adventage of mesenchymal stem cells (MSC) expansion directly from purified bone marrow CD105+ and CD271+ cells. *Folia Histochem Cytobiol,* 46**,** 307-14.

JI, B., CASE, L. C., LIU, K., SHAO, Z., LEE, X., YANG, Z., WANG, J., TIAN, T., SHULGA-MORSKAYA, S., SCOTT, M., HE, Z., RELTON, J. K. & MI, S. 2008. Assessment of functional recovery and axonal sprouting in oligodendrocyte-myelin glycoprotein (OMgp) null mice after spinal cord injury. *Mol Cell Neurosci,* 39**,** 258-67.

JIAO, J., MILWID, J., YARMUSH, M. & PAREKKADAN, B. 2011. A mesenchymal stem cell potency assay. *Methods in molecular biology,* 677**,** 221-231.

JIN, H., BAE, Y., KIM, M., KWON, S.-J., JEON, H., CHOI, S., KIM, S., YANG, Y., OH, W. & CHANG, J. 2013. Comparative Analysis of Human Mesenchymal Stem Cells from Bone Marrow, Adipose Tissue, and Umbilical Cord Blood as Sources of Cell Therapy. *International Journal of Molecular Sciences,* 14**,** 17986-18001.

KANG, E.-S., HA, K.-Y. & KIM, Y.-H. 2012. Fate of Transplanted Bone Marrow Derived Mesenchymal Stem Cells Following Spinal Cord Injury in Rats by Transplantation Routes. *J Korean Med Sci,* 27**,** 586-593.

KANG, K. N., KIM, D. Y., YOON, S. M., LEE, J. Y., LEE, B. N., KWON, J. S., SEO, H. W., LEE, I. W., SHIN, H. C., KIM, Y. M., KIM, H. S., KIM, J. H., MIN, B. H., LEE, H. B. & KIM, M. S. 2012. Tissue engineered regeneration of completely transected spinal cord using human mesenchymal stem cells. *Biomaterials*.

KARIMI-ABDOLREZAEE, S., EFTEKHARPOUR, E., WANG, J., SCHUT, D. & FEHLINGS, M. G. 2010. Synergistic effects of transplanted adult neural stem/progenitor cells, chondroitinase, and growth factors promote functional repair and plasticity of the chronically injured spinal cord. *J Neurosci,* 30**,** 1657-76.

KASSEM, M. 2004. Mesenchymal stem cells: biological characteristics and potential clinical applications. *Cloning Stem Cells,* 6**,** 369-74.

KATZ, A. J., THOLPADY, A., THOLPADY, S. S., SHANG, H. & OGLE, R. C. 2005. Cell surface and transcriptional characterization of human adipose-derived adherent stromal (hADAS) cells. *Stem Cells,* 23**,** 412-23.

KEIRSTEAD, H. S. & BLAKEMORE, W. 1997. Indentification of Post-mitotic Oligodendrocytes Incapable of Remyelination within the Demyelinated Adult Spinal Cord. *Journal of Neuropathology and Experimental Neurology,* 56**,** 1191-1201.

KEIRSTEAD, H. S., NISTOR, G., BERNAL, G., TOTOIU, M., CLOUTIER, F., SHARP, K. & STEWARD, O. 2005. Human embryonic stem cell-derived oligodendrocyte progenitor cell transplants remyelinate and restore locomotion after spinal cord injury. *J Neurosci,* 25**,** 4694-705.

KERSCHENSTEINER, M., SCHWAB, M. E., LICHTMAN, J. W. & MISGELD, T. 2005. In vivo imaging of axonal degeneration and regeneration in the injured spinal cord. *Nat Med,* 11**,** 572-577.

KIGERL, K. A. & POPOVICH, P. G. 2009. Toll-Like Receptors in Spinal Cord Injury. *Toll-Like Receptors: Roles in Infection and Neuropathology*. Berlin: Springer-Verlag Berlin.

KIM, B. J., SEO, J. H., BUBIEN, J. K. & OH, Y. S. 2002. Differentiation of adult bone marrow stem cells into neuroprogenitor cells in vitro. *Neuroreport,* 13**,** 1185-8.

KINNAIRD, T., STABILE, E., BURNETT, M. S., LEE, C. W., BARR, S., FUCHS, S. & EPSTEIN, S. E. 2004. Marrow-Derived Stromal Cells Express Genes Encoding a Broad Spectrum of Arteriogenic Cytokines and Promote In Vitro and In Vivo Arteriogenesis Through Paracrine Mechanisms. *Circulation Research,* 94**,** 678-685.

KLEIN-NULEND, J., BACABAC, R. G. & MULLENDER, M. G. 2005. Mechanobiology of bone tissue. *Pathologie Biologie,* 53**,** 576-580.

KOHAMA, I., LANKFORD, K. L., PREININGEROVA, J., WHITE, F. A., VOLLMER, T. L. & KOCSIS, J. D. 2001. Transplantation of cryopreserved adult human Schwann cells enhances axonal conduction in demyelinated spinal cord. *J Neurosci,* 21**,** 944-50.

KOLF, C. M., CHO, E. & TUAN, R. S. 2007. Mesenchymal stromal cells. Biology of adult mesenchymal stem cells: regulation of niche, self-renewal and differentiation. *Arthritis Res Ther,* 9**,** 204.

KOTOBUKI, N., HIROSE, M., MACHIDA, H., KATOU, Y., MURAKI, K., TAKAKURA, Y. & OHGUSHI, H. 2005. Viability and osteogenic potential of cryopreserved human bone marrow-derived mesenchymal cells. *Tissue Eng,* 11**,** 663-73.

KRETLOW, J. D., JIN, Y. Q., LIU, W., ZHANG, W. J., HONG, T. H., ZHOU, G., BAGGETT, L. S., MIKOS, A. G. & CAO, Y. 2008. Donor age and cell passage affects differentiation potential of murine bone marrow-derived stem cells. *BMC Cell Biol,* 9**,** 60.

LAKATOS, A., BARNETT, S. C. & FRANKLIN, R. J. 2003. Olfactory ensheathing cells induce less host astrocyte response and chondroitin sulphate proteoglycan expression than Schwann cells following transplantation into adult CNS white matter. *Exp Neurol,* 184**,** 237-46.

LAKATOS, A., FRANKLIN, R. J. M. & BARNETT, S. C. 2000. Olfactory ensheathing cells and Schwann cells differ in their in vitro interactions with astrocytes. *Glia,* 32**,** 214-225.

LAMMERTSE, D. P. 2012. Clinical trials in spinal cord injury: lessons learned on the path to translation. The 2011 International Spinal Cord Society Sir Ludwig Guttmann Lecture. *Spinal Cord,* 51**,** 2-9.

LANG, K. J., RATHJEN, J., VASSILIEVA, S. & RATHJEN, P. D. 2004. Differentiation of embryonic stem cells to a neural fate: a route to re-building the nervous system? *J Neurosci Res,* 76**,** 184-92.

LASIENE, J., SHUPE, L., PERLMUTTER, S. & HORNER, P. 2008. No evidence for chronic demyelination in spared axons after spinal cord injury in a mouse. *J Neurosci,* 28**,** 3887-96.

LAZARUS, H. M., HAYNESWORTH, S. E., GERSON, S. L., ROSENTHAL, N. S. & CAPLAN, A. I. 1995. Ex vivo expansion and subsequent infusion of human bone marrow-derived stromal progenitor cells (mesenchymal progenitor cells): implications for therapeutic use. *Bone Marrow Transplant,* 16**,** 557-64.

LE BLANC, K., RASMUSSON, I., SUNDBERG, B., GÃ¶THERSTRÃ¶M, C., HASSAN, M., UZUNEL, M. & RINGDÃ©N, O. 2004. Treatment of severe acute graft-versus-host disease with third party haploidentical mesenchymal stem cells. *The Lancet,* 363**,** 1439-1441.

LEE, D. C., HSU, Y. C., CHUNG, Y. F., HSIAO, C. Y., CHEN, S. L., CHEN, M. S., LIN, H. K. & CHIU, I. M. 2009. Isolation of neural stem/progenitor cells by using EGF/FGF1 and FGF1B promoter-driven green fluorescence from embryonic and adult mouse brains. *Mol Cell Neurosci,* 41**,** 348-63.

LEE, E. J., LEE, H. N., KANG, H. J., KIM, K. H., HUR, J., CHO, H. J., LEE, J., CHUNG, H. M., CHO, J., CHO, M. Y., OH, S. K., MOON, S. Y., PARK, Y. B. & KIM, H. S. 2010. Novel embryoid body-based method to derive mesenchymal stem cells from human embryonic stem cells. *Tissue Eng Part A,* 16**,** 705-15.

LEE, K. H., SUH-KIM, H., CHOI, J. S., JEUN, S. S., KIM, E. J., KIM, S. S., YOON DO, H. & LEE, B. H. 2007. Human mesenchymal stem cell transplantation promotes functional recovery following acute spinal cord injury in rats. *Acta Neurobiol Exp (Wars),* 67**,** 13-22.

LEE, M. W., KIM, D. S., YOO, K. H., KIM, H. R., JANG, I. K., LEE, J. H., KIM, S. Y., SON, M. H., LEE, S. H., JUNG, H. L., SUNG, K. W. & KOO, H. H. 2013. Human bone marrow-derived mesenchymal stem cell gene expression patterns vary with culture conditions. *Blood Res,* 48**,** 107-14.

LEE, R. H., HSU, S. C., MUNOZ, J., JUNG, J. S., LEE, N. R., POCHAMPALLY, R. & PROCKOP, D. J. 2006. A subset of human rapidly self-renewing marrow stromal cells preferentially engraft in mice. *Blood,* 107**,** 2153-61.

LI, M., SHIBATA, A., LI, C., BRAUN, P. E., MCKERRACHER, L., RODER, J., KATER, S. B. & DAVID, S. 1996. Myelin-associated glycoprotein inhibits neurite/axon growth and causes growth cone collapse. *J Neurosci Res,* 46**,** 404-14.

LI, X. J., DU, Z. W., ZARNOWSKA, E. D., PANKRATZ, M., HANSEN, L. O., PEARCE, R. A. & ZHANG, S. C. 2005. Specification of motoneurons from human embryonic stem cells. *Nat Biotechnol,* 23**,** 215-21.

LI, X. L., ZHANG, W., ZHOU, X., WANG, X. Y., ZHANG, H. T., QIN, D. X., ZHANG, H., LI, Q., LI, M. & WANG, T. H. 2007. Temporal changes in the expression of some neurotrophins in spinal cord transected adult rats. *Neuropeptides,* 41**,** 135-43.

LI, Y. & RAISMAN, G. 1994. Schwann cells induce sprouting in motor and sensory axons in the adult rat spinal cord. *J Neurosci,* 14**,** 4050-63.

LIAN, Q., LYE, E., SUAN YEO, K., KHIA WAY TAN, E., SALTO-TELLEZ, M., LIU, T. M., PALANISAMY, N., EL OAKLEY, R. M., LEE, E. H., LIM, B. & LIM, S. K. 2007. Derivation of clinically compliant MSCs from CD105+, CD24- differentiated human ESCs. *Stem Cells,* 25**,** 425-36.

LIANG, P., MORET, V., WIESENDANGER, M. & ROUILLER, E. M. 1991. Corticomotoneuronal connections in the rat: Evidence from double-labeling of motoneurons and corticospinal axon arborizations. *The Journal of Comparative Neurology,* 311**,** 356-366.

LIN, G., LIU, G., BANIE, L., WANG, G., NING, H., LUE, T. F. & LIN, C. S. 2011. Tissue distribution of mesenchymal stem cell marker Stro-1. *Stem Cells Dev,* 20**,** 1747-52.

LINDSAY, S. L., JOHNSTONE, S. A., MOUNTFORD, J. C., SHEIKH, S., ALLAN, D. B., CLARK, L. & BARNETT, S. C. 2013. Human mesenchymal stem cells isolated from

olfactory biopsies but not bone enhance CNS myelination in vitro. *Glia,* 61**,** 368-382.

LINGOR, P., KOCH, J., TÖNGES, L. & BÄHR, M. 2012. Axonal degeneration as a therapeutic target in the CNS. *Cell and Tissue Research,* 349**,** 289-311.

LIU, C. N. & CHAMBERS, W. W. 1958. Intraspinal sprouting of dorsal root axons; development of new collaterals and preterminals following partial denervation of the spinal cord in the cat. *AMA Arch Neurol Psychiatry,* 79**,** 46-61.

LIU, G., ZHOU, H., LI, Y., LI, G., CUI, L., LIU, W. & CAO, Y. 2008. Evaluation of the viability and osteogenic differentiation of cryopreserved human adipose-derived stem cells. *Cryobiology,* 57**,** 18-24.

LIU, S., QU, Y., STEWART, T. J., HOWARD, M. J., CHAKRABORTTY, S., HOLEKAMP, T. F. & MCDONALD, J. W. 2000. Embryonic stem cells differentiate into oligodendrocytes and myelinate in culture and after spinal cord transplantation. *Proc Natl Acad Sci U S A,* 97**,** 6126-31.

LIU, W. G., WANG, Z. Y. & HUANG, Z. S. 2011. Bone marrow-derived mesenchymal stem cells expressing the bFGF transgene promote axon regeneration and functional recovery after spinal cord injury in rats. *Neurol Res,* 33**,** 686-93.

LIU, X. Z., XU, X. M., HU, R., DU, C., ZHANG, S. X., MCDONALD, J. W., DONG, H. X., WU, Y. J., FAN, G. S., JACQUIN, M. F., HSU, C. Y. & CHOI, D. W. 1997. Neuronal and glial apoptosis after traumatic spinal cord injury. *J Neurosci,* 17**,** 5395-406.

LLADO, J., HAENGGELI, C., MARAGAKIS, N. J., SNYDER, E. Y. & ROTHSTEIN, J. D. 2004. Neural stem cells protect against glutamate-induced excitotoxicity and promote survival of injured motor neurons through the secretion of neurotrophic factors. *Mol Cell Neurosci,* 27**,** 322-31.

LONG, X., OLSZEWSKI, M., HUANG, W. & KLETZEL, M. 2005. Neural cell differentiation in vitro from adult human bone marrow mesenchymal stem cells. *Stem Cells Dev,* 14**,** 65-9.

LOPEZ-VALES, R., FORES, J., NAVARRO, X. & VERDU, E. 2006. Olfactory ensheathing glia graft in combination with FK506 administration promote repair after spinal cord injury. *Neurobiol Dis,* 24**,** 443-54.

LU, J., ASHWELL, K. W. & WAITE, P. 2000. Advances in secondary spinal cord injury: role of apoptosis. *Spine (Phila Pa 1976),* 25**,** 1859-66.

LU, L. L., LIU, Y. J., YANG, S. G., ZHAO, Q. J., WANG, X., GONG, W., HAN, Z. B., XU, Z. S., LU, Y. X., LIU, D., CHEN, Z. Z. & HAN, Z. C. 2006. Isolation and characterization of human umbilical cord mesenchymal stem cells with hematopoiesis-supportive function and other potentials. *Haematologica,* 91**,** 1017-26.

LU, P., JONES, L., SNYDER, E. Y. & TUSZYNSKI, M. H. 2003. Neural stem cells constitutively secrete neurotrophic factors and promote extensive host axonal growth after spinal cord injury. *Experimental Neurology,* 181**,** 115-129.

LU, P., JONES, L. L., SNYDER, E. Y. & TUSZYNSKI, M. H. 2003. Neural stem cells constitutively secrete neurotrophic factors and promote extensive host axonal growth after spinal cord injury. *Exp Neurol,* 181**,** 115-29.

LU, P., JONES, L. L. & TUSZYNSKI, M. H. 2005. BDNF-expressing marrow stromal cells support extensive axonal growth at sites of spinal cord injury. *Experimental Neurology,* 191**,** 344-360.

LU, P., JONES, L. L. & TUSZYNSKI, M. H. 2007. Axon regeneration through scars and into sites of chronic spinal cord injury. *Experimental Neurology,* 203**,** 8-21.

LU, P., WANG, Y., GRAHAM, L., MCHALE, K., GAO, M., WU, D., BROCK, J., BLESCH, A., ROSENZWEIG, EPHRONÂ S., HAVTON, LEIFÂ A., ZHENG, B., CONNER, JAMESÂ M., MARSALA, M. & TUSZYNSKI, MARKÂ H. 2012. Long-Distance Growth

and Connectivity of Neural Stem Cells after Severe Spinal Cord Injury. *Cell,* 150**,** 1264-1273.

LUO, J., ZHANG, H.-T., JIANG, X.-D., XUE, S. & KE, Y.-Q. 2009. Combination of bone marrow stromal cell transplantation with mobilization by granulocyte-colony stimulating factor promotes functional recovery after spinal cord transection. *Acta Neurochirurgica,* 151**,** 1483-1492.

MAJUMDAR, M. K., THIEDE, M. A., MOSCA, J. D., MOORMAN, M. & GERSON, S. L. 1998. Phenotypic and functional comparison of cultures of marrow-derived mesenchymal stem cells (MSCs) and stromal cells. *J Cell Physiol,* 176**,** 57-66.

MAMIDI, M. K., NATHAN, K. G., SINGH, G., THRICHELVAM, S. T., MOHD YUSOF, N. A. N., FAKHARUZI, N. A., ZAKARIA, Z., BHONDE, R., DAS, A. K. & MAJUMDAR, A. S. 2012. Comparative cellular and molecular analyses of pooled bone marrow multipotent mesenchymal stromal cells during continuous passaging and after successive cryopreservation. *Journal of Cellular Biochemistry,* 113**,** 3153-3164.

MARTINEZ, M., BREZUN, JM., BONNIER, L., XERI, C. A new rating scale for open field evaluation of behavioural recovery after cervical spinal cord injury in rats. *J Neurotrauma* 26:1043-1053

MCKEON, R. J., SCHREIBER, R. C., RUDGE, J. S. & SILVER, J. 1991. Reduction of neurite outgrowth in a model of glial scarring following CNS injury is correlated with the expression of inhibitory molecules on reactive astrocytes. *J Neurosci,* 11**,** 3398-411.

MCNEILL, D. L., CHUNG, K., CARLTON, S. M. & COGGESHALL, R. E. 1988. Calcitonin gene-related peptide immunostained axons provide evidence for fine primary afferent fibers in the dorsal and dorsolateral funiculi of the rat spinal cord. *J Comp Neurol,* 272**,** 303-8.

MELETIS, K., BARNABE-HEIDER, F., CARLEN, M., EVERGREN, E., TOMILIN, N., SHUPLIAKOV, O. & FRISEN, J. 2008. Spinal Cord Injury Reveals Multilineage Differentiation of Ependymal Cells. *PLOS Biology,* 6**,** 1494-1507.

MENICANIN, D., BARTOLD, P. M., ZANNETTINO, A. C. & GRONTHOS, S. 2010. Identification of a common gene expression signature associated with immature clonal mesenchymal cell populations derived from bone marrow and dental tissues. *Stem Cells Dev,* 19**,** 1501-10.

MILLER, M. W. 1987. The origin of corticospinal projection neurons in rat. *Exp Brain Res,* 67**,** 339-51.

MINAIRE, P., EDOUARD, C., ARLOT, M. & MEUNIER, P. J. 1984. Marrow changes in paraplegic patients. *Calcified Tissue International,* 36**,** 338-340.

MIURA, K., OKADA, Y., AOI, T., OKADA, A., TAKAHASHI, K., OKITA, K., NAKAGAWA, M., KOYANAGI, M., TANABE, K., OHNUKI, M., OGAWA, D., IKEDA, E., OKANO, H. & YAMANAKA, S. 2009. Variation in the safety of induced pluripotent stem cell lines. *Nat Biotechnol,* 27**,** 743-5.

MOLANDER, C., Xu, Q., Grant, G. 1984. The cytoarchitecture organization of the spinal cord in the rat: I. The lower thoracic and lumbosacral cord. *The Journal of Comparative Neurology*, 230, 133-141.

MOLANDER, C., Xu, Q., Rivero-Melian, C., Grant, G. 1989. Cytoarchitectonic organization of the spinal cord in the rat: II. The cervical and upper thoracic. *The Journal of Comparative Neurology*, 3, 375-385

MOON, L. D., ASHER, R. A., RHODES, K. E. & FAWCETT, J. W. 2001. Regeneration of CNS axons back to their target following treatment of adult rat brain with chondroitinase ABC. *Nat Neurosci,* 4**,** 465-6.

MORI, F., HIMES, B. T., KOWADA, M., MURRAY, M. & TESSLER, A. 1997. Fetal spinal cord transplants rescue some axotomized rubrospinal neurons from retrograde cell death in adult rats. *Exp Neurol,* 143**,** 45-60.

MORSHEAD, C. M., CRAIG, C. G. & VAN DER KOOY, D. 1998. In vivo clonal analyses reveal the properties of endogenous neural stem cell proliferation in the adult mammalian forebrain. *Development,* 125**,** 2251-61.

MOSNA, F., SENSEBE, L. & KRAMPERA, M. 2010. Human bone marrow and adipose tissue mesenchymal stem cells: a user's guide. *Stem Cells Dev,* 19**,** 1449-70.

MOUNTFORD, J. C. 2008. Human embryonic stem cells: origins, characteristics and potential for regenerative therapy. *Transfus Med,* 18**,** 1-12.

MUELLER, S. M. & GLOWACKI, J. 2001. Age-related decline in the osteogenic potential of human bone marrow cells cultured in three-dimensional collagen sponges. *J Cell Biochem,* 82**,** 583-90.

MUKHOPADHYAY, G., DOHERTY, P., WALSH, F. S., CROCKER, P. R. & FILBIN, M. T. 1994. A novel role for myelin-associated glycoprotein as an inhibitor of axonal regeneration. *Neuron,* 13**,** 757-67.

MURAGLIA, A., CANCEDDA, R. & QUARTO, R. 2000. Clonal mesenchymal progenitors from human bone marrow differentiate in vitro according to a hierarchical model. *J Cell Sci,* 113 (Pt 7)**,** 1161-6.

MUSINA, R. A., BEKCHANOVA, E. S. & SUKHIKH, G. T. 2005. Comparison of mesenchymal stem cells obtained from different human tissues. *Bull Exp Biol Med,* 139**,** 504-9.

NAKAJIMA, H., UCHIDA, K., GUERRERO, A. R., WATANABE, S., SUGITA, D., TAKEURA, N., YOSHIDA, A., LONG, G., WRIGHT, K. T., JOHNSON, W. E. B. & BABA, H. 2012. Transplantation of mesenchymal stem cells promotes an alternative pathway of macrophage activation and functional recovery after spinal cord injury. *Journal of neurotrauma,* 29**,** 1641-1625.

NANDOE TEWARIE, R., HURTADO, A., BARTELS, R., GROTENHUIS, A. & OUDEGA, M. 2009. Stem Cell-Based Therapies for spinal cord injury. *J Spinal Cord Med,* 32**,** 105-114.

NASHMI, R. & FEHLINGS, M. G. 2001. Mechanisms of axonal dysfunction after spinal cord injury: with an emphasis on the role of voltage-gated potassium channels. *Brain Research Reviews,* 38**,** 165-191.

National Institute of Health, 2013. Available from: http://clinicaltrials.gov (5 November 2013)

National Spinal Cord Injury Statistical Centre, 2012. Available from: Spinal cord injury: facts and figures at a glance, https: //www.nscisc.uab.edu (20 February 2013).

NEUBAUER, M., FISCHBACH, C., BAUER-KREISEL, P., LIEB, E., HACKER, M., TESSMAR, J., SCHULZ, M. B., GOEPFERICH, A. & BLUNK, T. 2004. Basic fibroblast growth factor enhances PPARgamma ligand-induced adipogenesis of mesenchymal stem cells. *FEBS Lett,* 577**,** 277-83.

NEUHUBER, B., TIMOTHY HIMES, B., SHUMSKY, J. S., GALLO, G. & FISCHER, I. 2005. Axon growth and recovery of function supported by human bone marrow stromal cells in the injured spinal cord exhibit donor variations. *Brain Research,* 1035**,** 73-85.

NIEHAGE, C., STEENBLOCK, C., PURSCHE, T., BORNHAUSER, M., CORBEIL, D. & HOFLACK, B. 2011. The cell surface proteome of human mesenchymal stromal cells. *PLoS One,* 6**,** e20399.

NIETO-SAMPEDRO, M., LEWIS, E. R., COTMAN, C. W., MANTHORPE, M., SKAPER, S. D., BARBIN, G., LONGO, F. M. & VARON, S. 1982. Brain injury causes a time-dependent increase in neuronotrophic activity at the lesion site. *Science,* 217**,** 860-1.

NISTOR, G. I., TOTOIU, M. O., HAQUE, N., CARPENTER, M. K. & KEIRSTEAD, H. S. 2005. Human embryonic stem cells differentiate into oligodendrocytes in high purity and myelinate after spinal cord transplantation. *Glia,* 49**,** 385-96.

NOEL, D., DJOUAD, F., BOUFFI, C., MRUGALA, D. & JORGENSEN, C. 2007. Multipotent mesenchymal stromal cells and immune tolerance. *Leuk Lymphoma,* 48**,** 1283-9.

NUNES, M. C., ROY, N. S., KEYOUNG, H. M., GOODMAN, R. R., MCKHANN, G., 2ND, JIANG, L., KANG, J., NEDERGAARD, M. & GOLDMAN, S. A. 2003.

Identification and isolation of multipotential neural progenitor cells from the subcortical white matter of the adult human brain. *Nat Med,* 9**,** 439-47.

NYGREN, L.-G. R., FUXE, K., JONSSON, G. S. & OLSON, L. 1974. Functional regeneration of 5-hydroxytryptamine nerve terminals in the rat spinal cord following 5,6-dihydroxytryptamine induced degeneration. *Brain Research,* 78**,** 377-394.

OGAWA, Y., SAWAMOTO, K., MIYATA, T., MIYAO, S., WATANABE, M., NAKAMURA, M., BREGMAN, B. S., KOIKE, M., UCHIYAMA, Y., TOYAMA, Y. & OKANO, H. 2002. Transplantation of in vitro-expanded fetal neural progenitor cells results in neurogenesis and functional recovery after spinal cord contusion injury in adult rats. *J Neurosci Res,* 69**,** 925-33.

OHTA, M., SUZUKI, Y., NODA, T., EJIRI, Y., DEZAWA, M., KATAOKA, K., CHOU, H., ISHIKAWA, N., MATSUMOTO, N., IWASHITA, Y., MIZUTA, E., KUNO, S. & IDE, C. 2004. Bone marrow stromal cells infused into the cerebrospinal fluid promote functional recovery of the injured rat spinal cord with reduced cavity formation. *Exp Neurol,* 187**,** 266-78.

O'LEARY, D. D. & TERASHIMA, T. 1988. Cortical axons branch to multiple subcortical targets by interstitial axon budding: implications for target recognition and "waiting periods". *Neuron,* 1**,** 901-10.

OLIVERI, R. S., BELLO, S. & BIERING-SØRENSEN, F. 2013. Mesenchymal stem cells improve locomotor recovery in traumatic spinal cord injury: Systematic review with meta-analyses of rat models. *Neurobiology of Disease*.

OLIVIER, E., RYBICKI, A. & BOUHASSIRA, E. 2006. Differentiation of human embryonic stem cells into bipotent mesenchymal stem cells. *Stem Cells,* 24**,** 1914-1922.

OLIVIER, E. N. & BOUHASSIRA, E. E. 2011. Differentiation of human embryonic stem cells into mesenchymal stem cells by the "raclure" method. *Methods Mol Biol,* 690**,** 183-93.

OSAKA, M., HONMOU, O., MURAKAMI, T., NONAKA, T., HOUKIN, K., HAMADA, H. & KOCSIS, J. D. 2010. Intravenous administration of mesenchymal stem cells derived from bone marrow after contusive spinal cord injury improves functional outcome. *Brain Research,* In Press, Corrected Proof.

PAL, R., GOPINATH, C., RAO, N. M., BANERJEE, P., KRISHNAMOORTHY, V., VENKATARAMANA, N. K. & TOTEY, S. 2010. Functional recovery after transplantation of bone marrow-derived human mesenchymal stromal cells in a rat model of spinal cord injury. *Cytotherapy,* 12**,** 792-806.

PAN, G. & THOMSON, J. A. 2007. Nanog and transcriptional networks in embryonic stem cell pluripotency. *Cell Res,* 17**,** 42-9.

PARK, H. C., SHIM, Y. S., HA, Y., YOON, S. H., PARK, S. R., CHOI, B. H. & PARK, H. S. 2005. Treatment of complete spinal cord injury patients by autologous bone marrow cell transplantation and administration of granulocyte-macrophage colony stimulating factor. *Tissue Eng,* 11**,** 913-22.

PARK, H. W., LIM, M. J., JUNG, H., LEE, S. P., PAIK, K. S. & CHANG, M. S. 2010. Human mesenchymal stem cell-derived Schwann cell-like cells exhibit neurotrophic effects, via distinct growth factor production, in a model of spinal cord injury. *Glia,* 58**,** 1118-32.

PARK, W., KIM, S., LEE, S., KIM, H.-W., PARK, J.-S. & HYUN, J. 2010. The effect of mesenchymal stem cell transplantation on the recovery of bladder and hindlimb function after spinal cord contusion in rats. *BMC Neuroscience,* 11**,** 119.

PATTERSON, J. T., COGGESHALL, R. E., LEE, W. T. & CHUNG, K. 1990. Long ascending unmyelinated primary afferent axons in the rat dorsal column: immunohistochemical localizations. *Neurosci Lett,* 108**,** 6-10.

PEDRAM, M. S., DEHGHAN, M. M., SOLEIMANI, M., SHARIFI, D., MARJANMEHR, S. H. & NASIRI, Z. 2010. Transplantation of a combination of autologous neural differentiated and undifferentiated mesenchymal stem cells into injured spinal cord of rats. *Spinal Cord,* 48**,** 457-63.

PEVSNER-FISCHER, M., LEVIN, S. & ZIPORI, D. 2011. The origins of mesenchymal stromal cell heterogeneity. *Stem Cell Rev,* 7**,** 560-8.

PHINNEY, D. G. & ISAKOVA, I. 2005. Plasticity and therapeutic potential of mesenchymal stem cells in the nervous system. *Curr Pharm Des,* 11**,** 1255-65.

PHINNEY, D. G. & PROCKOP, D. J. 2007. Concise review: mesenchymal stem/multipotent stromal cells: the state of transdifferentiation and modes of tissue repair--current views. *Stem Cells,* 25**,** 2896-902.

PIERUCCI, A., DUEK, E. A. & DE OLIVEIRA, A. L. 2009. Expression of basal lamina components by Schwann cells cultured on poly(lactic acid) (PLLA) and poly(caprolactone) (PCL) membranes. *J Mater Sci Mater Med,* 20**,** 489-95.

PITTENGER, M., MACKAY, A., BECK, S., JAISWAL, R., DOUGLAS, R., MOSCA, J., MOORMAN, M., SIMONETTI, D., CRAIG, S. & MARSHAK, D. 1999. Multilineage potential of adult human mesenchymal stem cells. *Science,* 284**,** 143 - 147.

PITTENGER, M. F. 2008. Mesenchymal stem cells from adult bone marrow. *Methods Mol Biol,* 449**,** 27-44.

PONTE, A. L., MARAIS, E., GALLAY, N., LANGONNE, A., DELORME, B., HERAULT, O., CHARBORD, P. & DOMENECH, J. 2007. The in vitro migration capacity of human bone marrow mesenchymal stem cells: comparison of chemokine and growth factor chemotactic activities. *Stem Cells,* 25**,** 1737-45.

PRICOLA, K. L., KUHN, N. Z., HALEEM-SMITH, H., SONG, Y. & TUAN, R. S. 2009. Interleukin-6 maintains bone marrow-derived mesenchymal stem cell stemness by an ERK1/2-dependent mechanism. *J Cell Biochem,* 108**,** 577-88.

PRINDULL, G. & ZIPORI, D. 2004. Environmental guidance of normal and tumor cell plasticity: epithelial mesenchymal transitions as a paradigm. *Blood,* 103**,** 2892-2899.

QUERTAINMONT, R., CANTINIEAUX, D., BOTMAN, O., SID, S., SCHOENEN, J. & FRANZEN, R. 2012. Mesenchymal Stem Cell Graft Improves Recovery after Spinal

Cord Injury in Adult Rats through Neurotrophic and Pro-Angiogenic Actions. *PLoS One,* 7**,** e39500.

RADOJICIC, M., REIER, P. J., STEWARD, O. & KEIRSTEAD, H. S. 2005. Septations in chronic spinal cord injury cavities contain axons. *Exp Neurol,* 196**,** 339-41.

RAISMAN, G. & LI, Y. 2007. Repair of neural pathways by olfactory ensheathing cells. *Nat Rev Neurosci,* 8**,** 312-319.

RAMÓN-CUETO, A. & AVILA, J. 1998. Olfactory ensheathing glia: properties and function. *Brain Research Bulletin,* 46**,** 175-187.

REUBINOFF, B. E., ITSYKSON, P., TURETSKY, T., PERA, M. F., REINHARTZ, E., ITZIK, A. & BEN-HUR, T. 2001. Neural progenitors from human embryonic stem cells. *Nat Biotechnol,* 19**,** 1134-40.

REYNOLDS, B. A. & WEISS, S. 1992. Generation of neurons and astrocytes from isolated cells of the adult mammalian central nervous system. *Science,* 255**,** 1707-10.

RICHARDSON, P. M., MCGUINNESS, U. M. & AGUAYO, A. J. 1980. Axons from CNS neurons regenerate into PNS grafts. *Nature,* 284**,** 264-5.

RICHTER, M. W. & ROSKAMS, A. J. 2008. Olfactory ensheathing cell transplantation following spinal cord injury: Hype or hope? *Experimental Neurology,* 209**,** 353-367.

RINGDEN, O., UZUNEL, M., RASMUSSON, I., REMBERGER, M., SUNDBERG, B., LONNIES, H., MARSCHALL, H.-U., DLUGOSZ, A., SZAKOS, A., HASSAN, Z., OMAZIC, B., ASCHAN, J., BARKHOLT, L. & LE BLANC, K. 2006. Mesenchymal stem cells for treatment of Therapy-resistant graft -versus -host disease. *Transplantation,* 81**,** 1390-1397.

RINGE, J., KAPS, C., BURMESTER, G.-R. & SITTINGER, M. 2002. Stem cells for regenerative medicine: advances in the engineering of tissues and organs. *Naturwissenschaften,* 89**,** 338-351.

ROLLS, A. & SCHWARTZ, M. 2006. Chondroitin sulfate proteoglycan and its degradation products in CNS repair. *Adv Pharmacol,* 53**,** 357-74.

ROSENBERG, L. J. & WRATHALL, J. R. 1997. Quantitative analysis of acute axonal pathology in experimental spinal cord contusion. *J Neurotrauma,* 14**,** 823-38.

ROSSI, S. L. & KEIRSTEAD, H. S. 2009. Stem cells and spinal cord regeneration. *Curr Opin Biotechnol,* 20**,** 552-62.

ROUILLER, E. M., LIANG, F., MORET, V. R. & WIESENDANGER, M. 1991. Trajectory of redirected corticospinal axons after unilateral lesion of the sensorimotor cortex in neonatal rat; A phaseolus vulgaris-leucoagglutinin (PHA-L) tracing study. *Experimental Neurology,* 114**,** 53-65.

ROWLAND, J. W., HAWRYLUK, G. W. J., KWON, B. & FEHLINGS, M. G. 2008. Current status of acute spinal cord injury pathophysiology and emerging therapies: promise on the horizon. *Neurosurgical Focus,* 25**,** E2.

RUFF, C. A., WILCOX, J. T. & FEHLINGS, M. G. 2012. Cell-based transplantation strategies to promote plasticity following spinal cord injury. *Experimental Neurology*.

SAHNI, V. & KESSLER, J. A. 2010. Stem cell therapies for spinal cord injury. *nat Rev Neurology,* 6**,** 363-372.

SALGADO-CEBALLOS, H., GUIZAR-SAHAGUN, G., FERIA-VELASCO, A., GRIJALVA, I., ESPITIA, L., IBARRA, A. & MADRAZO, I. 1998. Spontaneous long-term remyelination after traumatic spinal cord injury in rats. *Brain Res,* 782**,** 126-35.

SANCHEZ-RAMOS, J., SONG, S., CARDOZO-PELAEZ, F., HAZZI, C., STEDEFORD, T., WILLING, A., FREEMAN, T. B., SAPORTA, S., JANSSEN, W., PATEL, N., COOPER, D. R. & SANBERG, P. R. 2000. Adult Bone Marrow Stromal Cells Differentiate into Neural Cells in Vitro. *Experimental Neurology,* 164**,** 247-256.

SASAKI, M., RADTKE, C., TAN, A. M., ZHAO, P., HAMADA, H., HOUKIN, K., HONMOU, O. & KOCSIS, J. D. 2009. BDNF-Hypersecreting Human Mesenchymal

Stem Cells Promote Functional Recovery, Axonal Sprouting, and Protection of Corticospinal Neurons after Spinal Cord Injury. *Journal of Neuroscience,* 29**,** 14932-14941.

SCHAFER, M., FRUTTIGER, M., MONTAG, D., SCHACHNER, M. & MARTINI, R. 1996. Disruption of the gene for the myelin-associated glycoprotein improves axonal regrowth along myelin in C57BL/Wlds mice. *Neuron,* 16**,** 1107-13.

SCHMITTGEN, T. D. & LIVAK, K. J. 2008. Analyzing real-time PCR data by the comparative C(T) method. *Nat Protoc,* 3**,** 1101-8.

SCHNELL, L. & SCHWAB, M. E. 1990. Axonal regeneration in the rat spinal cord produced by an antibody against myelin-associated neurite growth inhibitors. *Nature,* 343**,** 269-72.

SCHWAB, J. M. & HE, Z. 2007. Mechanisms of Axon Regeneration

Intracellular Mechanisms for Neuritogenesis. *In:* CURTIS, I. (ed.). Springer US.

SEKIYA, I., LARSON, B. L., VUORISTO, J. T., CUI, J. G. & PROCKOP, D. J. 2004. Adipogenic differentiation of human adult stem cells from bone marrow stroma (MSCs). *J Bone Miner Res,* 19**,** 256-64.

SEO, J. H., JANG, I. K., KIM, H., YANG, M. S., LEE, J. E., KIM, H. E., EOM, Y.-W., LEE, D.-H., YU, J. H., KIM, J. Y., KIM, H. O. & CHO, S.-R. 2011. Early Immunomodulation by Intravenously Transplanted Mesenchymal Stem Cells Promotes Functional Recovery in Spinal Cord Injured Rats. *Cell Medicine,* 2**,** 55-67.

SHETH, R., MANZANO, G., LI, X. & LEVI, A. D. 2008. Transplantation of human bone marrow-derived stromal cells into the contused spinal cord of nude rats. *J Neurosurg Spine,* 8**,** 153-162.

SHIELDS, S. A., BLAKEMORE, W. F. & FRANKLIN, R. J. M. 2000. Schwann cell remyelination is restricted to astrocyte-deficient areas after transplantation into demyelinated adult rat brain. *Journal of Neuroscience Research,* 60**,** 571-578.

SIEGENTHALER, M., TU, M. & KEIRSTEAD, H. 2007. The extent of myelin pathology differs following contusion and transection spinal cord injury. *Journal of Neurotrauma,* 24**,** 1631-1646.

SILVA, W. A., JR., COVAS, D. T., PANEPUCCI, R. A., PROTO-SIQUEIRA, R., SIUFI, J. L., ZANETTE, D. L., SANTOS, A. R. & ZAGO, M. A. 2003. The profile of gene expression of human marrow mesenchymal stem cells. *Stem Cells,* 21**,** 661-9.

SILVER, J. & MILLER, J. H. 2004. Regeneration beyond the glial scar. *Nat Rev Neurosci,* 5**,** 146-56.

SIMMONS, P. & TOROK-STORB, B. 1991. Identification of stromal cell precursors in human bone marrow by a novel monoclonal antibody, STRO-1. *Blood,* 78**,** 55-62.

SMITH, J. R., POCHAMPALLY, R., PERRY, A., HSU, S. C. & PROCKOP, D. J. 2004. Isolation of a highly clonogenic and multipotential subfraction of adult stem cells from bone marrow stroma. *Stem Cells,* 22**,** 823-31.

SMITH, K. J. & BENNETT, B. J. 1987. Topographic and quantitative description of rat dorsal column fibres arising from the lumbar dorsal roots. *J Anat,* 153**,** 203-15.

SMITH, P. M. & JEFFERY, N. D. 2006. Histological and ultrastructural analysis of white matter damage after naturally-occurring spinal cord injury. *Brain Pathol,* 16**,** 99-109.

STENDERUP, K., JUSTESEN, J., CLAUSEN, C. & KASSEM, M. 2003. Aging is associated with decreased maximal life span and accelerated senescence of bone marrow stromal cells. *Bone,* 33**,** 919-26.

STICHEL, C. C. & MULLER, H. W. 1998. The CNS lesion scar: new vistas on an old regeneration barrier. *Cell Tissue Res,* 294**,** 1-9.

STICHEL, C. C. & MULLER, H. W. 1998. Experimental strategies to promote axonal regeneration after traumatic central nervous system injury. *Prog Neurobiol,* 56**,** 119-48.

STRIOGA, M., VISWANATHAN, S., DARINSKAS, A., SLABY, O. & MICHALEK, J. 2012. Same or not the same? Comparison of adipose tissue-derived versus bone marrow-derived mesenchymal stem and stromal cells. *Stem Cells Dev,* 21**,** 2724-52.

SYKOVA, E., HOMOLA, A., MAZANEC, R., LACHMANN, H., KONRADOVA, S. L., KOBYLKA, P., PADR, R., NEUWIRTH, J., KOMRSKA, V., VAVRA, V., STULIK, J. & BOJAR, M. 2006. Autologous bone marrow transplantation in patients with subacute and chronic spinal cord injury. *Cell Transplant,* 15**,** 675-87.

TABBARA, I., ZIMMERMAN, K., MORGAN, C. & NAHLEH, Z. 2002. Allogeneic hematopoietic stem cell transplantation. *Arch Intern Med,* 162**,** 1558-1566.

TAKAHASHI, K., TANABE, K., OHNUKI, M., NARITA, M., ICHISAKA, T., TOMODA, K. & YAMANAKA, S. 2007. Induction of Pluripotent Stem Cells from Adult Human Fibroblasts by Defined Factors. *Cell,* 131**,** 861-872.

TAKAHASHI, K. & YAMANAKA, S. 2006. Induction of pluripotent stem cells from mouse embryonic and adult fibroblast cultures by defined factors. *Cell,* 126**,** 663-76.

TAKASHIMA, Y., ERA, T., NAKAO, K., KONDO, S., KASUGA, M., SMITH, A. G. & NISHIKAWA, S. 2007. Neuroepithelial cells supply an initial transient wave of MSC differentiation. *Cell,* 129**,** 1377-88.

TAKEOKA, A., JINDRICH, D. L., MUNOZ-QUILES, C., ZHONG, H., VAN DEN BRAND, R., PHAM, D. L., ZIEGLER, M. D., RAMON-CUETO, A., ROY, R. R., EDGERTON, V. R. & PHELPS, P. E. 2011. Axon regeneration can facilitate or suppress hindlimb function after olfactory ensheathing glia transplantation. *J Neurosci,* 31**,** 4298-310.

TAMATANI, M., SENBA, E. & TOHYAMA, M. 1989. Calcitonin gene-related peptide- and substance P-containing primary afferent fibers in the dorsal column of the rat. *Brain Res,* 495**,** 122-30.

TANG, B. L. & LOW, C. B. 2007. Genetic manipulation of neural stem cells for transplantation into the injured spinal cord. *Cell Mol Neurobiol,* 27**,** 75-85.

TANG, S., WOODHALL, R. W., SHEN, Y. J., DEBELLARD, M. E., SAFFELL, J. L., DOHERTY, P., WALSH, F. S. & FILBIN, M. T. 1997. Soluble myelin-associated glycoprotein (MAG) found in vivo inhibits axonal regeneration. *Mol Cell Neurosci,* 9**,** 333-46.

TARASENKO, Y. I., GAO, J., NIE, L., JOHNSON, K. M., GRADY, J. J., HULSEBOSCH, C. E., MCADOO, D. J. & WU, P. 2007. Human fetal neural stem cells grafted into contusion-injured rat spinal cords improve behavior. *J Neurosci Res,* 85**,** 47-57.

TASSO, R. & PENNESI, G. 2009. When stem cells meet immunoregulation. *International Immunopharmacology,* 9**,** 596-598.

TERADA, N., HAMAZAKI, T., OKA, M., HOKI, M., MASTALERZ, D. M., NAKANO, Y., MEYER, E. M., MOREL, L., PETERSEN, B. E. & SCOTT, E. W. 2002. Bone marrow cells adopt the phenotype of other cells by spontaneous cell fusion. *Nature,* 416**,** 542-5.

TERASHIMA, T. 1995. Anatomy, development and lesion-induced plasticity of rodent corticospinal tract. *Neuroscience Research,* 22**,** 139-161.

TETZLAFF, W., OKON, E. B., KARIMI-ABDOLREZAEE, S., HILL, C. E., SPARLING, J. S., PLEMEL, J. R., PLUNET, W. T., TSAI, E. C., BAPTISTE, D., SMITHSON, L. J., KAWAJA, M. D., FEHLINGS, M. G. & KWON, B. K. 2011. A systematic review of cellular transplantation therapies for spinal cord injury. *J Neurotrauma,* 28**,** 1611-82.

THALLMAIR, M., METZ, G. A., Z'GRAGGEN, W. J., RAINETEAU, O., KARTJE, G. L. & SCHWAB, M. E. 1998. Neurite growth inhibitors restrict plasticity and

functional recovery following corticospinal tract lesions. *Nat Neurosci,* 1**,** 124-31.

THOMSON, J. A., ITSKOVITZ-ELDOR, J., SHAPIRO, S. S., WAKNITZ, M. A., SWIERGIEL, J. J., MARSHALL, V. S. & JONES, J. M. 1998. Embryonic stem cell lines derived from human blastocysts. *Science,* 282**,** 1145-7.

THURET, S., MOON, L. D. F. & GAGE, F. H. 2006. Therapeutic interventions after spinal cord injury. *Nat Rev Neurosci,* 7**,** 628-643.

TOBIAS, C. A., SHUMSKY, J. S., SHIBATA, M., TUSZYNSKI, M. H., FISCHER, I., TESSLER, A. & MURRAY, M. 2003. Delayed grafting of BDNF and NT-3 producing fibroblasts into the injured spinal cord stimulates sprouting, partially rescues axotomized red nucleus neurons from loss and atrophy, and provides limited regeneration. *Exp Neurol,* 184**,** 97-113.

TOFT, A., SCOTT, D. T., BARNETT, S. C. & RIDDELL, J. S. 2007. Electrophysiological evidence that olfactory cell transplants improve function after spinal cord injury. *Brain,* 130**,** 970-84.

TOFT, A., TOME, M., BARNETT, S. C. & RIDDELL, J. S. 2013. A comparative study of glial and non-neural cell properties for transplant-mediated repair of the injured spinal cord. *Glia,* 61**,** 513-528.

TOKUMINE, J., KAKINOHANA, O., CIZKOVA, D., SMITH, D. W. & MARSALA, M. 2003. Changes in spinal GDNF, BDNF, and NT-3 expression after transient spinal cord ischemia in the rat. *J Neurosci Res,* 74**,** 552-61.

TOTOIU, M. O. & KEIRSTEAD, H. S. 2005. Spinal cord injury is accompanied by chronic progressive demyelination. *The Journal of Comparative Neurology,* 486**,** 373-383.

TOTOIU, M. O., NISTOR, G. I., LANE, T. E. & KEIRSTEAD, H. S. 2004. Remyelination, axonal sparing, and locomotor recovery following transplantation of glial-committed progenitor cells into the MHV model of multiple sclerosis. *Exp Neurol,* 187**,** 254-65.

TRIVEDI, P. & HEMATTI, P. 2008. Derivation and immunological characterization of mesenchymal stromal cells from human embryonic stem cells. *Exp Hematol,* 36**,** 350-9.

TSAI, M. S., HWANG, S. M., CHEN, K. D., LEE, Y. S., HSU, L. W., CHANG, Y. J., WANG, C. N., PENG, H. H., CHANG, Y. L., CHAO, A. S., CHANG, S. D., LEE, K. D., WANG, T. H., WANG, H. S. & SOONG, Y. K. 2007. Functional network analysis of the transcriptomes of mesenchymal stem cells derived from amniotic fluid, amniotic membrane, cord blood, and bone marrow. *Stem Cells,* 25**,** 2511-23.

TUREYEN, K., VEMUGANTI, R., BOWEN, K. K., SAILOR, K. A. & DEMPSEY, R. J. 2005. EGF and FGF-2 infusion increases post-ischemic neural progenitor cell proliferation in the adult rat brain. *Neurosurgery,* 57**,** 1254-63; discussion 1254-63.

TUSZYNSKI, M. H., PETERSON, D. A., RAY, J., BAIRD, A., NAKAHARA, Y. & GAGE, F. H. 1994. Fibroblasts genetically modified to produce nerve growth factor induce robust neuritic ingrowth after grafting to the spinal cord. *Exp Neurol,* 126**,** 1-14.

TUSZYNSKI, MARK H. & STEWARD, O. 2012. Concepts and Methods for the Study of Axonal Regeneration in the CNS. *Neuron,* 74**,** 777-791.

TUSZYNSKI, M. H., WEIDNER, N., MCCORMACK, M., MILLER, I., POWELL, H. & CONNER, J. 1998. Grafts of genetically modified Schwann cells to the spinal cord: survival, axon growth, and myelination. *Cell Transplant,* 7**,** 187-96.

TYNDALL, A., WALKER, U., COPE, A., DAZZI, F., DE BARI, C., FIBBE, W., GUIDUCCI, S., JONES, S., JORGENSEN, C., LE BLANC, K., LUYTEN, F., MCGONAGLE, D., MARTIN, I., BOCELLI-TYNDALL, C., PENNESI, G., PISTOIA, V., PITZALIS, C., UCCELLI, A., WULFFRAAT, N. & FELDMANN, M. 2007. Immunomodulatory properties of mesenchymal stem cells: a review based on an interdisciplinary meeting held at the Kennedy Institute of Rheumatology Division, London, UK, 31 October 2005. *Arthritis Research & Therapy,* 9**,** 301.

UCCELLI, A., MORETTA, L. & PISTOIA, V. 2008. Mesenchymal stem cells in health and disease. *Nat Rev Immunol,* 8**,** 726-736.

UCHIDA, K., BABA, H., MAEZAWA, Y., FURUKAWA, S., OMIYA, M., KOKUBO, Y., KUBOTA, C. & NAKAJIMA, H. 2003. Increased expression of neurotrophins and their receptors in the mechanically compressed spinal cord of the spinal hyperostotic mouse (twy/twy). *Acta Neuropathol,* 106**,** 29-36.

VARGAS, M. E. & BARRES, B. A. 2007. Why is Wallerian degeneration in the CNS so slow? *Annu Rev Neurosci,* 30**,** 153-79.

VAWDA, R., WILCOX, J. T. & FEHLINGS, M. G. 2012. Current stem cell treatments for spinal cord injury. *Indian Journal of Orthopaedics,* 46**,** 10-18.

VENKATARAMANA, N. K., KUMAR, S. K., BALARAJU, S., RADHAKRISHNAN, R. C., BANSAL, A., DIXIT, A., RAO, D. K., DAS, M., JAN, M., GUPTA, P. K. & TOTEY, S. M. 2010. Open-labeled study of unilateral autologous bone-marrow-derived mesenchymal stem cell transplantation in Parkinson's disease. *Transl Res,* 155**,** 62-70.

WADA, Y., SUGIYAMA, A., YAMAMOTO, T., NAITO, M., NOGUCHI, N., YOKOYAMA, S., TSUJITA, M., KAWABE, Y., KOBAYASHI, M., IZUMI, A., KOHRO, T., TANAKA, T., TANIGUCHI, H., KOYAMA, H., HIRANO, K., YAMASHITA, S., MATSUZAWA, Y., NIKI, E., HAMAKUBO, T. & KODAMA, T. 2002. Lipid accumulation in smooth muscle cells under LDL loading is independent of LDL receptor pathway and enhanced by hypoxic conditions. *Arterioscler Thromb Vasc Biol,* 22**,** 1712-9.

WAGNER, W., HORN, P., CASTOLDI, M., DIEHLMANN, A., BORK, S., SAFFRICH, R., BENES, V., BLAKE, J., PFISTER, S., ECKSTEIN, V. & HO, A. D. 2008. Replicative senescence of mesenchymal stem cells: a continuous and organized process. *PLoS One,* 3**,** e2213.

WANG, J. T., MEDRESS, Z. A. & BARRES, B. A. 2012. Axon degeneration: Molecular mechanisms of a self-destruction pathway. *The Journal of Cell Biology,* 196**,** 7-18.

WANG, K. C., KOPRIVICA, V., KIM, J. A., SIVASANKARAN, R., GUO, Y., NEVE, R. L. & HE, Z. 2002. Oligodendrocyte-myelin glycoprotein is a Nogo receptor ligand that inhibits neurite outgrowth. *Nature,* 417**,** 941-4.

WEIDNER, N., BLESCH, A., GRILL, R. J. & TUSZYNSKI, M. H. 1999. Nerve growth factor-hypersecreting Schwann cell grafts augment and guide spinal cord axonal growth and remyelinate central nervous system axons in a phenotypically appropriate manner that correlates with expression of L1. *J Comp Neurol,* 413**,** 495-506.

WIDENFALK, J., LUNDSTROMER, K., JUBRAN, M., BRENE, S. & OLSON, L. 2001. Neurotrophic factors and receptors in the immature and adult spinal cord after mechanical injury or kainic acid. *J Neurosci,* 21**,** 3457-75.

WILKINS, A., KEMP, K., GINTY, M., HARES, K., MALLAM, E. & SCOLDING, N. 2009. Human bone marrow-derived mesenchymal stem cells secrete brain-derived neurotrophic factor which promotes neuronal survival in vitro. *Stem Cell Research,* 3**,** 63-70.

WILLERTH, S. M. & SAKIYAMA-ELBERT, S. E. 2008. Cell therapy for spinal cord regeneration. *Adv Drug Deliv Rev,* 60**,** 263-76.

Concise Review: Bone Marrow for the Treatment of Spinal Cord Injury: Mechanisms and Clinical Applications, 2011. Directed by WRIGHT, K. T., MASRI, W. E., OSMAN, A., CHOWDHURY, J. & JOHNSON, W. E. B.: Wiley Subscription Services, Inc., A Wiley Company.

WRIGHT, K. T., MASRI, W. E., OSMAN, A., ROBERTS, S., TRIVEDI, J., ASHTON, B. A. & JOHNSON, W. E. B. 2008. The cell culture expansion of bone marrow stromal cells from humans with spinal cord injury: implications for future cell transplantation therapy. *Spinal Cord,* 46**,** 811-817.

WRIGHT, L. S., PROWSE, K. R., WALLACE, K., LINSKENS, M. H. & SVENDSEN, C. N. 2006. Human progenitor cells isolated from the developing cortex undergo decreased neurogenesis and eventual senescence following expansion in vitro. *Exp Cell Res,* 312**,** 2107-20.

WU, B. & REN, X.-J. 2008. Control of demyelination for recovery of spinal cord injury. *Chinese Journal of Traumatology (English Edition),* 11**,** 306-310.

WU, P., TARASENKO, Y. I., GU, Y., HUANG, L. Y., COGGESHALL, R. E. & YU, Y. 2002. Region-specific generation of cholinergic neurons from fetal human neural stem cells grafted in adult rat. *Nat Neurosci,* 5**,** 1271-8.

WU, R., GU, B., ZHAO, X., TAN, Z., CHEN, L., ZHU, J. & ZHANG, M. 2013. Derivation of multipotent nestin+/CD271/STRO-1 mesenchymal-like precursors from human embryonic stem cells in chemically defined conditions. *Human Cell***,** 1-9.

WU, S., SUZUKI, Y., EJIRI, Y., NODA, T., BAI, H., KITADA, M., KATAOKA, K., OHTA, M., CHOU, H. & IDE, C. 2003. Bone marrow stromal cells enhance differentiation of cocultured neurosphere cells and promote regeneration of injured spinal cord. *J Neurosci Res,* 72**,** 343-51.

XU, X. M., CHEN, A., GUENARD, V., KLEITMAN, N. & BUNGE, M. B. 1997. Bridging Schwann cell transplants promote axonal regeneration from both the rostral and caudal stumps of transected adult rat spinal cord. *J Neurocytol,* 26**,** 1-16.

XU, Y., LIU, Z., LIU, L., ZHAO, C., XIONG, F., ZHOU, C., LI, Y., SHAN, Y., PENG, F. & ZHANG, C. 2008. Neurospheres from rat adipose-derived stem cells could be induced into functional Schwann cell-like cells in vitro. *BMC Neurosci,* 9**,** 21.

YAN, J., XU, L., WELSH, A. M., HATFIELD, G., HAZEL, T., JOHE, K. & KOLIATSOS, V. E. 2007. Extensive neuronal differentiation of human neural stem cell grafts in adult rat spinal cord. *PLoS Med,* 4**,** e39.

YASUDA, A., TSUJI, O., SHIBATA, S., NORI, S., TAKANO, M., KOBAYASHI, Y., TAKAHASHI, Y., FUJIYOSHI, K., HARA, C. M., MIYAWAKI, A., OKANO, H. J., TOYAMA, Y., NAKAMURA, M. & OKANO, H. 2011. Significance of Remyelination by Neural Stem/Progenitor Cells Transplanted into the Injured Spinal Cord. *STEM CELLS,* 29**,** 1983-1994.

ZHANG, Y. J., ZHANG, W., LIN, C. G., DING, Y., HUANG, S. F., WU, J. L., LI, Y., DONG, H. & ZENG, Y. S. 2012. Neurotrophin-3 gene modified mesenchymal stem cells promote remyelination and functional recovery in the demyelinated spinal cord of rats. *J Neurol Sci,* 313**,** 64-74.

ZHOU, Z., CHEN, Y., ZHANG, H., MIN, S., YU, B., HE, B. & JIN, A. 2013. Comparison of mesenchymal stem cells from human bone marrow and adipose tissue for the treatment of spinal cord injury. *Cytotherapy*.

ZIEGLER, M. D., HSU, D., TAKEOKA, A., ZHONG, H., RAMON-CUETO, A., PHELPS, P. E., ROY, R. R. & EDGERTON, V. R. 2011. Further evidence of olfactory ensheathing glia facilitating axonal regeneration after a complete spinal cord transection. *Exp Neurol,* 229**,** 109-19.

ZIPORI, D. 2005. The Stem State: Plasticity Is Essential, Whereas Self-Renewal and Hierarchy Are Optional. *Stem Cells,* 23**,** 719-726.

ZIPORI, D. 2009. Stem Cells with No Tissue Specificity

Biology of Stem Cells and the Molecular Basis of the Stem State. Humana Press.

ZVAROVA, K., MURRAY, E. & VIZZARD, M. A. 2004. Changes in galanin immunoreactivity in rat lumbosacral spinal cord and dorsal root ganglia after spinal cord injury. *J Comp Neurol,* 475**,** 590-603.